Journal of Asian Earth Sciences xxx (2015) xxx–xxx

Contents lists available at ScienceDirect

Journal of Asian Earth Sciences

journal homepage: www.elsevier.com/locate/jseaes

# Emplacement ages, geochemical and Sr–Nd–Hf isotopic characterization of Mesozoic to early Cenozoic granitoids of the Sikhote-Alin Orogenic Belt, Russian Far East: Crustal growth and regional tectonic evolution

Bor-ming Jahn [a,*], Galina Valui [b], Nikolai Kruk [c,d], V. Gonevchuk [b], Masako Usuki [a], Jeremy T.J. Wu [a]

[a] Department of Geosciences, National Taiwan University, Taipei 106, Taiwan
[b] Far Eastern Geological Institute, Russian Academy of Sciences, Vladivostok, Russia
[c] Institute of Geology and Mineralogy of Siberian Branch, Russian Academy of Sciences, Novosibirsk, Russia
[d] Novosibirsk State University, Novosibirsk, Russia

ARTICLE INFO

*Article history:*
Received 18 May 2015
Received in revised form 10 August 2015
Accepted 10 August 2015
Available online xxxx

*Keywords:*
Sikhote-Alin
Accretionary orogen
Granitoids
Juvenile crust
Zircon age
Sr–Nd–Hf isotope compositions
Cretaceous magmatism

ABSTRACT

The Sikhote-Alin Range of the Russian Far East is an important accretionary orogen of the Western Pacific Orogenic Belt. In order to study the formation and tectonic evolution of the orogen, we performed zircon U–Pb dating, as well as geochemical and Sr–Nd–Hf isotopic analyses on 24 granitoid samples from various massifs in the Primorye and Khabarovsk regions. The zircon dating revealed that the granitoids were emplaced from 131 to 56 Ma (Cretaceous to Paleogene). In the Primorye Region, granitoids in the coastal Sikhote-Alin intruded the Cretaceous Taukha Accretionary Terrane from ca. 90 to 56 Ma, whereas those along the Central Sikhote-Alin Fault zone intruded the Jurassic Samarka Accretionary Terrane during ca. 110–75 Ma. The "oldest" monzogranite (131 Ma) was emplaced in the Lermontovka area of the NW Primorye Region. Granitoid massifs along the Central Sikhote-Alin Fault zone in the Khabarovsk Region formed from 109 to 58 Ma. Thus, the most important tectonothermal events in the Sikhote-Alin orogen took place in the Cretaceous.

Geochemical analysis indicates that most samples are I-type granitoids. They have initial $^{87}Sr/^{86}Sr$ ratios ranging from 0.7040 to 0.7083, and initial Nd isotopic ratios, expressed as $\varepsilon_{Nd}(t)$ values, from +3.0 to −6.0 (mostly 0 to −5). The data suggest that the granitoid magmas were generated by partial melting of sources with mixed lithologies, including the subducted accretionary complex ± hidden Paleozoic-Proterozoic basement rocks. Based on whole-rock Nd isotopic data, we estimated variable proportions (36–77%) of juvenile component (=mantle-derived basaltic rocks) in the generation of the granitic magmas. Furthermore, zircon Hf isotopic data ($\varepsilon_{Hf}(t)$ = 0 to +15) indicate that the zircon grains crystallized from melts of mixed sources and that crustal assimilation occurred during magmatic differentiation.

The quasi-continuous magmatism in the Sikhote-Alin orogen suggests that the Paleo-Pacific plate subduction was very active in the Late Cretaceous. The apparently regular progression of granitic intrusion ages from 80 to 56 Ma in the Taukha Terrane may reflect oblique underflow of the Paleo-Pacific plate beneath the Eurasian continental margin. Subduction was not only manifested by granitic intrusion, but also by abundant silicic volcanism. The Late Cretaceous Paleo-Pacific plate motion probably changed from parallel or sub-parallel to oblique relative to the continental margin of the Sikhote-Alin, leading to the change of magmatic source region and geochemical characteristics of the derived igneous rocks. Late Cretaceous rapid seafloor spreading at ca. 100 Ma induced highly active subduction and led to voluminous magmatism in the entire Circum-Pacific realm. Finally, the present age and isotopic study lends support to the hypothesis of geologic and tectonic correlation between Sikhote-Alin and SW Japan.



## 1. Introduction

The Asian continent is a complex mosaic composed of numerous tectonic blocks of various sizes. To simplify, the eastern part of Asia consists of four to five Precambrian cratons which are welded together by younger orogenic belts. A gigantic belt, the Altaids (Sengor et al., 1993) or Central Asian Orogenic Belt (CAOB; Jahn, 2004; Jahn et al., 2000a,b) between the Russian, Siberian and Tarim-North China cratons was formed by the successive accretion of island arcs and rifted microcontinents. The evolution of the CAOB is generally regarded to be related to the birth and death

* Corresponding author.
*E-mail address:* bmjahn@ntu.edu.tw (B.-m. Jahn).

http://dx.doi.org/10.1016/j.jseaes.2015.08.012
1367-9120/

of the Paleo-Asian Ocean, hence the CAOB represents the Paleo-Asian Tectonic Realm. Similarly, the second gigantic belt, the Tethysides, between the Tarim-North China and India-Arabian cratons, was also formed by stacking of arc and micro-continental terranes, with a final stage of continental collision that produced the Himalayan Range and elevated the Tibetan Plateau. Thus, the Tethysides belongs to the Tethyan Tectonic Realm. The orogenic belts the eastern margin of Asia comprise Mesozoic and younger continental and oceanic arcs formed by subduction of the Pacific Plate and its marginal seas. Rifted microcontinental blocks make up a small component. Thus, the third group of orogenic belts constitute the Pacific Tectonic Realm. Sengor and Natal'in (1996) coined this tectonic realm as the "Nipponides".

Through extensive field investigations, zircon age dating and Nd–Sr–Hf isotopic tracer studies in the last two decades, the CAOB is renowned for massive generation of juvenile continental crust (e.g., Sengor and Natal'in, 1996; Jahn, 2004; Jahn et al., 2000a,b). Isotopic studies on the crustal rocks of the Tethysides are comparatively rare; however, the available data and on-going research of S.L. Chung and co-workers have indicated that a significant proportion of these crustal rocks are also of juvenile characteristics (Chu et al., 2006; Lin et al., 2013). Though the orogenic belts of the Pacific Realm are known to comprise mainly accretionary orogens, the true crustal characteristics and evolution remain much debated. For example, the Japanese Islands have long been considered as the classic example of an accretionary orogen in which voluminous granitoids was transferred from the mantle to the crust via melting of subducted slabs (Isozaki, 1996, 1997; Maruyama, 1997; Maruyama et al., 1997). This model has not been supported by the available Nd–Sr isotopic data for SW Japan (Jahn, 2010), but probably is true for NE Japan and Hokkaido (Jahn et al., 2014).

The Sikhote-Alin Orogenic Belt of the Russian Far East is a part of the Pacific Tectonic Realm. Its geological and tectonic evolution has been correlated with that of SW Japan (Ishiwatari and Tsujimori, 2003; Khanchuk, 2001; Sato et al., 2004, 2006). In this work we carried out a comprehensive investigation on the emplacement ages and geochemical-isotopic characteristics of the granitoids from the Sikhote-Alin Belt. These data are used to discuss the granitoid petrogenesis and implications for the crustal and tectonic evolution in the Sikhote-Alin accretionary orogen.

## 2. Geological setting of the Sikhote-Alin Orogenic Belt

The Sikhote-Alin Orogenic Belt is composed of Mesozoic tectonostratigraphic terranes lying to the east of the late-Precambrian crustal blocks – Bureya, Jiamusi and Khanka (Fig. 1). Structural nappes, ophiolite mélanges, and chaotic olistostromes occur widely in the belt (Geology of the USSR, 1971; Melnikov and Golozubov, 1980; Khanchuk et al., 1988; Zonenshain et al., 1990a,b). Parfenov (1984) was the first to interpret the Sikhote-Alin Belt as an accretionary orogen, and this interpretation was further elaborated by Natal'in (1991).

The Pre-Mesozoic tectonic units include (1) the Neoproterozoic Bureya, Jiamusi and Khanka Blocks (Wilde, in press), and (2) the Paleozoic Dzhagdy-Kerbinsky, Galamsky and Laoelin-Grodekovo terranes (Fig. 1). The Laoelin-Grodekovo terrane is the southern extension of the Zhangguangcai Range of NE China. The Khanka Block consists of Precambrian continental basement overlain by thick Paleozoic continental margin deposits, including Cambrian calcareous sediments and post-Silurian non-marine strata. It is probably part of a larger continental segment (=Amuria superterrane or microcontinent) that includes the Bureya and Jiamusi blocks to the north (Khanchuk, 2001; Khanchuk et al., 1996). A basic granulite (two-pyroxene-amphibole schist; $SiO_2$ = 47%, $Al_2O_3$ = 17.1%, MgO = 8.6%) from the Khanka Block near the Khanka Lake has been dated using SHRIMP analysis on zircon grains (Khanchuk et al., 2010). Type 1 zircon grains (inner cores) yielded 757 ± 4 Ma, and type-2 zircon grains (structureless and rims of zoned zircons) gave 507 ± 3 Ma. The age of 757 Ma probably represents the formation time of the protolith (basaltic) and 507 Ma the time of the granulite facies metamorphism. In NE China, the pre-Mesozoic basement (Jamusi Block) is composed of the Mashan

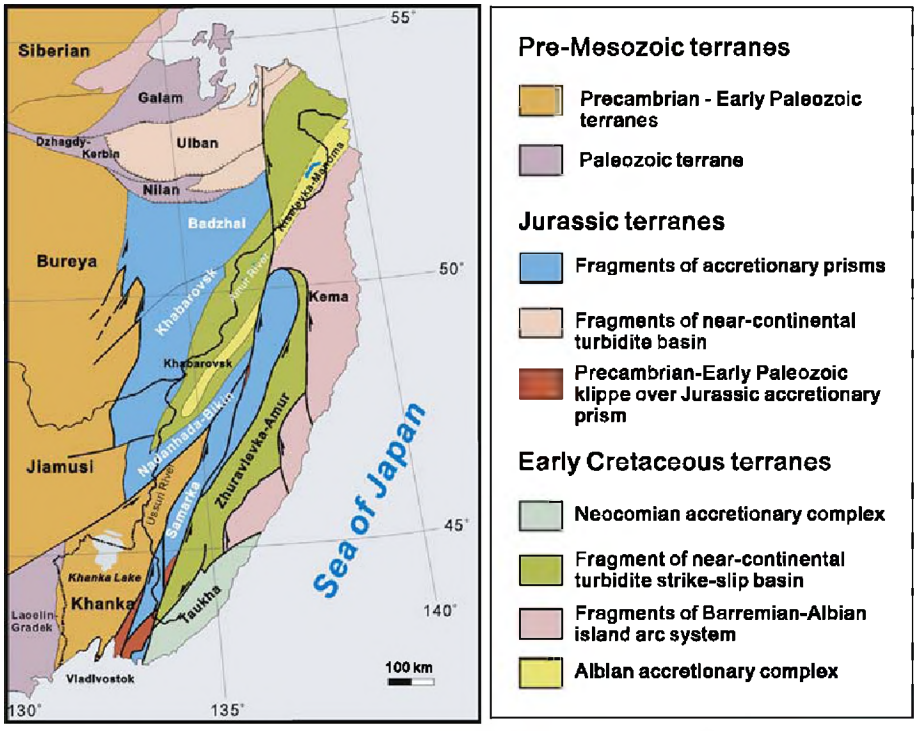


**Fig. 1.** Principal tectonostratigraphic terranes in the Sikhote-Alin Orogenic Belt, Russian Far East (after Golozoubov, 2006).

Please cite this article in press as: Jahn, B.-m., et al. Emplacement ages, geochemical and Sr–Nd–Hf isotopic characterization of Mesozoic to early Cenozoic granitoids of the Sikhote-Alin Orogenic Belt, Russian Far East: Crustal growth and regional tectonic evolution. Journal of Asian Earth Sciences (2015), http://dx.doi.org/10.1016/j.jseaes.2015.08.012

and Heilongjiang Complexes and Permian granites (Wilde et al., 2003; Wilde, in press; Wu et al., 2011; Zhou et al., 2010; Zhou and Wilde, 2013). The high-grade metamorphic rocks of the Khanka Block are comparable to those of the Mashan Complex, whose metamorphic ages have been well determined at ca. 500 Ma (Wilde et al., 1997, 2000, 2003; Wilde, in press). In fact, a very important work in NE China has been the recognition of a huge khondalite belt along the China-Russia border. The khondalitic metasedimentary rocks and associated igneous rocks were metamorphosed to granulite facies at ca. 500 Ma. This event is registered in the northern parts of the Erguna and Xing'an Blocks (Zhou et al., 2011) as well as in the Jiamusi and Khanka Blocks (Wilde et al., 2000, 2003, 2010; Wilde, in press).

As shown in Fig. 1, the Sikhote-Alin Orogenic Belt proper is constituted by several Mesozoic terranes. The Jurassic terranes comprise four accretionary prisms (=Samarka, Nadanhada-Bikin, Khabarovsk and Badzhal terranes), a turbidite basin (=the Ulban terrane) and a Precambrian-Early Paleozoic klippe (=the Sergeevka terrane) overlying accretionary complexes. The Early Cretaceous terranes include: (1) the Taukha Terrane, an accretionary complex; (2) the Zhuravlevka Terrane, a fragment of near-continental turbidite basin; (3) the Kema Terrane, mainly composed of island arc assemblages; and (4) the Kiselevka-Manoma Terrane, another accretionary complex to the north and west of the Kema terrane. All the Mesozoic terranes are intruded by Late Cretaceous to Eocene granitic rocks or covered by vast contemporaneous volcanic and volcanisedimentary rocks (Kemkin and Khanchuk, 1994; Kojima et al., 2000).

The Jurassic Samarka accretionary prism consists mainly of terrigenous sediments (sandstones and siltstones). Fragments of oceanic basalts, mainly OIB, are often associated with clastic sediments. Blocks of limestone and chert also occur. The Cretaceous **Zhuravlevka** Terrane is a vast expanse of turbidite that mainly occurs to the east of the Central Sikhote-Alin Fault (Fig. 1; Golozoubov and Khanchuk, 1996). Kojima (1989) considered the Samarka Terrane to be equivalent to the Mino-Tamba belt in SW Japan and the Nadanhada Terrane in China, and they were fragments of the same Jurassic accretionary complex.

The **Kema Terrane** of eastern Sikhote-Alin is mainly composed of flysch deposits and volcanisedimentary sequences; the volcanic rocks are basalt, andesite and rhyolite of Cretaceous to Paleocene ages (e.g., Grebennikov and Popov, 2014). The youngest volcanic rocks are the Miocene-Pliocene plateau basalt that occurs in the northern Kema Terrane, in the Khabarovsk Region. Several researchers considered the Kema Terrane to be of island arc or back-arc origin (e.g., Malinovsky et al., 2006, 2008; Golozoubov, 2006; Grebennikov and Popov, 2014).

The **Taukha Terrane** in the southeastern part of the Primorye Region is mainly a Cretaceous accretionary complex, intruded by numerous granitoid plutons and stocks (e.g., Kemkin and Taketani, 2008). The nature of the basement is largely unknown, but some workers consider it to be composed predominantly of tholeiitic basalts, similar to that of the Kema Terrane.

A distinctive feature of the Sikhote-Alin Belt is that it is broken by a system of sinistral strike-slip faults, the most striking being the **Central Sikhote-Alin Fault** (Figs. 1 and 2) with a displacement of ca. 200 km. The Fault was most active during the Early Cretaceous, and the activity was terminated in the Late Cretaceous (Utkin, 1980).

Mesozoic-Cenozoic magmatic activity in Sikhote-Alin is mainly manifested in the Central Sikhote-Alin magmatic belt and the East Sikhote-Alin Volcanic-Plutonic Belt (**ESAVPB**). The "Central Sikhote-Alin magmatic belt" includes numerous granitoid plutons in the Zhuravlevka, Samarka and Nadanhada terranes. In addition, small volumes of basalt and andesite also occur (Simanenko et al., 2002). The granitoid plutons and volcanic rocks were mostly emplaced during the Early Cretaceous and rarely in the Late Cretaceous to early Cenozoic (Sakhno, 2001; Khanchuk, 2006).

The East Sikhote-Alin Volcanic-Plutonic Belt (**ESAVPB**) comprises a large volume of volcanic rocks overlying the Kema and Taukha terranes. These volcanic rocks, including basalt, andesite and rhyolite, were emplaced in the Late Cretaceous to Middle Paleogene. According to Khanchuk (2001) and Khanchuk and Kemkin (2003), during the period from Cenomanian (ca. 95 Ma) to Maastrichtian (70–65 Ma), the tectonic regime of the **ESAVPB** was of a supra-subduction nature, but it changed to a transform or strike-slip setting in the Paleocene-Eocene. Volcanic activity was accompanied by the emplacement of numerous granitoid plutons in the same areas.

A correlation between the tectonic units of Sikhote-Alin and the Japanese Islands has been proposed by Kojima (1989) and Khanchuk (2001), and further supported by Ishiwatari and Tsujimori (2003) based on their study of the distribution and emplacement of the ophiolite-blueschist complexes. Because the correlation will be further discussed in the last section, a brief description of the main features of SW Japan is given in the Appendix A.

## 3. Occurrences of granitic rocks in Sikhote-Alin and description of sampling localities

Fig. 2 shows the distribution of granitoid intrusions in the Primorye region. The granitoid samples were collected from four general areas: (1) the East Sikhote-Alin Volcanic-Plutonic Belt (**ESAVPB**), along the Japan Sea and south of 45°N (**Valui samples**; from the Oprichnensky, Vladimirsky, Olginsky and Valentinovsky massifs); (2) along the Central Sikhote-Alin Fault zone (**Gonevchuk samples** from the Shumninsky, Berezovsky, Sadovsky and Ladoshinsky massifs; **Kruk samples** from the Dalnensky area including the Dalnensky and Vostok-2 massifs; and also from the southernmost tip of Sikhote-Alin: the Ovseenko Cape and Vrangel massifs of the Uspensky area); (3) the Lermontovka area of the NW Primorye Region (**Kruk samples**, Gorbun and Chaplievsky massifs), and (4) to the north of Fig. 2 map area, in the Khabarovsk Region (N49°20′ to 50°35′), including the Chalba and West-Anuy massifs and small unnamed stocks (**Gonevchuk and Kruk samples**). A description of the four areas is given below. This is done as a brief review for the international reader as the original Russian literature is hard to access or difficult to understand for non-Russian reader.

### 3.1. The East Sikhote-Alin Volcanic-Plutonic Belt (ESAVPB)

According to Valui (2004, 2014) and Valui et al. (2008), the four plutons of the ESAVPB (**Oprichninsky, Vladimirsky, Olginsky, and Valentinovsky**) are mainly composed of diorite, granodiorite and granite. The plutons of the western part of the ESAVPB, within the Dalnegorsk district, are mono-phase granitic porphyry of the ilmenite series. K–Ar ages of 83, 69–72, and 60–63 Ma were obtained for the Dalnegorsk gabbro-diorites, granodiorites, and granites, respectively (Valui et al., 2008). Many plutons are accompanied by important mineralization, for example, borosilicate and base metal deposits in the Dalnegorsk district.

The granitoids of the coastal ESAVPB show various stages of differentiation and levels of emplacement (Valui et al., 2008). The lithological and petrographic characteristics of the plutons may be represented by two massifs – the Olginsky and Valentinovsky massifs.

The **Olginsky massif** is multi-phased, composed of diorite, granodiorite and coarse-grained granite. As a whole, coarse-grained

Please cite this article in press as: Jahn, B.-m., et al. Emplacement ages, geochemical and Sr–Nd–Hf isotopic characterization of Mesozoic to early Cenozoic granitoids of the Sikhote-Alin Orogenic Belt, Russian Far East: Crustal growth and regional tectonic evolution. Journal of Asian Earth Sciences (2015), http://dx.doi.org/10.1016/j.jseaes.2015.08.012

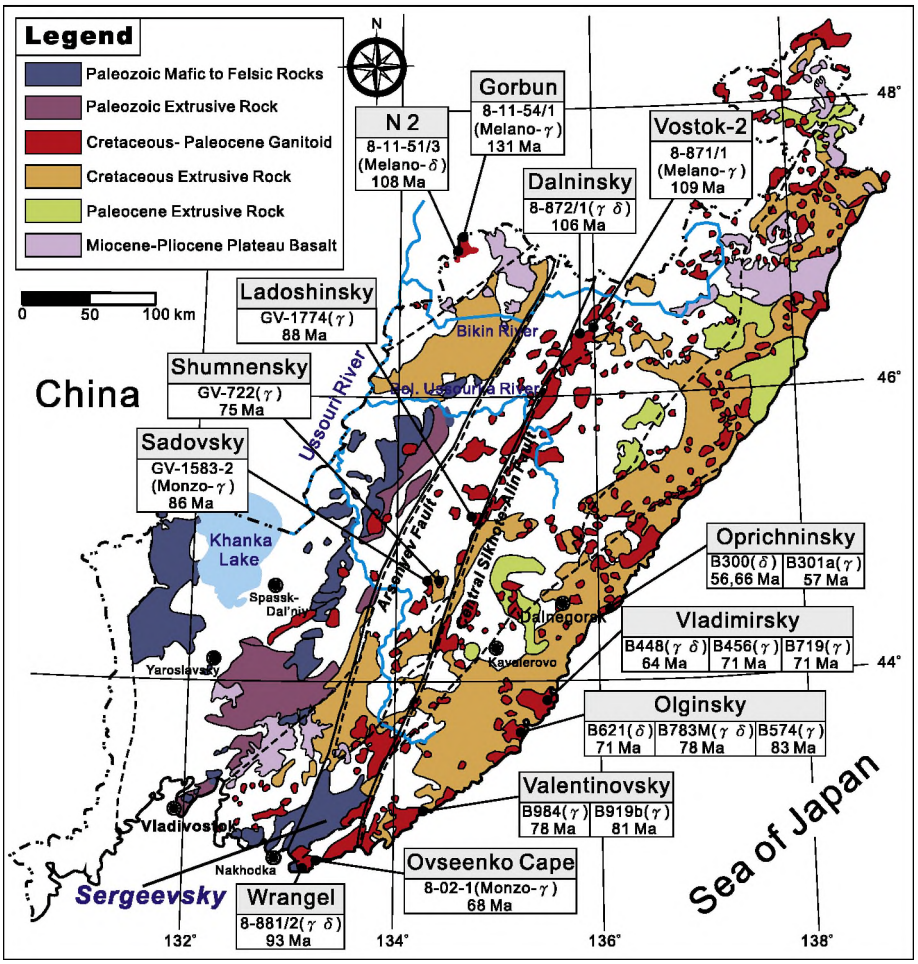


**Fig. 2.** Distribution of granitoids and extrusive (volcanic) rocks in the Primorye region, Sikhote-Alin (Khanchuk, 2006). The sampling localities and new zircon age data are also shown. At each sample locality, the sample number, rock-type and zircon age are given in a rectangular box. Symbols: γ = granite, δ = diorite, γδ = granodiorite. The Sergeevsky Massif or Complex, located in the southern part of Sikhote-Alin and near Vladivostok, is a tectonic "klippe", composed mainly of early Paleozoic metabasic to metagranitoid rocks.

granite is dominant, but diorite is the earliest phase. Granitic bodies are intruded by stocks of miarolitic granite and aplitic dikes. Diorite is generally massive, grey-green and fine-to-medium-grained. Granodiorite crops out only in the Manevsky Cape area. It is cut by granite in many places. Granite is generally massive, porphyritic and coarse-grained. Three samples from the Olginsky massif were selected for the present study – a diorite (B-621), a granodiorite (B-783M), and a granite (B-574).

The **Valentinovsky massif** in southern Sikhote-Alin extends along the Japan Sea coast for more than 50 km, with a total exposure of about 200 km$^2$. The massif shows a complicated structure and comprises diorite, quartz diorite, granodiorite, granite, aplite and granite porphyry. As in the Olginsky massif, the earliest intrusive phase is diorite, which occurs as a small stock between the Bodisko and Tumannyi capes. The northern part of the massif is composed of uniform granodiorite. In the central part of the massif, a large block (0.5 × 2.5 km) of sedimentary rock is found in granodiorite. K–Ar dating suggests that the Valentinovsky massif was emplaced during a prolonged period from late Cretaceous (ca. 95 Ma; diorites) to Eocene–Oligocene (alkaline granites and granite-porphyries of the Tasovaya Bay) (Valui, 2014). A granodiorite (**B919-b**) and a granite (**B984**) samples were chosen for the present study. In terms of mineralization, the intrusions of the coastal region host only very minor magnetite–skarn and molybdenum deposits.

### 3.2. The Central Sikhote-Alin Fault zone

Numerous granitoid intrusions were emplaced along the Central Sikhote-Alin Fault zone. Large granitoid massifs, such as Dalnensky and Biserny, occur in the **Dalnensky area** in the northern Primorye Region (Fig. 2). The granitoid intrusions are accompanied by small stocks and dikes of basic to silicic compositions (Soloviev and Krivoshchekov, 2011). The Dalnensky monzonite–granodiorite pluton is associated with the celebrated tungsten deposit "**Vostok-2**". The granitoids in the Dalnensky area intruded into the Jurassic terrigenous siliceous-volcanic strata of the Samarka Terrane and early Paleozoic amphibolite of the **Sergeevsky** metamorphic complex.

The principal rock-types of the granitoid massifs are medium-grained biotite- and biotite-hornblende granodiorite and melanocratic granite. In the Dalnensky massif, amphibole-biotite (± pyroxene) diorite, quartz diorite and monzodiorite form the early phase. The granitoids were intruded by dikes and small bodies of biotite granite porphyry, leucocratic granite and aplite. **Samples 8-871/1** (Vostok-2 stock) and **8-872/1** (Dalnensky massif) are representative of the granitoids from the Dalnensky area.

In the middle segment of the Central Sikhote-Alin Fault zone, or in the geographic center of the Primorye Region (Fig. 2), granitoid samples were collected from four massifs – from north to south, Ladoshinsky (granite sample **GV-1774**), Sadovsky (granite sample

Please cite this article in press as: Jahn, B.-m., et al. Emplacement ages, geochemical and Sr–Nd–Hf isotopic characterization of Mesozoic to early Cenozoic granitoids of the Sikhote-Alin Orogenic Belt, Russian Far East: Crustal growth and regional tectonic evolution. Journal of Asian Earth Sciences (2015), http://dx.doi.org/10.1016/j.jseaes.2015.08.012

**GV-1583-2**), Shumnensky (granite sample **GV-722**) and Berezovsky (monzogranite sample **GV-1401**). The first two massifs intruded into clastic and volcaniclastic rocks of the Samarka terrane of the Jurassic accretionary prism; whereas the last two massifs intruded into the clastic sedimentary rocks of the Zhuravlevka turbidite basin.

The **Ladoshinsky** massif is characterized by medium-grained biotite and biotite-hornblende granites. These granites are often cut by small leucocratic granite porphyry and aplite, and are associated with minor gabbro and diorite bodies. They are also accompanied by tungsten mineralization, such as the Skrytoye deposit (Soloviev, 1995).

The **Sadovsky** massif is a large granite intrusion (>100 km$^2$) with zonal structure. The central part of the massif is composed of medium- and coarse-grained biotite granite, often with schlieren texture and thin veins of muscovite pegmatite. The marginal part is characterized by fine-grained porphyritic granite. In addition, small bodies of melanocratic granite, granodiorite, and alkaline gabbro are also associated with the Sadovsky massif.

The **Shumnensky** and **Berezovsky** massifs occur in the Kavalerovo magmatic area. The area has more than 10 massifs of different compositions and emplacement ages, many of them are accompanied by tin (Sn) mineralization. The rock-types include gabbro (Ararat massif), monzodiorite, syenite and monzogranite (Berezovsky massif), granodiorite and plagiogranite (Porubsky massif), granite and leucogranite (Shumnensky) (Rub et al., 1982; Sakhno et al., 2011; Gonevchuk et al., 2011; Kruk et al., 2014a). The Shumnensky massif is composed of medium-grained porphyritic biotite granite, and it was dated at 85–70 Ma by the K–Ar method on biotite (Gonevchuk, 2002). The Berezovsky massif was dated at 100–85 Ma by the K–Ar and Rb–Sr methods (Gonevchuk, 2002; Gonevchuk et al., 2011).

The **Uspensky area** is located in the southernmost part of Sikhote-Alin (Fig. 2). To the east of this area is the southern part of the ESAVPB and to the west the Khanka block. The area is bounded by two major faults – the Central Sikhote-Alin Fault in the east and the Arsenyev Fault in the west. It includes the Early Cretaceous Uspensky and Wrangel Massifs and Late Cretaceous Ovseenko Cape Massif and several small intrusive bodies. The granitoids intruded the Jurassic terrigenous siliceous volcaniclastic deposits of the Samarka Terrane and Early Paleozoic amphibolites of the **Sergeevsky** complex. Together with the overlying Permian volcanisedimentary sequences, the **Sergeevsky** complex forms a tectonic allochthon (klippe). The granitoid massifs were dated by the Rb–Sr and K–Ar methods at 112–98 Ma (Krimskii et al., 1998; Gvozdev, 2010). Metamorphic ages of metagabbro, metadiorite and amphibolites from the Sergeevsky complex have recently been dated at 480–490 Ma at National Taiwan University (zircon U–Pb; unpublished data).

The **Uspensky Massif** is a linear body of ca. 40 km long and 10 km wide. The western part of the massif is composed of coarse-grained garnet-bearing biotite and two-mica leucocratic granites; whereas the eastern and central parts are dominated by medium-grained biotite (±amphibole) granodiorite and melanocratic granite. Khanchuk et al. (2008) published two zircon U–Pb ages (103 ± 2 and 99 ± 2 Ma) for the Uspensky granitoids. Recently, Nd isotopic compositions were determined for a garnet-bearing leucogranite ($\varepsilon_{Nd}(t) = -3.8$) by Moskalenko et al. (2011) and for biotite-amphibole granodiorites and granites (−0.7 to −2.4) by Kruk et al. (2014a).

The **Vrangel Massif** (about 50 km$^2$) is mostly composed of medium-grained equigranular biotite-hornblende granodiorite and weakly porphyritic biotite granite. Mafic enclaves are frequently found in the granitoids. In places the massif was cut by dikes of granite porphyry and aplites.

**The Ovseenko Cape massif** is an isometric body with an exposure area of about 35 km$^2$. The massif is homogeneous and composed of coarse-grained biotite granites. Two granitoid samples from the Uspensky area were subject to analysis in this work – **sample 8-881/1** represents the Wrangel massif and **sample 8-02-1**, the Ovseenko Cape massif.

### 3.3. The Lermontovka area of the NW Primorye Region

In the **Lermontovka area** several Cretaceous granitoid massifs intruded and metamorphosed the Late Jurassic clastic and volcaniclastic rocks of the eastern part of the **Nadanhada Terrane**. The massifs also intruded sub-latitudinal mafic dikes (pyroxenite, gabbro and diorite). The granitoids belong to two associations. The first comprises large massifs (Shivka, Gorbun and Olimpiada) and small stocks, with one massif connected with the Lermontovka tungsten deposit. The predominant rock types of the massifs are coarse- to medium-grained biotite or two-mica cordierite-bearing granodiorites and melanocratic granites. In places, they are intruded by fine-grained leucogranitic dikes. **Sample 8-11-54/1** is a melanocratic monzogranite from the **Gorbun massif**.

The second association is represented by the Chaplievsky massif and several small satellite bodies. The association comprises fine-grained pyroxene-amphibole monzodiorite and quartz monzodiorite. Mafic enclaves (fine-grained monzogabbro) and fine-grained biotite-amphibole monzogranite veins also occur in the monzodiorites. **Sample 8-11-51/3** is representative of the monzodiorite.

### 3.4. Khabarovsk Region (N49°20′ to 50°35′)

A number of granitoid massifs of Early Cretaceous and Paleogene age occur in the basin of the Anuy River, a triburaty of the Amur River. The largest massif is the **Gobilly intrusion** emplaced at 105 ± 2 Ma (Natal'in et al., 1994). The granitoids intruded into deformed Jurassic strata of the Samarka Terrane and metamorphic rocks of the Anuy Dome, which is a Mesozoic core complex (Kruk et al., 2014b). Contact metamorphism produced aureoles of biotite- and cordierite-bearing hornfels up to 1 km wide.

Large intrusions (up to 100 km$^2$) of Early Cretaceous granitoids occur in sub-meridional to NE orientation. They consist mainly of coarse-grained biotite granodiorite or porphyritic melanocratic granite. Dikes of fine-grained granite and aplite occur but rarely. A monzogranite sample (**AN-2-11**) was chosen for the present study.

Granitoids of Paleogene age usually make up small massifs or stocks (<15 km$^2$). They are composed of medium- and fine-grained biotite and biotite-amphibole leucocratic granites. A leucocratic granite sample (**AN-3-11**) was selected for the present analysis.

Two more granitoid samples came from two complexes of the **Komsomolsk** magmatic area – a monzogranite of the **Silinka complex** (**ЧГ-332**) and a porphyritic granite of the **Chalba complex** (**ЧГ-410**). The granitoids intruded into the terrigenous rocks of the **Badzal Terrane** of the Jurassic accretionary prism.

**The Silinka complex** is composed of trachyandesite and a suite of intrusive rocks ranging from gabbro to leucogranite, with a predominance of quartz diorite and granodiorite. Quartz diorite and granodiorite often occur as small intrusive bodies and dikes. The Silinka complex was emplaced from 102 to 80 Ma based on the K–Ar and Rb–Sr geochronology (Gonevchuk, 2002; Gonevchuk et al., 2011).

**The Chalba complex** is characterized by granitic rocks (>80%) with coarse-grained biotite granite in the central part and biotite-hornblende-bearing granite porphyry in the border. K–Ar dating suggests that the complex was formed during 90–92 Ma.

A summary of rock types, intrusive age information, sample localities, pluton names, principal geological features, and mineral assemblages for all the granitoid samples analyzed in this work is presented in Table 1.

Please cite this article in press as: Jahn, B.-m., et al. Emplacement ages, geochemical and Sr–Nd–Hf isotopic characterization of Mesozoic to early Cenozoic granitoids of the Sikhote-Alin Orogenic Belt, Russian Far East: Crustal growth and regional tectonic evolution. Journal of Asian Earth Sciences (2015), http://dx.doi.org/10.1016/j.jseaes.2015.08.012

Please cite this article in press as: Jahn, B.-m., et al. Emplacement ages, geochemical and Sr–Nd–Hf isotopic characterization of Mesozoic to early Cenozoic granitoids of the Sikhote-Alin Orogenic Belt, Russian Far East: Crustal growth and regional tectonic evolution. Journal of Asian Earth Sciences (2015), http://dx.doi.org/10.1016/j.jseaes.2015.08.012

**Table 1**
Brief description of the analyzed granitoid samples from Sikhote-Alin.

| Sample No. | Rock type (original appellation in parentheses) | Literature age information (Ma) | Sample locality (Coordinates) | Name of Pluton or intrusive body | Geological and structural features; associated rocks | Petrographic texture | Mineral assemblage or characteristic phases[a] |
|---|---|---|---|---|---|---|---|
| B-300 | Quartz monzodiorite (Diorite) | 81 (K–Ar) | E 136°10′13″, N 44°30′04″ | Oprichnensky (central. Part.) | Located in the central part of pluton | Massive, medium-to-coarse-grained | Pl 64%, Hbl 9%, Px 1%, Bt 9%, Qz 10%, Kfs 5%. Accessory (2%): Mag, Ilm, Ap, Zrn, cassiterite, fergusonite |
| B-301a (=B-257) | Alkali feldspar granite (Granite) | 57.5 (K–Ar) | E 136°07′29″, N 44°29′17″ | Oprichnensky (central. Part.) | Located in the south-central part of pluton | Coarse-grained, equigranular | Pl 27%, Qz 32%, Kfs 35%, Bt 5%. Accessory (1%): Mag, Ap, Zrn, Au, fergusonite |
| B-448 (=B433) | Granodiorite | 68 (K–Ar) | E 135°28′01″, N 43°55′36″ | Vladimirsky | Located in the northern part of pluton | Medium-to-fine grained, hetrogeneous | Pl 46%, Qz 21%, Kfs 18%, Bt 8%, Hbl 5%. Accessory (2%): Mag, Ap, Zrn, Aln |
| B-456 (=B-494) | Granodiorite (Granite) | 68 (K–Ar) | E 135°28′10″, N 43°55′02″ | Vladimirsky | Located in the middle of the western coast of the Vladimir Bay | Coarse-grained, equigranular | Pl 28%, Qz 36%,Kfs 33%, Bt (2%). Accessory (1%): Mag, Ap, Zrn, Aln |
| B-719 (=B-720) | Granite | 70 (K–Ar) | E 135°27′57″, N 43°48′35″ | Vladimirsky | Located in the southern part of pluton | Coarse-grained, equigranular | Pl 30%, Qz 36%, Kfs 30%, Bt 2%, Hbl 1%. Accessory (1%): Mag, Ap, Zrn, Aln |
| B-574 | Granite | 59 (K–Ar) | E 135°13′17″, N 43°38′36″ | Olginsky | Located in the southern part of pluton | Coarse-grained, equigranular | Pl 33%, Kfs 30%, Qz 32%, Bt 3%, Hbl 1%. Accessory (1%): Mag, Ap, Zrn, Aln, fergusonite, cassiterite |
| B-617a, B-621 (=B611) | Granodiorite (Diorite) | | E 135°13′35″, N 43°40′14″ | Olginsky | Located in the central part of pluton | Fine-to-medium-grained, equigranular | Pl 60%, Px 15%, Hbl 10%, Qz 10%, Kfs 2%. Accessory (3%): Mag, Ilm, Ap, Zrn ± Aln ± cassiterite |
| B-783M (=B-781) | Granite (Granodiorite) | 60, 65 (K–Ar) | E 135°13′03″, N 43°37′59″ | Olginsky | Located in the southern part of pluton | Medium-grained, heterogeneous | Pl 46%, Qz 26%, Kfs 20%, Hbl 4%, Bt 3%. Accessory (1%): Mag, Ap, Zrn, Aln, cassiterite |
| B-919b (=B909A) | Granite (Granodiorite) | 69, 62 (K–Ar) | E 134°21′21″, N 43°07′09″ | Valentinovsky | Located in northern part of pluton | Coarse-to-medium-grained, equigranular | Pl 36%, Qz 34%, Kfs 12%, Hbl 3%, Bt 14%. Accessory (1%): Mag, Ap, Zrn, Aln, cassiterite, fergusonite |
| B-984 (=B-995) | Granite | 57 (K–Ar) | E 134°10′01″, N 43°01′49″ | Valentinovsky | Located in the southern part of pluton | Coarse-grained, equigranular | Pl 23%, Qz 40%, Kfs 27%, Hbl 3%, Bt 6%. Accessory (1%): Mag, Ap, Zrn, fergusonite |
| GV-722 | Granite | 76 ± 2 (K–Ar) | E 134°20′, N 44°15′ | Shumny | Located within the Central Sikhote-Alin fault zone. Leucocratic granites with biotite and rarely hornblende. | Coarse-grained | Qz 40%, Kfs 35%, Pl 20%, Bt 4%, Hbl ⩽1% |
| GV-1401 | Granite (Monzogranite) | 102–105 (K–Ar) | E 134°43′, N 44°25′ | Berezovsky | The intrusive body comprises gabbro and younger monzogranite | | Qz 35%, Pl 30%, Kfs 25%, Bt 6%, Px 2%, Hb 2% |
| GV1583-2 | Granite (Monzogranite) | 90 ± 2 (K–Ar) | E. 134°15′, N 44°33′ | Bisersky complex, Sadovy intrusive body | Biotite granite prevails in the Sadovy body. Small pegmatite or leucogranite dikes are also present. | Coarse-grained | Qz 45%, Kfs 25%, Pl 25%, Bt 4%, Hbl ⩽ 1% |
| GV1774 | Granite | 87 ± 2 (K–Ar) | E 134°50′, N 45°10′ | Ladoshin intrusive body | Located in the central part of the Malinovka area. Early granite stock (phase I) is intruded by biotite-muscovite granite, which is cut by dikes of fine-grained biotite granites (phase II). | Coarse-grained | Qz 40%, Kfs 30%, Pl 25%, Bt 4%, Hbl ⩽ 1% |
| ЧG-332 | Granite (Monzogranite) | 94 ± 2 (K–Ar) | E 136°00′, N 50°35′ | Silinka Complex | Granite forms small intrusive body. Sharp contact with granite. K–Ar and Rb–Sr ages = 102–80 Ma | | Qz 35%, Kfs 30%, Pl 25%, Bt 5%, Px 3%, Hbl 2% |
| ЧG-410 | Granite | 90 ± 2 (K–Ar) | E 136°10′, N 50°35′ | Chalba Complex | It occurs in the contact zone of the Chalba intrusive body (K–Ar age = 90–92 Ma). | Porphyritic | Qz 40%, Kfs 30%, Pl 25%, Bt 4%, Hbl 1% |
| 8-11-54/1 | Granite (Monzogranite) | 120–127 (Rb–Sr) | E 134°35′24″; N 47°02′05″ | Gorbun | It occurs in the northern part of massif, about 250 m from the border; melanocratic | Coarse-grained, equigranular | Qz 25%, Pl 28%, Kfs 35%, Bt 12% |
| 8-11-51/3 | Quartz monzodiorite (Monzodiorite) | K2 (?) | E 134°30′23″; N 47°02′53″ | unnamed | Southern part of the massif, about 50 m from the contact. | Fine-grained, equigranular | Pl 45%, Kfs 15%, Qz 5%, Cpx 2–3%, Hbl 25%, Bt 5% |

**Table 1** (*continued*)

| Sample No. | Rock type (original appellation in parentheses) | Literature age information (Ma) | Sample locality (Coordinates) | Name of Pluton or intrusive body | Geological and structural features; associated rocks | Petrographic texture | Mineral assemblage or characteristic phases[a] |
|---|---|---|---|---|---|---|---|
| 8-871-1 | Granodiorite (Melanogranite) | 95–100 (Rb–Sr) | E 135°53′48″; N 46°30′03″ | Vostok-II stock | Central part of the stock; melanocratic | Medium-grained, equigranular | Pl 45%, Kfs 20%, Qz 22%, Hbl 4% Bt 9% |
| 8-872-1 | Granodiorite | 100–102 (Rb–Sr) | E 135°49′38″; N 46°24′13″ | Dalnensky | Central part of the massif; melanocratic | Medium-grained, equigranular | Pl 45%, Kfs 15%, Qz 5%, Hbl 9%, Bt 6% |
| 8-02-01 | Alkali feldspar granite (Monzogranite) | 75 ± 3 (Ar/Ar) | E 133°02′18″; N 42°45′43″ | Ovseenko Cape | Northern part of the massif, about 100 m from the border; leucocratic | Medium-grained, equigranular | Qz 50%, Pl 20%, Kfs 25%, Bt 5% |
| 8-881-2 | Graodiorite | 91 ± 1 (Ar/Ar) | E 133°02′18″; N 42°41′04″ | Wrangel | Central part of the massif; melanocratic | Medium-grained, equigranular | Pl 32%, Kfs 33%, Qz 25%, Bt 8–9%, Hbl 1–2% |
| AN-2-11 | Granite (Melanogranite) | K1 (?) | E 137°48′11″; N 49°20′48″ | Unnamed | Central part of the massif; melanocratic | Coarse-grained, porphyritic | Qz 25%, Pl 30%, Kfs 35%, Bt 10% |
| AN-3-11 | Alkali feldspar granite (Leucogranite) | K2 (?) | E 137°37′26″; N 49°20′33″ | Unnamed | Central part of the massif; leucocratic | Fine-grained, equigranular | Qz 45%, Pl 20%, Kfs 30%, Bt 5% |

[a] Mineral name abbreviations (Whitney and Evans, 2010): Qz = quartz, Pl = plagioclase, Kfs = K-feldspar, Hbl = hornblende, Px = pyroxene, Cpx = clino-pyroxene, Bt = biotite, Mag = magnetite, Ilm = ilmenite, Aln = allnite, Zrn = zircon, Ap = apatite.

## 4. Analytical methods

### 4.1. Zircon U–Pb geochoronology and Lu–Hf isotope analysis

Zircon grains were separated from granitic samples using conventional techniques and final purification by hand-picking. They were mounted in epoxy resin bed and half-sectioned after the resin bed had dried. Cathodoluminescence (CL) images were taken at the Beijing SHRIMP Center, Chinese Academy of Geological Sciences, for examination of zircon internal structures and for selection of analytical spots. Zircon U–Pb isotopic analyses were performed using a New Wave UP213 laser ablation system combined with an Agilent 7500s quadrupole ICPMS (inductively coupled plasma mass spectrometer) at the Department of Geosciences, National Taiwan University (NTU-Geosciences). The LA-ICP-MS operating conditions and analytical procedures were the same as those reported in Chiu et al. (2009). Due to the small radiogenic growth of $^{207}Pb$ in the present zircon samples, only the weighted means of pooled $^{206}Pb/^{238}U$ ages are given to represent the ages of the zircon crystallization.

In-situ Hf isotopic analysis of zircon was performed using a multi-collector ICP-MS (Neptune), also at NTU-Geosciences. A New Wave UP193FX laser ablation system was used for spot vaporization. The Hf isotope analysis was done on the same zircon grains that were previously analyzed for U–Pb dating. Ablation time was about 26 s for each measurement with a beam diameter of ca. 40 μm, an 8 Hz repetition rate, and energy of 100 mJ. A detailed description of the analytical techniques can be found in Wu et al. (2006) and Xie et al. (2008). Harvard reference zircon 91500 and Australian Mud Tank carbonatite zircon were used as secondary standards for data quality assessment. During the data acquisition, $^{176}Hf/^{177}Hf$ ratios of 0.282293 ± 22 (2σ, $n = 16$) for Harvard 91500 and 0.282511 ± 25 (2σ, $n = 39$) for the Mud Tank standards were obtained. These values are in good agreement with those obtained by solution and ICP-MS methods reported in the literature (Goolaerts et al., 2004; Woodhead et al., 2004; Woodhead and Hergt, 2005; Griffin et al., 2006; Wu et al., 2006).

### 4.2. Major and trace element analyses

Samples were crushed in a stainless steel jaw crusher and then powdered in an agate mill. Major element contents were determined by X-ray fluorescence (XRF) spectroscopy on fused glass beads, using a Rigaku RIX-2000 spectrometer. For trace elements analysis, about 200 mg of powdered sample was dissolved in a mixture of HF and $HNO_3$ (2:1) in a screw-top Savillex Teflon beaker for 5–7 days at ~100 °C. This was followed by evaporation to dryness, refluxing in 6 N HCl and drying twice, and finally redissolution in 1 N HCl. The procedure was repeated until complete dissolution was achieved. The final solution was split in two parts; a small aliquot (about 10–20%) was used for subsequent trace element analysis by ICP-MS, and the rest for further chemical separation of Sr and Nd for isotopic analysis.

Trace element analysis was performed using an Agilent 7500s at NTU-Geosciences. The standard reference materials used for trace element analyses are AGV-2, BCR-2, BHVO-2, BIR9-1 and DNC-1. The details of analytical procedures may be found in Lin et al. (2012). Analytical errors are 0.5–3% for major elements and 1–10% for trace elements, depending on the concentrations.

### 4.3. Whole-rock Sr–Nd isotopic analyses

For Sr–Nd isotopic analysis, the chemical preparation and mass analysis were performed at Institute of Earth Sciences (IES), Academia Sinica, Taipei. Approximately 150–175 mg of rock powder was

Please cite this article in press as: Jahn, B.-m., et al. Emplacement ages, geochemical and Sr–Nd–Hf isotopic characterization of Mesozoic to early Cenozoic granitoids of the Sikhote-Alin Orogenic Belt, Russian Far East: Crustal growth and regional tectonic evolution. Journal of Asian Earth Sciences (2015), http://dx.doi.org/10.1016/j.jseaes.2015.08.012

dissolved using a HF-$HNO_3$ (2:1) mixture in a screw-top Teflon beaker for 5–7 days at ~100 °C. The same procedure was followed by evaporation to dryness, refluxing in 6 N HCl and drying twice, and then re-dissolution in 1 N HCl. The procedure was repeated until complete dissolution. The sample solution was split into two portions, a small portion (ca. 20%) for trace element analysis and the rest for further chemical separation of Sr and Nd using the conventional ion exchange technique. Sr and rare-earth elements (REEs) were separated in polyethylene columns with a 2.5 ml resin bed of AG 50W-X8, 100–200 mesh. Neodymium was separated from other REEs using 1 ml polyethylene columns packed with Eichrom Ln resin (Ln-B25-A) as a cation exchange medium. Sr and Nd isotope ratios were measured at IES using a Finnigan MAT 262 and a TRITON mass spectrometer, respectively. For the isotope measurement, Sr was loaded on a single Ta filament with H3PO4; whereas Nd was loaded on a Re filament with H3PO4 and measured using a double-Re-filament configuration. The effect of mass fractionation in Sr and Nd isotopic measurements was corrected by normalizing to $^{86}Sr/^{88}Sr = 0.1194$ and $^{146}Nd/^{144}Nd = 0.7219$, respectively. Analyses of NBS-987 Sr and JMC Nd standard throughout the period of data acquisition yielded $^{86}Sr/^{87}Sr = 0.710251 \pm 0.000020$ (2σ external precision) and $^{143}Nd/^{144}Nd = 0.511818 \pm 0.000010$ (2σ external precision). Procedural blanks were ca. 330 pg Sr and 300 pg Nd. Within-run or internal precision, expressed as $2\sigma_m$, was better than 0.000010 for both Sr and Nd. The procedures of chemical separation and mass analysis can be found in Jahn et al. (2009, 2014).

## 5. Analytical results

The results of zircon U–Pb age determination, whole-rock chemical and Sr–Nd isotopic and zircon Hf isotopic analyses are presented in Tables 2, 4 and 5, respectively. A summary of the new zircon age data is given in Table 3.

### 5.1. Zircon U–Pb age data

As a whole, the majority of zircon grains from the granitoids of Sikhote-Alin have a rather simple morphology of magmatic origin. Five representative CL images of zircon from each sample are displayed in Fig. 3a and b. The magmatic zoning and prismatic habit are clearly shown. Round spots of ca. 40 μm diameter are the analytical positions on zircon grains. Uranium concentrations show a large range from <100 to 5600 ppm, but the majority of these are lower than 1000 ppm (Table 2). Th/U ratios are exclusively higher than 0.1, and the majority are between 0.4 and 4.0. Such high ratios suggest that all the zircon grains analyzed have magmatic origin. This is consistent with the information derived from the CL images.

The zircon age data are illustrated in the Concordia plots (Fig. 4A–X). The color code of each data ellipse represents the Th/U ratio of the analyzed spot. In most cases, the data points form a tight cluster, yielding a well-defined $^{206}Pb/^{238}U$ age, which is interpreted as the time of magmatic intrusion. However, in rare cases, the zircon analyses revealed a more complicated thermal or zircon crystallization history. For example, the data of sample B-300 (Fig. 4A), a quartz monzodiorite (formerly mistermed as "diorite") from Oprichnensky, show two clearly defined clusters, yielding an age of 56.3 ± 0.7 Ma and another of 65.6 ± 0.9 Ma (Fig. 4A). Interpretation of the two ages is not straightforward. The CL images indicate that all the zircon crystals are of magmatic origin. An apparent difference between the older (66 Ma) and younger (56 Ma) zircon grains lies in their Th/U ratios. The older crystals have an average ratio of 2.19 (16 grains), whereas the younger ones have a ratio of 1.70 (10 grains). However, this is insufficient to provide a clear explanation why this rock reflects two distinct magmatic ages. Perhaps this rock was initially emplaced at 66 Ma, and some zircon grains lost some radiogenic Pb at 56 Ma when the associated granite (B-301a) intruded. Incidentally, the Hf isotopic compositions, which will be presented and discussed later, do not show any difference between the two zircon groups.

The second rare case is demonstrated by sample 8-11-54/1 (Fig. 4U, V). This is a granite (formerly named as biotite-bearing monzogranite) from the Gorbun locality near the China-Russia international border. The zircon crystals have complicated $^{206}Pb/^{238}U$ ages from 129 to 1316 Ma (Table 2). A partial set of data with a string of quasi-concordant data points yielded ages from 130 to 140 Ma (Fig. 4V). The youngest group of 9 spots defined an age of 131 ± 2 Ma. This is interpreted as the time of intrusion of the Gorbun granite. The older zircon grains with $^{206}Pb/^{238}U$ ages from 150 to 1316 Ma are likely to be inherited zircon crystals. However, the CL images of these older grains cannot be distinguished from those of the 130 Ma crystals (Fig. 3).

The new zircon ages are summarized in Table 3 and displayed in two age maps (Figs. 2 and 5). The age data are arranged for three groups of granitoids. The first group was for samples collected by **G. Valui** from the southeastern coastal areas of Sikhote-Alin. All granitic bodies occur within the Taukha Zone (Cretaceous accretionary complex). The age data indicate that the granitic plutons were emplaced from the Late Cretaceous (83 Ma) to Early Eocene (56 Ma), and they appear to show a younging trend toward the north (Fig. 2).

The second group was collected by **V. Gonevchuk** from several ore districts. Four of these (GV-722, GV-1401, GV-1583-2, GV-1774) are located in or near the Central Sikhote-Alin Fault zone in the Kavalerovo and Malinovka ore districts and intruded the Samarka (Jurassic to Cretaceous accretionary complex) and Zhuravlevka-Amur (Early Cretaceous turbidite basin) terranes of the Primorye Region. Two other samples (ЧG-332 and ЧG-410; also designated in English letters as CHG-332 and CHG-410; Fig. 5) are located in the Komsomolsk ore district (E136°00′, N50°35′) within the Badzhal terrane (analogue of the Samarka terrane) of the Khabarovsk Region (Fig. 5).

The new zircon dating yielded 74.4 ± 0.9 Ma for GV-722 (granite), 102.8 ± 1.7 Ma for GV-1405 (equivalent to GV-1401; monzogranite) from the Kavalerovo ore district, 86.0 ± 0.8 Ma for **GV-1583-2** (granite), and 88.3 ± 0.8 Ma for **GV-1774** (granite) from the Malinovka ore district. The two granitoid samples from the Komsomolsk ore district yielded two identical ages: 92.4 ± 0.8 Ma for ЧG-332 (monzogranite) and 91.5 ± 0.8 Ma for ЧG-410 (granite) (Table 3). Note that the newly obtained zircon ages are quite similar to the published K–Ar ages, suggesting that the plutons were emplaced at shallow levels and cooled rapidly.

The third group of granitoids was collected by **N. Kruk** from three different areas. Two samples (**8-02-1 and 8-881/2**) came from the southernmost part of Primorye (Sergeevka Terrane), and they were emplaced at 68 ± 1 Ma and 93 ± 1 Ma, respectively (Table 3). Two samples (**AH-2-11 and AH-3-11**; also in English letter as **AN-2-11 and AN-3-11**) from the Anyi area (Figs. 2 and 5) yielded two contrasting ages of 108 and 58 Ma (Table 3, Fig. 5). The rest of four samples are from the northern Primorye Region (Fig. 2). Two of these (8-871/1 and 8-872/1) occur close to the Central Fault and have zircon ages of 109 and 106 Ma; whereas the other two (**8-11-54/1 and 8-11-51/3**), from the western part of the Samarka Zone, were dated at 131 and 108 Ma, respectively (Table 3, Fig. 2).

### 5.2. Whole-rock geochemical data

The result of whole-rock chemical analysis is presented in Table 4. The silica contents of the 24 granitoid samples vary from

Please cite this article in press as: Jahn, B.-m., et al. Emplacement ages, geochemical and Sr–Nd–Hf isotopic characterization of Mesozoic to early Cenozoic granitoids of the Sikhote-Alin Orogenic Belt, Russian Far East: Crustal growth and regional tectonic evolution. Journal of Asian Earth Sciences (2015), http://dx.doi.org/10.1016/j.jseaes.2015.08.012

**Table 2**
Zircon U–Th–Pb isotopic data & calculated ages for granitoids from Sikhote-Alin.

| Analysis No. | Th (ppm) | U (ppm) | Th/U | $^{207}Pb/^{206}Pb$ | ±1σ | $^{207}Pb/^{235}U$ | ±1σ | $^{206}Pb/^{238}U$ |
|---|---|---|---|---|---|---|---|---|
| *B-300 wt. mean = 65.6 ± 0.9 Ma (2σ)* | | | | | | | | |
| B-300-01 | 570 | 205 | 2.78 | 0.05106 | 0.00123 | 0.06926 | 0.00301 | 0.00984 |
| B-300-02 | 1291 | 402 | 3.21 | 0.04676 | 0.00077 | 0.06388 | 0.00216 | 0.00991 |
| B-300-03 | 746 | 254 | 2.94 | 0.04523 | 0.00107 | 0.06223 | 0.00266 | 0.00998 |
| B-300-04 | 1215 | 488 | 2.49 | 0.04886 | 0.00070 | 0.06825 | 0.00214 | 0.01013 |
| B-300-05 | 153 | 90 | 1.69 | 0.05202 | 0.00253 | 0.07415 | 0.00525 | 0.01034 |
| B-300-06 | 93 | 611 | 0.15 | 0.04863 | 0.00122 | 0.06740 | 0.00317 | 0.01005 |
| B-300-08 | 153 | 84 | 1.83 | 0.04919 | 0.00311 | 0.07162 | 0.00627 | 0.01056 |
| B-300-10 | 961 | 309 | 3.11 | 0.04697 | 0.00100 | 0.06874 | 0.00283 | 0.01062 |
| B-300-12 | 474 | 204 | 2.32 | 0.04862 | 0.00121 | 0.06774 | 0.00303 | 0.01011 |
| B-300-15 | 283 | 122 | 2.32 | 0.04459 | 0.00202 | 0.06427 | 0.00431 | 0.01046 |
| B-300-18 | 319 | 139 | 2.29 | 0.05061 | 0.00182 | 0.07237 | 0.00411 | 0.01037 |
| B-300-19 | 357 | 254 | 1.41 | 0.04983 | 0.00107 | 0.07211 | 0.00290 | 0.01050 |
| B-300-20 | 128 | 176 | 0.73 | 0.04778 | 0.00226 | 0.06849 | 0.00463 | 0.01040 |
| B-300-21 | 227 | 99 | 2.30 | 0.04564 | 0.00251 | 0.06643 | 0.00515 | 0.01056 |
| B-300-22 | 1443 | 454 | 3.18 | 0.05030 | 0.00085 | 0.07085 | 0.00248 | 0.01022 |
| B-300-23 | 1119 | 487 | 2.30 | 0.04607 | 0.00203 | 0.06493 | 0.00380 | 0.01022 |
| =56.3 ± 0.7 Ma (2σ) | | | | | | | | |
| B-300-07 | 1136 | 395 | 2.88 | 0.05121 | 0.00089 | 0.06115 | 0.00213 | 0.00866 |
| B-300-072 | 557 | 273 | 2.04 | 0.04607 | 0.00138 | 0.05496 | 0.00249 | 0.00865 |
| B-300-09 | 312 | 189 | 1.65 | 0.05164 | 0.00158 | 0.06249 | 0.00319 | 0.00878 |
| B-300-112 | 311 | 170 | 1.83 | 0.04923 | 0.00352 | 0.06155 | 0.00564 | 0.00907 |
| B-300-13 | 162 | 113 | 1.44 | 0.05174 | 0.00257 | 0.06210 | 0.00448 | 0.00871 |
| B-300-14 | 261 | 194 | 1.35 | 0.04353 | 0.00210 | 0.05384 | 0.00387 | 0.00897 |
| B-300-16 | 396 | 217 | 1.82 | 0.04607 | 0.00251 | 0.05559 | 0.00390 | 0.00875 |
| B-300-17 | 145 | 126 | 1.15 | 0.05127 | 0.00389 | 0.06168 | 0.00607 | 0.00872 |
| B-300-24 | 272 | 202 | 1.35 | 0.04641 | 0.00290 | 0.05650 | 0.00448 | 0.00883 |
| B-300-25 | 400 | 274 | 1.46 | 0.04682 | 0.00122 | 0.05500 | 0.00252 | 0.00852 |
| *B-301a wt. mean = 57.1 ± 0.4 Ma (2σ)* | | | | | | | | |
| B301A-01 | 312 | 196 | 1.59 | 0.04978 | 0.00082 | 0.06093 | 0.00204 | 0.00888 |
| B301A-02 | 104 | 82 | 1.27 | 0.04536 | 0.00172 | 0.05626 | 0.00324 | 0.00900 |
| B301A-03 | 300 | 176 | 1.71 | 0.04863 | 0.00092 | 0.05984 | 0.00218 | 0.00893 |
| B301A-04 | 341 | 189 | 1.81 | 0.04786 | 0.00169 | 0.05931 | 0.00345 | 0.00899 |
| B301A-05 | 204 | 115 | 1.77 | 0.04571 | 0.00128 | 0.05594 | 0.00265 | 0.00888 |
| B301A-06 | 265 | 184 | 1.44 | 0.04937 | 0.00086 | 0.06030 | 0.00209 | 0.00886 |
| B301A-07 | 234 | 179 | 1.31 | 0.04759 | 0.00088 | 0.05825 | 0.00210 | 0.00888 |
| B301A-08 | 402 | 223 | 1.80 | 0.05196 | 0.00082 | 0.06276 | 0.00206 | 0.00876 |
| B301A-09 | 199 | 138 | 1.44 | 0.05084 | 0.00366 | 0.06273 | 0.00568 | 0.00895 |
| B301A-11 | 227 | 141 | 1.61 | 0.04321 | 0.00116 | 0.05310 | 0.00244 | 0.00891 |
| B301A-12 | 256 | 189 | 1.35 | 0.04656 | 0.00089 | 0.05683 | 0.00208 | 0.00885 |
| B301A-13 | 70 | 101 | 0.70 | 0.04974 | 0.00151 | 0.06095 | 0.00304 | 0.00889 |
| B301A-15 | 209 | 127 | 1.65 | 0.05159 | 0.00129 | 0.06255 | 0.00277 | 0.00879 |
| B301A-16 | 93 | 109 | 0.86 | 0.04565 | 0.00142 | 0.05572 | 0.00282 | 0.00885 |
| B301A-17 | 738 | 313 | 2.36 | 0.04686 | 0.00068 | 0.05864 | 0.00184 | 0.00908 |
| B301A-18 | 112 | 84 | 1.33 | 0.04553 | 0.00205 | 0.05650 | 0.00371 | 0.00900 |
| B301A-19 | 201 | 137 | 1.47 | 0.04529 | 0.00115 | 0.05467 | 0.00244 | 0.00876 |
| B301A-20 | 187 | 162 | 1.15 | 0.04454 | 0.00100 | 0.05484 | 0.00225 | 0.00893 |
| B301A-21 | 147 | 92 | 1.59 | 0.04841 | 0.00178 | 0.05877 | 0.00344 | 0.00880 |
| B301A-22 | 487 | 264 | 1.84 | 0.04403 | 0.00077 | 0.05444 | 0.00192 | 0.00897 |
| B301A-23 | 178 | 126 | 1.42 | 0.04572 | 0.00140 | 0.05707 | 0.00293 | 0.00905 |
| B301A-24 | 96 | 62 | 1.53 | 0.04734 | 0.00253 | 0.05795 | 0.00443 | 0.00888 |

| ±1σ | $^{208}Pb/^{232}Th$ | ±1σ | $^{207}Pb/^{206}Pb$ | ±1σ | $^{207}Pb/^{235}U$ | ±1σ | $^{206}Pb/^{238}U$ | ±1σ | $^{208}Pb/^{232}Th$ | ±1σ |
|---|---|---|---|---|---|---|---|---|---|---|
| 0.00024 | 0.00325 | 0.00010 | 244 | 56 | 68 | 3 | 63 | 2 | 66 | 2 |
| 0.00023 | 0.00321 | 0.00010 | 37 | 37 | 63 | 2 | 64 | 1 | 65 | 2 |
| 0.00024 | 0.00330 | 0.00011 | −8 | 44 | 61 | 3 | 64 | 2 | 67 | 2 |
| 0.00024 | 0.00332 | 0.00011 | 141 | 34 | 67 | 2 | 65 | 2 | 67 | 2 |
| 0.00027 | 0.00333 | 0.00013 | 286 | 111 | 73 | 5 | 66 | 2 | 67 | 3 |
| 0.00028 | 0.00320 | 0.00024 | 130 | 59 | 66 | 3 | 64 | 2 | 65 | 5 |
| 0.00030 | 0.00328 | 0.00015 | 157 | 144 | 70 | 6 | 68 | 2 | 66 | 3 |
| 0.00027 | 0.00325 | 0.00012 | 48 | 47 | 68 | 3 | 68 | 2 | 66 | 2 |
| 0.00025 | 0.00336 | 0.00013 | 130 | 59 | 67 | 3 | 65 | 2 | 68 | 3 |
| 0.00027 | 0.00349 | 0.00012 | −40 | 94 | 63 | 4 | 67 | 2 | 70 | 2 |
| 0.00026 | 0.00338 | 0.00012 | 223 | 84 | 71 | 4 | 67 | 2 | 68 | 2 |
| 0.00025 | 0.00349 | 0.00012 | 187 | 49 | 71 | 3 | 67 | 2 | 70 | 2 |
| 0.00027 | 0.00330 | 0.00011 | 88 | 104 | 67 | 4 | 67 | 2 | 67 | 2 |
| 0.00028 | 0.00338 | 0.00014 | −21 | 117 | 65 | 5 | 68 | 2 | 68 | 3 |
| 0.00025 | 0.00338 | 0.00013 | 209 | 39 | 70 | 2 | 66 | 2 | 68 | 3 |
| 0.00024 | 0.00336 | 0.00011 | 1 | 92 | 64 | 4 | 66 | 2 | 68 | 2 |
| 0.00020 | 0.00286 | 0.00010 | 250 | 40 | 60 | 2 | 56 | 1 | 58 | 2 |
| 0.00020 | 0.00286 | 0.00008 | 1 | 61 | 54 | 2 | 56 | 1 | 58 | 2 |
| 0.00022 | 0.00291 | 0.00011 | 270 | 70 | 62 | 3 | 56 | 1 | 59 | 2 |
| 0.00023 | 0.00287 | 0.00006 | 159 | 157 | 61 | 5 | 58 | 1 | 58 | 1 |
| 0.00023 | 0.00301 | 0.00012 | 274 | 114 | 61 | 4 | 56 | 1 | 61 | 2 |
| 0.00025 | 0.00290 | 0.00012 | −95 | 101 | 53 | 4 | 58 | 2 | 59 | 2 |
| 0.00023 | 0.00295 | 0.00015 | 1 | 118 | 55 | 4 | 56 | 1 | 60 | 3 |
| 0.00024 | 0.00275 | 0.00006 | 253 | 171 | 61 | 6 | 56 | 2 | 55 | 1 |
| 0.00022 | 0.00281 | 0.00011 | 19 | 133 | 56 | 4 | 57 | 1 | 57 | 2 |
| 0.00021 | 0.00278 | 0.00010 | 40 | 56 | 54 | 2 | 55 | 1 | 56 | 2 |
| 0.00020 | 0.00289 | 0.00007 | 185 | 39 | 60 | 2 | 57 | 1 | 58 | 1 |
| 0.00021 | 0.00286 | 0.00008 | −1 | 79 | 56 | 3 | 58 | 1 | 58 | 2 |
| 0.00020 | 0.00294 | 0.00007 | 130 | 46 | 59 | 2 | 57 | 1 | 59 | 1 |
| 0.00025 | 0.00243 | 0.00008 | 92 | 77 | 59 | 3 | 58 | 2 | 49 | 2 |
| 0.00021 | 0.00291 | 0.00008 | −17 | 53 | 55 | 3 | 57 | 1 | 59 | 2 |
| 0.00020 | 0.00287 | 0.00007 | 165 | 43 | 59 | 2 | 57 | 1 | 58 | 1 |
| 0.00020 | 0.00284 | 0.00008 | 79 | 40 | 57 | 2 | 57 | 1 | 57 | 2 |
| 0.00020 | 0.00282 | 0.00007 | 284 | 36 | 62 | 2 | 56 | 1 | 57 | 1 |
| 0.00022 | 0.00282 | 0.00005 | 234 | 159 | 62 | 5 | 57 | 1 | 57 | 1 |
| 0.00021 | 0.00310 | 0.00009 | −112 | 64 | 53 | 2 | 57 | 1 | 63 | 2 |
| 0.00020 | 0.00295 | 0.00009 | 27 | 38 | 56 | 2 | 57 | 1 | 60 | 2 |
| 0.00021 | 0.00318 | 0.00011 | 183 | 74 | 60 | 3 | 57 | 1 | 64 | 2 |
| 0.00021 | 0.00338 | 0.00009 | 267 | 60 | 62 | 3 | 56 | 1 | 68 | 2 |
| 0.00021 | 0.00310 | 0.00010 | −20 | 60 | 55 | 3 | 57 | 1 | 63 | 2 |
| 0.00021 | 0.00307 | 0.00008 | 42 | 35 | 58 | 2 | 58 | 1 | 62 | 2 |
| 0.00022 | 0.00337 | 0.00012 | −27 | 92 | 56 | 4 | 58 | 1 | 68 | 2 |
| 0.00021 | 0.00291 | 0.00008 | −5 | 54 | 54 | 2 | 56 | 1 | 59 | 2 |
| 0.00021 | 0.00290 | 0.00008 | −43 | 50 | 54 | 2 | 57 | 1 | 59 | 2 |
| 0.00023 | 0.00308 | 0.00010 | 119 | 78 | 58 | 3 | 56 | 1 | 62 | 2 |
| 0.00021 | 0.00289 | 0.00008 | −69 | 40 | 54 | 2 | 58 | 1 | 58 | 2 |
| 0.00023 | 0.00294 | 0.00010 | −17 | 59 | 56 | 3 | 58 | 1 | 59 | 2 |
| 0.00024 | 0.00288 | 0.00010 | 66 | 109 | 57 | 4 | 57 | 2 | 58 | 2 |

(*continued on next page*)

**Table 2** (*continued*)

| Analysis No. | Th (ppm) | U (ppm) | Th/U | $^{207}Pb/^{206}Pb$ | ±1σ | $^{207}Pb/^{235}U$ | ±1σ | $^{206}Pb/^{238}U$ | ±1σ | $^{208}Pb/^{232}Th$ | ±1σ | $^{207}Pb/^{206}Pb$ | ±1σ | $^{207}Pb/^{235}U$ | ±1σ | $^{206}Pb/^{238}U$ | ±1σ | $^{208}Pb/^{232}Th$ | ±1σ |
|---|---|---|---|---|---|---|---|---|---|---|---|---|---|---|---|---|---|---|---|
| *B-448 wt. mean = 64.0 ± 0.7 Ma (2σ)* | | | | | | | | | | | | | | | | | | | |
| B448-01 | 177 | 152 | 1.17 | 0.04248 | 0.00108 | 0.05717 | 0.00258 | 0.00976 | 0.00024 | 0.00326 | 0.00009 | −151 | 56 | 56 | 2 | 63 | 2 | 66 | 2 |
| B448-02 | 58 | 44 | 1.31 | 0.04183 | 0.00365 | 0.05709 | 0.00638 | 0.00990 | 0.00028 | 0.00341 | 0.00014 | −186 | 163 | 56 | 6 | 64 | 2 | 69 | 3 |
| B448-03 | 103 | 57 | 1.82 | 0.04514 | 0.00271 | 0.06267 | 0.00520 | 0.01007 | 0.00027 | 0.00358 | 0.00012 | −12 | 135 | 62 | 5 | 65 | 2 | 72 | 2 |
| B448-05 | 77 | 55 | 1.40 | 0.05109 | 0.00464 | 0.07105 | 0.00807 | 0.01009 | 0.00029 | 0.00318 | 0.00007 | 245 | 195 | 70 | 8 | 65 | 2 | 64 | 1 |
| B448-06 | 116 | 66 | 1.76 | 0.04394 | 0.00227 | 0.06095 | 0.00449 | 0.01006 | 0.00026 | 0.00365 | 0.00012 | −74 | 110 | 60 | 4 | 65 | 2 | 74 | 2 |
| B448-07 | 286 | 235 | 1.22 | 0.05344 | 0.00081 | 0.07541 | 0.00244 | 0.01024 | 0.00024 | 0.00374 | 0.00010 | 348 | 33 | 74 | 2 | 66 | 2 | 75 | 2 |
| B448-08 | 1197 | 980 | 1.22 | 0.04608 | 0.00104 | 0.06142 | 0.00243 | 0.00967 | 0.00023 | 0.00314 | 0.00009 | 2 | 44 | 61 | 2 | 62 | 1 | 63 | 2 |
| B448-09 | 96 | 75 | 1.28 | 0.04516 | 0.00195 | 0.06243 | 0.00406 | 0.01003 | 0.00026 | 0.00331 | 0.00011 | −11 | 87 | 61 | 4 | 64 | 2 | 67 | 2 |
| B448-10 | 82 | 51 | 1.62 | 0.04607 | 0.00231 | 0.06205 | 0.00438 | 0.00977 | 0.00028 | 0.00332 | 0.00016 | 1 | 106 | 61 | 4 | 63 | 2 | 67 | 3 |
| B448-11 | 247 | 186 | 1.33 | 0.04444 | 0.00091 | 0.06407 | 0.00255 | 0.01046 | 0.00026 | 0.00304 | 0.00009 | −48 | 41 | 63 | 2 | 67 | 2 | 61 | 2 |
| B448-12 | 128 | 78 | 1.63 | 0.04654 | 0.00183 | 0.06554 | 0.00398 | 0.01022 | 0.00026 | 0.00357 | 0.00012 | 26 | 86 | 64 | 4 | 66 | 2 | 72 | 2 |
| B448-13 | 123 | 73 | 1.67 | 0.03230 | 0.00221 | 0.04495 | 0.00407 | 0.01009 | 0.00026 | 0.00327 | 0.00010 | −185 | 97 | 45 | 4 | 65 | 2 | 66 | 2 |
| B448-14 | 79 | 39 | 2.04 | 0.03831 | 0.00426 | 0.05212 | 0.00714 | 0.00987 | 0.00029 | 0.00336 | 0.00012 | −390 | 229 | 52 | 7 | 63 | 2 | 68 | 2 |
| B448-15 | 143 | 93 | 1.54 | 0.04917 | 0.00335 | 0.06675 | 0.00625 | 0.00985 | 0.00030 | 0.00311 | 0.00008 | 156 | 150 | 66 | 6 | 63 | 2 | 63 | 2 |
| B448-16 | 511 | 470 | 1.09 | 0.04726 | 0.00060 | 0.06387 | 0.00184 | 0.00980 | 0.00023 | 0.00353 | 0.00010 | 62 | 32 | 63 | 2 | 63 | 1 | 71 | 2 |
| B448-17 | 80 | 44 | 1.81 | 0.05124 | 0.00317 | 0.07122 | 0.00610 | 0.01008 | 0.00028 | 0.00354 | 0.00012 | 252 | 146 | 70 | 6 | 65 | 2 | 71 | 2 |
| B448-18 | 178 | 113 | 1.58 | 0.04887 | 0.00141 | 0.06766 | 0.00332 | 0.01004 | 0.00025 | 0.00355 | 0.00011 | 142 | 67 | 66 | 3 | 64 | 2 | 72 | 2 |
| B448-19 | 122 | 70 | 1.75 | 0.03811 | 0.00235 | 0.05301 | 0.00444 | 0.01009 | 0.00026 | 0.00332 | 0.00012 | −403 | 224 | 52 | 4 | 65 | 2 | 67 | 2 |
| B448-20 | 168 | 98 | 1.72 | 0.04320 | 0.00179 | 0.05993 | 0.00378 | 0.01006 | 0.00026 | 0.00343 | 0.00012 | −112 | 87 | 59 | 4 | 65 | 2 | 69 | 2 |
| B448-21 | 237 | 129 | 1.84 | 0.04421 | 0.00154 | 0.05976 | 0.00334 | 0.00980 | 0.00025 | 0.00356 | 0.00012 | −60 | 75 | 59 | 3 | 63 | 2 | 72 | 2 |
| B448-22 | 188 | 111 | 1.70 | 0.04761 | 0.00158 | 0.06684 | 0.00362 | 0.01018 | 0.00026 | 0.00347 | 0.00012 | 80 | 72 | 66 | 3 | 65 | 2 | 70 | 2 |
| B448-23 | 70 | 39 | 1.81 | 0.04469 | 0.00444 | 0.06209 | 0.00783 | 0.01008 | 0.00031 | 0.00366 | 0.00015 | −35 | 186 | 61 | 7 | 65 | 2 | 74 | 3 |
| B448-24 | 220 | 105 | 2.09 | 0.03980 | 0.00179 | 0.05597 | 0.00377 | 0.01020 | 0.00027 | 0.00343 | 0.00012 | −301 | 111 | 55 | 4 | 65 | 2 | 69 | 2 |
| *B-456 wt. mean (one old core excepted) = 70.5 ± 0.9 Ma (2σ)* | | | | | | | | | | | | | | | | | | | |
| B-456-01 | 259 | 180 | 1.44 | 0.05333 | 0.00137 | 0.08358 | 0.00381 | 0.01137 | 0.00028 | 0.00420 | 0.00015 | 343 | 57 | 82 | 4 | 73 | 2 | 85 | 3 |
| B-456-02 | 226 | 183 | 1.24 | 0.04904 | 0.00284 | 0.07460 | 0.00586 | 0.01103 | 0.00029 | 0.00349 | 0.00008 | 150 | 131 | 73 | 6 | 71 | 2 | 70 | 2 |
| B-456-03 | 240 | 164 | 1.47 | 0.04495 | 0.00153 | 0.06798 | 0.00370 | 0.01097 | 0.00027 | 0.00375 | 0.00014 | −22 | 68 | 67 | 4 | 70 | 2 | 76 | 3 |
| B-456-04 | 446 | 633 | 0.70 | 0.04821 | 0.00071 | 0.07221 | 0.00230 | 0.01086 | 0.00026 | 0.00364 | 0.00014 | 110 | 35 | 71 | 2 | 70 | 2 | 73 | 3 |
| B-456-06 | 189 | 146 | 1.30 | 0.04916 | 0.00174 | 0.07535 | 0.00425 | 0.01112 | 0.00028 | 0.00367 | 0.00015 | 155 | 83 | 74 | 4 | 71 | 2 | 74 | 3 |
| B-456-07 | 376 | 187 | 2.01 | 0.05113 | 0.00128 | 0.07853 | 0.00354 | 0.01114 | 0.00028 | 0.00348 | 0.00012 | 247 | 59 | 77 | 3 | 71 | 2 | 70 | 2 |
| B-456-08 | 289 | 274 | 1.05 | 0.04871 | 0.00106 | 0.07512 | 0.00307 | 0.01118 | 0.00027 | 0.00368 | 0.00015 | 134 | 52 | 74 | 3 | 72 | 2 | 74 | 3 |
| B-456-09 | 480 | 565 | 0.85 | 0.04971 | 0.00069 | 0.07547 | 0.00231 | 0.01101 | 0.00026 | 0.00343 | 0.00013 | 181 | 33 | 74 | 2 | 71 | 2 | 69 | 3 |
| B-456-092 | 336 | 261 | 1.29 | 0.04767 | 0.00095 | 0.06979 | 0.00263 | 0.01062 | 0.00024 | 0.00364 | 0.00012 | 83 | 47 | 69 | 2 | 68 | 2 | 73 | 2 |
| B-456-11 | 300 | 95 | 3.15 | 0.05685 | 0.00402 | 0.08436 | 0.00831 | 0.01076 | 0.00035 | 0.00311 | 0.00016 | 486 | 157 | 82 | 8 | 69 | 2 | 63 | 3 |
| B-456-12 | 582 | 214 | 2.72 | 0.04684 | 0.00447 | 0.07225 | 0.00832 | 0.01119 | 0.00031 | 0.00356 | 0.00010 | 41 | 198 | 71 | 8 | 72 | 2 | 72 | 2 |
| B-456-13 | 289 | 217 | 1.33 | 0.04922 | 0.00123 | 0.07265 | 0.00324 | 0.01071 | 0.00026 | 0.00329 | 0.00011 | 158 | 59 | 71 | 3 | 69 | 2 | 66 | 2 |
| B-456-14 | 430 | 587 | 0.73 | 0.04729 | 0.00066 | 0.07144 | 0.00220 | 0.01096 | 0.00026 | 0.00350 | 0.00012 | 64 | 33 | 70 | 2 | 70 | 2 | 71 | 2 |
| B-456-15 | 160 | 128 | 1.25 | 0.04607 | 0.00116 | 0.06778 | 0.00281 | 0.01067 | 0.00026 | 0.00366 | 0.00018 | 1 | 49 | 67 | 3 | 68 | 2 | 74 | 4 |
| B-456-17 | 288 | 197 | 1.46 | 0.05462 | 0.00227 | 0.08301 | 0.00546 | 0.01103 | 0.00032 | 0.00326 | 0.00016 | 397 | 92 | 81 | 5 | 71 | 2 | 66 | 3 |
| B-456-18 | 332 | 214 | 1.55 | 0.05031 | 0.00126 | 0.07588 | 0.00340 | 0.01094 | 0.00027 | 0.00353 | 0.00013 | 209 | 59 | 74 | 3 | 70 | 2 | 71 | 3 |
| B-456-19 | 307 | 136 | 2.26 | 0.04851 | 0.00190 | 0.07366 | 0.00445 | 0.01101 | 0.00028 | 0.00363 | 0.00014 | 124 | 90 | 72 | 4 | 71 | 2 | 73 | 3 |
| B-456-192 | 191 | 105 | 1.82 | 0.04663 | 0.00345 | 0.06871 | 0.00630 | 0.01069 | 0.00027 | 0.00340 | 0.00011 | 30 | 156 | 67 | 6 | 69 | 2 | 69 | 2 |
| B-456-20 | 361 | 250 | 1.44 | 0.04987 | 0.00107 | 0.07779 | 0.00313 | 0.01131 | 0.00027 | 0.00364 | 0.00014 | 189 | 49 | 76 | 3 | 72 | 2 | 73 | 3 |
| B-456-21 | 864 | 364 | 2.37 | 0.04672 | 0.00085 | 0.07090 | 0.00257 | 0.01101 | 0.00026 | 0.00347 | 0.00013 | 35 | 40 | 70 | 2 | 71 | 2 | 70 | 3 |
| B-456-23 | 249 | 158 | 1.57 | 0.05331 | 0.00161 | 0.08117 | 0.00413 | 0.01104 | 0.00028 | 0.00360 | 0.00015 | 342 | 68 | 79 | 4 | 71 | 2 | 73 | 3 |
| B-456-16 (Core) | 717 | 681 | 1.05 | 0.04844 | 0.00062 | 0.09095 | 0.00261 | 0.01362 | 0.00032 | 0.00447 | 0.00015 | 121 | 30 | 88 | 2 | 87 | 2 | 90 | 3 |
| *B-719 wt. mean = 70.7 ± 0.8 Ma (2σ)* | | | | | | | | | | | | | | | | | | | |
| B-719-01 | 251 | 210 | 1.19 | 0.04676 | 0.00083 | 0.06952 | 0.00246 | 0.01078 | 0.00025 | 0.00343 | 0.00010 | 37 | 40 | 68 | 2 | 69 | 2 | 69 | 2 |
| B-719-02 | 310 | 260 | 1.19 | 0.04710 | 0.00073 | 0.07231 | 0.00233 | 0.01114 | 0.00025 | 0.00361 | 0.00010 | 54 | 37 | 71 | 2 | 71 | 2 | 73 | 2 |
| B-719-03 | 388 | 256 | 1.52 | 0.04769 | 0.00242 | 0.07194 | 0.00495 | 0.01094 | 0.00027 | 0.00347 | 0.00007 | 84 | 110 | 71 | 5 | 70 | 2 | 70 | 1 |
| B-719-04 | 279 | 201 | 1.39 | 0.04583 | 0.00084 | 0.06957 | 0.00250 | 0.01101 | 0.00025 | 0.00352 | 0.00010 | −11 | 34 | 68 | 2 | 71 | 2 | 71 | 2 |

Please cite this article in press as: Jahn, B.-m., et al. Emplacement ages, geochemical and Sr–Nd–Hf isotopic characterization of Mesozoic to early Cenozoic granitoids of the Sikhote-Alin Orogenic Belt, Russian Far East: Crustal growth and regional tectonic evolution. Journal of Asian Earth Sciences (2015), http://dx.doi.org/10.1016/j.jseaes.2015.08.012

**Table 2** (*continued*)

| Analysis No. | Th (ppm) | U (ppm) | Th/U | $^{207}Pb/^{206}Pb$ | ±1σ | $^{207}Pb/^{235}U$ | ±1σ | $^{206}Pb/^{238}U$ | ±1σ | $^{208}Pb/^{232}Th$ | ±1σ | $^{207}Pb/^{206}Pb$ | ±1σ | $^{207}Pb/^{235}U$ | ±1σ | $^{206}Pb/^{238}U$ | ±1σ | $^{208}Pb/^{232}Th$ | ±1σ |
|---|---|---|---|---|---|---|---|---|---|---|---|---|---|---|---|---|---|---|---|
| B-719-05 | 156 | 153 | 1.03 | 0.04683 | 0.00102 | 0.07030 | 0.00285 | 0.01089 | 0.00026 | 0.00345 | 0.00011 | 41 | 47 | 69 | 3 | 70 | 2 | 70 | 2 |
| B-719-06 | 228 | 220 | 1.04 | 0.04607 | 0.00112 | 0.07001 | 0.00285 | 0.01102 | 0.00026 | 0.00362 | 0.00011 | 1 | 47 | 69 | 3 | 71 | 2 | 73 | 2 |
| B-719-07 | 345 | 283 | 1.22 | 0.04563 | 0.00073 | 0.06972 | 0.00233 | 0.01108 | 0.00026 | 0.00342 | 0.00011 | −22 | 29 | 68 | 2 | 71 | 2 | 69 | 2 |
| B-719-08 | 190 | 129 | 1.47 | 0.04536 | 0.00122 | 0.06777 | 0.00314 | 0.01084 | 0.00026 | 0.00360 | 0.00012 | −1 | 54 | 67 | 3 | 70 | 2 | 73 | 2 |
| B-719-09 | 838 | 426 | 1.97 | 0.05240 | 0.00064 | 0.08060 | 0.00224 | 0.01116 | 0.00026 | 0.00359 | 0.00011 | 303 | 28 | 79 | 2 | 72 | 2 | 72 | 2 |
| B-719-10 | 320 | 271 | 1.18 | 0.04953 | 0.00077 | 0.07501 | 0.00248 | 0.01098 | 0.00026 | 0.00345 | 0.00012 | 173 | 37 | 73 | 2 | 70 | 2 | 70 | 2 |
| B-719-11 | 294 | 168 | 1.75 | 0.04687 | 0.00100 | 0.07084 | 0.00283 | 0.01096 | 0.00026 | 0.00361 | 0.00013 | 43 | 46 | 69 | 3 | 70 | 2 | 73 | 3 |
| B-719-12 | 211 | 159 | 1.33 | 0.04895 | 0.00106 | 0.07386 | 0.00299 | 0.01095 | 0.00026 | 0.00367 | 0.00013 | 145 | 52 | 72 | 3 | 70 | 2 | 74 | 3 |
| B-719-14 | 261 | 213 | 1.23 | 0.04846 | 0.00114 | 0.07377 | 0.00321 | 0.01104 | 0.00028 | 0.00339 | 0.00011 | 122 | 55 | 72 | 3 | 71 | 2 | 68 | 2 |
| B-719-15 | 477 | 660 | 0.72 | 0.04732 | 0.00057 | 0.07062 | 0.00194 | 0.01083 | 0.00025 | 0.00352 | 0.00010 | 65 | 29 | 69 | 2 | 69 | 2 | 71 | 2 |
| B-719-16 | 408 | 299 | 1.36 | 0.04921 | 0.00087 | 0.07578 | 0.00273 | 0.01117 | 0.00027 | 0.00361 | 0.00012 | 158 | 42 | 74 | 3 | 72 | 2 | 73 | 2 |
| B-719-17 | 363 | 299 | 1.21 | 0.04701 | 0.00104 | 0.07245 | 0.00303 | 0.01118 | 0.00028 | 0.00348 | 0.00013 | 50 | 49 | 71 | 3 | 72 | 2 | 70 | 3 |
| B-719-18 | 199 | 152 | 1.31 | 0.05196 | 0.00120 | 0.07884 | 0.00336 | 0.01101 | 0.00027 | 0.00346 | 0.00012 | 284 | 54 | 77 | 3 | 71 | 2 | 70 | 2 |
| B-719-19 | 169 | 157 | 1.08 | 0.04539 | 0.00119 | 0.06902 | 0.00317 | 0.01103 | 0.00027 | 0.00361 | 0.00013 | −34 | 51 | 68 | 3 | 71 | 2 | 73 | 3 |
| B-719-20 | 315 | 346 | 0.91 | 0.04807 | 0.00091 | 0.07386 | 0.00281 | 0.01114 | 0.00028 | 0.00359 | 0.00014 | 103 | 45 | 72 | 3 | 71 | 2 | 72 | 3 |
| B-719-21 | 496 | 344 | 1.44 | 0.04652 | 0.00071 | 0.07130 | 0.00231 | 0.01112 | 0.00026 | 0.00356 | 0.00012 | 25 | 33 | 70 | 2 | 71 | 2 | 72 | 2 |
| B-719-22 | 289 | 245 | 1.18 | 0.04646 | 0.00085 | 0.07016 | 0.00255 | 0.01095 | 0.00026 | 0.00351 | 0.00012 | 22 | 39 | 69 | 2 | 70 | 2 | 71 | 2 |
| B-719-23 | 138 | 109 | 1.27 | 0.04923 | 0.00169 | 0.07630 | 0.00420 | 0.01124 | 0.00028 | 0.00367 | 0.00014 | 159 | 79 | 75 | 4 | 72 | 2 | 74 | 3 |
| B-719-24 | 299 | 273 | 1.10 | 0.04668 | 0.00080 | 0.07072 | 0.00248 | 0.01099 | 0.00026 | 0.00337 | 0.00012 | 33 | 38 | 69 | 2 | 70 | 2 | 68 | 2 |
| *B-574 wt. mean = 82.7 ± 0.8 Ma (2σ)* | | | | | | | | | | | | | | | | | | | |
| B574-01 | 135 | 90 | 1.50 | 0.05592 | 0.00152 | 0.09956 | 0.00475 | 0.01291 | 0.00033 | 0.00519 | 0.00016 | 449 | 62 | 96 | 4 | 83 | 2 | 105 | 3 |
| B574-02 | 103 | 84 | 1.22 | 0.04836 | 0.00150 | 0.08932 | 0.00458 | 0.01340 | 0.00033 | 0.00452 | 0.00015 | 117 | 70 | 87 | 4 | 86 | 2 | 91 | 3 |
| B574-03 | 112 | 97 | 1.15 | 0.05672 | 0.00135 | 0.10167 | 0.00442 | 0.01300 | 0.00032 | 0.00520 | 0.00016 | 481 | 53 | 98 | 4 | 83 | 2 | 105 | 3 |
| B574-04 | 218 | 144 | 1.51 | 0.04561 | 0.00098 | 0.07914 | 0.00318 | 0.01258 | 0.00030 | 0.00435 | 0.00013 | −23 | 40 | 77 | 3 | 81 | 2 | 88 | 3 |
| B574-05 | 172 | 119 | 1.45 | 0.04773 | 0.00146 | 0.08667 | 0.00452 | 0.01317 | 0.00035 | 0.00469 | 0.00016 | 86 | 64 | 84 | 4 | 84 | 2 | 95 | 3 |
| B574-06 | 97 | 90 | 1.07 | 0.04886 | 0.00137 | 0.08583 | 0.00415 | 0.01274 | 0.00032 | 0.00451 | 0.00014 | 141 | 68 | 84 | 4 | 82 | 2 | 91 | 3 |
| B574-07 | 170 | 108 | 1.57 | 0.04821 | 0.00121 | 0.08728 | 0.00390 | 0.01313 | 0.00032 | 0.00449 | 0.00014 | 110 | 53 | 85 | 4 | 84 | 2 | 91 | 3 |
| B574-08 | 206 | 146 | 1.41 | 0.05782 | 0.00176 | 0.10629 | 0.00574 | 0.01333 | 0.00039 | 0.00447 | 0.00018 | 523 | 60 | 103 | 5 | 85 | 2 | 90 | 4 |
| B574-10 | 127 | 80 | 1.60 | 0.06273 | 0.00210 | 0.11398 | 0.00630 | 0.01318 | 0.00035 | 0.00533 | 0.00022 | 699 | 76 | 110 | 6 | 84 | 2 | 107 | 4 |
| B574-11 | 160 | 106 | 1.51 | 0.04530 | 0.00120 | 0.08069 | 0.00376 | 0.01292 | 0.00032 | 0.00451 | 0.00015 | −4 | 50 | 79 | 4 | 83 | 2 | 91 | 3 |
| B574-12 | 159 | 107 | 1.48 | 0.04695 | 0.00116 | 0.08394 | 0.00374 | 0.01297 | 0.00032 | 0.00448 | 0.00015 | 47 | 50 | 82 | 4 | 83 | 2 | 90 | 3 |
| B574-13 | 172 | 113 | 1.52 | 0.04842 | 0.00120 | 0.08552 | 0.00379 | 0.01281 | 0.00031 | 0.00428 | 0.00013 | 120 | 63 | 83 | 4 | 82 | 2 | 86 | 3 |
| B574-14 | 113 | 92 | 1.23 | 0.04277 | 0.00138 | 0.07660 | 0.00402 | 0.01299 | 0.00032 | 0.00447 | 0.00014 | −135 | 73 | 75 | 4 | 83 | 2 | 90 | 3 |
| B574-15 | 197 | 129 | 1.53 | 0.04740 | 0.00107 | 0.08250 | 0.00347 | 0.01262 | 0.00031 | 0.00447 | 0.00013 | 69 | 49 | 80 | 3 | 81 | 2 | 90 | 3 |
| B574-16 | 177 | 137 | 1.29 | 0.04927 | 0.00108 | 0.08804 | 0.00368 | 0.01296 | 0.00033 | 0.00448 | 0.00014 | 161 | 51 | 86 | 3 | 83 | 2 | 90 | 3 |
| B574-17 | 140 | 97 | 1.45 | 0.04759 | 0.00132 | 0.08379 | 0.00403 | 0.01277 | 0.00032 | 0.00432 | 0.00013 | 79 | 66 | 82 | 4 | 82 | 2 | 87 | 3 |
| B574-18 | 188 | 121 | 1.56 | 0.04992 | 0.00109 | 0.08689 | 0.00358 | 0.01262 | 0.00031 | 0.00435 | 0.00013 | 191 | 54 | 85 | 3 | 81 | 2 | 88 | 3 |
| B574-19 | 162 | 104 | 1.55 | 0.04913 | 0.00124 | 0.08634 | 0.00392 | 0.01275 | 0.00032 | 0.00435 | 0.00014 | 154 | 61 | 84 | 4 | 82 | 2 | 88 | 3 |
| B574-20 | 156 | 114 | 1.37 | 0.04391 | 0.00113 | 0.07812 | 0.00357 | 0.01291 | 0.00032 | 0.00439 | 0.00014 | −75 | 56 | 76 | 3 | 83 | 2 | 89 | 3 |
| B574-21 | 146 | 98 | 1.49 | 0.04804 | 0.00129 | 0.08566 | 0.00402 | 0.01293 | 0.00032 | 0.00454 | 0.00015 | 101 | 60 | 83 | 4 | 83 | 2 | 92 | 3 |
| B574-22 | 201 | 132 | 1.52 | 0.05050 | 0.00455 | 0.08818 | 0.00997 | 0.01267 | 0.00036 | 0.00399 | 0.00013 | 218 | 186 | 86 | 9 | 81 | 2 | 81 | 3 |
| B574-23 | 168 | 131 | 1.28 | 0.04555 | 0.00100 | 0.08081 | 0.00335 | 0.01287 | 0.00032 | 0.00448 | 0.00015 | −26 | 43 | 79 | 3 | 82 | 2 | 90 | 3 |
| B574-24 | 210 | 150 | 1.40 | 0.04713 | 0.00106 | 0.08165 | 0.00347 | 0.01257 | 0.00032 | 0.00418 | 0.00014 | 56 | 49 | 80 | 3 | 81 | 2 | 84 | 3 |
| *B-621 wt. mean (one old core excluded) = 70.8 ± 0.8 Ma (2σ)* | | | | | | | | | | | | | | | | | | | |
| B621D-02 | 530 | 257 | 2.07 | 0.04753 | 0.00090 | 0.07254 | 0.00269 | 0.01107 | 0.00026 | 0.00381 | 0.00013 | 76 | 44 | 71 | 3 | 71 | 2 | 77 | 3 |
| B621D-03 | 119 | 299 | 0.40 | 0.04556 | 0.00078 | 0.07042 | 0.00245 | 0.01121 | 0.00026 | 0.00363 | 0.00015 | −25 | 32 | 69 | 2 | 72 | 2 | 73 | 3 |
| B621D-04 | 337 | 210 | 1.60 | 0.04980 | 0.00151 | 0.07616 | 0.00393 | 0.01109 | 0.00029 | 0.00382 | 0.00016 | 186 | 70 | 75 | 4 | 71 | 2 | 77 | 3 |
| B621D-05 | 762 | 268 | 2.85 | 0.05649 | 0.00121 | 0.08656 | 0.00356 | 0.01111 | 0.00028 | 0.00359 | 0.00014 | 472 | 47 | 84 | 3 | 71 | 2 | 72 | 3 |
| B621D-06 | 529 | 181 | 2.93 | 0.04634 | 0.00436 | 0.06893 | 0.00764 | 0.01079 | 0.00028 | 0.00344 | 0.00010 | 16 | 196 | 68 | 7 | 69 | 2 | 69 | 2 |
| B621D-07 | 736 | 267 | 2.75 | 0.04864 | 0.00088 | 0.07432 | 0.00267 | 0.01108 | 0.00026 | 0.00368 | 0.00013 | 131 | 43 | 73 | 3 | 71 | 2 | 74 | 3 |
| B621D-08 | 1277 | 367 | 3.48 | 0.05576 | 0.00103 | 0.08623 | 0.00323 | 0.01122 | 0.00028 | 0.00384 | 0.00017 | 443 | 41 | 84 | 3 | 72 | 2 | 77 | 3 |
| B621D-09 | 778 | 290 | 2.69 | 0.05099 | 0.00144 | 0.07646 | 0.00375 | 0.01088 | 0.00028 | 0.00363 | 0.00014 | 240 | 65 | 75 | 4 | 70 | 2 | 73 | 3 |
| B621D-12 | 879 | 352 | 2.50 | 0.05181 | 0.00117 | 0.07738 | 0.00326 | 0.01083 | 0.00027 | 0.00359 | 0.00014 | 277 | 51 | 76 | 3 | 69 | 2 | 72 | 3 |
| B621D-13 | 2409 | 685 | 3.52 | 0.04635 | 0.00095 | 0.06929 | 0.00279 | 0.01084 | 0.00028 | 0.00349 | 0.00016 | 16 | 42 | 68 | 3 | 70 | 2 | 70 | 3 |

(*continued on next page*)



Please cite this article in press as: Jahn, B.-m., et al. Emplacement ages, geochemical and Sr–Nd–Hf isotopic characterization of Mesozoic to early Cenozoic granitoids of the Sikhote-Alin Orogenic Belt, Russian Far East: Crustal growth and regional tectonic evolution. Journal of Asian Earth Sciences (2015), http://dx.doi.org/10.1016/j.jseaes.2015.08.012

**Table 2** (*continued*)

| Analysis No. | Th (ppm) | U (ppm) | Th/U | $^{207}Pb/^{206}Pb$ | ±1σ | $^{207}Pb/^{235}U$ | ±1σ | $^{206}Pb/^{238}U$ | ±1σ | $^{208}Pb/^{232}Th$ | ±1σ | $^{207}Pb/^{206}Pb$ | ±1σ | $^{207}Pb/^{235}U$ | ±1σ | $^{206}Pb/^{238}U$ | ±1σ | $^{208}Pb/^{232}Th$ | ±1σ |
|---|---|---|---|---|---|---|---|---|---|---|---|---|---|---|---|---|---|---|---|
| B621D-14 | 1736 | 479 | 3.62 | 0.04512 | 0.00087 | 0.07093 | 0.00270 | 0.01140 | 0.00028 | 0.00357 | 0.00014 | −13 | 35 | 70 | 3 | 73 | 2 | 72 | 3 |
| B621D-15 | 829 | 281 | 2.95 | 0.05005 | 0.00165 | 0.07558 | 0.00418 | 0.01095 | 0.00030 | 0.00333 | 0.00016 | 197 | 77 | 74 | 4 | 70 | 2 | 67 | 3 |
| B621D-16 | 376 | 437 | 0.86 | 0.04530 | 0.00080 | 0.06804 | 0.00240 | 0.01089 | 0.00025 | 0.00403 | 0.00017 | −4 | 33 | 67 | 2 | 70 | 2 | 81 | 3 |
| B621D-18 | 430 | 237 | 1.82 | 0.04607 | 0.00200 | 0.06938 | 0.00402 | 0.01092 | 0.00026 | 0.00360 | 0.00013 | 2 | 91 | 68 | 4 | 70 | 2 | 73 | 3 |
| B621D-19 | 517 | 202 | 2.57 | 0.04533 | 0.00215 | 0.07078 | 0.00499 | 0.01132 | 0.00031 | 0.00372 | 0.00020 | −3 | 101 | 69 | 5 | 73 | 2 | 75 | 4 |
| B621D-20 | 615 | 300 | 2.05 | 0.04607 | 0.00198 | 0.07098 | 0.00402 | 0.01117 | 0.00026 | 0.00370 | 0.00015 | 1 | 89 | 70 | 4 | 72 | 2 | 75 | 3 |
| B621D-21 | 341 | 174 | 1.95 | 0.04941 | 0.00191 | 0.07355 | 0.00439 | 0.01080 | 0.00027 | 0.00376 | 0.00014 | 167 | 88 | 72 | 4 | 69 | 2 | 76 | 3 |
| B621D-22 | 490 | 176 | 2.78 | 0.04929 | 0.00237 | 0.07486 | 0.00532 | 0.01102 | 0.00030 | 0.00348 | 0.00014 | 162 | 108 | 73 | 5 | 71 | 2 | 70 | 3 |
| B621D-23 | 977 | 414 | 2.36 | 0.04944 | 0.00088 | 0.07610 | 0.00270 | 0.01117 | 0.00026 | 0.00360 | 0.00013 | 169 | 42 | 74 | 3 | 72 | 2 | 73 | 3 |
| B621D-24 | 611 | 227 | 2.69 | 0.04750 | 0.00145 | 0.07213 | 0.00366 | 0.01102 | 0.00027 | 0.00361 | 0.00014 | 74 | 68 | 71 | 3 | 71 | 2 | 73 | 3 |
| B621D-25 | 1174 | 406 | 2.89 | 0.04491 | 0.00094 | 0.06758 | 0.00268 | 0.01091 | 0.00026 | 0.00368 | 0.00015 | −24 | 39 | 66 | 3 | 70 | 2 | 74 | 3 |
| B621D-26 | 1629 | 447 | 3.64 | 0.05492 | 0.00088 | 0.08399 | 0.00281 | 0.01109 | 0.00026 | 0.00369 | 0.00014 | 409 | 36 | 82 | 3 | 71 | 2 | 74 | 3 |
| B621D-27 | 1208 | 441 | 2.74 | 0.04994 | 0.00206 | 0.07583 | 0.00496 | 0.01102 | 0.00032 | 0.00279 | 0.00016 | 192 | 95 | 74 | 5 | 71 | 2 | 56 | 3 |
| B621C-28 | 1499 | 439 | 3.41 | 0.04847 | 0.00116 | 0.07170 | 0.00315 | 0.01073 | 0.00027 | 0.00335 | 0.00015 | 122 | 56 | 70 | 3 | 69 | 2 | 68 | 3 |
| B621C-01 (Core) | 977 | 289 | 3.39 | 0.44060 | 0.00488 | 1.34656 | 0.03418 | 0.02216 | 0.00050 | 0.01971 | 0.00089 | 4054 | 16 | 866 | 15 | 141 | 3 | 395 | 18 |
| *B-783M wt. mean = 77.7 ± 0.9 Ma (2σ)* | | | | | | | | | | | | | | | | | | | |
| B-783M01 | 588 | 216 | 2.72 | 0.04608 | 0.00216 | 0.07694 | 0.00485 | 0.01211 | 0.00029 | 0.00395 | 0.00010 | 2 | 97 | 75 | 5 | 78 | 2 | 80 | 2 |
| B-783M02 | 678 | 201 | 3.38 | 0.04607 | 0.00209 | 0.07674 | 0.00475 | 0.01208 | 0.00029 | 0.00393 | 0.00009 | 1 | 95 | 75 | 4 | 77 | 2 | 79 | 2 |
| B-783M03 | 353 | 149 | 2.36 | 0.04822 | 0.00093 | 0.08038 | 0.00300 | 0.01209 | 0.00028 | 0.00410 | 0.00010 | 110 | 45 | 79 | 3 | 77 | 2 | 83 | 2 |
| B-783M04 | 504 | 198 | 2.55 | 0.05547 | 0.00103 | 0.09482 | 0.00352 | 0.01240 | 0.00030 | 0.00401 | 0.00011 | 431 | 42 | 92 | 3 | 79 | 2 | 81 | 2 |
| B-783M06 | 335 | 140 | 2.40 | 0.04607 | 0.00226 | 0.07723 | 0.00518 | 0.01216 | 0.00031 | 0.00393 | 0.00010 | 1 | 103 | 76 | 5 | 78 | 2 | 79 | 2 |
| B-783M08 | 885 | 271 | 3.26 | 0.04743 | 0.00067 | 0.08132 | 0.00247 | 0.01244 | 0.00028 | 0.00418 | 0.00011 | 71 | 33 | 79 | 2 | 80 | 2 | 84 | 2 |
| B-783M09 | 471 | 201 | 2.34 | 0.04837 | 0.00078 | 0.08184 | 0.00271 | 0.01227 | 0.00028 | 0.00408 | 0.00011 | 117 | 37 | 80 | 3 | 79 | 2 | 82 | 2 |
| B-783M10 | 1027 | 295 | 3.49 | 0.04826 | 0.00066 | 0.08229 | 0.00245 | 0.01237 | 0.00028 | 0.00404 | 0.00011 | 112 | 32 | 80 | 2 | 79 | 2 | 81 | 2 |
| B-783M12 | 416 | 149 | 2.80 | 0.05471 | 0.00115 | 0.09442 | 0.00381 | 0.01252 | 0.00031 | 0.00400 | 0.00013 | 400 | 48 | 92 | 4 | 80 | 2 | 81 | 3 |
| B-783M13 | 408 | 155 | 2.63 | 0.05360 | 0.00110 | 0.08892 | 0.00350 | 0.01203 | 0.00029 | 0.00390 | 0.00010 | 354 | 47 | 86 | 3 | 77 | 2 | 79 | 2 |
| B-783M14 | 483 | 175 | 2.76 | 0.04620 | 0.00303 | 0.07677 | 0.00641 | 0.01205 | 0.00030 | 0.00384 | 0.00009 | 8 | 140 | 75 | 6 | 77 | 2 | 78 | 2 |
| B-783M15 | 322 | 121 | 2.66 | 0.04608 | 0.00272 | 0.07741 | 0.00590 | 0.01218 | 0.00030 | 0.00391 | 0.00010 | 2 | 127 | 76 | 6 | 78 | 2 | 79 | 2 |
| B-783M18 | 306 | 144 | 2.12 | 0.05128 | 0.00437 | 0.08638 | 0.00946 | 0.01222 | 0.00036 | 0.00384 | 0.00008 | 254 | 192 | 84 | 9 | 78 | 2 | 78 | 2 |
| B-783M19 | 159 | 86 | 1.84 | 0.05404 | 0.00583 | 0.08884 | 0.01208 | 0.01192 | 0.00040 | 0.00373 | 0.00009 | 373 | 241 | 86 | 11 | 76 | 3 | 75 | 2 |
| B-783M20 | 384 | 147 | 2.61 | 0.05013 | 0.00122 | 0.08060 | 0.00356 | 0.01166 | 0.00029 | 0.00379 | 0.00011 | 201 | 56 | 79 | 3 | 75 | 2 | 76 | 2 |
| B-783M21 | 168 | 84 | 1.99 | 0.05188 | 0.00295 | 0.08482 | 0.00706 | 0.01186 | 0.00037 | 0.00368 | 0.00016 | 280 | 128 | 83 | 7 | 76 | 2 | 74 | 3 |
| B-783M22 | 364 | 141 | 2.58 | 0.05743 | 0.00148 | 0.09405 | 0.00439 | 0.01188 | 0.00031 | 0.00357 | 0.00012 | 508 | 57 | 91 | 4 | 76 | 2 | 72 | 2 |
| B-783M23 | 493 | 166 | 2.96 | 0.04719 | 0.00401 | 0.07911 | 0.00828 | 0.01216 | 0.00033 | 0.00387 | 0.00010 | 59 | 182 | 77 | 8 | 78 | 2 | 78 | 2 |
| *B-919B wt. mean = 80.8 ± 0.8 Ma (2σ)* | | | | | | | | | | | | | | | | | | | |
| B-919b-01 | 233 | 259 | 0.90 | 0.04972 | 0.00116 | 0.08524 | 0.00362 | 0.01243 | 0.00030 | 0.00400 | 0.00017 | 182 | 54 | 83 | 3 | 80 | 2 | 81 | 3 |
| B-919b-02 | 568 | 527 | 1.08 | 0.04710 | 0.00217 | 0.08016 | 0.00496 | 0.01234 | 0.00029 | 0.00393 | 0.00012 | 54 | 100 | 78 | 5 | 79 | 2 | 79 | 2 |
| B-919b-03 | 290 | 289 | 1.00 | 0.04472 | 0.00108 | 0.07785 | 0.00340 | 0.01263 | 0.00031 | 0.00391 | 0.00018 | −34 | 47 | 76 | 3 | 81 | 2 | 79 | 4 |
| B-919b-04 | 448 | 358 | 1.25 | 0.04811 | 0.00092 | 0.08234 | 0.00307 | 0.01242 | 0.00029 | 0.00410 | 0.00018 | 105 | 45 | 80 | 3 | 80 | 2 | 83 | 4 |
| B-919b-05 | 368 | 409 | 0.90 | 0.04665 | 0.00089 | 0.08194 | 0.00305 | 0.01274 | 0.00030 | 0.00417 | 0.00016 | 31 | 41 | 80 | 3 | 82 | 2 | 84 | 3 |
| B-919b-06 | 239 | 283 | 0.84 | 0.04311 | 0.00121 | 0.07603 | 0.00363 | 0.01279 | 0.00031 | 0.00427 | 0.00018 | −117 | 62 | 74 | 3 | 82 | 2 | 86 | 4 |
| B-919b-07 | 388 | 349 | 1.11 | 0.04553 | 0.00097 | 0.07866 | 0.00316 | 0.01253 | 0.00030 | 0.00392 | 0.00015 | −27 | 41 | 77 | 3 | 80 | 2 | 79 | 3 |
| B-919b-08 | 580 | 517 | 1.12 | 0.04429 | 0.00086 | 0.07594 | 0.00288 | 0.01244 | 0.00030 | 0.00427 | 0.00019 | −56 | 40 | 74 | 3 | 80 | 2 | 86 | 4 |
| B-919b-09 | 719 | 507 | 1.42 | 0.04770 | 0.00117 | 0.08482 | 0.00381 | 0.01290 | 0.00033 | 0.00412 | 0.00022 | 84 | 56 | 83 | 4 | 83 | 2 | 83 | 4 |
| B-919b-10 | 965 | 564 | 1.71 | 0.05413 | 0.00104 | 0.09490 | 0.00365 | 0.01272 | 0.00032 | 0.00402 | 0.00019 | 376 | 43 | 92 | 3 | 81 | 2 | 81 | 4 |
| B-919b-11 | 244 | 211 | 1.15 | 0.05109 | 0.00156 | 0.08841 | 0.00450 | 0.01255 | 0.00031 | 0.00454 | 0.00021 | 245 | 70 | 86 | 4 | 80 | 2 | 92 | 4 |
| B-919b-12 | 287 | 296 | 0.97 | 0.04796 | 0.00123 | 0.08118 | 0.00367 | 0.01228 | 0.00030 | 0.00415 | 0.00020 | 97 | 58 | 79 | 3 | 79 | 2 | 84 | 4 |
| B-919b-13 | 397 | 381 | 1.04 | 0.04445 | 0.00166 | 0.07714 | 0.00465 | 0.01259 | 0.00035 | 0.00380 | 0.00024 | −47 | 76 | 75 | 4 | 81 | 2 | 77 | 5 |
| B-919b-15 | 229 | 195 | 1.18 | 0.04730 | 0.00166 | 0.08255 | 0.00458 | 0.01266 | 0.00031 | 0.00386 | 0.00019 | 64 | 76 | 81 | 4 | 81 | 2 | 78 | 4 |
| B-919b-19 | 273 | 333 | 0.82 | 0.04745 | 0.00109 | 0.08331 | 0.00353 | 0.01274 | 0.00031 | 0.00424 | 0.00019 | 72 | 53 | 81 | 3 | 82 | 2 | 86 | 4 |
| B-919b-20 | 456 | 542 | 0.84 | 0.04709 | 0.00079 | 0.08174 | 0.00283 | 0.01259 | 0.00030 | 0.00421 | 0.00018 | 54 | 39 | 80 | 3 | 81 | 2 | 85 | 4 |
| B-919b-21 | 224 | 252 | 0.89 | 0.04659 | 0.00145 | 0.08098 | 0.00416 | 0.01261 | 0.00031 | 0.00410 | 0.00019 | 28 | 64 | 79 | 4 | 81 | 2 | 83 | 4 |
| B-919b-22 | 381 | 348 | 1.10 | 0.04662 | 0.00243 | 0.08174 | 0.00558 | 0.01272 | 0.00032 | 0.00405 | 0.00015 | 30 | 111 | 80 | 5 | 81 | 2 | 82 | 3 |

Please cite this article in press as: Jahn, B.-m., et al. Emplacement ages, geochemical and Sr–Nd–Hf isotopic characterization of Mesozoic to early Cenozoic granitoids of the Sikhote-Alin Orogenic Belt, Russian Far East: Crustal growth and regional tectonic evolution. Journal of Asian Earth Sciences (2015), http://dx.doi.org/10.1016/j.jseaes.2015.08.012

**Table 2** (*continued*)

| Analysis No. | Th (ppm) | U (ppm) | Th/U | $^{207}Pb/^{206}Pb$ | ±1σ | $^{207}Pb/^{235}U$ | ±1σ | $^{206}Pb/^{238}U$ | ±1σ | $^{208}Pb/^{232}Th$ | ±1σ | $^{207}Pb/^{206}Pb$ | ±1σ | $^{207}Pb/^{235}U$ | ±1σ | $^{206}Pb/^{238}U$ | ±1σ | $^{208}Pb/^{232}Th$ | ±1σ |
|---|---|---|---|---|---|---|---|---|---|---|---|---|---|---|---|---|---|---|---|
| B-919b-23 | 270 | 283 | 0.95 | 0.04432 | 0.00131 | 0.07667 | 0.00382 | 0.01255 | 0.00031 | 0.00398 | 0.00020 | −54 | 59 | 75 | 4 | 80 | 2 | 80 | 4 |
| B-919b-24 | 334 | 328 | 1.02 | 0.05310 | 0.00120 | 0.09220 | 0.00383 | 0.01259 | 0.00030 | 0.00474 | 0.00023 | 333 | 52 | 90 | 4 | 81 | 2 | 96 | 5 |
| B-919b-25 | 549 | 502 | 1.09 | 0.04530 | 0.00092 | 0.07679 | 0.00302 | 0.01230 | 0.00030 | 0.00410 | 0.00021 | −4 | 38 | 75 | 3 | 79 | 2 | 83 | 4 |
| B-919b-26 | 213 | 278 | 0.77 | 0.04708 | 0.00232 | 0.08166 | 0.00534 | 0.01258 | 0.00031 | 0.00400 | 0.00018 | 53 | 106 | 80 | 5 | 81 | 2 | 81 | 4 |
| B-919b-27 | 368 | 381 | 0.97 | 0.04691 | 0.00112 | 0.08228 | 0.00357 | 0.01272 | 0.00031 | 0.00431 | 0.00024 | 45 | 52 | 80 | 3 | 81 | 2 | 87 | 5 |
| B-919b-28 | 152 | 174 | 0.87 | 0.04509 | 0.00205 | 0.07959 | 0.00535 | 0.01280 | 0.00033 | 0.00422 | 0.00025 | −15 | 94 | 78 | 5 | 82 | 2 | 85 | 5 |
| *B-984 wt. mean = 78.1 ± 0.8 Ma (2σ)* | | | | | | | | | | | | | | | | | | | |
| B984-01 | 294 | 217 | 1.36 | 0.04703 | 0.00181 | 0.07893 | 0.00466 | 0.01217 | 0.00030 | 0.00415 | 0.00018 | 51 | 82 | 77 | 4 | 78 | 2 | 84 | 4 |
| B984-02 | 399 | 228 | 1.75 | 0.04597 | 0.00186 | 0.07606 | 0.00472 | 0.01200 | 0.00031 | 0.00406 | 0.00018 | −4 | 81 | 74 | 4 | 77 | 2 | 82 | 4 |
| B984-03 | 256 | 165 | 1.55 | 0.04293 | 0.00249 | 0.07039 | 0.00566 | 0.01189 | 0.00031 | 0.00403 | 0.00019 | −127 | 125 | 69 | 5 | 76 | 2 | 81 | 4 |
| B984-04 | 239 | 166 | 1.44 | 0.04691 | 0.00228 | 0.08053 | 0.00567 | 0.01245 | 0.00032 | 0.00387 | 0.00018 | 45 | 105 | 79 | 5 | 80 | 2 | 78 | 4 |
| B984-05 | 190 | 126 | 1.51 | 0.05498 | 0.00306 | 0.09469 | 0.00740 | 0.01249 | 0.00033 | 0.00425 | 0.00021 | 411 | 126 | 92 | 7 | 80 | 2 | 86 | 4 |
| B984-06 | 256 | 212 | 1.21 | 0.04537 | 0.00186 | 0.07599 | 0.00475 | 0.01215 | 0.00031 | 0.00391 | 0.00019 | −1 | 85 | 74 | 4 | 78 | 2 | 79 | 4 |
| B984-07 | 251 | 201 | 1.25 | 0.05065 | 0.00190 | 0.08633 | 0.00505 | 0.01236 | 0.00031 | 0.00425 | 0.00021 | 225 | 88 | 84 | 5 | 79 | 2 | 86 | 4 |
| B984-08 | 104 | 129 | 0.81 | 0.04425 | 0.00310 | 0.07467 | 0.00692 | 0.01224 | 0.00032 | 0.00437 | 0.00026 | −58 | 145 | 73 | 7 | 78 | 2 | 88 | 5 |
| B984-09 | 471 | 428 | 1.10 | 0.04525 | 0.00100 | 0.07602 | 0.00312 | 0.01219 | 0.00029 | 0.00382 | 0.00019 | −7 | 42 | 74 | 3 | 78 | 2 | 77 | 4 |
| B984-10 | 137 | 116 | 1.19 | 0.04652 | 0.00342 | 0.07923 | 0.00766 | 0.01235 | 0.00033 | 0.00401 | 0.00023 | 25 | 159 | 77 | 7 | 79 | 2 | 81 | 5 |
| B984-12 | 321 | 217 | 1.48 | 0.04686 | 0.00441 | 0.07815 | 0.00869 | 0.01210 | 0.00032 | 0.00385 | 0.00020 | 42 | 198 | 76 | 8 | 78 | 2 | 78 | 4 |
| B-984-13 | 666 | 578 | 1.15 | 0.04846 | 0.00053 | 0.08455 | 0.00212 | 0.01266 | 0.00028 | 0.00400 | 0.00009 | 122 | 26 | 82 | 2 | 81 | 2 | 81 | 2 |
| B-984-15 | 305 | 236 | 1.29 | 0.04880 | 0.00070 | 0.08069 | 0.00248 | 0.01199 | 0.00027 | 0.00383 | 0.00009 | 138 | 33 | 79 | 2 | 77 | 2 | 77 | 2 |
| B-984-16 | 301 | 204 | 1.48 | 0.05107 | 0.00077 | 0.08539 | 0.00269 | 0.01213 | 0.00027 | 0.00390 | 0.00010 | 244 | 35 | 83 | 3 | 78 | 2 | 79 | 2 |
| B-984-17 | 637 | 402 | 1.58 | 0.04889 | 0.00251 | 0.08554 | 0.00598 | 0.01269 | 0.00030 | 0.00402 | 0.00008 | 143 | 117 | 83 | 6 | 81 | 2 | 81 | 2 |
| B-984-18 | 327 | 227 | 1.44 | 0.04855 | 0.00071 | 0.07967 | 0.00248 | 0.01190 | 0.00027 | 0.00378 | 0.00010 | 126 | 35 | 78 | 2 | 76 | 2 | 76 | 2 |
| B-984-19 | 751 | 425 | 1.77 | 0.04754 | 0.00212 | 0.07818 | 0.00492 | 0.01193 | 0.00029 | 0.00379 | 0.00008 | 76 | 98 | 76 | 5 | 76 | 2 | 76 | 2 |
| B-984-20 | 240 | 276 | 0.87 | 0.04559 | 0.00063 | 0.07697 | 0.00230 | 0.01225 | 0.00027 | 0.00404 | 0.00011 | −24 | 26 | 75 | 2 | 78 | 2 | 81 | 2 |
| B-984-21 | 678 | 763 | 0.89 | 0.04854 | 0.00053 | 0.07995 | 0.00200 | 0.01195 | 0.00026 | 0.00388 | 0.00010 | 126 | 26 | 78 | 2 | 77 | 2 | 78 | 2 |
| B-984-22 | 612 | 379 | 1.61 | 0.05080 | 0.00061 | 0.08657 | 0.00237 | 0.01236 | 0.00028 | 0.00409 | 0.00011 | 232 | 27 | 84 | 2 | 79 | 2 | 82 | 2 |
| B-984-23 | 673 | 618 | 1.09 | 0.04834 | 0.00054 | 0.08044 | 0.00207 | 0.01207 | 0.00027 | 0.00390 | 0.00011 | 116 | 27 | 79 | 2 | 77 | 2 | 79 | 2 |
| B-984-24 | 622 | 563 | 1.10 | 0.04935 | 0.00057 | 0.08084 | 0.00212 | 0.01188 | 0.00026 | 0.00389 | 0.00011 | 164 | 27 | 79 | 2 | 76 | 2 | 78 | 2 |
| *GV-722 wt. mean = 74.4 ± 0.9 Ma (2σ)* | | | | | | | | | | | | | | | | | | | |
| GB72201 | 433 | 545 | 0.79 | 0.04753 | 0.00114 | 0.08160 | 0.00335 | 0.01245 | 0.00026 | 0.00396 | 0.00007 | 76 | 56 | 80 | 3 | 80 | 2 | 80 | 1 |
| GB72202 | 271 | 456 | 0.60 | 0.04896 | 0.00051 | 0.08219 | 0.00196 | 0.01218 | 0.00025 | 0.00393 | 0.00009 | 146 | 24 | 80 | 2 | 78 | 2 | 79 | 2 |
| GB72203 | 412 | 974 | 0.42 | 0.05668 | 0.00278 | 0.09032 | 0.00591 | 0.01156 | 0.00027 | 0.00359 | 0.00011 | 479 | 108 | 88 | 6 | 74 | 2 | 72 | 2 |
| GB72204 | 430 | 1015 | 0.42 | 0.04870 | 0.00080 | 0.07774 | 0.00250 | 0.01158 | 0.00023 | 0.00367 | 0.00007 | 133 | 39 | 76 | 2 | 74 | 1 | 74 | 1 |
| GB72205 | 328 | 313 | 1.05 | 0.04611 | 0.00119 | 0.07036 | 0.00289 | 0.01107 | 0.00024 | 0.00354 | 0.00008 | 3 | 52 | 69 | 3 | 71 | 2 | 71 | 2 |
| GB72206 | 553 | 1979 | 0.28 | 0.04837 | 0.00045 | 0.07684 | 0.00163 | 0.01152 | 0.00023 | 0.00357 | 0.00008 | 117 | 22 | 75 | 2 | 74 | 1 | 72 | 2 |
| GB72207 | 373 | 393 | 0.95 | 0.04828 | 0.00053 | 0.07869 | 0.00194 | 0.01182 | 0.00024 | 0.00379 | 0.00009 | 113 | 26 | 77 | 2 | 76 | 2 | 76 | 2 |
| GB72208 | 494 | 493 | 1.00 | 0.04894 | 0.00059 | 0.07916 | 0.00209 | 0.01173 | 0.00024 | 0.00371 | 0.00010 | 145 | 28 | 77 | 2 | 75 | 2 | 75 | 2 |
| GB72209 | 579 | 805 | 0.72 | 0.04752 | 0.00047 | 0.07782 | 0.00176 | 0.01188 | 0.00024 | 0.00379 | 0.00009 | 75 | 24 | 76 | 2 | 76 | 2 | 76 | 2 |
| GB72210 | 397 | 845 | 0.47 | 0.04812 | 0.00047 | 0.07780 | 0.00175 | 0.01173 | 0.00023 | 0.00396 | 0.00010 | 105 | 23 | 76 | 2 | 75 | 1 | 80 | 2 |
| GB72211 | 1197 | 2346 | 0.51 | 0.05410 | 0.00139 | 0.05316 | 0.00224 | 0.00713 | 0.00015 | 0.00223 | 0.00004 | 375 | 57 | 53 | 2 | 45.8 | 1 | 45 | 0.9 |
| GB72212 | 1403 | 1908 | 0.74 | 0.05171 | 0.00049 | 0.08277 | 0.00180 | 0.01161 | 0.00023 | 0.00423 | 0.00011 | 273 | 22 | 81 | 2 | 74 | 1 | 85 | 2 |
| GB72213 | 344 | 358 | 0.96 | 0.04830 | 0.00053 | 0.07950 | 0.00197 | 0.01194 | 0.00024 | 0.00391 | 0.00009 | 114 | 26 | 78 | 2 | 77 | 2 | 79 | 2 |
| GB72214 | 194 | 158 | 1.23 | 0.04981 | 0.00072 | 0.08178 | 0.00246 | 0.01191 | 0.00025 | 0.00379 | 0.00009 | 186 | 34 | 80 | 2 | 76 | 2 | 76 | 2 |
| GB72215 | 181 | 118 | 1.53 | 0.04789 | 0.00085 | 0.07818 | 0.00268 | 0.01184 | 0.00025 | 0.00386 | 0.00009 | 94 | 42 | 76 | 3 | 76 | 2 | 78 | 2 |
| GB72216 | 588 | 837 | 0.70 | 0.04835 | 0.00047 | 0.07794 | 0.00175 | 0.01169 | 0.00023 | 0.00385 | 0.00009 | 116 | 23 | 76 | 2 | 75 | 1 | 78 | 2 |
| GB72217 | 1253 | 1132 | 1.11 | 0.05274 | 0.00057 | 0.08368 | 0.00205 | 0.01151 | 0.00024 | 0.00364 | 0.00009 | 318 | 24 | 82 | 2 | 74 | 2 | 73 | 2 |
| GB72218 | 1230 | 2761 | 0.45 | 0.04691 | 0.00153 | 0.05957 | 0.00276 | 0.00921 | 0.00019 | 0.00293 | 0.00012 | 45 | 69 | 59 | 3 | 59 | 1 | 59 | 2 |
| GB72219 | 340 | 291 | 1.17 | 0.04892 | 0.00058 | 0.07980 | 0.00209 | 0.01183 | 0.00024 | 0.00385 | 0.00009 | 144 | 27 | 78 | 2 | 76 | 2 | 78 | 2 |
| GB72220 | 1489 | 956 | 1.56 | 0.04609 | 0.00139 | 0.06992 | 0.00309 | 0.01100 | 0.00023 | 0.00354 | 0.00008 | 2 | 61 | 69 | 3 | 71 | 1 | 71 | 2 |
| GB72221 | 885 | 1811 | 0.49 | 0.05212 | 0.00177 | 0.07777 | 0.00396 | 0.01082 | 0.00025 | 0.00340 | 0.00007 | 290 | 78 | 76 | 4 | 69 | 2 | 69 | 1 |
| GB72222 | 560 | 780 | 0.72 | 0.04784 | 0.00048 | 0.07949 | 0.00183 | 0.01205 | 0.00024 | 0.00388 | 0.00009 | 91 | 24 | 78 | 2 | 77 | 2 | 78 | 2 |
| GB72223 | 480 | 852 | 0.56 | 0.04781 | 0.00051 | 0.07791 | 0.00188 | 0.01182 | 0.00024 | 0.00382 | 0.00010 | 90 | 25 | 76 | 2 | 76 | 2 | 77 | 2 |
| GB72224 | 852 | 1723 | 0.49 | 0.04973 | 0.00052 | 0.07787 | 0.00186 | 0.01136 | 0.00024 | 0.00358 | 0.00010 | 182 | 24 | 76 | 2 | 73 | 2 | 72 | 2 |

(*continued on next page*)



Please cite this article in press as: Jahn, B.-m., et al. Emplacement ages, geochemical and Sr–Nd–Hf isotopic characterization of Mesozoic to early Cenozoic granitoids of the Sikhote-Alin Orogenic Belt, Russian Far East: Crustal growth and regional tectonic evolution. Journal of Asian Earth Sciences (2015), http://dx.doi.org/10.1016/j.jseaes.2015.08.012

**Table 2** (*continued*)

| Analysis No. | Th (ppm) | U (ppm) | Th/U | $^{207}Pb/^{206}Pb$ | ±1σ | $^{207}Pb/^{235}U$ | ±1σ | $^{206}Pb/^{238}U$ | ±1σ | $^{208}Pb/^{232}Th$ | ±1σ | $^{207}Pb/^{206}Pb$ | ±1σ | $^{207}Pb/^{235}U$ | ±1σ | $^{206}Pb/^{238}U$ | ±1σ | $^{208}Pb/^{232}Th$ | ±1σ |
|---|---|---|---|---|---|---|---|---|---|---|---|---|---|---|---|---|---|---|---|
| *GV-1583-2 wt. mean = 86.0 ± 0.8 Ma (2σ)* | | | | | | | | | | | | | | | | | | | |
| GV158301 | 153 | 120 | 1.28 | 0.04860 | 0.00082 | 0.08973 | 0.00296 | 0.01339 | 0.00028 | 0.00440 | 0.00010 | 129 | 39 | 87 | 3 | 86 | 2 | 89 | 2 |
| GV158302 | 527 | 507 | 0.87 | 0.04878 | 0.00048 | 0.08974 | 0.00202 | 0.01334 | 0.00026 | 0.00434 | 0.00009 | 137 | 23 | 87 | 2 | 85 | 2 | 88 | 2 |
| GV158303 | 363 | 171 | 2.12 | 0.04613 | 0.00246 | 0.08486 | 0.00570 | 0.01334 | 0.00029 | 0.00426 | 0.00011 | 4 | 111 | 83 | 5 | 85 | 2 | 86 | 2 |
| GV158304 | 202 | 226 | 0.90 | 0.04773 | 0.00061 | 0.08626 | 0.00235 | 0.01311 | 0.00026 | 0.00430 | 0.00010 | 86 | 31 | 84 | 2 | 84 | 2 | 87 | 2 |
| GV158305 | 94 | 79 | 1.20 | 0.05167 | 0.00262 | 0.09383 | 0.00660 | 0.01317 | 0.00031 | 0.00414 | 0.00008 | 271 | 116 | 91 | 6 | 84 | 2 | 84 | 2 |
| GV158306 | 343 | 263 | 1.30 | 0.05005 | 0.00059 | 0.08991 | 0.00233 | 0.01303 | 0.00026 | 0.00426 | 0.00010 | 197 | 27 | 87 | 2 | 83 | 2 | 86 | 2 |
| GV158307 | 297 | 334 | 0.89 | 0.04763 | 0.00053 | 0.08644 | 0.00216 | 0.01316 | 0.00026 | 0.00414 | 0.00010 | 81 | 27 | 84 | 2 | 84 | 2 | 84 | 2 |
| GV158308 | 154 | 132 | 1.16 | 0.04770 | 0.00075 | 0.08975 | 0.00281 | 0.01365 | 0.00028 | 0.00436 | 0.00011 | 84 | 37 | 87 | 3 | 87 | 2 | 88 | 2 |
| GV158309 | 401 | 414 | 0.97 | 0.04997 | 0.00053 | 0.09246 | 0.00221 | 0.01342 | 0.00027 | 0.00434 | 0.00010 | 194 | 24 | 90 | 2 | 86 | 2 | 88 | 2 |
| GV158310 | 570 | 560 | 1.02 | 0.04952 | 0.00050 | 0.09400 | 0.00217 | 0.01377 | 0.00027 | 0.00438 | 0.00011 | 173 | 24 | 91 | 2 | 88 | 2 | 88 | 2 |
| GV158311 | 293 | 369 | 0.79 | 0.04926 | 0.00053 | 0.09361 | 0.00227 | 0.01378 | 0.00027 | 0.00435 | 0.00011 | 160 | 26 | 91 | 2 | 88 | 2 | 88 | 2 |
| GV158312 | 170 | 130 | 1.31 | 0.05397 | 0.00080 | 0.10128 | 0.00308 | 0.01361 | 0.00028 | 0.00438 | 0.00011 | 370 | 33 | 98 | 3 | 87 | 2 | 88 | 2 |
| GV158313 | 235 | 146 | 1.61 | 0.05125 | 0.00073 | 0.09446 | 0.00282 | 0.01337 | 0.00028 | 0.00418 | 0.00009 | 252 | 33 | 92 | 3 | 86 | 2 | 84 | 2 |
| GV158314 | 568 | 476 | 1.19 | 0.04951 | 0.00050 | 0.09220 | 0.00212 | 0.01351 | 0.00027 | 0.00419 | 0.00009 | 172 | 23 | 90 | 2 | 87 | 2 | 85 | 2 |
| GV158315 | 277 | 337 | 0.82 | 0.04788 | 0.00052 | 0.09150 | 0.00223 | 0.01386 | 0.00028 | 0.00431 | 0.00010 | 93 | 25 | 89 | 2 | 89 | 2 | 87 | 2 |
| GV158316 | 360 | 272 | 1.33 | 0.05179 | 0.00059 | 0.09647 | 0.00243 | 0.01351 | 0.00027 | 0.00438 | 0.00010 | 276 | 26 | 94 | 2 | 87 | 2 | 88 | 2 |
| GV158317 | 355 | 347 | 1.02 | 0.04837 | 0.00053 | 0.08915 | 0.00221 | 0.01337 | 0.00027 | 0.00420 | 0.00009 | 117 | 25 | 87 | 2 | 86 | 2 | 85 | 2 |
| GV158318 | 725 | 698 | 1.04 | 0.04790 | 0.00047 | 0.08753 | 0.00196 | 0.01325 | 0.00026 | 0.00411 | 0.00009 | 94 | 24 | 85 | 2 | 85 | 2 | 83 | 2 |
| GV158319 | 135 | 103 | 1.31 | 0.05582 | 0.00089 | 0.10439 | 0.00337 | 0.01356 | 0.00029 | 0.00443 | 0.00011 | 445 | 36 | 101 | 3 | 87 | 2 | 89 | 2 |
| GV158320 | 91 | 65 | 1.40 | 0.05130 | 0.00119 | 0.09609 | 0.00393 | 0.01359 | 0.00030 | 0.00418 | 0.00011 | 254 | 53 | 93 | 4 | 87 | 2 | 84 | 2 |
| GV158321 | 262 | 324 | 0.81 | 0.04848 | 0.00054 | 0.08965 | 0.00225 | 0.01341 | 0.00027 | 0.00420 | 0.00010 | 123 | 27 | 87 | 2 | 86 | 2 | 85 | 2 |
| GV158323 | 225 | 337 | 0.67 | 0.04873 | 0.00055 | 0.08944 | 0.00225 | 0.01331 | 0.00027 | 0.00459 | 0.00012 | 135 | 26 | 87 | 2 | 85 | 2 | 93 | 2 |
| GV158324 | 180 | 148 | 1.22 | 0.04826 | 0.00073 | 0.08977 | 0.00277 | 0.01349 | 0.00028 | 0.00421 | 0.00011 | 112 | 35 | 87 | 3 | 86 | 2 | 85 | 2 |
| *GV-1774 wt. mean = 88.3 ± 0.8 Ma (2σ)* | | | | | | | | | | | | | | | | | | | |
| GV177401 | 765 | 668 | 1.14 | 0.05010 | 0.00050 | 0.09614 | 0.00218 | 0.01392 | 0.00028 | 0.00452 | 0.00010 | 200 | 23 | 93 | 2 | 89 | 2 | 91 | 2 |
| GV177402 | 369 | 364 | 1.01 | 0.04640 | 0.00158 | 0.08798 | 0.00424 | 0.01375 | 0.00029 | 0.00438 | 0.00012 | 18 | 70 | 86 | 4 | 88 | 2 | 88 | 2 |
| GV177403 | 441 | 459 | 0.96 | 0.05314 | 0.00058 | 0.10139 | 0.00250 | 0.01384 | 0.00028 | 0.00515 | 0.00014 | 335 | 25 | 98 | 2 | 89 | 2 | 104 | 3 |
| GV177404 | 452 | 371 | 1.22 | 0.04971 | 0.00054 | 0.09465 | 0.00232 | 0.01381 | 0.00028 | 0.00442 | 0.00011 | 181 | 26 | 92 | 2 | 88 | 2 | 89 | 2 |
| GV177407 | 183 | 299 | 0.61 | 0.04876 | 0.00056 | 0.09568 | 0.00244 | 0.01423 | 0.00029 | 0.00462 | 0.00012 | 136 | 27 | 93 | 2 | 91 | 2 | 93 | 2 |
| GV177408 | 345 | 293 | 1.18 | 0.04892 | 0.00057 | 0.09252 | 0.00241 | 0.01372 | 0.00028 | 0.00425 | 0.00011 | 144 | 28 | 90 | 2 | 88 | 2 | 86 | 2 |
| GV177409 | 292 | 231 | 1.27 | 0.04881 | 0.00062 | 0.09105 | 0.00251 | 0.01353 | 0.00028 | 0.00426 | 0.00011 | 139 | 30 | 88 | 2 | 87 | 2 | 86 | 2 |
| GV177410 | 282 | 277 | 1.02 | 0.04714 | 0.00056 | 0.09065 | 0.00240 | 0.01395 | 0.00029 | 0.00432 | 0.00012 | 56 | 28 | 88 | 2 | 89 | 2 | 87 | 2 |
| GV177411 | 561 | 654 | 0.86 | 0.04867 | 0.00050 | 0.09098 | 0.00214 | 0.01356 | 0.00027 | 0.00436 | 0.00012 | 132 | 24 | 88 | 2 | 87 | 2 | 88 | 2 |
| GV177412 | 308 | 336 | 0.92 | 0.05111 | 0.00058 | 0.09550 | 0.00244 | 0.01355 | 0.00028 | 0.00445 | 0.00012 | 246 | 26 | 93 | 2 | 87 | 2 | 90 | 2 |
| GV177413 | 333 | 301 | 1.11 | 0.04878 | 0.00057 | 0.09147 | 0.00239 | 0.01360 | 0.00028 | 0.00449 | 0.00010 | 137 | 27 | 89 | 2 | 87 | 2 | 91 | 2 |
| GV177414 | 333 | 297 | 1.12 | 0.04956 | 0.00058 | 0.09241 | 0.00241 | 0.01352 | 0.00028 | 0.00439 | 0.00010 | 174 | 27 | 90 | 2 | 87 | 2 | 89 | 2 |
| GV177415 | 470 | 502 | 0.94 | 0.04975 | 0.00052 | 0.09496 | 0.00225 | 0.01384 | 0.00028 | 0.00438 | 0.00010 | 183 | 24 | 92 | 2 | 89 | 2 | 88 | 2 |
| GV177416 | 363 | 343 | 1.06 | 0.04871 | 0.00055 | 0.09325 | 0.00236 | 0.01389 | 0.00029 | 0.00440 | 0.00010 | 134 | 26 | 91 | 2 | 89 | 2 | 89 | 2 |
| GV177417 | 479 | 373 | 1.29 | 0.04939 | 0.00194 | 0.09319 | 0.00532 | 0.01368 | 0.00030 | 0.00433 | 0.00008 | 166 | 91 | 90 | 5 | 88 | 2 | 87 | 2 |
| GV177418 | 263 | 252 | 1.04 | 0.04907 | 0.00175 | 0.09263 | 0.00500 | 0.01369 | 0.00031 | 0.00433 | 0.00008 | 151 | 82 | 90 | 5 | 88 | 2 | 87 | 2 |
| GV177419 | 466 | 522 | 0.89 | 0.04830 | 0.00051 | 0.09114 | 0.00219 | 0.01369 | 0.00028 | 0.00427 | 0.00010 | 114 | 25 | 89 | 2 | 88 | 2 | 86 | 2 |
| GV177420 | 395 | 337 | 1.17 | 0.04841 | 0.00055 | 0.09239 | 0.00238 | 0.01384 | 0.00029 | 0.00433 | 0.00011 | 119 | 27 | 90 | 2 | 89 | 2 | 87 | 2 |
| GV177421 | 472 | 404 | 1.17 | 0.05128 | 0.00057 | 0.09814 | 0.00247 | 0.01388 | 0.00029 | 0.00453 | 0.00011 | 253 | 26 | 95 | 2 | 89 | 2 | 91 | 2 |
| GV177422 | 355 | 269 | 1.32 | 0.05209 | 0.00063 | 0.10012 | 0.00267 | 0.01394 | 0.00029 | 0.00457 | 0.00012 | 289 | 28 | 97 | 2 | 89 | 2 | 92 | 2 |
| GV177423 | 261 | 208 | 1.25 | 0.04956 | 0.00067 | 0.09355 | 0.00271 | 0.01369 | 0.00029 | 0.00427 | 0.00011 | 174 | 31 | 91 | 3 | 88 | 2 | 86 | 2 |
| GV177424 | 159 | 102 | 1.56 | 0.05036 | 0.00096 | 0.09522 | 0.00345 | 0.01371 | 0.00030 | 0.00425 | 0.00012 | 212 | 43 | 92 | 3 | 88 | 2 | 86 | 2 |
| *YG-332 wt. mean = 92.4 ± 0.8 Ma (2σ)* | | | | | | | | | | | | | | | | | | | |
| CG332-01 | 230 | 149 | 1.54 | 0.04792 | 0.00076 | 0.09561 | 0.00302 | 0.01447 | 0.00030 | 0.00472 | 0.00011 | 95 | 37 | 93 | 3 | 93 | 2 | 95 | 2 |
| CG332-02 | 257 | 146 | 1.76 | 0.04818 | 0.00078 | 0.09565 | 0.00307 | 0.01440 | 0.00030 | 0.00468 | 0.00011 | 108 | 38 | 93 | 3 | 92 | 2 | 94 | 2 |
| CG332-03 | 331 | 187 | 1.77 | 0.05058 | 0.00070 | 0.09946 | 0.00288 | 0.01426 | 0.00029 | 0.00459 | 0.00011 | 222 | 32 | 96 | 3 | 91 | 2 | 93 | 2 |
| CG332-04 | 493 | 254 | 1.94 | 0.05100 | 0.00078 | 0.10040 | 0.00318 | 0.01428 | 0.00031 | 0.00447 | 0.00012 | 241 | 36 | 97 | 3 | 91 | 2 | 90 | 2 |
| CG332-05 | 292 | 171 | 1.71 | 0.04961 | 0.00282 | 0.09843 | 0.00731 | 0.01439 | 0.00032 | 0.00455 | 0.00008 | 177 | 128 | 95 | 7 | 92 | 2 | 92 | 2 |

Please cite this article in press as: Jahn, B.-m., et al. Emplacement ages, geochemical and Sr–Nd–Hf isotopic characterization of Mesozoic to early Cenozoic granitoids of the Sikhote-Alin Orogenic Belt, Russian Far East: Crustal growth and regional tectonic evolution. Journal of Asian Earth Sciences (2015), http://dx.doi.org/10.1016/j.jseaes.2015.08.012

**Table 2** (*continued*)

| Analysis No. | Th (ppm) | U (ppm) | Th/U | $^{207}Pb/^{206}Pb$ | ±1σ | $^{207}Pb/^{235}U$ | ±1σ | $^{206}Pb/^{238}U$ |
|---|---|---|---|---|---|---|---|---|
| CG332-06 | 402 | 213 | 1.89 | 0.04827 | 0.00063 | 0.09711 | 0.00272 | 0.01459 |
| CG332-07 | 123 | 113 | 1.09 | 0.04999 | 0.00253 | 0.09943 | 0.00699 | 0.01443 |
| CG332-08 | 325 | 236 | 1.38 | 0.04753 | 0.00061 | 0.09377 | 0.00259 | 0.01431 |
| CG332-09 | 133 | 117 | 1.13 | 0.04616 | 0.00089 | 0.09138 | 0.00327 | 0.01436 |
| CG332-10 | 235 | 185 | 1.27 | 0.04815 | 0.00218 | 0.09711 | 0.00602 | 0.01463 |
| CG332-11 | 402 | 226 | 1.78 | 0.04696 | 0.00066 | 0.09399 | 0.00277 | 0.01452 |
| CG332-12 | 329 | 229 | 1.44 | 0.04608 | 0.00062 | 0.09079 | 0.00257 | 0.01429 |
| CG332-13 | 379 | 222 | 1.71 | 0.04868 | 0.00062 | 0.09554 | 0.00263 | 0.01424 |
| CG332-14 | 155 | 127 | 1.22 | 0.05043 | 0.00085 | 0.10047 | 0.00330 | 0.01445 |
| CG332-15 | 484 | 298 | 1.62 | 0.04814 | 0.00056 | 0.09405 | 0.00242 | 0.01417 |
| CG332-16 | 253 | 174 | 1.45 | 0.04778 | 0.00213 | 0.09864 | 0.00607 | 0.01497 |
| CG332-18 | 285 | 188 | 1.52 | 0.05024 | 0.00069 | 0.09885 | 0.00285 | 0.01427 |
| CG332-19 | 368 | 219 | 1.68 | 0.04871 | 0.00063 | 0.09735 | 0.00272 | 0.01450 |
| CG332-20 | 417 | 230 | 1.81 | 0.04845 | 0.00062 | 0.09739 | 0.00270 | 0.01458 |
| CG332-21 | 213 | 147 | 1.45 | 0.04886 | 0.00076 | 0.09988 | 0.00314 | 0.01483 |
| CG332-22 | 196 | 124 | 1.58 | 0.04830 | 0.00083 | 0.09578 | 0.00319 | 0.01439 |
| CG332-23 | 566 | 265 | 2.13 | 0.04749 | 0.00058 | 0.09605 | 0.00258 | 0.01467 |
| CG332-24 | 235 | 151 | 1.55 | 0.04647 | 0.00076 | 0.09206 | 0.00298 | 0.01437 |
| *¶G-410 wt. mean = 91.5 ± 0.8 Ma (2σ)* | | | | | | | | |
| CG410-01 | 227 | 179 | 1.27 | 0.04562 | 0.00065 | 0.09253 | 0.00276 | 0.01471 |
| CG410-02 | 637 | 714 | 0.89 | 0.04793 | 0.00132 | 0.09537 | 0.00423 | 0.01443 |
| CG410-03 | 234 | 220 | 1.06 | 0.04722 | 0.00061 | 0.09395 | 0.00262 | 0.01443 |
| CG410-04 | 297 | 216 | 1.38 | 0.05000 | 0.00065 | 0.09820 | 0.00272 | 0.01425 |
| CG410-05 | 259 | 444 | 0.58 | 0.04816 | 0.00051 | 0.09549 | 0.00230 | 0.01438 |
| CG410-06 | 415 | 578 | 0.72 | 0.04798 | 0.00049 | 0.09319 | 0.00218 | 0.01409 |
| CG410-08 | 350 | 325 | 1.08 | 0.04877 | 0.00056 | 0.09382 | 0.00241 | 0.01395 |
| CG410-10 | 491 | 716 | 0.69 | 0.05096 | 0.00051 | 0.10275 | 0.00235 | 0.01462 |
| CG410-11 | 198 | 287 | 0.69 | 0.04862 | 0.00057 | 0.09961 | 0.00261 | 0.01486 |
| CG410-12 | 433 | 575 | 0.75 | 0.04837 | 0.00050 | 0.09532 | 0.00226 | 0.01429 |
| CG410-13 | 743 | 910 | 0.82 | 0.05118 | 0.00133 | 0.09540 | 0.00409 | 0.01352 |
| CG410-14 | 220 | 302 | 0.73 | 0.05012 | 0.00057 | 0.09967 | 0.00254 | 0.01443 |
| CG410-15 | 363 | 559 | 0.65 | 0.04955 | 0.00051 | 0.09764 | 0.00228 | 0.01429 |
| CG410-16 | 373 | 594 | 0.63 | 0.04755 | 0.00048 | 0.09311 | 0.00217 | 0.01420 |
| CG410-17 | 266 | 243 | 1.09 | 0.04671 | 0.00059 | 0.09064 | 0.00249 | 0.01408 |
| CG410-18 | 456 | 701 | 0.65 | 0.04753 | 0.00106 | 0.09108 | 0.00356 | 0.01390 |
| CG410-19 | 164 | 228 | 0.72 | 0.04745 | 0.00124 | 0.09307 | 0.00403 | 0.01422 |
| CG410-20 | 548 | 724 | 0.76 | 0.04836 | 0.00048 | 0.09425 | 0.00216 | 0.01414 |
| CG410-21 | 375 | 500 | 0.75 | 0.04857 | 0.00051 | 0.09832 | 0.00235 | 0.01468 |
| CG410-22 | 554 | 333 | 1.66 | 0.04937 | 0.00056 | 0.09949 | 0.00253 | 0.01462 |
| CG410-23 | 722 | 823 | 0.88 | 0.04786 | 0.00048 | 0.09427 | 0.00215 | 0.01429 |
| CG410-24 | 574 | 732 | 0.78 | 0.04729 | 0.00127 | 0.09312 | 0.00403 | 0.01428 |
| *8-02-1 wt. mean = 67.8 ± 0.8 Ma (2σ); Average calculation except the young 4 components* | | | | | | | | |
| 8-02-1 01 | 202 | 142 | 1.43 | 0.04838 | 0.00153 | 0.07077 | 0.00352 | 0.01061 |
| 8-02-1 02 | 92 | 82 | 1.12 | 0.04941 | 0.00323 | 0.07436 | 0.00642 | 0.01091 |
| 8-02-1 04 | 432 | 381 | 1.13 | 0.04899 | 0.00072 | 0.07183 | 0.00218 | 0.01063 |
| 8-02-1 05 | 385 | 201 | 1.91 | 0.04762 | 0.00110 | 0.07005 | 0.00279 | 0.01067 |
| 8-02-1 07 | 567 | 355 | 1.60 | 0.05565 | 0.00577 | 0.08358 | 0.01030 | 0.01089 |
| 8-02-1 08 | 1849 | 1456 | 1.27 | 0.05037 | 0.00052 | 0.07414 | 0.00174 | 0.01068 |
| 8-02-1 09 | 1190 | 1226 | 0.97 | 0.04882 | 0.00060 | 0.07319 | 0.00198 | 0.01087 |
| 8-02-1 10 | 557 | 324 | 1.72 | 0.05357 | 0.00387 | 0.07458 | 0.00711 | 0.01010 |
| 8-02-1-11 | 622 | 396 | 1.57 | 0.05409 | 0.00115 | 0.07901 | 0.00309 | 0.01060 |
| 8-02-1-12 | 891 | 1198 | 0.74 | 0.05428 | 0.00158 | 0.07932 | 0.00356 | 0.01060 |
| 8-02-1-18 | 2196 | 2594 | 0.85 | 0.05549 | 0.00377 | 0.07712 | 0.00644 | 0.01008 |
| 8-02-1-19 | 332 | 242 | 1.37 | 0.04908 | 0.00103 | 0.07009 | 0.00266 | 0.01036 |

| ±1σ | $^{208}Pb/^{232}Th$ | ±1σ | $^{207}Pb/^{206}Pb$ | ±1σ | $^{207}Pb/^{235}U$ | ±1σ | $^{206}Pb/^{238}U$ | ±1σ | $^{208}Pb/^{232}Th$ | ±1σ |
|---|---|---|---|---|---|---|---|---|---|---|
| 0.00030 | 0.00462 | 0.00011 | 113 | 30 | 94 | 3 | 93 | 2 | 93 | 2 |
| 0.00035 | 0.00455 | 0.00009 | 194 | 115 | 96 | 6 | 92 | 2 | 92 | 2 |
| 0.00029 | 0.00455 | 0.00012 | 76 | 31 | 91 | 2 | 92 | 2 | 92 | 2 |
| 0.00030 | 0.00459 | 0.00013 | 6 | 38 | 89 | 3 | 92 | 2 | 93 | 3 |
| 0.00032 | 0.00464 | 0.00009 | 107 | 99 | 94 | 6 | 94 | 2 | 94 | 2 |
| 0.00030 | 0.00449 | 0.00012 | 47 | 33 | 91 | 3 | 93 | 2 | 91 | 2 |
| 0.00029 | 0.00450 | 0.00012 | 2 | 27 | 88 | 2 | 91 | 2 | 91 | 2 |
| 0.00029 | 0.00450 | 0.00010 | 132 | 31 | 93 | 2 | 91 | 2 | 91 | 2 |
| 0.00030 | 0.00461 | 0.00012 | 215 | 39 | 97 | 3 | 92 | 2 | 93 | 2 |
| 0.00029 | 0.00446 | 0.00010 | 106 | 27 | 91 | 2 | 91 | 2 | 90 | 2 |
| 0.00033 | 0.00475 | 0.00009 | 89 | 98 | 96 | 6 | 96 | 2 | 96 | 2 |
| 0.00029 | 0.00464 | 0.00012 | 206 | 31 | 96 | 3 | 91 | 2 | 94 | 2 |
| 0.00030 | 0.00457 | 0.00011 | 134 | 31 | 94 | 3 | 93 | 2 | 92 | 2 |
| 0.00030 | 0.00462 | 0.00012 | 121 | 31 | 94 | 2 | 93 | 2 | 93 | 2 |
| 0.00031 | 0.00464 | 0.00012 | 141 | 37 | 97 | 3 | 95 | 2 | 94 | 2 |
| 0.00030 | 0.00455 | 0.00012 | 114 | 41 | 93 | 3 | 92 | 2 | 92 | 2 |
| 0.00030 | 0.00451 | 0.00012 | 74 | 29 | 93 | 2 | 94 | 2 | 91 | 2 |
| 0.00030 | 0.00457 | 0.00013 | 22 | 35 | 89 | 3 | 92 | 2 | 92 | 3 |
| 0.00031 | 0.00472 | 0.00011 | −22 | 27 | 90 | 3 | 94 | 2 | 95 | 2 |
| 0.00031 | 0.00458 | 0.00008 | 96 | 63 | 92 | 4 | 92 | 2 | 92 | 2 |
| 0.00030 | 0.00454 | 0.00011 | 60 | 31 | 91 | 2 | 92 | 2 | 92 | 2 |
| 0.00029 | 0.00453 | 0.00011 | 195 | 30 | 95 | 3 | 91 | 2 | 91 | 2 |
| 0.00029 | 0.00473 | 0.00012 | 107 | 25 | 93 | 2 | 92 | 2 | 95 | 2 |
| 0.00028 | 0.00452 | 0.00011 | 98 | 24 | 90 | 2 | 90 | 2 | 91 | 2 |
| 0.00029 | 0.00462 | 0.00012 | 137 | 26 | 91 | 2 | 89 | 2 | 93 | 2 |
| 0.00030 | 0.00479 | 0.00012 | 239 | 23 | 99 | 2 | 94 | 2 | 97 | 2 |
| 0.00031 | 0.00475 | 0.00013 | 130 | 28 | 96 | 2 | 95 | 2 | 96 | 3 |
| 0.00029 | 0.00470 | 0.00013 | 117 | 24 | 92 | 2 | 91 | 2 | 95 | 3 |
| 0.00028 | 0.00426 | 0.00008 | 249 | 61 | 93 | 4 | 87 | 2 | 86 | 2 |
| 0.00029 | 0.00459 | 0.00011 | 201 | 27 | 96 | 2 | 92 | 2 | 93 | 2 |
| 0.00029 | 0.00467 | 0.00011 | 174 | 24 | 95 | 2 | 91 | 2 | 94 | 2 |
| 0.00029 | 0.00455 | 0.00011 | 77 | 24 | 90 | 2 | 91 | 2 | 92 | 2 |
| 0.00029 | 0.00443 | 0.00011 | 34 | 29 | 88 | 2 | 90 | 2 | 89 | 2 |
| 0.00029 | 0.00441 | 0.00008 | 76 | 50 | 89 | 3 | 89 | 2 | 89 | 2 |
| 0.00030 | 0.00452 | 0.00008 | 72 | 59 | 90 | 4 | 91 | 2 | 91 | 2 |
| 0.00028 | 0.00443 | 0.00011 | 117 | 24 | 91 | 2 | 91 | 2 | 89 | 2 |
| 0.00030 | 0.00459 | 0.00012 | 127 | 25 | 95 | 2 | 94 | 2 | 93 | 2 |
| 0.00030 | 0.00440 | 0.00011 | 165 | 26 | 96 | 2 | 94 | 2 | 89 | 2 |
| 0.00029 | 0.00444 | 0.00011 | 92 | 23 | 91 | 2 | 91 | 2 | 90 | 2 |
| 0.00031 | 0.00454 | 0.00009 | 64 | 60 | 90 | 4 | 91 | 2 | 92 | 2 |
| 0.00023 | 0.00346 | 0.00010 | 118 | 72 | 69 | 3 | 68 | 1 | 70 | 2 |
| 0.00027 | 0.00345 | 0.00008 | 167 | 147 | 73 | 6 | 70 | 2 | 70 | 2 |
| 0.00022 | 0.00332 | 0.00008 | 147 | 35 | 70 | 2 | 68 | 1 | 67 | 2 |
| 0.00022 | 0.00328 | 0.00008 | 80 | 53 | 69 | 3 | 68 | 1 | 66 | 2 |
| 0.00027 | 0.00339 | 0.00008 | 438 | 232 | 82 | 10 | 70 | 2 | 68 | 2 |
| 0.00021 | 0.00345 | 0.00008 | 212 | 24 | 73 | 2 | 68 | 1 | 70 | 2 |
| 0.00023 | 0.00329 | 0.00008 | 139 | 29 | 72 | 2 | 70 | 1 | 66 | 2 |
| 0.00027 | 0.00316 | 0.00006 | 353 | 159 | 73 | 7 | 65 | 2 | 64 | 1 |
| 0.00024 | 0.00333 | 0.00011 | 375 | 48 | 77 | 3 | 68 | 2 | 67 | 2 |
| 0.00022 | 0.00331 | 0.00006 | 383 | 65 | 78 | 3 | 68 | 1 | 67 | 1 |
| 0.00022 | 0.00314 | 0.00007 | 432 | 152 | 75 | 6 | 65 | 1 | 63 | 1 |
| 0.00022 | 0.00327 | 0.00011 | 152 | 49 | 69 | 3 | 66 | 1 | 66 | 2 |

(continued on next page)

**Table 2** (*continued*)

| Analysis No. | Th (ppm) | U (ppm) | Th/U | $^{207}Pb/^{206}Pb$ | ±1σ | $^{207}Pb/^{235}U$ | ±1σ | $^{206}Pb/^{238}U$ | ±1σ | $^{208}Pb/^{232}Th$ | ±1σ | $^{207}Pb/^{206}Pb$ | ±1σ | $^{207}Pb/^{235}U$ | ±1σ | $^{206}Pb/^{238}U$ | ±1σ | $^{208}Pb/^{232}Th$ | ±1σ |
|---|---|---|---|---|---|---|---|---|---|---|---|---|---|---|---|---|---|---|---|
| 8-02-1-21 | 204 | 200 | 1.02 | 0.05022 | 0.00123 | 0.07218 | 0.00301 | 0.01042 | 0.00022 | 0.00334 | 0.00012 | 205 | 56 | 71 | 3 | 67 | 1 | 67 | 2 |
| 8-02-1-22 | 118 | 126 | 0.94 | 0.04926 | 0.00170 | 0.07388 | 0.00391 | 0.01088 | 0.00024 | 0.00331 | 0.00014 | 160 | 79 | 72 | 4 | 70 | 2 | 67 | 3 |
| 8-02-1 23 | 413 | 356 | 1.16 | 0.05720 | 0.00188 | 0.08290 | 0.00454 | 0.01052 | 0.00028 | 0.00327 | 0.00016 | 499 | 74 | 81 | 4 | 67 | 2 | 66 | 3 |
| 8-02-1 24 | 1692 | 1892 | 0.89 | 0.05139 | 0.00059 | 0.07581 | 0.00198 | 0.01070 | 0.00023 | 0.00335 | 0.00010 | 258 | 27 | 74 | 2 | 69 | 1 | 68 | 2 |
| 8-02-1 06 (young) | 4630 | 1865 | 2.48 | 0.13443 | 0.00533 | 0.16200 | 0.00952 | 0.00874 | 0.00020 | 0.00248 | 0.00005 | 2157 | 69 | 152 | 8 | 56 | 1 | 50 | 1 |
| 8-02-1-14 (young) | 1134 | 373 | 3.04 | 0.12056 | 0.00969 | 0.12162 | 0.01279 | 0.00732 | 0.00022 | 0.00210 | 0.00005 | 1964 | 146 | 117 | 12 | 47 | 1 | 42 | 1 |
| 8-02-1-15 (young) | 1873 | 2163 | 0.87 | 0.05385 | 0.00833 | 0.05979 | 0.01029 | 0.00805 | 0.00020 | 0.00252 | 0.00020 | 365 | 326 | 59 | 10 | 52 | 1 | 51 | 4 |
| 8-02-1-16 (young) | 819 | 822 | 1.00 | 0.07003 | 0.01060 | 0.07751 | 0.01346 | 0.00803 | 0.00023 | 0.00244 | 0.00012 | 929 | 325 | 76 | 13 | 52 | 1 | 49 | 2 |
| *8-881/2 wt. mean = 92.9 ± 0.9 Ma (2σ)* | | | | | | | | | | | | | | | | | | | |
| 8-881/2 01 | 932 | 594 | 1.57 | 0.05320 | 0.00057 | 0.10300 | 0.00249 | 0.01404 | 0.00028 | 0.00464 | 0.00012 | 337 | 24 | 100 | 2 | 90 | 2 | 94 | 2 |
| 8-881/2 02 | 1435 | 616 | 2.33 | 0.04697 | 0.00051 | 0.09227 | 0.00225 | 0.01425 | 0.00028 | 0.00425 | 0.00011 | 48 | 26 | 90 | 2 | 91 | 2 | 86 | 2 |
| 8-881/2 03 | 769 | 391 | 1.96 | 0.04838 | 0.00060 | 0.09618 | 0.00259 | 0.01442 | 0.00029 | 0.00449 | 0.00012 | 118 | 29 | 93 | 2 | 92 | 2 | 91 | 2 |
| 8-881/2 04 | 428 | 306 | 1.40 | 0.05185 | 0.00069 | 0.10267 | 0.00288 | 0.01436 | 0.00029 | 0.00464 | 0.00013 | 279 | 30 | 99 | 3 | 92 | 2 | 94 | 3 |
| 8-881/2 05 | 990 | 706 | 1.40 | 0.04948 | 0.00052 | 0.09853 | 0.00234 | 0.01445 | 0.00029 | 0.00446 | 0.00012 | 171 | 24 | 95 | 2 | 92 | 2 | 90 | 2 |
| 8-881/2 06 | 1496 | 526 | 2.85 | 0.04985 | 0.00059 | 0.09724 | 0.00251 | 0.01415 | 0.00028 | 0.00449 | 0.00013 | 188 | 27 | 94 | 2 | 91 | 2 | 91 | 3 |
| 8-881/2 07 | 627 | 433 | 1.45 | 0.04840 | 0.00059 | 0.09542 | 0.00253 | 0.01430 | 0.00029 | 0.00448 | 0.00013 | 119 | 28 | 93 | 2 | 92 | 2 | 90 | 3 |
| 8-881/2 08 | 428 | 259 | 1.65 | 0.04793 | 0.00072 | 0.09612 | 0.00295 | 0.01455 | 0.00030 | 0.00451 | 0.00014 | 96 | 35 | 93 | 3 | 93 | 2 | 91 | 3 |
| 8-881/2 09 | 1216 | 807 | 1.51 | 0.04793 | 0.00054 | 0.09510 | 0.00238 | 0.01439 | 0.00029 | 0.00444 | 0.00014 | 96 | 26 | 92 | 2 | 92 | 2 | 90 | 3 |
| 8-881/2 10 | 2503 | 4558 | 0.55 | 0.05594 | 0.00109 | 0.11125 | 0.00425 | 0.01442 | 0.00035 | 0.00439 | 0.00032 | 450 | 44 | 107 | 4 | 92 | 2 | 89 | 6 |
| 8-881/2-11 | 1933 | 1216 | 1.59 | 0.04826 | 0.00045 | 0.10020 | 0.00213 | 0.01506 | 0.00029 | 0.00466 | 0.00011 | 112 | 22 | 97 | 2 | 96 | 2 | 94 | 2 |
| 8-881/2-12 | 1820 | 2168 | 0.84 | 0.05235 | 0.00176 | 0.10777 | 0.00544 | 0.01493 | 0.00033 | 0.00469 | 0.00009 | 301 | 78 | 104 | 5 | 96 | 2 | 94 | 2 |
| 8-881/2-13 | 1134 | 694 | 1.63 | 0.04787 | 0.00048 | 0.09587 | 0.00219 | 0.01453 | 0.00028 | 0.00452 | 0.00011 | 93 | 24 | 93 | 2 | 93 | 2 | 91 | 2 |
| 8-881/2-14 | 4662 | 1546 | 3.02 | 0.06237 | 0.00088 | 0.12820 | 0.00387 | 0.01491 | 0.00033 | 0.00461 | 0.00020 | 687 | 30 | 122 | 3 | 95 | 2 | 93 | 4 |
| 8-881/2-15 | 4123 | 1161 | 3.55 | 0.06841 | 0.00103 | 0.13347 | 0.00403 | 0.01415 | 0.00028 | 0.00459 | 0.00023 | 881 | 31 | 127 | 4 | 91 | 2 | 93 | 5 |
| 8-881/2-16 | 1745 | 816 | 2.14 | 0.04876 | 0.00048 | 0.10161 | 0.00228 | 0.01511 | 0.00029 | 0.00455 | 0.00012 | 136 | 23 | 98 | 2 | 97 | 2 | 92 | 2 |
| 8-881/2-17 | 666 | 572 | 1.16 | 0.04620 | 0.00146 | 0.09570 | 0.00422 | 0.01502 | 0.00029 | 0.00479 | 0.00012 | 8 | 65 | 93 | 4 | 96 | 2 | 97 | 2 |
| 8-881/2-18 | 1323 | 643 | 2.06 | 0.04853 | 0.00050 | 0.09638 | 0.00226 | 0.01440 | 0.00028 | 0.00450 | 0.00012 | 125 | 25 | 93 | 2 | 92 | 2 | 91 | 2 |
| *AH-2-11 wt. mean = 108.1 ± 1.3 Ma (2σ)* | | | | | | | | | | | | | | | | | | | |
| AH-2-11-01 | 250 | 238 | 1.05 | 0.05166 | 0.00067 | 0.12355 | 0.00337 | 0.01735 | 0.00034 | 0.00526 | 0.00015 | 270 | 30 | 118 | 3 | 111 | 2 | 106 | 3 |
| AH-2-11-02 | 390 | 312 | 1.25 | 0.05495 | 0.00086 | 0.13328 | 0.00411 | 0.01759 | 0.00035 | 0.00592 | 0.00024 | 410 | 35 | 127 | 4 | 112 | 2 | 119 | 5 |
| AH-2-11-03 | 86 | 135 | 0.64 | 0.05160 | 0.00089 | 0.12366 | 0.00408 | 0.01738 | 0.00035 | 0.00575 | 0.00020 | 268 | 39 | 118 | 4 | 111 | 2 | 116 | 4 |
| AH-2-11-04 | 136 | 202 | 0.67 | 0.05162 | 0.00071 | 0.12349 | 0.00352 | 0.01735 | 0.00034 | 0.00572 | 0.00018 | 269 | 32 | 118 | 3 | 111 | 2 | 115 | 4 |
| AH-2-11-05 | 627 | 448 | 1.40 | 0.05030 | 0.00054 | 0.12567 | 0.00301 | 0.01812 | 0.00035 | 0.00586 | 0.00014 | 209 | 25 | 120 | 3 | 116 | 2 | 118 | 3 |
| AH-2-11-06 | 1225 | 1236 | 0.99 | 0.05700 | 0.00185 | 0.13313 | 0.00624 | 0.01694 | 0.00033 | 0.00526 | 0.00009 | 491 | 72 | 127 | 6 | 108 | 2 | 106 | 2 |
| AH-2-11-07 | 380 | 363 | 1.05 | 0.05036 | 0.00057 | 0.12436 | 0.00313 | 0.01791 | 0.00035 | 0.00578 | 0.00015 | 212 | 26 | 119 | 3 | 114 | 2 | 116 | 3 |
| AH-2-11-08 | 457 | 553 | 0.83 | 0.05006 | 0.00174 | 0.12489 | 0.00617 | 0.01809 | 0.00036 | 0.00571 | 0.00010 | 198 | 80 | 119 | 6 | 116 | 2 | 115 | 2 |
| AH-2-11-09 | 606 | 736 | 0.82 | 0.04780 | 0.00049 | 0.11078 | 0.00258 | 0.01681 | 0.00032 | 0.00523 | 0.00015 | 89 | 24 | 107 | 2 | 107 | 2 | 105 | 3 |
| AH-2-11-10 | 329 | 401 | 0.82 | 0.04938 | 0.00057 | 0.11287 | 0.00286 | 0.01658 | 0.00032 | 0.00525 | 0.00015 | 166 | 27 | 109 | 3 | 106 | 2 | 106 | 3 |
| AH-2-11-11 | 335 | 883 | 0.38 | 0.04843 | 0.00093 | 0.10975 | 0.00386 | 0.01644 | 0.00034 | 0.00521 | 0.00010 | 120 | 45 | 106 | 4 | 105 | 2 | 105 | 2 |
| AH-2-11-12 | 249 | 472 | 0.53 | 0.04811 | 0.00054 | 0.10659 | 0.00265 | 0.01607 | 0.00031 | 0.00519 | 0.00015 | 105 | 26 | 103 | 2 | 103 | 2 | 105 | 3 |
| AH-2-11-13 | 343 | 782 | 0.44 | 0.04895 | 0.00049 | 0.10795 | 0.00247 | 0.01599 | 0.00031 | 0.00565 | 0.00016 | 145 | 24 | 104 | 2 | 102 | 2 | 114 | 3 |
| AH-2-11-14 | 695 | 766 | 0.91 | 0.05029 | 0.00051 | 0.11454 | 0.00262 | 0.01652 | 0.00032 | 0.00527 | 0.00015 | 208 | 24 | 110 | 2 | 106 | 2 | 106 | 3 |
| AH-2-11-15 | 653 | 1570 | 0.42 | 0.04980 | 0.00060 | 0.11574 | 0.00309 | 0.01686 | 0.00035 | 0.00561 | 0.00022 | 186 | 28 | 111 | 3 | 108 | 2 | 113 | 4 |
| AH-2-11-16 | 514 | 849 | 0.61 | 0.05115 | 0.00057 | 0.12009 | 0.00303 | 0.01703 | 0.00035 | 0.00536 | 0.00019 | 248 | 26 | 115 | 3 | 109 | 2 | 108 | 4 |
| AH-2-11-17 | 171 | 282 | 0.61 | 0.05029 | 0.00065 | 0.11716 | 0.00322 | 0.01690 | 0.00034 | 0.00564 | 0.00015 | 208 | 30 | 112 | 3 | 108 | 2 | 114 | 3 |
| AH-2-11-18 | 122 | 409 | 0.30 | 0.04864 | 0.00055 | 0.11189 | 0.00282 | 0.01669 | 0.00033 | 0.00542 | 0.00016 | 131 | 26 | 108 | 3 | 107 | 2 | 109 | 3 |
| AH-2-11-19 | 776 | 1618 | 0.48 | 0.04838 | 0.00104 | 0.11121 | 0.00418 | 0.01667 | 0.00035 | 0.00528 | 0.00010 | 118 | 50 | 107 | 4 | 107 | 2 | 107 | 2 |
| AH-2-11-20 | 618 | 591 | 1.04 | 0.04970 | 0.00052 | 0.11634 | 0.00275 | 0.01698 | 0.00033 | 0.00532 | 0.00014 | 181 | 24 | 112 | 3 | 109 | 2 | 107 | 3 |
| AH-2-11-21 | 368 | 662 | 0.56 | 0.04874 | 0.00051 | 0.11422 | 0.00270 | 0.01700 | 0.00033 | 0.00552 | 0.00015 | 135 | 24 | 110 | 2 | 109 | 2 | 111 | 3 |
| AH-2-11-22 | 203 | 301 | 0.67 | 0.04898 | 0.00064 | 0.11300 | 0.00313 | 0.01674 | 0.00033 | 0.00535 | 0.00016 | 147 | 31 | 109 | 3 | 107 | 2 | 108 | 3 |

Please cite this article in press as: Jahn, B.-m., et al. Emplacement ages, geochemical and Sr–Nd–Hf isotopic characterization of Mesozoic to early Cenozoic granitoids of the Sikhote-Alin Orogenic Belt, Russian Far East: Crustal growth and regional tectonic evolution. Journal of Asian Earth Sciences (2015), http://dx.doi.org/10.1016/j.jseaes.2015.08.012

**Table 2** (*continued*)

| Analysis No. | Th (ppm) | U (ppm) | Th/U | $^{207}Pb/^{206}Pb$ | ±1σ | $^{207}Pb/^{235}U$ | ±1σ | $^{206}Pb/^{238}U$ | ±1σ | $^{208}Pb/^{232}Th$ | ±1σ | $^{207}Pb/^{206}Pb$ | ±1σ | $^{207}Pb/^{235}U$ | ±1σ | $^{206}Pb/^{238}U$ | ±1σ | $^{208}Pb/^{232}Th$ | ±1σ |
|---|---|---|---|---|---|---|---|---|---|---|---|---|---|---|---|---|---|---|---|
| AH-2-11-23 | 208 | 224 | 0.93 | 0.05534 | 0.00116 | 0.13288 | 0.00515 | 0.01742 | 0.00039 | 0.00550 | 0.00022 | 426 | 47 | 127 | 5 | 111 | 2 | 111 | 4 |
| AH-2-11-24 | 273 | 299 | 0.91 | 0.04967 | 0.00185 | 0.11414 | 0.00611 | 0.01667 | 0.00035 | 0.00527 | 0.00009 | 179 | 85 | 110 | 6 | 107 | 2 | 106 | 2 |
| *AH-3-11 wt. mean = 57.8 ± 1.1 Ma (2σ)* | | | | | | | | | | | | | | | | | | | |
| AH-3-11-02 | 2596 | 1206 | 2.15 | 0.07034 | 0.00088 | 0.08762 | 0.00240 | 0.00904 | 0.00019 | 0.00176 | 0.00007 | 938 | 26 | 85 | 2 | 58 | 1 | 36 | 1 |
| AH-3-11-03 | 337 | 280 | 1.20 | 0.06071 | 0.00115 | 0.07865 | 0.00280 | 0.00940 | 0.00020 | 0.00302 | 0.00011 | 629 | 41 | 77 | 3 | 60 | 1 | 61 | 2 |
| AH-3-11-04 | 127 | 55 | 2.32 | 0.10227 | 0.00349 | 0.13253 | 0.00742 | 0.00940 | 0.00025 | 0.00286 | 0.00011 | 1666 | 63 | 126 | 7 | 60 | 2 | 58 | 2 |
| AH-3-11-05 | 1906 | 925 | 2.06 | 0.06018 | 0.00068 | 0.07324 | 0.00183 | 0.00883 | 0.00017 | 0.00245 | 0.00008 | 610 | 25 | 72 | 2 | 57 | 1 | 49 | 2 |
| AH-3-11-06 | 162 | 178 | 0.91 | 0.04773 | 0.00204 | 0.05957 | 0.00363 | 0.00905 | 0.00020 | 0.00287 | 0.00007 | 86 | 94 | 59 | 3 | 58 | 1 | 58 | 1 |
| AH-3-11-07 | 2879 | 3519 | 0.82 | 0.05478 | 0.00057 | 0.06646 | 0.00158 | 0.00880 | 0.00018 | 0.00217 | 0.00006 | 403 | 23 | 65 | 2 | 56 | 1 | 44 | 1 |
| AH-3-11-08 | 1343 | 4205 | 0.32 | 0.04695 | 0.00044 | 0.05744 | 0.00123 | 0.00887 | 0.00017 | 0.00288 | 0.00007 | 47 | 23 | 57 | 1 | 57 | 1 | 58 | 1 |
| AH-3-11-09 | 4321 | 5606 | 0.77 | 0.04840 | 0.00056 | 0.06060 | 0.00151 | 0.00908 | 0.00017 | 0.00292 | 0.00013 | 119 | 27 | 60 | 1 | 58 | 1 | 59 | 3 |
| *8-11-54/1 wt. mean of most concentrated part = 131.4 ± 2.0 Ma (2σ)* | | | | | | | | | | | | | | | | | | | |
| 8-11-54/1-01 | 121 | 91 | 1.33 | 0.05285 | 0.00105 | 0.19018 | 0.00692 | 0.02610 | 0.00054 | 0.00869 | 0.00026 | 322 | 45 | 177 | 6 | 166 | 3 | 175 | 5 |
| 8-11-54/1-02 | 98 | 261 | 0.37 | 0.05054 | 0.00066 | 0.14401 | 0.00397 | 0.02067 | 0.00041 | 0.00673 | 0.00022 | 220 | 31 | 137 | 4 | 132 | 3 | 136 | 4 |
| 8-11-54/1-03 | 135 | 264 | 0.51 | 0.05096 | 0.00067 | 0.14201 | 0.00394 | 0.02021 | 0.00040 | 0.00658 | 0.00020 | 239 | 30 | 135 | 4 | 129 | 3 | 133 | 4 |
| 8-11-54/1-04 | 58 | 51 | 1.14 | 0.04945 | 0.00246 | 0.16221 | 0.01154 | 0.02379 | 0.00060 | 0.00738 | 0.00038 | 169 | 113 | 153 | 10 | 152 | 4 | 149 | 8 |
| 8-11-54/1-05 | 175 | 88 | 1.98 | 0.05500 | 0.00083 | 0.41681 | 0.01259 | 0.05497 | 0.00109 | 0.01711 | 0.00058 | 412 | 34 | 354 | 9 | 345 | 7 | 343 | 12 |
| 8-11-54/1-06 | 76 | 331 | 0.23 | 0.05062 | 0.00092 | 0.14299 | 0.00486 | 0.02049 | 0.00042 | 0.00646 | 0.00013 | 223 | 43 | 136 | 4 | 131 | 3 | 130 | 3 |
| 8-11-54/1-07 | 195 | 175 | 1.12 | 0.05043 | 0.00074 | 0.17002 | 0.00508 | 0.02445 | 0.00049 | 0.00800 | 0.00025 | 215 | 34 | 159 | 4 | 156 | 3 | 161 | 5 |
| 8-11-54/1-08 | 219 | 291 | 0.75 | 0.05487 | 0.00071 | 0.46261 | 0.01285 | 0.06115 | 0.00124 | 0.02174 | 0.00098 | 407 | 29 | 386 | 9 | 383 | 8 | 435 | 19 |
| 8-11-54/1-09 | 90 | 157 | 0.57 | 0.10777 | 0.00121 | 2.93315 | 0.07236 | 0.19740 | 0.00366 | 0.05720 | 0.00104 | 1762 | 21 | 1391 | 19 | 1161 | 20 | 1124 | 20 |
| 8-11-54/1-10 | 200 | 325 | 0.62 | 0.05514 | 0.00050 | 0.49987 | 0.01046 | 0.06575 | 0.00126 | 0.02127 | 0.00050 | 418 | 20 | 412 | 7 | 410 | 8 | 425 | 10 |
| 8-11-54/1-11 | 46 | 180 | 0.26 | 0.05066 | 0.00061 | 0.14485 | 0.00384 | 0.02074 | 0.00042 | 0.00687 | 0.00021 | 225 | 28 | 137 | 3 | 132 | 3 | 138 | 4 |
| 8-11-54/1-12 | 94 | 403 | 0.23 | 0.05132 | 0.00072 | 0.14505 | 0.00435 | 0.02050 | 0.00045 | 0.00688 | 0.00026 | 255 | 33 | 138 | 4 | 131 | 3 | 139 | 5 |
| 8-11-54/1-13 | 47 | 343 | 0.14 | 0.04909 | 0.00057 | 0.15083 | 0.00393 | 0.02229 | 0.00046 | 0.01027 | 0.00034 | 152 | 28 | 143 | 3 | 142 | 3 | 207 | 7 |
| 8-11-54/1-14 | 170 | 227 | 0.75 | 0.05030 | 0.00134 | 0.14335 | 0.00623 | 0.02067 | 0.00043 | 0.00652 | 0.00012 | 209 | 61 | 136 | 6 | 132 | 3 | 131 | 2 |
| 8-11-54/1-15 | 116 | 189 | 0.61 | 0.04961 | 0.00060 | 0.14486 | 0.00380 | 0.02118 | 0.00042 | 0.00718 | 0.00019 | 177 | 28 | 137 | 3 | 135 | 3 | 145 | 4 |
| 8-11-54/1-16 | 113 | 504 | 0.22 | 0.04948 | 0.00078 | 0.13890 | 0.00420 | 0.02036 | 0.00040 | 0.00644 | 0.00013 | 171 | 36 | 132 | 4 | 130 | 3 | 130 | 3 |
| 8-11-54/1-17 | 208 | 315 | 0.66 | 0.05059 | 0.00051 | 0.20338 | 0.00468 | 0.02915 | 0.00057 | 0.01062 | 0.00028 | 222 | 24 | 188 | 4 | 185 | 4 | 214 | 6 |
| 8-11-54/1-18 | 123 | 137 | 0.90 | 0.05228 | 0.00070 | 0.23854 | 0.00670 | 0.03309 | 0.00066 | 0.01060 | 0.00035 | 298 | 31 | 217 | 5 | 210 | 4 | 213 | 7 |
| 8-11-54/1-19 | 104 | 242 | 0.43 | 0.05002 | 0.00057 | 0.14109 | 0.00358 | 0.02046 | 0.00041 | 0.00674 | 0.00020 | 196 | 27 | 134 | 3 | 131 | 3 | 136 | 4 |
| 8-11-54/1-20 | 108 | 349 | 0.31 | 0.10972 | 0.00107 | 3.42503 | 0.07664 | 0.22642 | 0.00455 | 0.06147 | 0.00212 | 1795 | 18 | 1510 | 18 | 1316 | 24 | 1206 | 40 |
| *8-11-51/3 wt. mean = 108.1 ± 1.1 Ma (2σ)* | | | | | | | | | | | | | | | | | | | |
| 8-11-51/3 01 | 283 | 179 | 1.58 | 0.04829 | 0.00070 | 0.11069 | 0.00329 | 0.01663 | 0.00034 | 0.00514 | 0.00013 | 114 | 34 | 107 | 3 | 106 | 2 | 104 | 3 |
| 8-11-51/3 02 | 135 | 106 | 1.28 | 0.05103 | 0.00092 | 0.11941 | 0.00407 | 0.01697 | 0.00035 | 0.00531 | 0.00014 | 242 | 41 | 115 | 4 | 108 | 2 | 107 | 3 |
| 8-11-51/3 03 | 107 | 82 | 1.32 | 0.04943 | 0.00111 | 0.11680 | 0.00460 | 0.01714 | 0.00036 | 0.00541 | 0.00015 | 168 | 52 | 112 | 4 | 110 | 2 | 109 | 3 |
| 8-11-51/3 04 | 154 | 93 | 1.66 | 0.05051 | 0.00103 | 0.11626 | 0.00432 | 0.01670 | 0.00035 | 0.00540 | 0.00015 | 219 | 48 | 112 | 4 | 107 | 2 | 109 | 3 |
| 8-11-51/3 05 | 233 | 121 | 1.94 | 0.05076 | 0.00085 | 0.11875 | 0.00389 | 0.01697 | 0.00035 | 0.00536 | 0.00014 | 230 | 39 | 114 | 4 | 108 | 2 | 108 | 3 |
| 8-11-51/3 06 | 118 | 87 | 1.36 | 0.04899 | 0.00244 | 0.11455 | 0.00779 | 0.01696 | 0.00038 | 0.00537 | 0.00010 | 147 | 113 | 110 | 7 | 108 | 2 | 108 | 2 |
| 8-11-51/3 07 | 146 | 124 | 1.18 | 0.04903 | 0.00113 | 0.11571 | 0.00473 | 0.01712 | 0.00038 | 0.00555 | 0.00018 | 149 | 54 | 111 | 4 | 109 | 2 | 112 | 4 |
| 8-11-51/3 08 | 157 | 127 | 1.24 | 0.04922 | 0.00084 | 0.11861 | 0.00388 | 0.01748 | 0.00035 | 0.00553 | 0.00016 | 158 | 41 | 114 | 4 | 112 | 2 | 111 | 3 |
| 8-11-51/3 09 | 334 | 180 | 1.86 | 0.04915 | 0.00069 | 0.11595 | 0.00334 | 0.01711 | 0.00034 | 0.00544 | 0.00015 | 155 | 33 | 111 | 3 | 109 | 2 | 110 | 3 |
| 8-11-51/3 10 | 120 | 88 | 1.36 | 0.04805 | 0.00218 | 0.11578 | 0.00773 | 0.01748 | 0.00044 | 0.00623 | 0.00035 | 102 | 100 | 111 | 7 | 112 | 3 | 126 | 7 |
| 8-11-51/3 11 | 372 | 213 | 1.75 | 0.04856 | 0.00081 | 0.11417 | 0.00375 | 0.01705 | 0.00036 | 0.00521 | 0.00017 | 127 | 39 | 110 | 3 | 109 | 2 | 105 | 3 |
| 8-11-51/3 12 | 191 | 121 | 1.58 | 0.05304 | 0.00112 | 0.12355 | 0.00476 | 0.01690 | 0.00037 | 0.00526 | 0.00018 | 331 | 48 | 118 | 4 | 108 | 2 | 106 | 4 |
| 8-11-51/3 13 | 170 | 140 | 1.21 | 0.04873 | 0.00077 | 0.11681 | 0.00366 | 0.01739 | 0.00035 | 0.00542 | 0.00014 | 135 | 38 | 112 | 3 | 111 | 2 | 109 | 3 |
| 8-11-51/3 14 | 261 | 148 | 1.77 | 0.04893 | 0.00077 | 0.11718 | 0.00366 | 0.01737 | 0.00035 | 0.00542 | 0.00013 | 144 | 37 | 113 | 3 | 111 | 2 | 109 | 3 |
| 8-11-51/3 15 | 110 | 95 | 1.16 | 0.04812 | 0.00104 | 0.11130 | 0.00427 | 0.01678 | 0.00035 | 0.00549 | 0.00015 | 105 | 51 | 107 | 4 | 107 | 2 | 111 | 3 |
| 8-11-51/3 16 | 198 | 185 | 1.07 | 0.04974 | 0.00067 | 0.12152 | 0.00343 | 0.01772 | 0.00035 | 0.00564 | 0.00014 | 183 | 32 | 116 | 3 | 113 | 2 | 114 | 3 |
| 8-11-51/3 17 | 299 | 170 | 1.76 | 0.05236 | 0.00072 | 0.12186 | 0.00351 | 0.01688 | 0.00034 | 0.00528 | 0.00013 | 301 | 31 | 117 | 3 | 108 | 2 | 106 | 3 |
| 8-11-51/3 19 | 300 | 165 | 1.82 | 0.05037 | 0.00308 | 0.11494 | 0.00899 | 0.01655 | 0.00036 | 0.00522 | 0.00009 | 212 | 139 | 110 | 8 | 106 | 2 | 105 | 2 |
| 8-11-51/3 20 | 160 | 144 | 1.11 | 0.04984 | 0.00210 | 0.11311 | 0.00677 | 0.01646 | 0.00036 | 0.00520 | 0.00009 | 187 | 97 | 109 | 6 | 105 | 2 | 105 | 2 |
| 8-11-51/3 21 | 401 | 226 | 1.77 | 0.05016 | 0.00065 | 0.11311 | 0.00308 | 0.01636 | 0.00032 | 0.00514 | 0.00014 | 202 | 30 | 109 | 3 | 105 | 2 | 104 | 3 |

(*continued on next page*)

Please cite this article in press as: Jahn, B.-m., et al. Emplacement ages, geochemical and Sr–Nd–Hf isotopic characterization of Mesozoic to early Cenozoic granitoids of the Sikhote-Alin Orogenic Belt, Russian Far East: Crustal growth and regional tectonic evolution. Journal of Asian Earth Sciences (2015), http://dx.doi.org/10.1016/j.jseaes.2015.08.012

**Table 2** (*continued*)

| Analysis No. | Th (ppm) | U (ppm) | Th/U | $^{207}Pb/^{206}Pb$ | ±1σ | $^{207}Pb/^{235}U$ | ±1σ | $^{206}Pb/^{238}U$ | ±1σ | $^{208}Pb/^{232}Th$ | ±1σ | $^{207}Pb/^{206}Pb$ | ±1σ | $^{207}Pb/^{235}U$ | ±1σ | $^{206}Pb/^{238}U$ | ±1σ | $^{208}Pb/^{232}Th$ | ±1σ |
|---|---|---|---|---|---|---|---|---|---|---|---|---|---|---|---|---|---|---|---|
| 8-11-51/3 22 | 133 | 100 | 1.32 | 0.05012 | 0.00107 | 0.11258 | 0.00429 | 0.01629 | 0.00034 | 0.00524 | 0.00016 | 201 | 50 | 108 | 4 | 104 | 2 | 106 | 3 |
| 8-11-51/3 23 | 183 | 177 | 1.04 | 0.04921 | 0.00073 | 0.11259 | 0.00337 | 0.01659 | 0.00033 | 0.00540 | 0.00016 | 158 | 35 | 108 | 3 | 106 | 2 | 109 | 3 |
| 8-11-51/3 24 | 229 | 198 | 1.16 | 0.05042 | 0.00069 | 0.11415 | 0.00326 | 0.01642 | 0.00033 | 0.00526 | 0.00015 | 214 | 31 | 110 | 3 | 105 | 2 | 106 | 3 |
| *8-871/1 wt. mean = 108.8 ± 0.8 Ma (2σ)* | | | | | | | | | | | | | | | | | | | |
| 8-871-1 01 | 181 | 241 | 0.75 | 0.05109 | 0.00063 | 0.12032 | 0.00322 | 0.01708 | 0.00034 | 0.00540 | 0.00014 | 245 | 28 | 115 | 3 | 109 | 2 | 109 | 3 |
| 8-871-1 02 | 190 | 264 | 0.72 | 0.04813 | 0.00060 | 0.11245 | 0.00299 | 0.01695 | 0.00033 | 0.00516 | 0.00013 | 106 | 29 | 108 | 3 | 108 | 2 | 104 | 3 |
| 8-871-1 03 | 230 | 309 | 0.74 | 0.04804 | 0.00057 | 0.11219 | 0.00288 | 0.01694 | 0.00033 | 0.00523 | 0.00014 | 101 | 28 | 108 | 3 | 108 | 2 | 105 | 3 |
| 8-871-1 04 | 318 | 370 | 0.86 | 0.04966 | 0.00055 | 0.11607 | 0.00287 | 0.01695 | 0.00033 | 0.00534 | 0.00014 | 179 | 26 | 112 | 3 | 108 | 2 | 108 | 3 |
| 8-871-1 05 | 142 | 188 | 0.76 | 0.04846 | 0.00070 | 0.11319 | 0.00336 | 0.01694 | 0.00034 | 0.00528 | 0.00015 | 122 | 34 | 109 | 3 | 108 | 2 | 106 | 3 |
| 8-871-1 06 | 146 | 161 | 0.91 | 0.04951 | 0.00076 | 0.11478 | 0.00354 | 0.01682 | 0.00034 | 0.00536 | 0.00015 | 172 | 36 | 110 | 3 | 108 | 2 | 108 | 3 |
| 8-871-1 07 | 482 | 931 | 0.52 | 0.04983 | 0.00060 | 0.11643 | 0.00308 | 0.01695 | 0.00035 | 0.00519 | 0.00018 | 187 | 28 | 112 | 3 | 108 | 2 | 105 | 4 |
| 8-871-1 08 | 493 | 903 | 0.55 | 0.04853 | 0.00056 | 0.11544 | 0.00295 | 0.01725 | 0.00035 | 0.00468 | 0.00016 | 125 | 27 | 111 | 3 | 110 | 2 | 94 | 3 |
| 8-871-1 09 | 198 | 277 | 0.72 | 0.05192 | 0.00064 | 0.12413 | 0.00330 | 0.01734 | 0.00034 | 0.00539 | 0.00016 | 282 | 28 | 119 | 3 | 111 | 2 | 109 | 3 |
| 8-871-1 10 | 266 | 398 | 0.67 | 0.04924 | 0.00055 | 0.11764 | 0.00294 | 0.01733 | 0.00034 | 0.00541 | 0.00016 | 159 | 26 | 113 | 3 | 111 | 2 | 109 | 3 |
| 8-871-1 11 | 240 | 314 | 0.77 | 0.04908 | 0.00078 | 0.11338 | 0.00361 | 0.01676 | 0.00035 | 0.00546 | 0.00020 | 152 | 37 | 109 | 3 | 107 | 2 | 110 | 4 |
| 8-871-1 12 | 701 | 846 | 0.83 | 0.05068 | 0.00053 | 0.11829 | 0.00280 | 0.01693 | 0.00033 | 0.00542 | 0.00017 | 226 | 24 | 114 | 3 | 108 | 2 | 109 | 3 |
| 8-871-1 13 | 216 | 279 | 0.77 | 0.04938 | 0.00060 | 0.11553 | 0.00307 | 0.01697 | 0.00034 | 0.00552 | 0.00015 | 166 | 28 | 111 | 3 | 108 | 2 | 111 | 3 |
| 8-871-1 14 | 419 | 546 | 0.77 | 0.05091 | 0.00093 | 0.11834 | 0.00427 | 0.01686 | 0.00039 | 0.00479 | 0.00019 | 237 | 42 | 114 | 4 | 108 | 2 | 97 | 4 |
| 8-871-1 15 | 305 | 349 | 0.87 | 0.04958 | 0.00056 | 0.11889 | 0.00297 | 0.01739 | 0.00034 | 0.00545 | 0.00014 | 175 | 26 | 114 | 3 | 111 | 2 | 110 | 3 |
| 8-871-1 16 | 715 | 860 | 0.83 | 0.04943 | 0.00144 | 0.11739 | 0.00530 | 0.01722 | 0.00036 | 0.00544 | 0.00010 | 169 | 68 | 113 | 5 | 110 | 2 | 110 | 2 |
| 8-871-1 17 | 268 | 349 | 0.77 | 0.04953 | 0.00057 | 0.11482 | 0.00291 | 0.01681 | 0.00033 | 0.00550 | 0.00014 | 173 | 27 | 110 | 3 | 107 | 2 | 111 | 3 |
| 8-871-1 18 | 160 | 191 | 0.84 | 0.05171 | 0.00072 | 0.12175 | 0.00351 | 0.01708 | 0.00034 | 0.00555 | 0.00015 | 273 | 32 | 117 | 3 | 109 | 2 | 112 | 3 |
| 8-871-1 19 | 358 | 313 | 1.14 | 0.05743 | 0.00066 | 0.13468 | 0.00342 | 0.01701 | 0.00034 | 0.00504 | 0.00013 | 508 | 25 | 128 | 3 | 109 | 2 | 102 | 3 |
| 8-871-1 20 | 203 | 236 | 0.86 | 0.04850 | 0.00066 | 0.11479 | 0.00324 | 0.01717 | 0.00034 | 0.00562 | 0.00016 | 124 | 32 | 110 | 3 | 110 | 2 | 113 | 3 |
| 8-871-1 21 | 196 | 284 | 0.69 | 0.04814 | 0.00060 | 0.11228 | 0.00303 | 0.01692 | 0.00034 | 0.00528 | 0.00015 | 106 | 29 | 108 | 3 | 108 | 2 | 106 | 3 |
| 8-871-1 22 | 325 | 349 | 0.93 | 0.05829 | 0.00073 | 0.13749 | 0.00374 | 0.01711 | 0.00035 | 0.00559 | 0.00017 | 541 | 27 | 131 | 3 | 109 | 2 | 113 | 3 |
| 8-871-1 23 | 213 | 245 | 0.87 | 0.05421 | 0.00068 | 0.12954 | 0.00350 | 0.01733 | 0.00035 | 0.00549 | 0.00016 | 380 | 28 | 124 | 3 | 111 | 2 | 111 | 3 |
| 8-871-1 24 | 217 | 245 | 0.89 | 0.04994 | 0.00066 | 0.11591 | 0.00324 | 0.01684 | 0.00034 | 0.00511 | 0.00015 | 192 | 31 | 111 | 3 | 108 | 2 | 103 | 3 |
| *8-872/1 wt. mean = 105.9 ± 1.0 Ma (2σ)* | | | | | | | | | | | | | | | | | | | |
| 8-872-1 01 | 196 | 163 | 1.20 | 0.05302 | 0.00079 | 0.12138 | 0.00363 | 0.01660 | 0.00033 | 0.00536 | 0.00014 | 330 | 33 | 116 | 3 | 106 | 2 | 108 | 3 |
| 8-872-1 02 | 134 | 120 | 1.12 | 0.04756 | 0.00092 | 0.11096 | 0.00391 | 0.01692 | 0.00034 | 0.00545 | 0.00015 | 77 | 45 | 107 | 4 | 108 | 2 | 110 | 3 |
| 8-872-1 03 | 297 | 198 | 1.50 | 0.05236 | 0.00098 | 0.12039 | 0.00423 | 0.01668 | 0.00035 | 0.00519 | 0.00017 | 301 | 42 | 115 | 4 | 107 | 2 | 105 | 3 |
| 8-872-1 04 | 214 | 179 | 1.20 | 0.05411 | 0.00075 | 0.12414 | 0.00357 | 0.01664 | 0.00033 | 0.00535 | 0.00014 | 376 | 31 | 119 | 3 | 106 | 2 | 108 | 3 |
| 8-872-1 05 | 110 | 107 | 1.03 | 0.04758 | 0.00231 | 0.10899 | 0.00718 | 0.01662 | 0.00038 | 0.00528 | 0.00014 | 78 | 105 | 105 | 7 | 106 | 2 | 106 | 3 |
| 8-872-1 06 | 290 | 206 | 1.41 | 0.05162 | 0.00248 | 0.11732 | 0.00764 | 0.01648 | 0.00035 | 0.00518 | 0.00009 | 269 | 110 | 113 | 7 | 105 | 2 | 104 | 2 |
| 8-872-1 07 | 493 | 462 | 1.07 | 0.05009 | 0.00062 | 0.11676 | 0.00313 | 0.01691 | 0.00034 | 0.00544 | 0.00018 | 199 | 29 | 112 | 3 | 108 | 2 | 110 | 4 |
| 8-872-1 08 | 183 | 146 | 1.26 | 0.05317 | 0.00086 | 0.12358 | 0.00393 | 0.01686 | 0.00034 | 0.00543 | 0.00016 | 336 | 37 | 118 | 4 | 108 | 2 | 109 | 3 |
| 8-872-1 09 | 186 | 159 | 1.17 | 0.05045 | 0.00230 | 0.11557 | 0.00719 | 0.01661 | 0.00036 | 0.00524 | 0.00009 | 216 | 103 | 111 | 7 | 106 | 2 | 106 | 2 |
| 8-872-1 10 | 251 | 203 | 1.24 | 0.05081 | 0.00076 | 0.12084 | 0.00366 | 0.01725 | 0.00035 | 0.00564 | 0.00018 | 232 | 35 | 116 | 3 | 110 | 2 | 114 | 4 |
| 8-872-1 11 | 346 | 259 | 1.34 | 0.05065 | 0.00123 | 0.12116 | 0.00519 | 0.01735 | 0.00040 | 0.00558 | 0.00027 | 225 | 56 | 116 | 5 | 111 | 3 | 112 | 5 |
| 8-872-1 12 | 274 | 193 | 1.42 | 0.04886 | 0.00265 | 0.11112 | 0.00786 | 0.01649 | 0.00037 | 0.00522 | 0.00011 | 141 | 123 | 107 | 7 | 105 | 2 | 105 | 2 |
| 8-872-1 13 | 142 | 138 | 1.03 | 0.05023 | 0.00099 | 0.11720 | 0.00423 | 0.01692 | 0.00035 | 0.00563 | 0.00016 | 206 | 44 | 113 | 4 | 108 | 2 | 113 | 3 |
| 8-872-1 14 | 245 | 167 | 1.47 | 0.04701 | 0.00099 | 0.10659 | 0.00401 | 0.01645 | 0.00034 | 0.00524 | 0.00015 | 50 | 47 | 103 | 4 | 105 | 2 | 106 | 3 |
| 8-872-1 15 | 987 | 933 | 1.06 | 0.04854 | 0.00053 | 0.10720 | 0.00263 | 0.01602 | 0.00032 | 0.00507 | 0.00014 | 126 | 26 | 103 | 2 | 102 | 2 | 102 | 3 |
| 8-872-1 16 | 257 | 194 | 1.33 | 0.05420 | 0.00105 | 0.12659 | 0.00457 | 0.01694 | 0.00036 | 0.00546 | 0.00018 | 379 | 43 | 121 | 4 | 108 | 2 | 110 | 4 |
| 8-872-1 17 | 140 | 104 | 1.34 | 0.05147 | 0.00125 | 0.11392 | 0.00473 | 0.01605 | 0.00034 | 0.00528 | 0.00016 | 262 | 55 | 110 | 4 | 103 | 2 | 106 | 3 |
| 8-872-1 18 | 151 | 140 | 1.08 | 0.05300 | 0.00100 | 0.11712 | 0.00412 | 0.01603 | 0.00033 | 0.00530 | 0.00016 | 329 | 44 | 112 | 4 | 103 | 2 | 107 | 3 |
| 8-872-1 19 | 159 | 120 | 1.32 | 0.05135 | 0.00113 | 0.11345 | 0.00439 | 0.01603 | 0.00033 | 0.00485 | 0.00016 | 257 | 51 | 109 | 4 | 103 | 2 | 98 | 3 |
| 8-872-1 20 | 262 | 200 | 1.31 | 0.05255 | 0.00079 | 0.11870 | 0.00360 | 0.01638 | 0.00033 | 0.00528 | 0.00016 | 309 | 34 | 114 | 3 | 105 | 2 | 106 | 3 |
| 8-872-1 21 | 173 | 153 | 1.14 | 0.04889 | 0.00095 | 0.10960 | 0.00389 | 0.01626 | 0.00033 | 0.00518 | 0.00017 | 143 | 45 | 106 | 4 | 104 | 2 | 104 | 3 |

Please cite this article in press as: Jahn, B.-m., et al. Emplacement ages, geochemical and Sr–Nd–Hf isotopic characterization of Mesozoic to early Cenozoic granitoids of the Sikhote-Alin Orogenic Belt, Russian Far East: Crustal growth and regional tectonic evolution. Journal of Asian Earth Sciences (2015), http://dx.doi.org/10.1016/j.jseaes.2015.08.012

**Table 3**
Chemical data for Mesozoic and Early Cenozoic granitoids from Sikhote-Alin.

| Sample No. | B-300 | B-257 | B-433 | B-494 | B-720 | B-574 | B-611 | B-781 | B-909A | B-995 | GV-722 | GV-1401 | GV-1583-2 | GV-1774 | ЧG-332 | ЧG-410 | 2/8/2001 | 8-881/2 | AN-2-11 | AN-3-11 | 8-11-54/1 | 8-11-51/3 | 8-871/1 | 8-872/1 |
|---|---|---|---|---|---|---|---|---|---|---|---|---|---|---|---|---|---|---|---|---|---|---|---|---|
| Rock-type | Quartz monzodiorite | Alkali feldspar granite | Granodiorite | Granodiorite | Granite | Granite | Granodiorite | Granite | Granite | Granite | Granite | Granite | Granite | Granite | Granite | Granite | Alkali feldspar granite | Granodiorite | Granite | Alkali feldspar granite | Granite | Qtz monzodiorite | Granodiorite | Granodiorite |
| *Major element (in %)* | | | | | | | | | | | | | | | | | | | | | | | | |
| SiO2 | 59.74 | 74.06 | 68.96 | 70.16 | 72.57 | 71.49 | 64.54 | 69.87 | 65.66 | 72.45 | 69.35 | 67.48 | 74.41 | 73.07 | 69.90 | 72.86 | 78.32 | 68.17 | 68.55 | 76.07 | 69.48 | 56.54 | 69.63 | 67.49 |
| TiO2 | 0.77 | 0.22 | 0.46 | 0.34 | 0.25 | 0.28 | 0.59 | 0.36 | 0.63 | 0.22 | 0.33 | 0.42 | 0.19 | 0.25 | 0.32 | 0.25 | 0.03 | 0.52 | 0.44 | 0.09 | 0.47 | 1.08 | 0.42 | 0.51 |
| Al2O3 | 15.38 | 12.94 | 14.95 | 14.82 | 13.92 | 13.86 | 15.88 | 14.42 | 13.97 | 14.12 | 15.26 | 15.04 | 13.25 | 13.88 | 13.73 | 13.22 | 11.11 | 15.10 | 14.73 | 12.69 | 14.78 | 16.41 | 15.02 | 14.54 |
| Fe2O3 | 7.85 | 3.18 | 4.08 | 3.14 | 2.57 | 3.42 | 6.57 | 4.29 | 7.61 | 3.11 | 3.21 | 3.56 | 1.99 | 2.55 | 3.93 | 3.28 | 1.22 | 0.95 | 3.74 | 1.60 | 5.03 | 8.36 | 3.20 | 4.55 |
| MnO | 0.12 | 0.13 | 0.07 | 0.07 | 0.06 | 0.11 | 0.13 | 0.11 | 0.13 | 0.04 | 0.12 | 0.08 | 0.05 | 0.06 | 0.07 | 0.04 | 0.02 | 2.85 | 0.06 | 0.04 | 0.06 | 0.13 | 0.04 | 0.07 |
| MgO | 4.22 | 0.29 | 0.95 | 0.90 | 0.61 | 0.50 | 1.19 | 0.71 | 1.30 | 0.52 | 0.54 | 1.32 | 0.26 | 0.35 | 1.28 | 0.45 | 0.08 | 1.54 | 1.15 | 0.03 | 1.07 | 3.70 | 1.67 | 1.97 |
| CaO | 6.12 | 0.53 | 2.87 | 2.71 | 2.22 | 2.00 | 3.87 | 2.47 | 3.29 | 2.30 | 1.58 | 2.37 | 0.91 | 1.46 | 2.36 | 1.50 | 0.59 | 3.67 | 2.19 | 0.57 | 1.37 | 6.43 | 2.65 | 3.68 |
| Na2O | 2.95 | 4.61 | 3.86 | 3.85 | 3.68 | 3.63 | 3.93 | 3.55 | 3.43 | 3.05 | 4.21 | 3.12 | 3.79 | 4.05 | 2.74 | 2.81 | 3.62 | 3.70 | 3.69 | 3.82 | 3.13 | 3.15 | 3.32 | 2.71 |
| K2O | 2.10 | 3.58 | 3.43 | 3.32 | 3.49 | 4.01 | 2.26 | 3.70 | 3.40 | 4.19 | 4.27 | 5.38 | 4.56 | 3.82 | 4.66 | 5.09 | 4.27 | 2.52 | 4.00 | 4.67 | 4.19 | 3.03 | 2.98 | 3.98 |
| P2O5 | 0.15 | 0.05 | 0.11 | 0.10 | 0.07 | 0.07 | 0.21 | 0.11 | 0.16 | 0.06 | 0.10 | 0.12 | 0.05 | 0.07 | 0.08 | 0.06 | 0.03 | 0.17 | 0.11 | 0.02 | 0.20 | 0.30 | 0.11 | 0.15 |
| LOI | 0.33 | 0.45 | 0.22 | 0.38 | 0.30 | 0.32 | 0.87 | 0.51 | 0.22 | 0.25 | 0.76 | 0.91 | 0.44 | 无样 | 0.26 | 0.15 | 0.56 | 0.96 | 0.48 | 0.43 | 0.28 | 0.47 | 1.24 | 0.80 |
| Total | 99.73 | 100.04 | 99.96 | 99.79 | 99.74 | 99.69 | 100.04 | 100.10 | 99.80 | 100.31 | 99.73 | 99.80 | 99.90 | 99.56 | 99.33 | 99.71 | 99.85 | 100.14 | 99.12 | 100.02 | 100.05 | 99.61 | 100.28 | 100.45 |
| $Na_2O/K_2O$ | 1.40 | 1.29 | 1.13 | 1.16 | 1.05 | 0.91 | 1.74 | 0.96 | 1.01 | 0.73 | 0.99 | 0.58 | 0.83 | 1.06 | 0.59 | 0.55 | 0.85 | 1.47 | 0.92 | 0.82 | 0.75 | 1.04 | 1.11 | 0.68 |
| *Trace element (in ppm)* | | | | | | | | | | | | | | | | | | | | | | | | |
| P | 534 | 294 | 482 | 415 | 352 | 332 | 1052 | 448 | 711 | 280 | 415 | 574 | 235 | 342 | 345 | 257 | 103 | 827 | 537 | 88 | 1004 | 1570 | 550 | 748 |
| Sc | 17.7 | 10.7 | 8.5 | 6.2 | 5.2 | 4.9 | 12.4 | 6.7 | 14.2 | 3.8 | 8.7 | 9.4 | 2.9 | 3 | 7.4 | 5.8 | 39.1 | 6.6 | 7.6 | 8.7 | 6 | 19 | 6.8 | 10.2 |
| Ti | 4314 | 1662 | 2615 | 1965 | 1759 | 1562 | 3916 | 2060 | 3848 | 1284 | 1872 | 2588 | 1101 | 1565 | 1818 | 1391 | 431 | 2885 | 2445 | 405.9 | 2637 | 6024 | 2442 | 2857 |
| V | 138 | 2 | 41 | 33 | 28 | 14 | 55 | 20 | 71 | 18 | 16 | 69 | 7 | 10 | 52 | 16 | 1.74 | 48 | 28 | 2 | 30 | 177 | 34 | 85 |
| Cr | 91 | 292 | 12 | 8 | 9 | 10 | 20 | 12 | 23 | 10 | 4 | 99 | 2 | 58 | 39 | 9 | 16 | 38 | 63 | 25 | 136 | 54 | 59 | 48 |
| Mn | 849 | 1261 | 484 | 506 | 529 | 827 | 1124 | 813 | 1060 | 306 | 862 | 637 | 369 | 423 | 479 | 310 | 151 | 491 | 435 | 281 | 425 | 994 | 344 | 571 |
| Co | 20 | 1.5 | 4.9 | 4.5 | 3.8 | 3.5 | 9.4 | 4.5 | 10.4 | 3.7 | 2.4 | 7.6 | 1.4 | 1.8 | 6.7 | 2.7 | 0.6 | 7.9 | 6.5 | 0.7 | 7.3 | 21.3 | 7.1 | 9.8 |
| Ni | 43.6 | 18.3 | 12.1 | 9.1 | 11.6 | 12.3 | 23.4 | 16.5 | 18.2 | 10.4 | 1.5 | 11.5 | 1.2 | 1.9 | 8.8 | 7.8 | 9.101 | 9.2 | 18.6 | 5.4 | 38.6 | 18.1 | 23.4 | 9.9 |
| Cu | 34.6 | 17.6 | 7.6 | 12.0 | 5.6 | 9.5 | 29.3 | 12.4 | 20.6 | 16.3 | 5.0 | 17.4 | 2.6 | 2.5 | 12.3 | 6.3 | 13.79 | 7.0 | 15.3 | 5.9 | 34.8 | 80.9 | 6.9 | 11.3 |
| Zn | 65 | 106 | 40 | 50 | 34 | 73 | 185 | 69 | 69 | 31 | 62 | 56 | 54 | 60 | 45 | 52 | 23.3 | 37 | 47 | 26 | 53 | 83 | 33 | 40 |
| Ga | 16 | 24 | 17 | 16 | 18 | 16 | 23 | 16 | 19 | 15 | 24 | 19 | 21 | 21 | 16 | 15 | 17.3 | 18 | 19 | 25 | 20 | 20 | 20 | 15 |
| Rb | 74 | 135 | 106 | 119 | 156 | 145 | 95 | 127 | 155 | 149 | 344 | 233 | 222 | 187 | 197 | 189 | 403.9 | 123 | 155 | 447 | 177 | 120 | 128 | 142 |
| Sr | 357 | 107 | 250 | 231 | 230 | 159 | 376 | 189 | 222 | 197 | 76 | 312 | 95 | 140 | 170 | 128 | 20 | 389 | 153 | 18 | 155 | 508 | 344 | 356 |
| Y | 19.9 | 59.2 | 26.6 | 20 | 20.5 | 24.6 | 35.3 | 25.7 | 27.9 | 12.5 | 110.5 | 24.2 | 27.1 | 26.2 | 21.5 | 20.9 | 36.5 | 14.7 | 24.6 | 62.3 | 17.5 | 25.7 | 15.3 | 15.6 |
| Zr | 30 | 146 | 60 | 45 | 57 | 68 | 69 | 68 | 66 | 40 | 212 | 189 | 86 | 95 | 60 | 55 | 104 | 56 | 57 | 110 | 50 | 42 | 74 | 21 |
| Nb | 7.1 | 21.2 | 11.6 | 11.6 | 13.3 | 10 | 15.6 | 11.3 | 16.3 | 7 | 42.6 | 16.6 | 21.8 | 17.6 | 10.5 | 14.6 | 16 | 9.7 | 13 | 33.3 | 13.2 | 13.5 | 10.6 | 8.1 |
| Cs | 3.8 | 3.6 | 4.2 | 3.3 | 4.6 | 3.1 | 3.6 | 2.7 | 7.4 | 4.4 | 24.0 | 11.0 | 12.4 | 10.7 | 13.3 | 9.5 | 17.34 | 6.7 | 6.1 | 19.0 | 6.8 | 5.1 | 4.3 | 6.0 |
| Ba | 400 | 1105 | 745 | 522 | 542 | 581 | 687 | 556 | 422 | 483 | 129 | 251 | 269 | 203 | 432 | 341 | 39 | 394 | 579 | 55 | 498 | 618 | 562 | 388 |
| La | 18.1 | 53.4 | 38.7 | 26.6 | 24.4 | 34.3 | 36.3 | 26 | 49.4 | 33.7 | 48.6 | 39.8 | 26.3 | 33.7 | 31.4 | 36.9 | 31.8 | 31.7 | 21.4 | 23.2 | 27 | 30.8 | 27.8 | 32.6 |
| Ce | 41.7 | 121.3 | 80.1 | 56.1 | 51.7 | 69.2 | 81.3 | 56.2 | 99.3 | 62.8 | 111.8 | 85.6 | 70.7 | 72.9 | 66.5 | 81.3 | 65.5 | 60.9 | 47.7 | 59.9 | 59.9 | 65.6 | 57.7 | 56.9 |
| Pr | 4.51 | 14.01 | 8.56 | 5.57 | 5.19 | 7.04 | 8.99 | 5.91 | 10.11 | 5.77 | 12.93 | 8.99 | 6.61 | 7.82 | 6.83 | 7.61 | 8.175 | 6.08 | 5.03 | 7.10 | 6.66 | 7.55 | 5.92 | 5.37 |
| Nd | 17.7 | 53.8 | 30.9 | 18.8 | 17.5 | 23.6 | 33.9 | 21.1 | 33.4 | 17.3 | 46.9 | 30.9 | 22.8 | 26.8 | 22.4 | 25.1 | 30.29 | 21.1 | 18.8 | 27.1 | 25.3 | 30.0 | 21.7 | 18.5 |
| Sm | 3.87 | 11.33 | 5.99 | 3.53 | 3.41 | 4.42 | 7.11 | 4.44 | 5.92 | 2.73 | 12.08 | 5.8 | 4.94 | 5.37 | 4.17 | 4.59 | 7.35 | 3.5 | 4.07 | 7.43 | 5 | 5.83 | 3.89 | 3.18 |
| Eu | 0.93 | 1.82 | 1.39 | 0.75 | 0.79 | 0.84 | 1.72 | 0.96 | 0.94 | 0.71 | 0.33 | 0.76 | 0.42 | 0.54 | 0.61 | 0.52 | 0.178 | 0.89 | 0.71 | 0.12 | 0.72 | 1.42 | 0.88 | 0.89 |
| Gd | 3.71 | 10.11 | 5.24 | 3.13 | 3.06 | 3.96 | 6.46 | 4.22 | 4.83 | 2.1 | 12.4 | 4.64 | 4.3 | 4.53 | 3.51 | 3.76 | 6.37 | 2.75 | 3.95 | 7.34 | 3.95 | 4.94 | 3.02 | 2.69 |
| Tb | 0.57 | 1.62 | 0.81 | 0.51 | 0.51 | 0.64 | 0.99 | 0.68 | 0.75 | 0.33 | 2.24 | 0.72 | 0.72 | 0.72 | 0.57 | 0.60 | 1.052 | 0.45 | 0.72 | 1.49 | 0.62 | 0.79 | 0.48 | 0.45 |
| Dy | 3.43 | 9.81 | 4.73 | 3.14 | 3.12 | 3.96 | 5.93 | 4.2 | 4.41 | 1.89 | 14.97 | 4.18 | 4.35 | 4.27 | 3.42 | 3.6 | 6.33 | 2.38 | 4.13 | 9.41 | 3.11 | 4.31 | 2.52 | 2.55 |
| Ho | 0.71 | 2.07 | 0.96 | 0.68 | 0.69 | 0.84 | 1.21 | 0.89 | 0.92 | 0.40 | 3.31 | 0.86 | 0.91 | 0.88 | 0.72 | 0.74 | 1.199 | 0.48 | 0.87 | 2.05 | 0.59 | 0.89 | 0.51 | 0.54 |
| Er | 1.93 | 5.82 | 2.61 | 1.99 | 2.05 | 2.45 | 3.26 | 2.51 | 2.59 | 1.18 | 9.93 | 2.42 | 2.59 | 2.49 | 2.06 | 2.09 | 3.68 | 1.36 | 2.39 | 6.33 | 1.58 | 2.47 | 1.4 | 1.53 |
| Tm | 0.295 | 0.894 | 0.386 | 0.327 | 0.341 | 0.392 | 0.479 | 0.394 | 0.410 | 0.192 | 1.666 | 0.375 | 0.426 | 0.400 | 0.329 | 0.329 | 0.6073 | 0.205 | 0.354 | 1.092 | 0.232 | 0.366 | 0.205 | 0.237 |
| Yb | 1.93 | 5.77 | 2.46 | 2.25 | 2.36 | 2.63 | 3.04 | 2.59 | 2.75 | 1.36 | 11.17 | 2.48 | 2.88 | 2.65 | 2.21 | 2.15 | 4.36 | 1.3 | 2.17 | 7.24 | 1.4 | 2.26 | 1.3 | 1.49 |
| Lu | 0.284 | 0.841 | 0.355 | 0.347 | 0.37 | 0.398 | 0.442 | 0.383 | 0.417 | 0.217 | 1.624 | 0.366 | 0.418 | 0.387 | 0.325 | 0.308 | 0.641 | 0.196 | 0.318 | 1.078 | 0.195 | 0.332 | 0.193 | 0.226 |
| Hf | 1.13 | 5.05 | 2.08 | 1.76 | 2.21 | 2.47 | 2.3 | 2.41 | 2.24 | 1.44 | 6.37 | 5.61 | 3.18 | 3.61 | 2.2 | 2.08 | 4.22 | 1.85 | 1.86 | 5.23 | 1.48 | 1.56 | 2.29 | 0.9 |
| Ta | 0.56 | 1.33 | 0.91 | 1.15 | 1.50 | 0.95 | 1.05 | 1.01 | 1.46 | 0.87 | 7.87 | 1.24 | 1.99 | 1.75 | 1.48 | 1.29 | 4.257 | 1.16 | 1.25 | 5.58 | 1.28 | 0.97 | 0.97 | 0.76 |
| W | 1.00 | 1.53 | 2.01 | 0.64 | 1.58 | 3.40 | 3.08 | 1.17 | 2.07 | 1.33 | 0.96 | 6.14 | 4.61 | 3.04 | 3.20 | 2.79 | 13.43 | 0.53 | 0.56 | 2.07 | 2.99 | 1.15 | 0.43 | 1.63 |
| Tl | 0.47 | 1.09 | 0.62 | 0.59 | 0.89 | 1.22 | 0.97 | 0.89 | 0.92 | 0.82 | 1.95 | 0.89 | 1.18 | 1.06 | 1.03 | 0.94 | - | 0.70 | 0.83 | 2.64 | 0.85 | 0.48 | 0.57 | 0.64 |
| Pb | 18.3 | 26.6 | 15.6 | 24.4 | 19.1 | 23.5 | 63.5 | 20.3 | 23.6 | 18.4 | 104.9 | 28.8 | 22.3 | 15.0 | 23.7 | 23.0 | 25.18 | 12.1 | 20.5 | 25.3 | 21.4 | 14.1 | 17.8 | 15.0 |
| Th | 7.04 | 14.86 | 13.19 | 14.18 | 26.24 | 14.29 | 11.43 | 12.42 | 25.35 | 16.73 | 66.59 | 28.59 | 20.92 | 20.98 | 18.05 | 17.32 | 40.59 | 21.62 | 9.42 | 34.31 | 12.57 | 10.05 | 10.8 | 11.88 |
| U | 1.22 | 2.79 | 1.63 | 3.04 | 6.49 | 2.01 | 2.05 | 2.32 | 4.28 | 2.47 | 11.3 | 3.87 | 3.19 | 3.62 | 1.86 | 2.27 | 10.48 | 3.27 | 2.99 | 8.26 | 3.53 | 2.98 | 1.62 | 1.25 |

Please cite this article in press as: Jahn, B.-m., et al. Emplacement ages, geochemical and Sr–Nd–Hf isotopic characterization of Mesozoic to early Cenozoic granitoids of the Sikhote-Alin Orogenic Belt, Russian Far East: Crustal growth and regional tectonic evolution. Journal of Asian Earth Sciences (2015), http://dx.doi.org/10.1016/j.jseaes.2015.08.012

**Table 4**
Sr–Nd isotopic compositions of granitoids from Sikhote-Alin.

| Sample No. | Rock type | Age (Ma) | [Rb] (ppm) | [Sr] (ppm) | $^{87}Rb/^{86}Sr$ | $^{87}Sr/^{86}Sr$ | ±2σm | I (Sr) | [Sm] (ppm) | [Nd] (ppm) | $^{147}Sm/^{144}Nd$ | $^{143}Nd/^{144}Nd$ | ±2σm | $\varepsilon_{Nd}(0)$ | $\varepsilon_{Nd}(t)$ | $f(Sm/Nd)$ | $T_{DM}$-1 (Ma) | $T_{DM}$-2 (Ma) |
|---|---|---|---|---|---|---|---|---|---|---|---|---|---|---|---|---|---|---|
| B-300 | Quartz monzodiorite | 66 | 74 | 357 | 0.60 | 0.705894 | 9 | 0.70533 | 3.87 | 17.69 | 0.1323 | 0.512543 | 4 | −1.8 | −1.3 | −0.33 | 1135 | 980 |
| B-301a (=B-257) | Alkali feldspar granite | 57 | 135 | 107 | 3.64 | 0.708052 | 7 | 0.70511 | 11.33 | 53.82 | 0.1273 | 0.512568 | 6 | −1.4 | −0.9 | −0.35 | 1027 | 937 |
| B-448 (=B-433) | Granodiorite | 64 | 106 | 250 | 1.22 | 0.706652 | 8 | 0.70554 | 5.99 | 30.91 | 0.1172 | 0.512516 | 6 | −2.4 | −1.7 | −0.40 | 1000 | 1013 |
| B-456 (=B-494) | Granodiorite | 71 | 119 | 231 | 1.49 | 0.706831 | 7 | 0.70533 | 3.53 | 18.77 | 0.1137 | 0.512551 | 6 | −1.7 | −1.0 | −0.42 | 914 | 955 |
| B-719 (=B-720) | Granite | 71 | 156 | 230 | 1.97 | 0.707364 | 7 | 0.70538 | 3.41 | 17.53 | 0.1176 | 0.512539 | 6 | −1.9 | −1.2 | −0.40 | 969 | 976 |
| B-574 | Granite | 83 | 145 | 159 | 2.63 | 0.708559 | 7 | 0.70546 | 4.42 | 23.62 | 0.1131 | 0.512510 | 6 | −2.5 | −1.6 | −0.42 | 970 | 1019 |
| B-621 (=B-611) | Granodiorite | 71 | 95 | 376 | 0.73 | 0.706449 | 7 | 0.70571 | 7.11 | 33.92 | 0.1267 | 0.512509 | 6 | −2.5 | −1.9 | −0.36 | 1123 | 1032 |
| B-783M (=B-781) | Granite | 78 | 127 | 189 | 1.94 | 0.707735 | 8 | 0.70559 | 4.44 | 21.13 | 0.1270 | 0.512502 | 8 | −2.6 | −2.0 | −0.35 | 1138 | 1043 |
| B-919B (=B-909A) | Granite | 81 | 155 | 222 | 2.01 | 0.708111 | 9 | 0.70579 | 5.92 | 33.39 | 0.1072 | 0.512468 | 6 | −3.3 | −2.4 | −0.46 | 976 | 1081 |
| B-984 (=B-995) | Granite | 78 | 149 | 197 | 2.19 | 0.708547 | 9 | 0.70612 | 2.73 | 17.34 | 0.0952 | 0.512459 | 6 | −3.5 | −2.5 | −0.52 | 889 | 1087 |
| GV-722 | Granite | 75 | 344 | 76 | 13.11 | 0.721149 | 10 | 0.70718 | 12.08 | 46.91 | 0.1557 | 0.512409 | 6 | −4.5 | −4.1 | −0.21 | 1940 | 1214 |
| GV-1401 | Granite | 75 | 233 | 312 | 2.16 | 0.708179 | 8 | 0.70588 | 5.80 | 30.89 | 0.1135 | 0.512450 | 6 | −3.7 | −2.9 | −0.42 | 1064 | 1116 |
| GV-1583-2 | Granite | 86 | 222 | 95 | 6.76 | 0.713472 | 7 | 0.70522 | 4.94 | 22.84 | 0.1308 | 0.512580 | 6 | −1.1 | −0.4 | −0.34 | 1047 | 923 |
| GV-1774 | Granite | 88 | 187 | 140 | 3.87 | 0.709852 | 7 | 0.70502 | 5.37 | 26.78 | 0.1212 | 0.512595 | 6 | −0.8 | 0.0 | −0.38 | 915 | 891 |
| YG-332 | Granite | 92 | 197 | 170 | 3.35 | 0.710498 | 10 | 0.70611 | 4.17 | 22.36 | 0.1127 | 0.512391 | 6 | −4.8 | −3.8 | −0.43 | 1145 | 1208 |
| YG-410 | Granite | 92 | 189 | 128 | 4.28 | 0.711447 | 9 | 0.70586 | 4.59 | 25.14 | 0.1104 | 0.512423 | 6 | −4.2 | −3.2 | −0.44 | 1073 | 1156 |
| B-881/2 | Granodiorite | 93 | 123 | 389 | 0.915 | 0.706582 | 8 | 0.70537 | 3.50 | 21.11 | 0.1002 | 0.512564 | 6 | −1.4 | −0.3 | −0.49 | 788 | 920 |
| AN-2-11 | Granite | 108 | 155 | 153 | 2.93 | 0.710603 | 8 | 0.70611 | 4.07 | 18.84 | 0.1306 | 0.512548 | 6 | −1.8 | −0.8 | −0.34 | 1104 | 978 |
| AN-3-11 | Alkali feldspar granite | 58 | 447 | 18.0 | 72.2 | 0.767241 | 8 | 0.70796 | 7.43 | 27.13 | 0.1656 | 0.512651 | 6 | 0.3 | 0.5 | −0.16 | 1576 | 827 |
| B-11-54/1 | Granite | 131 | 177 | 155 | 3.31 | 0.714511 | 8 | 0.70832 | 5.00 | 25.31 | 0.1194 | 0.512361 | 4 | −5.4 | −4.1 | −0.39 | 1275 | 1264 |
| B-11-51/3 | Qtz monzodiorite | 108 | 120 | 508 | 0.684 | 0.705076 | 8 | 0.70403 | 5.83 | 29.95 | 0.1177 | 0.512738 | 6 | 1.9 | 3.0 | −0.40 | 655 | 659 |
| B-871/1 | Granodiorite | 109 | 128 | 344 | 1.08 | 0.708169 | 8 | 0.70650 | 3.89 | 21.73 | 0.1082 | 0.512358 | 6 | −5.5 | −4.2 | −0.45 | 1144 | 1256 |
| B-872/1 | Granodiorite | 106 | 142 | 356 | 1.16 | 0.706298 | 8 | 0.70456 | 3.18 | 18.50 | 0.1039 | 0.512563 | 6 | −1.5 | −0.2 | −0.47 | 816 | 924 |

$\varepsilon_{Nd}(0) = 10^4 * ((^{143}Nd/^{144}Nd)_{sample(0)}/(^{143}Nd/^{144}Nd)_{CHUR(0)} - 1)$.
$\varepsilon_{Nd}(t) = \varepsilon_{Nd}(0) - Q_{Nd} \times f_s \times t$ ($t$ in Ga).
$f_s = f_{Sm/Nd,\ sample(0)} = (^{147}Sm/^{144}Nd)_{sample(0)}/(^{147}Sm/^{144}Nd)_{CHUR(0)} - 1$.
$T_{DM-1} = (1/\lambda_{147}) \times \log_e\{1 + [(^{143}Nd/^{144}Nd)_{sample(0)} - (^{143}Nd/^{144}Nd)_{DM(0)}]/[(^{147}Sm/^{144}Nd)_{sample(0)} - (^{147}Sm/^{144}Nd)_{DM(0)}]\}$.
$T_{DM-2} = ((\varepsilon Nd_{DM(0)} - \varepsilon Nd_{sample(0)} + Q \times t \times (f_s - f_{cc}))/(Q \times (f_{DM} - f_{cc})) \times 1000$ (Ma).
$Q = 10^4 \times \lambda_{147} \times (^{147}Sm/^{144}Nd)_{CHUR(0)}/(^{143}Nd/^{144}Nd)_{CHUR(0)} = 25.1$ (/Ga).
$\lambda_{147} = 6.54 \times 10^{-6}$/Ma.
$(^{143}Nd/^{144}Nd)_{CHUR(0)} = 0.512638$.
$(^{147}Sm/^{144}Nd)_{CHUR(0)} = 0.1967$.
$(^{143}Nd/^{144}Nd)_{DM(0)} = 0.51315$; $(^{147}Sm/^{144}Nd)_{DM(0)} = 0.2137$.
$f_{cc} = (^{147}Sm/^{144}Nd)_{aver.cont.crust}/(^{147}Sm/^{144}Nd)_{CHUR} - 1 = -0.4$.

Please cite this article in press as: Jahn, B.-m., et al. Emplacement ages, geochemical and Sr–Nd–Hf isotopic characterization of Mesozoic to early Cenozoic granitoids of the Sikhote-Alin Orogenic Belt, Russian Far East: Crustal growth and regional tectonic evolution. Journal of Asian Earth Sciences (2015), http://dx.doi.org/10.1016/j.jseaes.2015.08.012

**Table 5**
Zircon Lu–Hf isotopic compositions of granitoids from Sikhote-Alin.

| Spot | Individual spot age (Ma) | ±2σ | Sample mean age (Ma) | $^{176}Hf/^{177}Hf$ | ±2σ | $^{176}Lu/^{177}Hf$ | ±2σ | $^{176}Yb/^{177}Hf$ | ±2σ | $^{176}Hf/^{177}Hf$ CHUR($t$) | $\varepsilon_{Hf}(0)$ | $\varepsilon_{Hf}(t)$ | $T_{DM}$ | $T^{c}_{DM}$ |
|---|---|---|---|---|---|---|---|---|---|---|---|---|---|---|
| B-300 01-1 | 63.0 | 4 | 65.6 | 0.283022 | 29 | 0.000519 | 8.8 | 0.019078 | 230 | 0.282745 | 8.4 | 9.8 | 370 | 612 |
| B-300 02 | 64.0 | 2 | 65.6 | 0.282989 | 27 | 0.001925 | 11 | 0.075801 | 1600 | 0.282745 | 7.2 | 8.6 | 442 | 711 |
| B-300 03-2 | 64.0 | 4 | 65.6 | 0.283003 | 36 | 0.000932 | 25 | 0.033451 | 1700 | 0.282745 | 7.7 | 9.1 | 406 | 667 |
| B-300 04-2 | 65.0 | 4 | 65.6 | 0.282951 | 35 | 0.001830 | 39 | 0.061239 | 2000 | 0.282744 | 5.9 | 7.3 | 505 | 820 |
| B-300 05 | 66.0 | 4 | 65.6 | 0.282912 | 35 | 0.000711 | 4.9 | 0.029377 | 240 | 0.282744 | 4.5 | 6.0 | 551 | 928 |
| B-300 07-2 | 56.0 | 2 | 65.6 | 0.282981 | 29 | 0.002729 | 40 | 0.090135 | 1700 | 0.282750 | 6.9 | 8.2 | 468 | 742 |
| B-300 07 | 56.0 | 2 | 65.6 | 0.283103 | 29 | 0.004402 | 170 | 0.155781 | 8400 | 0.282750 | 11.2 | 12.5 | 271 | 395 |
| B-300 08 | 68.0 | 4 | 65.6 | 0.282959 | 36 | 0.000769 | 9.2 | 0.031410 | 650 | 0.282742 | 6.2 | 7.7 | 476 | 791 |
| B-300 10 | 68.0 | 4 | 65.6 | 0.283093 | 23 | 0.001454 | 41 | 0.057242 | 2600 | 0.282742 | 10.9 | 12.4 | 263 | 406 |
| B-300 11 | 58.0 | 2 | 65.6 | 0.283022 | 32 | 0.002014 | 81 | 0.081943 | 3200 | 0.282749 | 8.4 | 9.7 | 388 | 620 |
| B-300 12 | 65.0 | 4 | 65.6 | 0.282994 | 19 | 0.001609 | 56 | 0.065508 | 1400 | 0.282744 | 7.4 | 8.8 | 430 | 695 |
| B-300 13 | 56.0 | 2 | 65.6 | 0.283080 | 35 | 0.002665 | 78 | 0.083651 | 1300 | 0.282750 | 10.4 | 11.7 | 295 | 456 |
| B-300 14 | 58.0 | 4 | 65.6 | 0.282990 | 29 | 0.001990 | 40 | 0.076908 | 1600 | 0.282749 | 7.2 | 8.5 | 442 | 713 |
| B-300 15 | 67.0 | 4 | 65.6 | 0.283018 | 46 | 0.001230 | 51 | 0.047127 | 420 | 0.282743 | 8.2 | 9.7 | 385 | 623 |
| B-300 16 | 56.0 | 2 | 65.6 | 0.282956 | 23 | 0.002863 | 78 | 0.114855 | 4300 | 0.282750 | 6.0 | 7.3 | 513 | 815 |
| B-300 17 | 56.0 | 4 | 65.6 | 0.283059 | 24 | 0.002522 | 120 | 0.094330 | 3500 | 0.282750 | 9.7 | 10.9 | 330 | 516 |
| B-300 18 | 67.0 | 4 | 65.6 | 0.282962 | 19 | 0.000871 | 15 | 0.035873 | 1100 | 0.282743 | 6.3 | 7.7 | 472 | 783 |
| B-300 19 | 67.0 | 4 | 65.6 | 0.283090 | 17 | 0.001805 | 100 | 0.074971 | 3500 | 0.282743 | 10.8 | 12.3 | 271 | 417 |
| B-300 20 | 67.0 | 4 | 65.6 | 0.282875 | 41 | 0.000532 | 5.6 | 0.020881 | 630 | 0.282743 | 3.2 | 4.7 | 608 | 1033 |
| B-300 21 | 68.0 | 4 | 65.6 | 0.283103 | 30 | 0.001459 | 84 | 0.063996 | 2900 | 0.282742 | 11.2 | 12.8 | 246 | 377 |
| B-300 22 | 66.0 | 4 | 65.6 | 0.282918 | 22 | 0.001367 | 40 | 0.060285 | 1100 | 0.282744 | 4.7 | 6.2 | 552 | 913 |
| B-300 23 | 66.0 | 4 | 65.6 | 0.282908 | 24 | 0.000967 | 15 | 0.042830 | 480 | 0.282744 | 4.3 | 5.8 | 562 | 940 |
| B-300 24 | 57.0 | 2 | 65.6 | 0.282997 | 34 | 0.001989 | 26 | 0.083453 | 1400 | 0.282749 | 7.5 | 8.8 | 430 | 693 |
| B-301a 01 | 57.0 | 2 | 57.1 | 0.283032 | 22 | 0.002217 | 14 | 0.089297 | 1600 | 0.282749 | 8.7 | 10.0 | 373 | 593 |
| B-301a 02 | 58.0 | 2 | 57.1 | 0.282919 | 19 | 0.001174 | 7.9 | 0.043224 | 830 | 0.282749 | 4.7 | 6.0 | 547 | 915 |
| B-301a 03 | 57.0 | 2 | 57.1 | 0.283061 | 21 | 0.002327 | 71 | 0.090649 | 3400 | 0.282749 | 9.8 | 11.0 | 325 | 509 |
| B-301a 04 | 58.0 | 4 | 57.1 | 0.283028 | 30 | 0.003087 | 170 | 0.112485 | 4400 | 0.282749 | 8.6 | 9.9 | 391 | 606 |
| B-301a 05 | 57.0 | 2 | 57.1 | 0.283062 | 25 | 0.002299 | 53 | 0.093810 | 2200 | 0.282749 | 9.8 | 11.1 | 323 | 506 |
| B-301a 06 | 57.0 | 2 | 57.1 | 0.283030 | 26 | 0.002430 | 85 | 0.086611 | 2300 | 0.282749 | 8.7 | 9.9 | 379 | 599 |
| B-301a 07 | 57.0 | 2 | 57.1 | 0.283024 | 34 | 0.002102 | 160 | 0.072592 | 3800 | 0.282749 | 8.5 | 9.7 | 385 | 616 |
| B-301a 09 | 57.0 | 2 | 57.1 | 0.283060 | 18 | 0.002619 | 33 | 0.096071 | 1600 | 0.282749 | 9.7 | 11.0 | 330 | 513 |
| B-301a 10 | 58.0 | 2 | 57.1 | 0.282890 | 29 | 0.002607 | 100 | 0.100606 | 2700 | 0.282749 | 3.7 | 5.0 | 623 | 1003 |
| B-301a 11 | 57.0 | 2 | 57.1 | 0.282955 | 37 | 0.002111 | 79 | 0.069048 | 1900 | 0.282749 | 6.0 | 7.3 | 503 | 815 |
| B-301a 12 | 57.0 | 2 | 57.1 | 0.283109 | 20 | 0.002357 | 59 | 0.091370 | 1500 | 0.282749 | 11.5 | 12.7 | 243 | 370 |
| B-301a 13 | 57.0 | 2 | 57.1 | 0.282992 | 22 | 0.001693 | 75 | 0.064472 | 2400 | 0.282749 | 7.3 | 8.6 | 434 | 707 |
| B-301a 14 | 56.0 | 4 | 57.1 | 0.282974 | 21 | 0.001278 | 44 | 0.051526 | 2800 | 0.282750 | 6.7 | 7.9 | 458 | 758 |
| B-301a 15 | 56.0 | 2 | 57.1 | 0.283055 | 27 | 0.002002 | 61 | 0.074212 | 1300 | 0.282750 | 9.5 | 10.8 | 332 | 526 |
| B-301a 16 | 57.0 | 2 | 57.1 | 0.283074 | 23 | 0.001871 | 30 | 0.073796 | 600 | 0.282749 | 10.2 | 11.5 | 298 | 470 |
| B-301a 17 | 58.0 | 2 | 57.1 | 0.283014 | 40 | 0.003686 | 150 | 0.130123 | 2100 | 0.282749 | 8.1 | 9.4 | 424 | 649 |
| B-301a 18 | 58.0 | 2 | 57.1 | 0.282963 | 37 | 0.002258 | 100 | 0.099962 | 5800 | 0.282749 | 6.3 | 7.6 | 491 | 791 |
| B-301a 19 | 56.0 | 2 | 57.1 | 0.283080 | 30 | 0.002295 | 48 | 0.101900 | 1400 | 0.282750 | 10.4 | 11.7 | 292 | 455 |
| B-301a 20 | 57.0 | 2 | 57.1 | 0.282994 | 27 | 0.001391 | 7.3 | 0.060316 | 550 | 0.282749 | 7.4 | 8.7 | 427 | 700 |
| B-301a 21 | 56.0 | 2 | 57.1 | 0.282954 | 36 | 0.002263 | 33 | 0.094012 | 1700 | 0.282750 | 6.0 | 7.2 | 507 | 819 |
| B-301a 22 | 58.0 | 2 | 57.1 | 0.283091 | 23 | 0.003287 | 130 | 0.150549 | 3900 | 0.282749 | 10.8 | 12.1 | 282 | 425 |
| B-301a 24 | 57.0 | 4 | 57.1 | 0.282954 | 27 | 0.001965 | 26 | 0.093454 | 2700 | 0.282749 | 6.0 | 7.2 | 502 | 817 |
| B448 01 | 63.0 | 4 | 64.0 | 0.282950 | 23 | 0.001351 | 35 | 0.051359 | 1000 | 0.282745 | 5.8 | 7.2 | 499 | 822 |
| B448 02 | 63.0 | 4 | 64.0 | 0.282886 | 26 | 0.000888 | 4.3 | 0.032100 | 630 | 0.282745 | 3.6 | 5.0 | 596 | 1005 |
| B448 03 | 63.0 | 4 | 64.0 | 0.282886 | 20 | 0.001475 | 16 | 0.056406 | 1300 | 0.282745 | 3.6 | 5.0 | 607 | 1007 |
| B448 04 | 63.0 | 4 | 64.0 | 0.282875 | 25 | 0.001126 | 46 | 0.040384 | 1300 | 0.282745 | 3.2 | 4.6 | 619 | 1038 |
| B448 05 | 63.0 | 4 | 64.0 | 0.282894 | 26 | 0.001319 | 18 | 0.049125 | 500 | 0.282745 | 3.9 | 5.3 | 591 | 984 |
| B448 06(near) | 63.0 | 4 | 64.0 | 0.282893 | 24 | 0.001329 | 8.9 | 0.047996 | 970 | 0.282745 | 3.8 | 5.2 | 593 | 987 |
| B448 07 | 63.0 | 4 | 64.0 | 0.282903 | 27 | 0.001484 | 30 | 0.054701 | 1700 | 0.282745 | 4.2 | 5.6 | 579 | 958 |
| B448 08 | 63.0 | 4 | 64.0 | 0.282879 | 16 | 0.002174 | 69 | 0.077621 | 3700 | 0.282745 | 3.3 | 4.7 | 633 | 1030 |
| B448 09 | 63.0 | 4 | 64.0 | 0.282904 | 27 | 0.000792 | 11 | 0.027067 | 740 | 0.282745 | 4.2 | 5.6 | 565 | 953 |

(continued on next page)

**Table 5** (*continued*)

| Spot | Individual spot age (Ma) | ±2σ | Sample mean age (Ma) | $^{176}Hf/^{177}Hf$ | ±2σ | $^{176}Lu/^{177}Hf$ | ±2σ | $^{176}Yb/^{177}Hf$ | ±2σ | $^{176}Hf/^{177}Hf$ CHUR($t$) | $\varepsilon_{Hf}(0)$ | $\varepsilon_{Hf}(t)$ | $T_{DM}$ | $T_{DM}^{c}$ |
|---|---|---|---|---|---|---|---|---|---|---|---|---|---|---|
| B448 10 | 63.0 | 4 | 64.0 | 0.282838 | 31 | 0.001505 | 35 | 0.054671 | 870 | 0.282745 | 1.9 | 3.3 | 687 | 1145 |
| B448 11 | 63.0 | 4 | 64.0 | 0.282848 | 29 | 0.001263 | 22 | 0.045459 | 1400 | 0.282745 | 2.2 | 3.6 | 666 | 1116 |
| B448 12 | 63.0 | 4 | 64.0 | 0.282954 | 26 | 0.001426 | 29 | 0.050552 | 1200 | 0.282745 | 6.0 | 7.4 | 494 | 811 |
| B448 13 | 63.0 | 4 | 64.0 | 0.282904 | 25 | 0.001328 | 24 | 0.054037 | 1200 | 0.282745 | 4.2 | 5.6 | 575 | 955 |
| B448 14 | 63.0 | 4 | 64.0 | 0.283074 | 26 | 0.001857 | 90 | 0.077302 | 3100 | 0.282745 | 10.2 | 11.6 | 298 | 466 |
| B448 15 | 63.0 | 4 | 64.0 | 0.282919 | 29 | 0.001676 | 67 | 0.065485 | 2700 | 0.282745 | 4.7 | 6.1 | 556 | 913 |
| B448 16 | 63.0 | 4 | 64.0 | 0.282929 | 27 | 0.001414 | 19 | 0.058277 | 1500 | 0.282745 | 5.1 | 6.5 | 535 | 883 |
| B448 17 | 63.0 | 4 | 64.0 | 0.282887 | 25 | 0.001084 | 13 | 0.043423 | 880 | 0.282745 | 3.6 | 5.0 | 598 | 1003 |
| B448 18 | 64.0 | 4 | 64.0 | 0.282977 | 29 | 0.001686 | 20 | 0.071871 | 830 | 0.282745 | 6.8 | 8.2 | 459 | 745 |
| B448 19 | 65.0 | 4 | 64.0 | 0.282920 | 24 | 0.001210 | 22 | 0.049246 | 800 | 0.282744 | 4.8 | 6.2 | 546 | 907 |
| B448 20 | 65.0 | 4 | 64.0 | 0.282888 | 22 | 0.000985 | 21 | 0.040159 | 1300 | 0.282744 | 3.6 | 5.1 | 595 | 998 |
| B-448 21 | 63.0 | 4 | 64.0 | 0.282945 | 15 | 0.001499 | 28 | 0.065401 | 1700 | 0.282745 | 5.7 | 7.1 | 510 | 837 |
| B-448 22 | 65.0 | 4 | 64.0 | 0.282987 | 28 | 0.001500 | 43 | 0.064644 | 1300 | 0.282744 | 7.1 | 8.6 | 440 | 715 |
| B-448 23 | 65.0 | 4 | 64.0 | 0.282915 | 20 | 0.001373 | 25 | 0.061341 | 440 | 0.282744 | 4.6 | 6.0 | 557 | 922 |
| B-448 24 | 65.0 | 4 | 64.0 | 0.282920 | 16 | 0.001554 | 24 | 0.065570 | 1800 | 0.282744 | 4.8 | 6.2 | 552 | 908 |
| B-456 01 | 73.0 | 4 | 70.5 | 0.282955 | 31 | 0.000808 | 5.6 | 0.032022 | 910 | 0.282739 | 6.0 | 7.6 | 483 | 799 |
| B-456 02 | 71.0 | 4 | 70.5 | 0.282978 | 25 | 0.001142 | 51 | 0.047563 | 2500 | 0.282740 | 6.8 | 8.4 | 450 | 735 |
| B-456 03 | 70.0 | 4 | 70.5 | 0.282898 | 27 | 0.000796 | 17 | 0.032591 | 1500 | 0.282741 | 4.0 | 5.6 | 575 | 965 |
| B-456 04 | 70.0 | 4 | 70.5 | 0.282985 | 15 | 0.001815 | 23 | 0.080187 | 740 | 0.282741 | 7.1 | 8.6 | 448 | 718 |
| B-456 06 | 71.0 | 4 | 70.5 | 0.282848 | 29 | 0.000853 | 21 | 0.034055 | 450 | 0.282740 | 2.2 | 3.8 | 658 | 1108 |
| B-456 07 | 71.0 | 4 | 70.5 | 0.282948 | 22 | 0.001992 | 78 | 0.080558 | 2600 | 0.282740 | 5.8 | 7.3 | 513 | 825 |
| B-456 08 | 72.0 | 4 | 70.5 | 0.282898 | 27 | 0.001212 | 8.4 | 0.047627 | 1100 | 0.282740 | 4.0 | 5.6 | 583 | 965 |
| B-456 09 | 71.0 | 4 | 70.5 | 0.282976 | 19 | 0.001349 | 38 | 0.053723 | 1300 | 0.282740 | 6.8 | 8.3 | 456 | 742 |
| B-456 09-2 | 68.0 | 4 | 70.5 | 0.282888 | 22 | 0.001493 | 42 | 0.060735 | 970 | 0.282742 | 3.6 | 5.2 | 604 | 998 |
| B-456 11 | 69.0 | 4 | 70.5 | 0.282907 | 28 | 0.001105 | 15 | 0.043777 | 1100 | 0.282742 | 4.3 | 5.8 | 566 | 941 |
| B-456 12 | 72.0 | 4 | 70.5 | 0.282970 | 22 | 0.001267 | 27 | 0.049986 | 1600 | 0.282740 | 6.5 | 8.1 | 465 | 758 |
| B-456 13 | 69.0 | 4 | 70.5 | 0.282961 | 24 | 0.000853 | 42 | 0.031014 | 2200 | 0.282742 | 6.2 | 7.8 | 474 | 784 |
| B-456 14 | 70.0 | 4 | 70.5 | 0.282981 | 22 | 0.001727 | 23 | 0.063829 | 670 | 0.282741 | 6.9 | 8.5 | 453 | 729 |
| B-456 15 | 68.0 | 4 | 70.5 | 0.282830 | 29 | 0.000763 | 12 | 0.027289 | 85 | 0.282742 | 1.6 | 3.1 | 685 | 1162 |
| B-456 16 | 87.0 | 4 | 70.5 | 0.282926 | 29 | 0.001282 | 73 | 0.047284 | 2800 | 0.282730 | 5.0 | 6.9 | 538 | 874 |
| B-456 18 | 70.0 | 4 | 70.5 | 0.282957 | 19 | 0.001163 | 37 | 0.039698 | 1700 | 0.282741 | 6.1 | 7.6 | 485 | 796 |
| B-456 19-1 | 71.0 | 4 | 70.5 | 0.282930 | 20 | 0.001377 | 40 | 0.049460 | 1200 | 0.282740 | 5.1 | 6.7 | 533 | 874 |
| B-456 19-2 | 69.0 | 4 | 70.5 | 0.282887 | 35 | 0.001155 | 44 | 0.039805 | 2200 | 0.282742 | 3.6 | 5.1 | 600 | 999 |
| B-456 20 | 72.0 | 4 | 70.5 | 0.282953 | 23 | 0.001294 | 31 | 0.046636 | 950 | 0.282740 | 5.9 | 7.5 | 493 | 807 |
| B-456 21 | 71.0 | 4 | 70.5 | 0.282996 | 31 | 0.002041 | 81 | 0.068810 | 4200 | 0.282740 | 7.5 | 9.0 | 432 | 686 |
| B-456 22 | 68.0 | 4 | 70.5 | 0.282929 | 22 | 0.002035 | 69 | 0.071007 | 3100 | 0.282742 | 5.1 | 6.6 | 545 | 882 |
| B-456 23 | 71.0 | 4 | 70.5 | 0.282965 | 29 | 0.001447 | 36 | 0.047639 | 500 | 0.282740 | 6.4 | 7.9 | 476 | 774 |
| B-719 01 | 69.0 | 4 | 70.7 | 0.282969 | 25 | 0.001356 | 11 | 0.044165 | 600 | 0.282742 | 6.5 | 8.0 | 468 | 763 |
| B-719 02 | 71.0 | 4 | 70.7 | 0.282876 | 24 | 0.001692 | 30 | 0.054621 | 1400 | 0.282740 | 3.2 | 4.8 | 628 | 1031 |
| B-719 03 | 70.0 | 4 | 70.7 | 0.282954 | 27 | 0.001420 | 19 | 0.045471 | 620 | 0.282741 | 6.0 | 7.5 | 493 | 806 |
| B-719 04 | 71.0 | 4 | 70.7 | 0.282917 | 27 | 0.001616 | 65 | 0.049571 | 1500 | 0.282740 | 4.7 | 6.2 | 558 | 913 |
| B-719 05 | 70.0 | 4 | 70.7 | 0.282898 | 25 | 0.000902 | 10 | 0.026950 | 290 | 0.282741 | 4.0 | 5.6 | 577 | 966 |
| B-719 06 | 71.0 | 4 | 70.7 | 0.282942 | 28 | 0.001258 | 13 | 0.037360 | 850 | 0.282740 | 5.6 | 7.1 | 511 | 839 |
| B-719 07 | 71.0 | 4 | 70.7 | 0.282806 | 29 | 0.001114 | 51 | 0.034993 | 1600 | 0.282740 | 0.7 | 2.3 | 732 | 1230 |
| B-719 08 | 70.0 | 4 | 70.7 | 0.282974 | 27 | 0.001847 | 27 | 0.062392 | 1100 | 0.282741 | 6.7 | 8.2 | 466 | 750 |
| B-719 09 | 72.0 | 4 | 70.7 | 0.282963 | 28 | 0.003441 | 110 | 0.116555 | 5100 | 0.282740 | 6.3 | 7.9 | 511 | 786 |
| B-719 10 | 70.0 | 4 | 70.7 | 0.282966 | 21 | 0.001198 | 9.7 | 0.040112 | 870 | 0.282741 | 6.4 | 8.0 | 470 | 771 |
| B-719 11 | 70.0 | 4 | 70.7 | 0.282987 | 22 | 0.001887 | 57 | 0.066419 | 2400 | 0.282741 | 7.1 | 8.7 | 445 | 713 |
| B-719 12 | 70.0 | 4 | 70.7 | 0.282957 | 26 | 0.001580 | 40 | 0.057452 | 2700 | 0.282741 | 6.1 | 7.6 | 491 | 798 |
| B-719 14 | 71.0 | 4 | 70.7 | 0.282922 | 21 | 0.001215 | 43 | 0.044343 | 1500 | 0.282740 | 4.8 | 6.4 | 543 | 897 |
| B-719 15 | 69.0 | 4 | 70.7 | 0.282931 | 18 | 0.001683 | 25 | 0.066136 | 1500 | 0.282742 | 5.2 | 6.7 | 536 | 874 |
| B-719 16 | 72.0 | 4 | 70.7 | 0.282954 | 22 | 0.002000 | 75 | 0.073205 | 1800 | 0.282740 | 6.0 | 7.6 | 503 | 807 |
| B-719 17 | 72.0 | 4 | 70.7 | 0.282963 | 22 | 0.001212 | 23 | 0.045726 | 1100 | 0.282740 | 6.3 | 7.9 | 475 | 778 |
| B-719 18 | 71.0 | 4 | 70.7 | 0.282922 | 23 | 0.001627 | 87 | 0.061487 | 3900 | 0.282740 | 4.8 | 6.4 | 550 | 898 |
| B-719 19 | 71.0 | 4 | 70.7 | 0.282925 | 21 | 0.001330 | 24 | 0.047239 | 650 | 0.282740 | 5.0 | 6.5 | 540 | 889 |

Please cite this article in press as: Jahn, B.-m., et al. Emplacement ages, geochemical and Sr–Nd–Hf isotopic characterization of Mesozoic to early Cenozoic granitoids of the Sikhote-Alin Orogenic Belt, Russian Far East: Crustal growth and regional tectonic evolution. Journal of Asian Earth Sciences (2015), http://dx.doi.org/10.1016/j.jseaes.2015.08.012

**Table 5** (*continued*)

| Spot | Individual spot age (Ma) | ±2σ | Sample mean age (Ma) | $^{176}Hf/^{177}Hf$ | ±2σ | $^{176}Lu/^{177}Hf$ | ±2σ | $^{176}Yb/^{177}Hf$ | ±2σ | $^{176}Hf/^{177}Hf$ CHUR($t$) | $\varepsilon_{Hf}(0)$ | $\varepsilon_{Hf}(t)$ | $T_{DM}$ | $T^{c}_{DM}$ |
|---|---|---|---|---|---|---|---|---|---|---|---|---|---|---|
| B-719 20 | 71.0 | 4 | 70.7 | 0.282947 | 22 | 0.001911 | 61 | 0.070373 | 1100 | 0.282740 | 5.7 | 7.3 | 513 | 827 |
| B-719 21 | 71.0 | 4 | 70.7 | 0.282900 | 25 | 0.001942 | 49 | 0.075610 | 1800 | 0.282740 | 4.1 | 5.6 | 593 | 963 |
| B-719 22 | 70.0 | 4 | 70.7 | 0.282954 | 20 | 0.001072 | 30 | 0.038617 | 600 | 0.282741 | 6.0 | 7.5 | 488 | 805 |
| B-719 23 | 72.0 | 4 | 70.7 | 0.283019 | 22 | 0.001115 | 50 | 0.042081 | 2600 | 0.282740 | 8.3 | 9.9 | 382 | 616 |
| B-719 24 | 70.0 | 4 | 70.7 | 0.282988 | 29 | 0.001136 | 11 | 0.042549 | 790 | 0.282741 | 7.2 | 8.7 | 433 | 707 |
| B-574 01 | 83.0 | 4 | 82.7 | 0.282937 | 32 | 0.001180 | 16 | 0.045464 | 1200 | 0.282733 | 5.4 | 7.2 | 518 | 844 |
| B-574 02 | 86.0 | 4 | 82.7 | 0.282960 | 24 | 0.001189 | 34 | 0.042885 | 1200 | 0.282731 | 6.2 | 8.1 | 480 | 776 |
| B-574 03 | 83.0 | 4 | 82.7 | 0.282878 | 32 | 0.001031 | 16 | 0.038083 | 240 | 0.282733 | 3.3 | 5.1 | 612 | 1014 |
| B-574 04 | 81.0 | 4 | 82.7 | 0.282933 | 21 | 0.001565 | 23 | 0.053729 | 1400 | 0.282734 | 5.2 | 7.0 | 531 | 859 |
| B-574 05 | 84.0 | 4 | 82.7 | 0.282807 | 20 | 0.001312 | 29 | 0.044971 | 550 | 0.282732 | 0.8 | 2.6 | 734 | 1218 |
| B-574 06 | 82.0 | 4 | 82.7 | 0.282904 | 22 | 0.000921 | 34 | 0.031722 | 880 | 0.282734 | 4.2 | 6.0 | 568 | 939 |
| B-574 07 | 84.0 | 4 | 82.7 | 0.282883 | 32 | 0.001356 | 22 | 0.049942 | 1200 | 0.282732 | 3.5 | 5.3 | 610 | 1000 |
| B-574 08 | 85.0 | 4 | 82.7 | 0.282916 | 18 | 0.001320 | 16 | 0.049436 | 1300 | 0.282732 | 4.6 | 6.5 | 555 | 904 |
| B-574 09 | 86.0 | 4 | 82.7 | 0.282956 | 24 | 0.001983 | 190 | 0.064575 | 4600 | 0.282731 | 6.0 | 8.0 | 499 | 791 |
| B-574 10 | 84.0 | 4 | 82.7 | 0.282739 | 28 | 0.001335 | 37 | 0.050189 | 850 | 0.282732 | −1.6 | 0.2 | 847 | 1413 |
| B-574 11 | 83.0 | 4 | 82.7 | 0.283004 | 22 | 0.001470 | 22 | 0.054875 | 390 | 0.282733 | 7.7 | 9.6 | 411 | 652 |
| B-574 12 | 83.0 | 4 | 82.7 | 0.282974 | 21 | 0.001023 | 24 | 0.039020 | 1500 | 0.282733 | 6.7 | 8.5 | 455 | 737 |
| B-574 13 | 82.0 | 4 | 82.7 | 0.282901 | 22 | 0.001398 | 16 | 0.055121 | 1100 | 0.282734 | 4.1 | 5.9 | 581 | 950 |
| B-574 14 | 83.0 | 4 | 82.7 | 0.282918 | 32 | 0.001358 | 29 | 0.055448 | 680 | 0.282733 | 4.7 | 6.5 | 552 | 900 |
| B-574 15 | 81.0 | 4 | 82.7 | 0.282990 | 23 | 0.001596 | 24 | 0.064578 | 1600 | 0.282734 | 7.2 | 9.0 | 436 | 695 |
| B-574 16 | 83.0 | 4 | 82.7 | 0.283003 | 22 | 0.001523 | 94 | 0.063286 | 3400 | 0.282733 | 7.7 | 9.6 | 413 | 655 |
| B-574 17 | 82.0 | 4 | 82.7 | 0.282862 | 19 | 0.001250 | 12 | 0.052758 | 490 | 0.282734 | 2.7 | 4.5 | 643 | 1061 |
| B-574 18 | 81.0 | 4 | 82.7 | 0.282847 | 20 | 0.001253 | 17 | 0.054294 | 1800 | 0.282734 | 2.2 | 4.0 | 667 | 1105 |
| B-574 19 | 82.0 | 4 | 82.7 | 0.282969 | 22 | 0.001566 | 48 | 0.064918 | 560 | 0.282734 | 6.5 | 8.3 | 471 | 755 |
| B-574 20 | 83.0 | 4 | 82.7 | 0.282928 | 18 | 0.001205 | 21 | 0.049641 | 1700 | 0.282733 | 5.1 | 6.9 | 533 | 870 |
| B-574 21 | 83.0 | 4 | 82.7 | 0.282968 | 29 | 0.001412 | 13 | 0.060375 | 1000 | 0.282733 | 6.5 | 8.3 | 470 | 756 |
| B-574 22 | 81.0 | 4 | 82.7 | 0.282847 | 31 | 0.001048 | 8 | 0.046166 | 1100 | 0.282734 | 2.2 | 4.0 | 663 | 1104 |
| B-574 23 | 82.0 | 4 | 82.7 | 0.283047 | 24 | 0.001366 | 23 | 0.058001 | 1600 | 0.282734 | 9.3 | 11.1 | 338 | 528 |
| B-574 24 | 81.0 | 4 | 82.7 | 0.282939 | 27 | 0.000959 | 24 | 0.038997 | 1400 | 0.282734 | 5.4 | 7.2 | 511 | 839 |
| B-621d 02 | 71.0 | 4 | 70.8 | 0.282850 | 32 | 0.001778 | 65 | 0.074440 | 710 | 0.282740 | 2.3 | 3.9 | 673 | 1106 |
| B-621d 03 | 72.0 | 4 | 70.8 | 0.282947 | 40 | 0.000547 | 36 | 0.020478 | 610 | 0.282740 | 5.7 | 7.3 | 492 | 821 |
| B-621d 04 | 71.0 | 4 | 70.8 | 0.282967 | 51 | 0.001102 | 22 | 0.044112 | 890 | 0.282740 | 6.4 | 8.0 | 467 | 767 |
| B-621d 05 | 71.0 | 4 | 70.8 | 0.283004 | 21 | 0.002076 | 42 | 0.098522 | 1500 | 0.282740 | 7.7 | 9.3 | 419 | 663 |
| B-621d 06 | 69.0 | 4 | 70.8 | 0.282971 | 33 | 0.000968 | 21 | 0.045244 | 1400 | 0.282742 | 6.6 | 8.1 | 459 | 756 |
| B-621d 07 | 71.0 | 4 | 70.8 | 0.283091 | 24 | 0.002183 | 44 | 0.102712 | 1900 | 0.282740 | 10.8 | 12.4 | 272 | 412 |
| B-621d 08 | 72.0 | 4 | 70.8 | 0.282879 | 42 | 0.001716 | 90 | 0.080165 | 6600 | 0.282740 | 3.3 | 4.9 | 624 | 1022 |
| B-621d 09 | 70.0 | 4 | 70.8 | 0.282978 | 35 | 0.001913 | 66 | 0.089446 | 3300 | 0.282741 | 6.8 | 8.4 | 461 | 739 |
| B-621d 12 | 69.0 | 4 | 70.8 | 0.282963 | 30 | 0.001527 | 60 | 0.062229 | 1700 | 0.282742 | 6.3 | 7.8 | 480 | 781 |
| B-621d 13 | 70.0 | 4 | 70.8 | 0.282905 | 33 | 0.001156 | 69 | 0.049926 | 3700 | 0.282741 | 4.2 | 5.8 | 570 | 946 |
| B-621d 14 | 73.0 | 4 | 70.8 | 0.282918 | 22 | 0.001739 | 55 | 0.069724 | 1100 | 0.282739 | 4.7 | 6.3 | 559 | 909 |
| B-621d 15 | 70.0 | 4 | 70.8 | 0.282869 | 33 | 0.001386 | 65 | 0.054181 | 1800 | 0.282741 | 3.0 | 4.5 | 634 | 1051 |
| B-621d 16 | 70.0 | 4 | 70.8 | 0.283010 | 27 | 0.001909 | 120 | 0.074854 | 2500 | 0.282741 | 8.0 | 9.5 | 407 | 646 |
| B-621d 18 | 70.0 | 4 | 70.8 | 0.282946 | 37 | 0.001169 | 60 | 0.044113 | 890 | 0.282741 | 5.7 | 7.2 | 503 | 828 |
| B-621d 19 | 73.0 | 4 | 70.8 | 0.282968 | 23 | 0.001358 | 14 | 0.056832 | 1000 | 0.282739 | 6.5 | 8.1 | 469 | 763 |
| B-621d 20 | 72.0 | 4 | 70.8 | 0.282940 | 41 | 0.001061 | 23 | 0.039542 | 910 | 0.282740 | 5.5 | 7.1 | 511 | 844 |
| B-621d 21 | 69.0 | 4 | 70.8 | 0.282881 | 38 | 0.001018 | 18 | 0.040267 | 1600 | 0.282742 | 3.4 | 4.9 | 607 | 1016 |
| B-621d 22 | 71.0 | 4 | 70.8 | 0.283005 | 21 | 0.001519 | 55 | 0.060828 | 870 | 0.282740 | 7.8 | 9.4 | 410 | 658 |
| B-621d 23 | 72.0 | 4 | 70.8 | 0.282905 | 25 | 0.001410 | 26 | 0.056309 | 2600 | 0.282740 | 4.2 | 5.8 | 575 | 946 |
| B-621d 24 | 71.0 | 4 | 70.8 | 0.282960 | 26 | 0.001254 | 34 | 0.048944 | 940 | 0.282740 | 6.2 | 7.8 | 481 | 787 |
| B-621d 25 | 70.0 | 4 | 70.8 | 0.283030 | 15 | 0.002067 | 62 | 0.082775 | 2200 | 0.282741 | 8.7 | 10.2 | 375 | 589 |
| B-621d 26 | 71.0 | 4 | 70.8 | 0.283014 | 23 | 0.001869 | 55 | 0.075742 | 3600 | 0.282740 | 8.1 | 9.7 | 399 | 634 |
| B-621d 27 | 71.0 | 4 | 70.8 | 0.282794 | 39 | 0.001293 | 22 | 0.046630 | 240 | 0.282740 | 0.3 | 1.9 | 755 | 1265 |
| B-621d 28 | 69.0 | 4 | 70.8 | 0.282988 | 27 | 0.001444 | 45 | 0.057770 | 3100 | 0.282742 | 7.2 | 8.7 | 437 | 709 |
| B-783M 01 | 78.0 | 4 | 77.7 | 0.282988 | 28 | 0.002826 | 47 | 0.125259 | 5100 | 0.282736 | 7.2 | 8.9 | 457 | 708 |
| B-783M 02 | 77.0 | 4 | 77.7 | 0.283188 | 31 | 0.003515 | 60 | 0.158930 | 6700 | 0.282737 | 14.3 | 16.0 | 111 | 132 |

(*continued on next page*)



Please cite this article in press as: Jahn, B.-m., et al. Emplacement ages, geochemical and Sr–Nd–Hf isotopic characterization of Mesozoic to early Cenozoic granitoids of the Sikhote-Alin Orogenic Belt, Russian Far East: Crustal growth and regional tectonic evolution. Journal of Asian Earth Sciences (2015), http://dx.doi.org/10.1016/j.jseaes.2015.08.012

**Table 5** (*continued*)

| Spot | Individual spot age (Ma) | ±2σ | Sample mean age (Ma) | $^{176}Hf/^{177}Hf$ | ±2σ | $^{176}Lu/^{177}Hf$ | ±2σ | $^{176}Yb/^{177}Hf$ | ±2σ | $^{176}Hf/^{177}Hf$ CHUR($t$) | $\varepsilon_{Hf}(0)$ | $\varepsilon_{Hf}(t)$ | $T_{DM}$ | $T_{DM}^{C}$ |
|---|---|---|---|---|---|---|---|---|---|---|---|---|---|---|
| B-783M 03 | 77.0 | 4 | 77.7 | 0.282981 | 23 | 0.002313 | 76 | 0.099093 | 4900 | 0.282737 | 6.9 | 8.6 | 461 | 727 |
| B-783M 04 | 79.0 | 4 | 77.7 | 0.282929 | 34 | 0.002356 | 53 | 0.092809 | 3000 | 0.282735 | 5.1 | 6.8 | 551 | 875 |
| B-783M 06 | 78.0 | 4 | 77.7 | 0.282980 | 30 | 0.001819 | 69 | 0.081862 | 4300 | 0.282736 | 6.9 | 8.6 | 456 | 727 |
| B-783M 08 | 80.0 | 4 | 77.7 | 0.283068 | 29 | 0.003998 | 110 | 0.173601 | 8400 | 0.282735 | 10.0 | 11.8 | 331 | 480 |
| B-783M 09 | 79.0 | 4 | 77.7 | 0.282964 | 32 | 0.002683 | 92 | 0.105543 | 1500 | 0.282735 | 6.3 | 8.1 | 496 | 776 |
| B-783M 10 | 79.0 | 4 | 77.7 | 0.283171 | 33 | 0.005048 | 120 | 0.216789 | 8500 | 0.282735 | 13.6 | 15.4 | 149 | 187 |
| B-783M 12 | 80.0 | 4 | 77.7 | 0.283046 | 24 | 0.002810 | 120 | 0.115046 | 6100 | 0.282735 | 9.2 | 11.0 | 356 | 539 |
| B-783M 13 | 77.0 | 4 | 77.7 | 0.282975 | 26 | 0.003764 | 110 | 0.146863 | 2300 | 0.282737 | 6.7 | 8.4 | 495 | 750 |
| B-783M 14 | 77.0 | 4 | 77.7 | 0.283026 | 23 | 0.003686 | 61 | 0.137283 | 4500 | 0.282737 | 8.5 | 10.2 | 402 | 602 |
| B-783M 15 | 78.0 | 4 | 77.7 | 0.282965 | 19 | 0.001977 | 73 | 0.068015 | 2500 | 0.282736 | 6.4 | 8.1 | 484 | 771 |
| B-783M 18 | 78.0 | 4 | 77.7 | 0.283035 | 35 | 0.002355 | 100 | 0.089281 | 3700 | 0.282736 | 8.8 | 10.6 | 370 | 570 |
| B-783M 19 | 76.0 | 6 | 77.7 | 0.282907 | 110 | 0.001500 | 18 | 0.056466 | 700 | 0.282737 | 4.3 | 6.0 | 573 | 937 |
| B-783M 20 | 75.0 | 4 | 77.7 | 0.282978 | 34 | 0.002622 | 66 | 0.104769 | 3300 | 0.282738 | 6.8 | 8.5 | 471 | 738 |
| B-783M 21 | 76.0 | 4 | 77.7 | 0.283043 | 34 | 0.002896 | 210 | 0.117582 | 10000 | 0.282737 | 9.1 | 10.8 | 362 | 551 |
| B-783M 23 | 78.0 | 4 | 77.7 | 0.283100 | 54 | 0.003432 | 170 | 0.134546 | 3800 | 0.282736 | 11.1 | 12.9 | 267 | 387 |
| B-919b 01 | 80.0 | 4 | 80.8 | 0.282907 | 17 | 0.001001 | 25 | 0.038583 | 800 | 0.282735 | 4.3 | 6.1 | 564 | 932 |
| B-919b 02 | 79.0 | 4 | 80.8 | 0.282844 | 21 | 0.001409 | 37 | 0.060001 | 2300 | 0.282735 | 2.1 | 3.8 | 675 | 1116 |
| B-919b 03 | 81.0 | 4 | 80.8 | 0.282893 | 28 | 0.000794 | 12 | 0.033307 | 330 | 0.282734 | 3.8 | 5.6 | 583 | 971 |
| B-919b 04 | 80.0 | 4 | 80.8 | 0.282864 | 24 | 0.001640 | 35 | 0.073601 | 1400 | 0.282735 | 2.8 | 4.6 | 647 | 1059 |
| B-919b 05 | 82.0 | 4 | 80.8 | 0.282866 | 33 | 0.001133 | 72 | 0.049779 | 940 | 0.282734 | 2.9 | 4.7 | 634 | 1049 |
| B-919b 06 | 82.0 | 4 | 80.8 | 0.282876 | 29 | 0.001452 | 61 | 0.067036 | 4200 | 0.282734 | 3.2 | 5.0 | 623 | 1022 |
| B-919b 07 | 80.0 | 4 | 80.8 | 0.283000 | 21 | 0.001785 | 44 | 0.074224 | 930 | 0.282735 | 7.6 | 9.4 | 422 | 667 |
| B-919b 08 | 80.0 | 4 | 80.8 | 0.282964 | 17 | 0.001657 | 37 | 0.069377 | 2500 | 0.282735 | 6.3 | 8.1 | 480 | 771 |
| B-919b 09 | 83.0 | 4 | 80.8 | 0.282697 | 28 | 0.001648 | 39 | 0.067767 | 2700 | 0.282733 | −3.1 | −1.3 | 925 | 1536 |
| B-919b 10 | 81.0 | 4 | 80.8 | 0.282911 | 27 | 0.001565 | 40 | 0.063309 | 2900 | 0.282734 | 4.5 | 6.3 | 567 | 922 |
| B-919b 11 | 80.0 | 4 | 80.8 | 0.282839 | 32 | 0.000895 | 33 | 0.036098 | 1100 | 0.282735 | 1.9 | 3.7 | 673 | 1128 |
| B-919b 12 | 79.0 | 4 | 80.8 | 0.282867 | 20 | 0.001481 | 26 | 0.061609 | 1100 | 0.282735 | 2.9 | 4.7 | 639 | 1050 |
| B-919b 13 | 81.0 | 4 | 80.8 | 0.282990 | 30 | 0.000737 | 11 | 0.028689 | 860 | 0.282734 | 7.2 | 9.0 | 425 | 691 |
| B-919b 14 | 78.0 | 4 | 80.8 | 0.282786 | 32 | 0.001115 | 18 | 0.047383 | 1500 | 0.282736 | 0.0 | 1.8 | 764 | 1282 |
| B-919b 15 | 81.0 | 4 | 80.8 | 0.282730 | 26 | 0.001165 | 77 | 0.045019 | 2200 | 0.282734 | −1.9 | −0.1 | 857 | 1441 |
| B-919b 17 | 65.0 | 4 | 80.8 | 0.282955 | 23 | 0.001358 | 39 | 0.056056 | 2100 | 0.282744 | 6.0 | 7.5 | 491 | 807 |
| B-919b 18 | 69.0 | 4 | 80.8 | 0.282949 | 22 | 0.001588 | 61 | 0.059534 | 1800 | 0.282742 | 5.8 | 7.3 | 504 | 822 |
| B-919b 19 | 82.0 | 4 | 80.8 | 0.282987 | 31 | 0.001315 | 60 | 0.055747 | 1700 | 0.282734 | 7.1 | 9.0 | 437 | 701 |
| B-919b 20 | 81.0 | 4 | 80.8 | 0.282847 | 24 | 0.000873 | 22 | 0.035861 | 1300 | 0.282734 | 2.2 | 4.0 | 660 | 1104 |
| B-919b 21 | 81.0 | 4 | 80.8 | 0.282851 | 29 | 0.000906 | 15 | 0.032056 | 540 | 0.282734 | 2.3 | 4.1 | 654 | 1092 |
| B-919b 22 | 81.0 | 4 | 80.8 | 0.282823 | 18 | 0.001125 | 78 | 0.045303 | 730 | 0.282734 | 1.3 | 3.1 | 704 | 1174 |
| B-919b 23 | 80.0 | 4 | 80.8 | 0.282802 | 22 | 0.001239 | 15 | 0.045701 | 240 | 0.282735 | 0.6 | 2.4 | 741 | 1235 |
| B-919b 24 | 81.0 | 4 | 80.8 | 0.282805 | 23 | 0.001023 | 11 | 0.034534 | 670 | 0.282734 | 0.7 | 2.5 | 731 | 1225 |
| B-919b 25 | 79.0 | 4 | 80.8 | 0.282875 | 23 | 0.001354 | 34 | 0.045564 | 860 | 0.282735 | 3.2 | 4.9 | 623 | 1027 |
| B-919b 26 | 81.0 | 4 | 80.8 | 0.282847 | 100 | 0.001125 | 33 | 0.036708 | 830 | 0.282734 | 2.2 | 4.0 | 665 | 1105 |
| B-919b 27 | 81.0 | 4 | 80.8 | 0.282997 | 25 | 0.001094 | 11 | 0.035941 | 710 | 0.282734 | 7.5 | 9.3 | 418 | 672 |
| B-919b 28 | 82.0 | 4 | 80.8 | 0.282821 | 36 | 0.000805 | 45 | 0.027773 | 420 | 0.282734 | 1.3 | 3.1 | 700 | 1177 |
| B984 01 | 78.0 | 4 | 78.1 | 0.283031 | 23 | 0.001054 | 20 | 0.044611 | 1100 | 0.282736 | 8.7 | 10.4 | 361 | 576 |
| B984 02 | 77.0 | 4 | 78.1 | 0.283065 | 29 | 0.002085 | 46 | 0.088584 | 1500 | 0.282737 | 9.9 | 11.6 | 315 | 483 |
| B984 03 | 76.0 | 4 | 78.1 | 0.282879 | 29 | 0.001910 | 21 | 0.080220 | 620 | 0.282737 | 3.3 | 5.0 | 627 | 1020 |
| B984 04 | 80.0 | 4 | 78.1 | 0.282956 | 22 | 0.001611 | 26 | 0.070051 | 1500 | 0.282735 | 6.0 | 7.8 | 493 | 794 |
| B984 05 | 80.0 | 4 | 78.1 | 0.282926 | 42 | 0.000895 | 35 | 0.037382 | 2200 | 0.282735 | 5.0 | 6.8 | 531 | 877 |
| B984 06 | 78.0 | 4 | 78.1 | 0.282839 | 28 | 0.001526 | 37 | 0.062468 | 1100 | 0.282736 | 1.9 | 3.6 | 686 | 1132 |
| B984 07 | 79.0 | 4 | 78.1 | 0.282972 | 23 | 0.001492 | 69 | 0.062195 | 2200 | 0.282735 | 6.6 | 8.4 | 465 | 748 |
| B984 08 | 78.0 | 4 | 78.1 | 0.282876 | 27 | 0.000942 | 92 | 0.037813 | 3400 | 0.282736 | 3.2 | 5.0 | 614 | 1023 |
| B984 09 | 78.0 | 4 | 78.1 | 0.283019 | 28 | 0.002494 | 91 | 0.112396 | 4800 | 0.282736 | 8.3 | 10.0 | 399 | 617 |
| B984 10 | 79.0 | 4 | 78.1 | 0.283059 | 20 | 0.001686 | 100 | 0.069088 | 3600 | 0.282735 | 9.7 | 11.4 | 322 | 497 |
| B984 12 | 78.0 | 4 | 78.1 | 0.282873 | 32 | 0.001270 | 34 | 0.049851 | 1100 | 0.282736 | 3.1 | 4.8 | 625 | 1033 |
| B984 13 | 81.0 | 4 | 78.1 | 0.282945 | 30 | 0.001469 | 16 | 0.064241 | 950 | 0.282734 | 5.7 | 7.5 | 509 | 824 |
| B984 15 | 77.0 | 4 | 78.1 | 0.283075 | 27 | 0.001470 | 31 | 0.059127 | 700 | 0.282737 | 10.3 | 12.0 | 293 | 451 |

Please cite this article in press as: Jahn, B.-m., et al. Emplacement ages, geochemical and Sr–Nd–Hf isotopic characterization of Mesozoic to early Cenozoic granitoids of the Sikhote-Alin Orogenic Belt, Russian Far East: Crustal growth and regional tectonic evolution. Journal of Asian Earth Sciences (2015), http://dx.doi.org/10.1016/j.jseaes.2015.08.012

**Table 5** (*continued*)

| Spot | Individual spot age (Ma) | ±2σ | Sample mean age (Ma) | $^{176}Hf/^{177}Hf$ | ±2σ | $^{176}Lu/^{177}Hf$ | ±2σ | $^{176}Yb/^{177}Hf$ | ±2σ | $^{176}Hf/^{177}Hf$ CHUR($t$) | $\varepsilon_{Hf}(0)$ | $\varepsilon_{Hf}(t)$ | $T_{DM}$ | $T_{DM}^{c}$ |
|---|---|---|---|---|---|---|---|---|---|---|---|---|---|---|
| B984 16 | 78.0 | 4 | 78.1 | 0.283025 | 30 | 0.001884 | 56 | 0.076523 | 1500 | 0.282736 | 8.5 | 10.2 | 381 | 597 |
| B984 17 | 81.0 | 4 | 78.1 | 0.283021 | 28 | 0.002839 | 53 | 0.110594 | 2800 | 0.282734 | 8.3 | 10.1 | 400 | 611 |
| B984 18 | 76.0 | 4 | 78.1 | 0.283043 | 35 | 0.001802 | 50 | 0.065343 | 600 | 0.282737 | 9.1 | 10.8 | 350 | 546 |
| B984 19 | 76.0 | 4 | 78.1 | 0.282924 | 36 | 0.002221 | 92 | 0.081520 | 870 | 0.282737 | 4.9 | 6.6 | 557 | 891 |
| B984 20 | 78.0 | 4 | 78.1 | 0.282868 | 31 | 0.001295 | 13 | 0.052802 | 1100 | 0.282736 | 2.9 | 4.7 | 634 | 1047 |
| B984 21 | 77.0 | 4 | 78.1 | 0.282846 | 35 | 0.001876 | 32 | 0.075328 | 1100 | 0.282737 | 2.2 | 3.9 | 682 | 1114 |
| B984 22 | 79.0 | 4 | 78.1 | 0.282993 | 25 | 0.001780 | 43 | 0.068885 | 1600 | 0.282735 | 7.4 | 9.1 | 434 | 688 |
| B984 23 | 77.0 | 4 | 78.1 | 0.282927 | 23 | 0.001919 | 84 | 0.070206 | 1900 | 0.282737 | 5.0 | 6.7 | 547 | 881 |
| B984 24 | 76.0 | 4 | 78.1 | 0.283176 | 120 | 0.002281 | 150 | 0.083552 | 4300 | 0.282737 | 13.8 | 15.5 | 127 | 163 |
| GV-722 02 | 78.0 | 4 | 74.8 | 0.282836 | 27 | 0.002192 | 190 | 0.079225 | 6100 | 0.282736 | 1.8 | 3.5 | 706 | 1143 |
| GV-722 03 | 74.0 | 4 | 74.8 | 0.282832 | 19 | 0.003335 | 270 | 0.148830 | 12000 | 0.282739 | 1.7 | 3.3 | 740 | 1161 |
| GV-722 04 | 74.0 | 2 | 74.8 | 0.282770 | 22 | 0.001104 | 11 | 0.039173 | 620 | 0.282739 | −0.5 | 1.1 | 790 | 1331 |
| GV-722 05 | 71.0 | 4 | 74.8 | 0.282695 | 26 | 0.001587 | 91 | 0.061365 | 2600 | 0.282740 | −3.2 | −1.6 | 926 | 1550 |
| GV-722 06 | 74.0 | 2 | 74.8 | 0.282786 | 24 | 0.002594 | 92 | 0.096472 | 2600 | 0.282739 | 0.0 | 1.7 | 801 | 1291 |
| GV-722 07 | 76.0 | 4 | 74.8 | 0.282779 | 26 | 0.000994 | 13 | 0.035766 | 850 | 0.282737 | −0.2 | 1.5 | 773 | 1303 |
| GV-722 08 | 75.0 | 4 | 74.8 | 0.282754 | 36 | 0.000935 | 44 | 0.034422 | 2100 | 0.282738 | −1.1 | 0.6 | 812 | 1376 |
| GV-722 09 | 76.0 | 4 | 74.8 | 0.282748 | 26 | 0.001049 | 8 | 0.037428 | 510 | 0.282737 | −1.3 | 0.4 | 825 | 1392 |
| GV-722 10 | 75.0 | 2 | 74.8 | 0.282720 | 30 | 0.001848 | 100 | 0.067099 | 4500 | 0.282738 | −2.3 | −0.6 | 892 | 1476 |
| GV-722 12 | 74.0 | 2 | 74.8 | 0.282779 | 27 | 0.001667 | 27 | 0.062919 | 1400 | 0.282739 | −0.2 | 1.4 | 789 | 1307 |
| GV-722 13 | 77.0 | 4 | 74.8 | 0.282749 | 20 | 0.000769 | 2.4 | 0.028216 | 470 | 0.282737 | −1.3 | 0.4 | 816 | 1388 |
| GV-722 14 | 76.0 | 4 | 74.8 | 0.282768 | 24 | 0.002555 | 250 | 0.090776 | 8600 | 0.282737 | −0.6 | 1.1 | 831 | 1341 |
| GV-722 15 | 76.0 | 4 | 74.8 | 0.282783 | 31 | 0.001662 | 86 | 0.058393 | 2800 | 0.282737 | −0.1 | 1.6 | 782 | 1294 |
| GV-722 16 | 75.0 | 2 | 74.8 | 0.282737 | 24 | 0.001088 | 58 | 0.036068 | 2400 | 0.282738 | −1.7 | 0.0 | 844 | 1425 |
| GV-722 17 | 74.0 | 4 | 74.8 | 0.282754 | 33 | 0.001487 | 140 | 0.055419 | 6200 | 0.282739 | −1.1 | 0.5 | 826 | 1378 |
| GV-722 19 | 76.0 | 4 | 74.8 | 0.282717 | 21 | 0.001138 | 63 | 0.040474 | 2600 | 0.282737 | −2.4 | −0.7 | 878 | 1482 |
| GV-722 22 | 77.0 | 4 | 74.8 | 0.282892 | 31 | 0.001639 | 120 | 0.061254 | 4300 | 0.282737 | 3.8 | 5.5 | 600 | 980 |
| GV-722 23 | 76.0 | 4 | 74.8 | 0.282867 | 25 | 0.001945 | 100 | 0.068926 | 3400 | 0.282737 | 2.9 | 4.6 | 648 | 1054 |
| GV-722 24 | 73.0 | 4 | 74.8 | 0.282669 | 18 | 0.001216 | 80 | 0.045757 | 3400 | 0.282739 | −4.1 | −2.5 | 958 | 1621 |
| GV-1583-2 01 | 86.0 | 4 | 86.0 | 0.282928 | 26 | 0.001058 | 21 | 0.038960 | 890 | 0.282731 | 5.1 | 7.0 | 531 | 868 |
| GV-1583-2 02 | 85.0 | 4 | 86.0 | 0.282900 | 19 | 0.000906 | 19 | 0.032044 | 1200 | 0.282732 | 4.1 | 6.0 | 574 | 948 |
| GV-1583-2 03 | 85.0 | 4 | 86.0 | 0.282829 | 29 | 0.001621 | 93 | 0.061377 | 4400 | 0.282732 | 1.6 | 3.4 | 705 | 1156 |
| GV-1583-2 04 | 84.0 | 4 | 86.0 | 0.282839 | 23 | 0.000689 | 6.7 | 0.023752 | 180 | 0.282732 | 1.9 | 3.8 | 669 | 1124 |
| GV-1583-2 05 | 84.0 | 4 | 86.0 | 0.282846 | 25 | 0.001263 | 25 | 0.044088 | 940 | 0.282732 | 2.2 | 4.0 | 669 | 1106 |
| GV-1583-2 06 | 83.0 | 4 | 86.0 | 0.282893 | 24 | 0.000882 | 74 | 0.031073 | 3000 | 0.282733 | 3.8 | 5.7 | 585 | 970 |
| GV-1583-2 07 | 84.0 | 4 | 86.0 | 0.282972 | 23 | 0.000854 | 33 | 0.034068 | 2000 | 0.282732 | 6.6 | 8.5 | 456 | 741 |
| GV-1583-2 08 | 87.0 | 4 | 86.0 | 0.282870 | 15 | 0.001638 | 94 | 0.068116 | 3600 | 0.282730 | 3.0 | 4.9 | 637 | 1036 |
| GV-1583-2 09 | 86.0 | 4 | 86.0 | 0.282947 | 28 | 0.001084 | 42 | 0.044514 | 2500 | 0.282731 | 5.7 | 7.6 | 500 | 813 |
| GV-1583-2 10 | 88.0 | 4 | 86.0 | 0.282996 | 23 | 0.000872 | 46 | 0.035833 | 2400 | 0.282730 | 7.5 | 9.4 | 417 | 669 |
| GV-1583-2 11 | 88.0 | 4 | 86.0 | 0.282960 | 18 | 0.001272 | 32 | 0.050947 | 1000 | 0.282730 | 6.2 | 8.1 | 481 | 775 |
| GV-1583-2 12 | 87.0 | 4 | 86.0 | 0.283040 | 26 | 0.001644 | 86 | 0.060744 | 1400 | 0.282730 | 9.0 | 11.0 | 353 | 546 |
| GV-1583-2 13 | 86.0 | 4 | 86.0 | 0.282805 | 31 | 0.001042 | 64 | 0.042387 | 2800 | 0.282731 | 0.7 | 2.6 | 732 | 1221 |
| GV-1583-2 14 | 87.0 | 4 | 86.0 | 0.282908 | 19 | 0.001033 | 26 | 0.043725 | 1800 | 0.282730 | 4.3 | 6.3 | 563 | 924 |
| GV-1583-2 15 | 89.0 | 4 | 86.0 | 0.282897 | 17 | 0.001061 | 33 | 0.047069 | 890 | 0.282729 | 4.0 | 5.9 | 581 | 955 |
| GV-1583-2 16 | 87.0 | 4 | 86.0 | 0.282956 | 26 | 0.001939 | 50 | 0.088195 | 1900 | 0.282730 | 6.0 | 8.0 | 498 | 790 |
| GV-1583-2 17 | 86.0 | 4 | 86.0 | 0.283017 | 22 | 0.001758 | 110 | 0.077484 | 3400 | 0.282731 | 8.2 | 10.1 | 393 | 614 |
| GV-1583-2 18 | 85.0 | 4 | 86.0 | 0.282863 | 15 | 0.001898 | 54 | 0.085921 | 2100 | 0.282732 | 2.8 | 4.6 | 654 | 1059 |
| GV-1583-2 19 | 87.0 | 4 | 86.0 | 0.282954 | 16 | 0.000948 | 39 | 0.039798 | 1200 | 0.282730 | 6.0 | 7.9 | 486 | 791 |
| GV-1583-2 20 | 87.0 | 4 | 86.0 | 0.283065 | 25 | 0.000965 | 2.6 | 0.041022 | 590 | 0.282730 | 9.9 | 11.8 | 305 | 471 |
| GV-1583-2 21 | 86.0 | 4 | 86.0 | 0.283035 | 19 | 0.000828 | 11 | 0.034219 | 980 | 0.282731 | 8.8 | 10.8 | 352 | 558 |
| GV-1583-2 23 | 85.0 | 4 | 86.0 | 0.283062 | 17 | 0.001021 | 17 | 0.041053 | 510 | 0.282732 | 9.8 | 11.7 | 310 | 481 |
| GV-1583-2 24 | 86.0 | 4 | 86.0 | 0.282974 | 30 | 0.001169 | 46 | 0.049295 | 1100 | 0.282731 | 6.7 | 8.6 | 457 | 735 |
| GV-1774 01 | 89.0 | 4 | 88.3 | 0.283021 | 35 | 0.000935 | 8.7 | 0.033055 | 730 | 0.282729 | 8.3 | 10.3 | 376 | 596 |
| GV-1774 02 | 88.0 | 4 | 88.3 | 0.282912 | 29 | 0.000711 | 46 | 0.025340 | 2300 | 0.282730 | 4.5 | 6.4 | 551 | 911 |
| GV-1774 03 | 89.0 | 4 | 88.3 | 0.282900 | 20 | 0.000895 | 8.7 | 0.032169 | 900 | 0.282729 | 4.1 | 6.0 | 574 | 945 |
| GV-1774 04 | 88.0 | 4 | 88.3 | 0.282929 | 24 | 0.001788 | 52 | 0.062370 | 2700 | 0.282730 | 5.1 | 7.0 | 541 | 867 |

(*continued on next page*)



Please cite this article in press as: Jahn, B.-m., et al. Emplacement ages, geochemical and Sr–Nd–Hf isotopic characterization of Mesozoic to early Cenozoic granitoids of the Sikhote-Alin Orogenic Belt, Russian Far East: Crustal growth and regional tectonic evolution. Journal of Asian Earth Sciences (2015), http://dx.doi.org/10.1016/j.jseaes.2015.08.012

**Table 5** (*continued*)

| Spot | Individual spot age (Ma) | ±2σ | Sample mean age (Ma) | $^{176}Hf/^{177}Hf$ | ±2σ | $^{176}Lu/^{177}Hf$ | ±2σ | $^{176}Yb/^{177}Hf$ | ±2σ | $^{176}Hf/^{177}Hf$ CHUR($t$) | $\varepsilon_{Hf}(0)$ | $\varepsilon_{Hf}(t)$ | $T_{DM}$ | $T_{DM}^{c}$ |
|---|---|---|---|---|---|---|---|---|---|---|---|---|---|---|
| GV-1774 07 | 91.0 | 4 | 88.3 | 0.283067 | 23 | 0.001578 | 83 | 0.056968 | 3600 | 0.282728 | 10.0 | 12.0 | 307 | 465 |
| GV-1774 08 | 88.0 | 4 | 88.3 | 0.282983 | 28 | 0.001238 | 67 | 0.049255 | 3500 | 0.282730 | 7.0 | 9.0 | 443 | 708 |
| GV-1774 09 | 87.0 | 4 | 88.3 | 0.282895 | 25 | 0.002055 | 37 | 0.078404 | 980 | 0.282730 | 3.9 | 5.8 | 603 | 966 |
| GV-1774 10 | 89.0 | 4 | 88.3 | 0.282895 | 18 | 0.001172 | 21 | 0.042218 | 740 | 0.282729 | 3.9 | 5.9 | 587 | 961 |
| GV-1774 11 | 87.0 | 4 | 88.3 | 0.282931 | 31 | 0.000838 | 28 | 0.029862 | 1300 | 0.282730 | 5.2 | 7.1 | 522 | 857 |
| GV-1774 12 | 87.0 | 4 | 88.3 | 0.282884 | 23 | 0.001124 | 37 | 0.041837 | 1700 | 0.282730 | 3.5 | 5.4 | 604 | 994 |
| GV-1774 13 | 87.0 | 4 | 88.3 | 0.282909 | 32 | 0.000740 | 26 | 0.030225 | 1400 | 0.282730 | 4.4 | 6.3 | 556 | 920 |
| GV-1774 14 | 87.0 | 4 | 88.3 | 0.282960 | 29 | 0.001652 | 12 | 0.067773 | 1000 | 0.282730 | 6.2 | 8.1 | 487 | 777 |
| GV-1774 15 | 89.0 | 4 | 88.3 | 0.282985 | 23 | 0.001143 | 16 | 0.045187 | 1100 | 0.282729 | 7.1 | 9.1 | 438 | 701 |
| GV-1774 16 | 89.0 | 4 | 88.3 | 0.282883 | 18 | 0.001286 | 19 | 0.050336 | 930 | 0.282729 | 3.5 | 5.4 | 609 | 996 |
| GV-1774 17 | 88.0 | 4 | 88.3 | 0.282844 | 25 | 0.000872 | 13 | 0.035676 | 900 | 0.282730 | 2.1 | 4.0 | 664 | 1107 |
| GV-1774 18 | 88.0 | 4 | 88.3 | 0.282989 | 23 | 0.001357 | 69 | 0.050975 | 2700 | 0.282730 | 7.2 | 9.2 | 435 | 691 |
| GV-1774 19 | 88.0 | 4 | 88.3 | 0.282965 | 22 | 0.001516 | 17 | 0.063901 | 1500 | 0.282730 | 6.4 | 8.3 | 477 | 761 |
| GV-1774 20 | 89.0 | 4 | 88.3 | 0.283094 | 31 | 0.001584 | 40 | 0.068746 | 3400 | 0.282729 | 10.9 | 12.9 | 262 | 388 |
| GV-1774 21 | 89.0 | 4 | 88.3 | 0.282999 | 22 | 0.001071 | 21 | 0.046128 | 1500 | 0.282729 | 7.6 | 9.5 | 414 | 660 |
| GV-1774 22 | 89.0 | 4 | 88.3 | 0.282974 | 26 | 0.001413 | 22 | 0.058629 | 1500 | 0.282729 | 6.7 | 8.7 | 460 | 734 |
| GV-1774 23 | 88.0 | 4 | 88.3 | 0.282955 | 22 | 0.000976 | 42 | 0.038162 | 2300 | 0.282730 | 6.0 | 8.0 | 485 | 788 |
| GV-1774 24 | 88.0 | 4 | 88.3 | 0.282923 | 27 | 0.001654 | 15 | 0.068683 | 650 | 0.282730 | 4.9 | 6.8 | 549 | 883 |
| ЧG-332 01 | 93.0 | 4 | 92.4 | 0.282763 | 27 | 0.000683 | 21 | 0.023970 | 1100 | 0.282727 | −0.8 | 1.3 | 791 | 1335 |
| ЧG-332 02 | 92.0 | 4 | 92.4 | 0.282821 | 28 | 0.001229 | 74 | 0.044466 | 2300 | 0.282727 | 1.3 | 3.3 | 710 | 1172 |
| ЧG-332 03 | 91.0 | 4 | 92.4 | 0.282786 | 22 | 0.001144 | 16 | 0.040974 | 570 | 0.282728 | 0.0 | 2.1 | 765 | 1273 |
| ЧG-332 04 | 91.0 | 4 | 92.4 | 0.282836 | 27 | 0.001473 | 18 | 0.054241 | 1300 | 0.282728 | 1.8 | 3.8 | 690 | 1130 |
| ЧG-332 05 | 92.0 | 4 | 92.4 | 0.282749 | 29 | 0.000864 | 14 | 0.031724 | 1200 | 0.282727 | −1.3 | 0.8 | 818 | 1377 |
| ЧG-332 06 | 93.0 | 4 | 92.4 | 0.282783 | 29 | 0.000974 | 17 | 0.035756 | 1500 | 0.282727 | −0.1 | 2.0 | 766 | 1279 |
| ЧG-332 07 | 92.0 | 4 | 92.4 | 0.282753 | 24 | 0.000687 | 35 | 0.023289 | 1100 | 0.282727 | −1.1 | 0.9 | 808 | 1364 |
| ЧG-332 08 | 92.0 | 4 | 92.4 | 0.282662 | 22 | 0.000669 | 10 | 0.024423 | 780 | 0.282727 | −4.3 | −2.3 | 954 | 1625 |
| ЧG-332 09 | 92.0 | 4 | 92.4 | 0.282775 | 33 | 0.000596 | 7.2 | 0.021292 | 160 | 0.282727 | −0.4 | 1.7 | 770 | 1301 |
| ЧG-332 10 | 94.0 | 4 | 92.4 | 0.282808 | 25 | 0.000679 | 9.4 | 0.025831 | 610 | 0.282726 | 0.8 | 2.9 | 719 | 1205 |
| ЧG-332 11 | 93.0 | 4 | 92.4 | 0.282713 | 29 | 0.001021 | 43 | 0.037906 | 1700 | 0.282727 | −2.5 | −0.5 | 881 | 1480 |
| ЧG-332 12 | 91.0 | 4 | 92.4 | 0.282725 | 26 | 0.000887 | 4.4 | 0.031750 | 340 | 0.282728 | −2.1 | −0.1 | 858 | 1446 |
| ЧG-332 13 | 91.0 | 4 | 92.4 | 0.282734 | 25 | 0.000830 | 14 | 0.030520 | 1100 | 0.282728 | −1.8 | 0.2 | 842 | 1420 |
| ЧG-332 14 | 92.0 | 4 | 92.4 | 0.282757 | 29 | 0.000525 | 7.7 | 0.019160 | 230 | 0.282727 | −1.0 | 1.1 | 797 | 1352 |
| ЧG-332 15 | 91.0 | 4 | 92.4 | 0.282819 | 19 | 0.000939 | 26 | 0.035849 | 1100 | 0.282728 | 1.2 | 3.2 | 706 | 1177 |
| ЧG-332 16 | 96.0 | 4 | 92.4 | 0.282775 | 27 | 0.000898 | 32 | 0.035336 | 1100 | 0.282725 | −0.4 | 1.8 | 777 | 1299 |
| ЧG-332 18 | 91.0 | 4 | 92.4 | 0.282697 | 17 | 0.000661 | 18 | 0.025329 | 920 | 0.282728 | −3.1 | −1.1 | 897 | 1525 |
| ЧG-332 19 | 93.0 | 4 | 92.4 | 0.282833 | 21 | 0.000800 | 20 | 0.030593 | 940 | 0.282727 | 1.7 | 3.8 | 681 | 1134 |
| ЧG-332 20 | 93.0 | 4 | 92.4 | 0.282678 | 19 | 0.000957 | 8.5 | 0.038190 | 780 | 0.282727 | −3.8 | −1.7 | 936 | 1580 |
| ЧG-332 21 | 95.0 | 4 | 92.4 | 0.282832 | 17 | 0.000874 | 11 | 0.033722 | 710 | 0.282725 | 1.7 | 3.8 | 684 | 1136 |
| ЧG-332 22 | 92.0 | 4 | 92.4 | 0.282835 | 26 | 0.000771 | 24 | 0.032908 | 1500 | 0.282727 | 1.8 | 3.8 | 677 | 1129 |
| ЧG-332 23 | 94.0 | 4 | 92.4 | 0.282763 | 25 | 0.001289 | 30 | 0.052989 | 2400 | 0.282726 | −0.8 | 1.3 | 806 | 1337 |
| ЧG-332 24 | 92.0 | 4 | 92.4 | 0.282732 | 34 | 0.000533 | 11 | 0.021710 | 880 | 0.282727 | −1.9 | 0.2 | 838 | 1424 |
| ЧG-410 01 | 94.0 | 4 | 91.5 | 0.282855 | 24 | 0.001115 | 29 | 0.042387 | 1300 | 0.282726 | 2.5 | 4.6 | 651 | 1072 |
| ЧG-410 02 | 92.0 | 4 | 91.5 | 0.282787 | 24 | 0.001075 | 36 | 0.038887 | 1300 | 0.282727 | 0.1 | 2.1 | 762 | 1269 |
| ЧG-410 03 | 92.0 | 4 | 91.5 | 0.282769 | 25 | 0.000952 | 24 | 0.032872 | 1300 | 0.282727 | −0.6 | 1.5 | 788 | 1320 |
| ЧG-410 04 | 91.0 | 4 | 91.5 | 0.282810 | 16 | 0.001423 | 45 | 0.050260 | 1100 | 0.282728 | 0.9 | 2.9 | 732 | 1205 |
| ЧG-410 05 | 92.0 | 4 | 91.5 | 0.282831 | 33 | 0.000862 | 33 | 0.028466 | 1000 | 0.282727 | 1.6 | 3.7 | 685 | 1141 |
| ЧG-410 06 | 90.0 | 4 | 91.5 | 0.282823 | 29 | 0.000948 | 39 | 0.033231 | 1200 | 0.282728 | 1.3 | 3.3 | 700 | 1166 |
| ЧG-410 08 | 89.0 | 4 | 91.5 | 0.282888 | 20 | 0.001301 | 23 | 0.045756 | 210 | 0.282729 | 3.6 | 5.6 | 601 | 982 |
| ЧG-410 11 | 95.0 | 4 | 91.5 | 0.282701 | 24 | 0.000597 | 17 | 0.021430 | 1100 | 0.282725 | −3.0 | −0.9 | 889 | 1511 |
| ЧG-410 10 | 94.0 | 4 | 91.5 | 0.282747 | 24 | 0.000696 | 8.4 | 0.023961 | 610 | 0.282726 | −1.3 | 0.7 | 818 | 1380 |
| ЧG-410 12 | 91.0 | 4 | 91.5 | 0.282780 | 24 | 0.000707 | 18 | 0.024133 | 980 | 0.282728 | −0.2 | 1.8 | 765 | 1288 |
| ЧG-410 13 | 87.0 | 4 | 91.5 | 0.282778 | 19 | 0.000813 | 16 | 0.028032 | 770 | 0.282730 | −0.2 | 1.7 | 770 | 1297 |
| ЧG-410 14 | 92.0 | 4 | 91.5 | 0.282822 | 28 | 0.001135 | 35 | 0.039052 | 1200 | 0.282727 | 1.3 | 3.4 | 706 | 1168 |
| ЧG-410 15 | 91.0 | 4 | 91.5 | 0.282803 | 28 | 0.000699 | 12 | 0.023671 | 250 | 0.282728 | 0.6 | 2.7 | 727 | 1222 |

Please cite this article in press as: Jahn, B.-m., et al. Emplacement ages, geochemical and Sr–Nd–Hf isotopic characterization of Mesozoic to early Cenozoic granitoids of the Sikhote-Alin Orogenic Belt, Russian Far East: Crustal growth and regional tectonic evolution. Journal of Asian Earth Sciences (2015), http://dx.doi.org/10.1016/j.jseaes.2015.08.012

**Table 5** (*continued*)

| Spot | Individual spot age (Ma) | ±2σ | Sample mean age (Ma) | $^{176}Hf/^{177}Hf$ | ±2σ | $^{176}Lu/^{177}Hf$ | ±2σ | $^{176}Yb/^{177}Hf$ | ±2σ | $^{176}Hf/^{177}Hf$ CHUR(t) | $\varepsilon_{Hf}(0)$ | $\varepsilon_{Hf}(t)$ | $T_{DM}$ | $T_{DM}^{C}$ |
|---|---|---|---|---|---|---|---|---|---|---|---|---|---|---|
| ЧG-410 16 | 91.0 | 4 | 91.5 | 0.282818 | 20 | 0.000517 | 3.6 | 0.018146 | 220 | 0.282728 | 1.2 | 3.2 | 699 | 1178 |
| ЧG-410 17 | 90.0 | 4 | 91.5 | 0.282789 | 20 | 0.000901 | 8.1 | 0.035206 | 600 | 0.282728 | 0.1 | 2.1 | 754 | 1264 |
| ЧG-410 18 | 89.0 | 4 | 91.5 | 0.282765 | 15 | 0.000772 | 25 | 0.027525 | 1100 | 0.282729 | −0.7 | 1.3 | 790 | 1333 |
| ЧG-410 19 | 91.0 | 4 | 91.5 | 0.282839 | 19 | 0.000611 | 12 | 0.024051 | 730 | 0.282728 | 1.9 | 3.9 | 667 | 1118 |
| ЧG-410 20 | 91.0 | 4 | 91.5 | 0.282809 | 18 | 0.000866 | 2.3 | 0.034978 | 430 | 0.282728 | 0.8 | 2.9 | 721 | 1205 |
| ЧG-410 21 | 94.0 | 4 | 91.5 | 0.282736 | 19 | 0.000647 | 16 | 0.025833 | 1100 | 0.282726 | −1.7 | 0.4 | 834 | 1411 |
| ЧG-410 22 | 94.0 | 4 | 91.5 | 0.282817 | 17 | 0.000974 | 57 | 0.038927 | 2700 | 0.282726 | 1.1 | 3.2 | 711 | 1180 |
| ЧG-410 23 | 91.0 | 4 | 91.5 | 0.282837 | 18 | 0.000827 | 2.2 | 0.033439 | 410 | 0.282728 | 1.8 | 3.9 | 675 | 1125 |
| ЧG-410 24 | 91.0 | 4 | 91.5 | 0.282862 | 16 | 0.001082 | 14 | 0.043353 | 640 | 0.282728 | 2.7 | 4.7 | 639 | 1054 |
| 8-871-1 01 | 109.0 | 4 | 108.8 | 0.282913 | 22 | 0.001318 | 33 | 0.052022 | 960 | 0.282717 | 4.5 | 6.9 | 560 | 895 |
| 8-871-1 02 | 108.0 | 4 | 108.8 | 0.282786 | 27 | 0.001312 | 26 | 0.052050 | 1400 | 0.282717 | 0.0 | 2.4 | 769 | 1261 |
| 8-871-1 03 | 108.0 | 4 | 108.8 | 0.282876 | 16 | 0.000834 | 23 | 0.028814 | 1300 | 0.282717 | 3.2 | 5.6 | 612 | 999 |
| 8-871-1 04 | 108.0 | 4 | 108.8 | 0.282786 | 17 | 0.001466 | 3.7 | 0.054774 | 840 | 0.282717 | 0.0 | 2.4 | 773 | 1262 |
| 8-871-1 05 | 108.0 | 4 | 108.8 | 0.282800 | 23 | 0.001143 | 32 | 0.041301 | 910 | 0.282717 | 0.5 | 2.9 | 742 | 1220 |
| 8-871-1 06 | 108.0 | 4 | 108.8 | 0.282822 | 28 | 0.001005 | 16 | 0.042411 | 560 | 0.282717 | 1.3 | 3.7 | 703 | 1156 |
| 8-871-1 07 | 108.0 | 4 | 108.8 | 0.282527 | 28 | 0.001536 | 36 | 0.063802 | 1300 | 0.282717 | −9.1 | −6.7 | 1202 | 2002 |
| 8-871-1 08 | 110.0 | 4 | 108.8 | 0.282598 | 26 | 0.001253 | 51 | 0.047562 | 1800 | 0.282716 | −6.6 | −4.2 | 1075 | 1797 |
| 8-871-1 09 | 111.0 | 4 | 108.8 | 0.282615 | 20 | 0.000672 | 7 | 0.028387 | 540 | 0.282715 | −6.0 | −3.5 | 1029 | 1744 |
| 8-871-1 10 | 111.0 | 4 | 108.8 | 0.282821 | 23 | 0.001215 | 16 | 0.050844 | 460 | 0.282715 | 1.3 | 3.7 | 709 | 1157 |
| 8-871-1 11 | 107.0 | 4 | 108.8 | 0.282831 | 18 | 0.001087 | 19 | 0.042458 | 1000 | 0.282718 | 1.6 | 4.0 | 690 | 1131 |
| 8-871-1 12 | 108.0 | 4 | 108.8 | 0.282825 | 22 | 0.001376 | 51 | 0.049292 | 900 | 0.282717 | 1.4 | 3.8 | 706 | 1149 |
| 8-871-1 13 | 108.0 | 4 | 108.8 | 0.282900 | 25 | 0.001668 | 76 | 0.058928 | 1200 | 0.282717 | 4.1 | 6.5 | 588 | 935 |
| 8-871-1 14 | 108.0 | 4 | 108.8 | 0.282849 | 30 | 0.001537 | 58 | 0.059389 | 1900 | 0.282717 | 2.3 | 4.7 | 670 | 1081 |
| 8-871-1 15 | 111.0 | 4 | 108.8 | 0.282863 | 21 | 0.001559 | 23 | 0.057889 | 260 | 0.282715 | 2.8 | 5.2 | 647 | 1039 |
| 8-871-1 16 | 110.0 | 4 | 108.8 | 0.282792 | 23 | 0.001253 | 16 | 0.045914 | 1400 | 0.282716 | 0.2 | 2.7 | 758 | 1242 |
| 8-871-1 17 | 107.0 | 4 | 108.8 | 0.282769 | 25 | 0.001149 | 55 | 0.039679 | 1700 | 0.282718 | −0.6 | 1.8 | 793 | 1309 |
| 8-871-1 18 | 109.0 | 4 | 108.8 | 0.282818 | 19 | 0.000677 | 16 | 0.024698 | 1000 | 0.282717 | 1.2 | 3.6 | 702 | 1164 |
| 8-871-1 19 | 109.0 | 4 | 108.8 | 0.282833 | 29 | 0.001084 | 17 | 0.040836 | 1100 | 0.282717 | 1.7 | 4.1 | 687 | 1124 |
| 8-871-1 20 | 110.0 | 4 | 108.8 | 0.282774 | 26 | 0.001360 | 65 | 0.045460 | 750 | 0.282716 | −0.4 | 2.1 | 790 | 1294 |
| 8-871-1 21 | 108.0 | 4 | 108.8 | 0.282837 | 22 | 0.001632 | 38 | 0.064229 | 680 | 0.282717 | 1.8 | 4.2 | 692 | 1116 |
| 8-871-1 23 | 111.0 | 4 | 108.8 | 0.282816 | 20 | 0.001550 | 68 | 0.059606 | 2300 | 0.282715 | 1.1 | 3.6 | 725 | 1174 |
| 8-871-1 22-2 | 109.0 | 4 | 108.8 | 0.282886 | 21 | 0.001251 | 82 | 0.051312 | 4300 | 0.282717 | 3.6 | 6.0 | 603 | 972 |
| 8-871-1 24 | 108.0 | 4 | 108.8 | 0.282784 | 22 | 0.001322 | 25 | 0.054167 | 1100 | 0.282717 | 0.0 | 2.4 | 772 | 1266 |

Please cite this article in press as: Jahn, B.-m., et al. Emplacement ages, geochemical and Sr–Nd–Hf isotopic characterization of Mesozoic to early Cenozoic granitoids of the Sikhote-Alin Orogenic Belt, Russian Far East: Crustal growth and regional tectonic evolution. Journal of Asian Earth Sciences (2015), http://dx.doi.org/10.1016/j.jseaes.2015.08.012

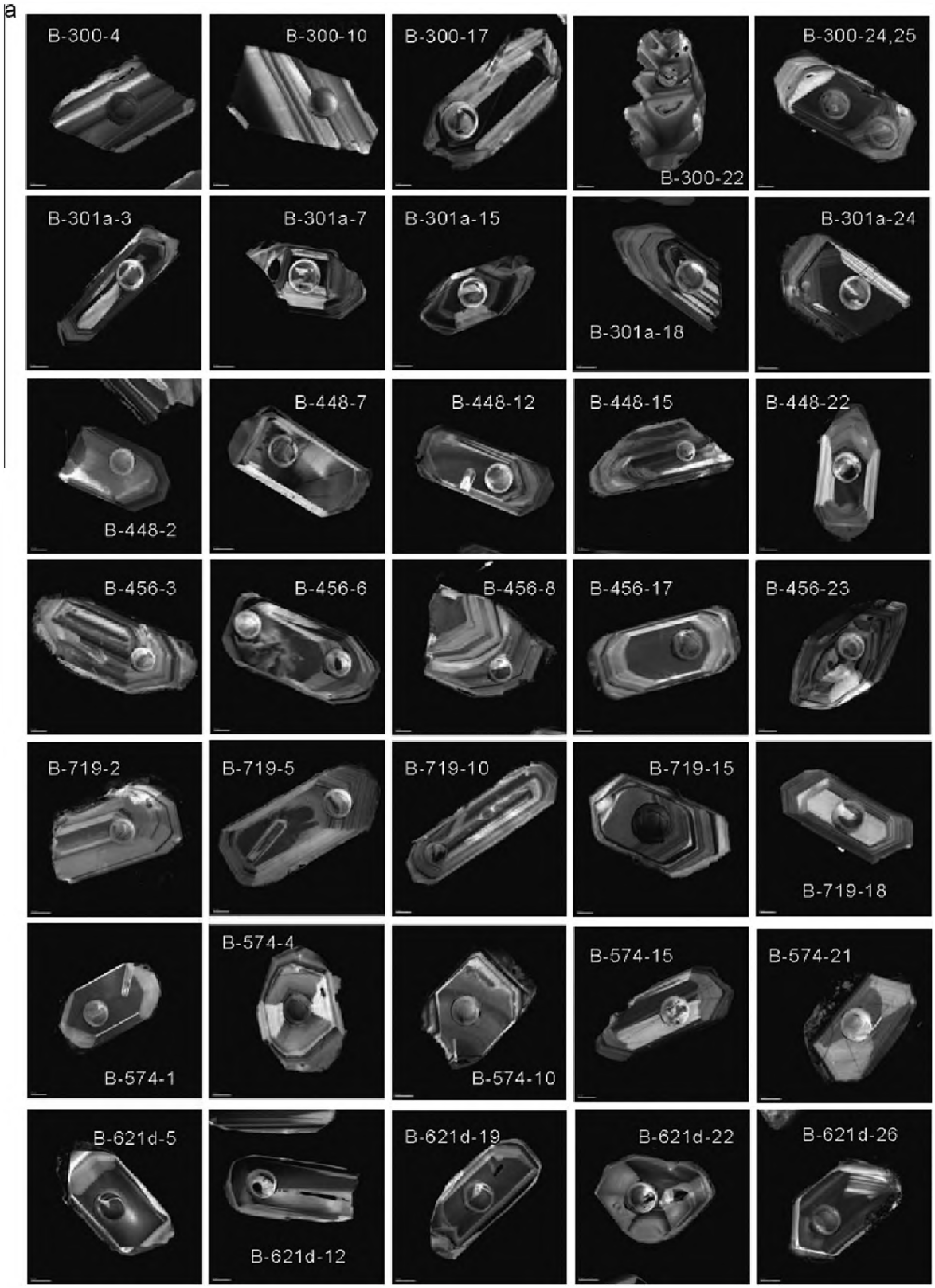


**Fig. 3.** Cathodoluminescence (CL) images of zircon samples. The CL images were taken at the Beijing SHRIMP Center, Beijing. The rounded spot sizes after U–Pb isotopic analyses by ICP-MS are about 40 μm.

57% to 78%, whereas the potash contents from 2.1% to 5.4%. Based on their normative compositions and the Q′ vs ANOR classification (Streckeisen and Le Maitre, 1979), the granitoid samples fall into 4 rock types: quartze monzodiorite (2 samples), granodiorite (6), granite (13) and alkali feldspar granite (3; Fig. 6A). In the A/CNK vs A/NK diagram (Fig. 6B), about half of the granitoids are metaluminous and the rest slightly peraluminous except for two. All of them may be considered as I-type granitoids except for the two samples

Please cite this article in press as: Jahn, B.-m., et al. Emplacement ages, geochemical and Sr–Nd–Hf isotopic characterization of Mesozoic to early Cenozoic granitoids of the Sikhote-Alin Orogenic Belt, Russian Far East: Crustal growth and regional tectonic evolution. Journal of Asian Earth Sciences (2015), http://dx.doi.org/10.1016/j.jseaes.2015.08.012

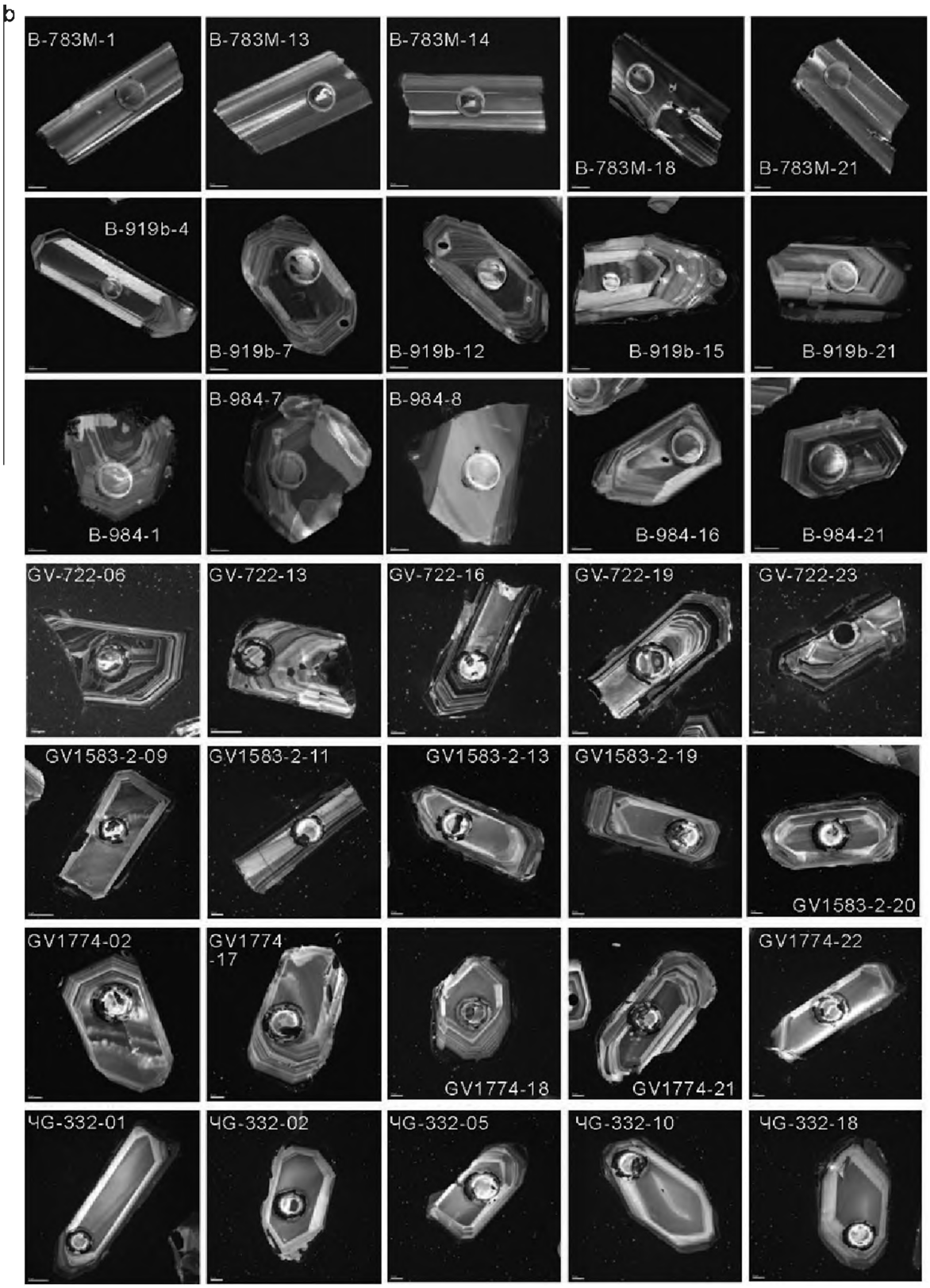


**Fig. 3** (*continued*)

which fall in the category of "S-type". In the FeO*/MgO vs (Zr + Nb + Ce + Y) plot of Whalen et al. (1987), most samples show variable degrees of fractional crystallization, and a few belong to A-type granitoids (Fig. 6C). Based on the $FeO_{total}/(FeO_{total} + MgO)$ vs $SiO_2$ plot of Frost et al. (2001), most granitic samples fall in the "magnesian" or "Cordilleran-type" granites (Fig. 6E). Samples in the "ferroan" field include some A-type granitoids or alkali feldspar granites. In the "modified alkali-lime index" (MALI = $Na_2O + K_2O - CaO$) vs $SiO_2$

Please cite this article in press as: Jahn, B.-m., et al. Emplacement ages, geochemical and Sr–Nd–Hf isotopic characterization of Mesozoic to early Cenozoic granitoids of the Sikhote-Alin Orogenic Belt, Russian Far East: Crustal growth and regional tectonic evolution. Journal of Asian Earth Sciences (2015), http://dx.doi.org/10.1016/j.jseaes.2015.08.012

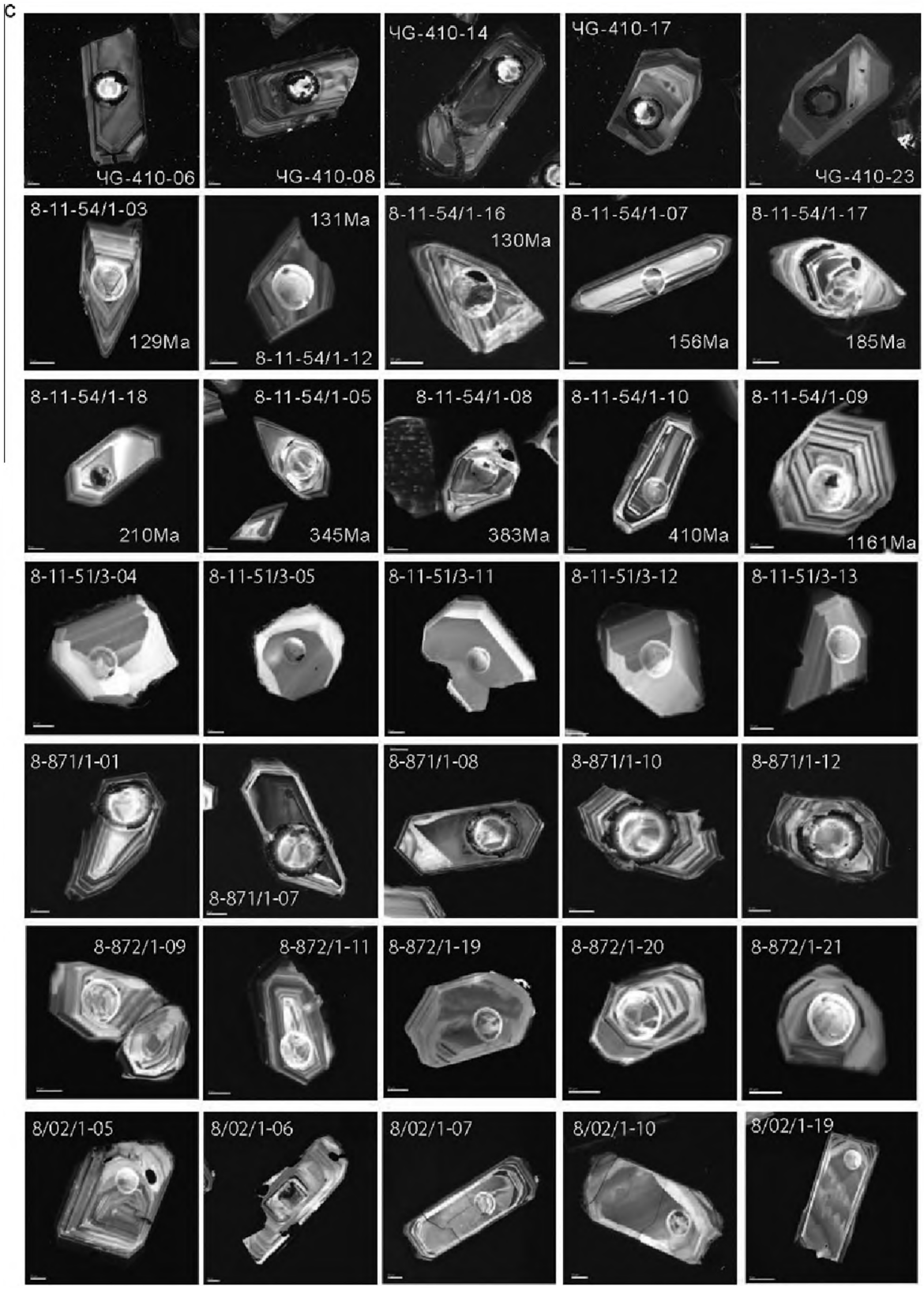


**Fig. 3** (*continued*)

diagram of Frost et al. (2001), most samples are found in the "calc-alkalic" field, and only three in the "alkali-calcic" field (Fig. 6F). According to a tectonic discrimination diagram of Pearce et al. (1984), most of the rocks plot in volcanic arc setting except for three A-type granites in within-plate environment (Fig. 6D).

Chondrite-normalized REE patterns are shown in Fig. 7A–E. Most of these have "typical granitic patterns" with light REE enrichment ($La_N$ = 100–200X, $Lu_N$ = 10–20X), conspicuous negative Eu anomaly and 10–20 times chondritic abundance for heavy REE. However, a few exceptional patterns are also noticed. Samples

Please cite this article in press as: Jahn, B.-m., et al. Emplacement ages, geochemical and Sr–Nd–Hf isotopic characterization of Mesozoic to early Cenozoic granitoids of the Sikhote-Alin Orogenic Belt, Russian Far East: Crustal growth and regional tectonic evolution. Journal of Asian Earth Sciences (2015), http://dx.doi.org/10.1016/j.jseaes.2015.08.012

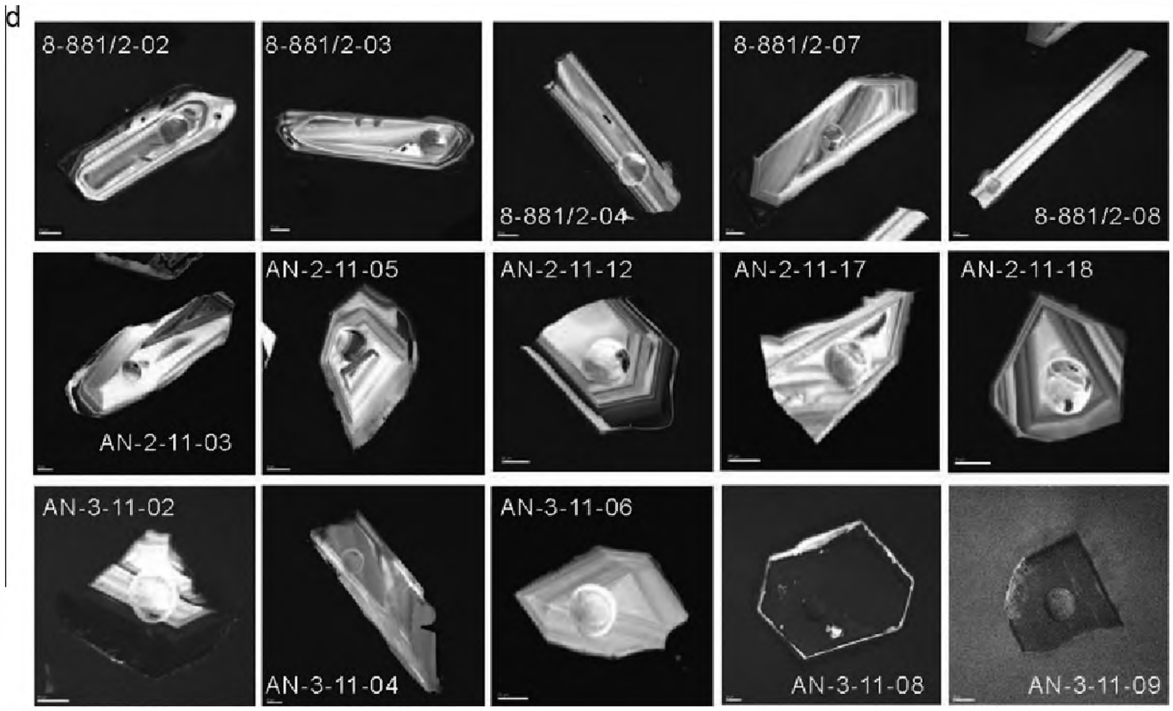


**Fig. 3** (*continued*)

B-995 (Fig. 7B; a granite, equivalent to zircon sample B-984; 78 Ma; 73% $SiO_2$), 8-02-1 (Fig. 7D; an alkali feldspar granite; 68 Ma; 78% $SiO_2$), 8-881-2 (Fig. 7D; a granodiorite; 93 Ma; 68% $SiO_2$), and 8-872/1 (Fig. 7E; a granodiorite; 106 Ma; 67% $SiO_2$) do not display any Eu anomalies. All the four patterns are similarly fractionated, but they do not show any correlation with the emplacement ages nor the silica contents. In addition, two samples, GV-722 (Fig. 7B; a granite; 78 Ma; 69% $SiO_2$) and AH-3-11 (Fig. 7D; an alkali feldspar granite; 58 Ma; 76% $SiO_2$) show REE patterns of highly differentiated granites with high and near-flat heavy REE patterns (40–60X chondritic abundances) and extremely large negative Eu anomalies. Such REE patterns appear to have a faint feature of the "lanthanide tetrad effect" as shown in many highly evolved A-type granites (e.g., Jahn et al., 2001, 2004; Wu et al., 2004). In addition, these granites are often characterized by high Rb and low Sr concentrations, hence very high Rb/Sr ratios. Their Zr/Hf (33–21) and Nb/Ta (6.0–5.4) ratios are lower than the average crustal rocks (average crustal rocks have ratios of 35–40 and 14–20, respectively).

Primitive-mantle-normalized spidergrams of the granitoids are shown in Fig. 8A–E. In principle, trace elements in the spidergrams are arranged in the ascending order, from left to right, of their compatibilities with N-MORB basaltic liquid (Sun and McDonough, 1989). The application of such diagrams to granitic rocks also serves to identify fractionation of particular mineral phases during the generation and differentiation of granitic liquids. The present spidergrams show depletion or negative anomalies in Nb–Ta, Sr, P, Zr and Ti. Such a feature of "negative TNT (Ti–Nb–Ta) anomaly" is most characteristic of granitic rocks, island arc volcanic rocks and the continental crust in general. The significance of such anomalies and other features will be discussed later.

### 5.3. Whole-rock Sr–Nd isotopic data

The data of whole-rock Sr and Nd isotopic analyses are given in Table 5, and further illustrated in Fig. 9. The Rb concentrations range from 22 to 447 ppm, whereas Sr from 18 to 790 ppm. The calculated initial $^{87}Sr/^{86}Sr$ ratios ($I_{Sr}$ values) range from 0.7040 to 0.7083; and the age-corrected initial $^{143}Nd/^{144}Nd$ ratios, expressed as $\varepsilon_{Nd}(t)$ values, vary from +3.0 to −6.0, but in most cases they are near zero or slightly negative (Fig. 9A). In Fig. 9A the only available coupled Sr–Nd isotopic data from the literature (Valui and Moskalenko, 2010) are also shown for comparison.

The present new analyses yielded single-stage Sm–Nd model ages between 655 and 1940 Ma and two-stage model ages from 650 to 1370 Ma (Table 5; Fig. 9). In Fig. 9B–D, the literature Nd isotopic data (Valui and Moskalenko, 2010; Khanchuk et al., 2013; Kruk et al., 2014a) are also shown for comparison. In all cases, the published and new data are quite comparable.

Correct use of single-stage and two-stage model ages may not be easy for many readers. Single-stage model assumes that the protolith (source rocks) of a rock, regardless of its composition, has evolved in a milieu with Sm/Nd ratio similar to that of the analyzed sample. That is, during the partial melting of a source rock, Sm/Nd ratio was not fractionated between the melt produced and the source rock. However, Sm/Nd fractionation frequently occurred during subsequent magma differentiation, leading to a ratio different from that of the initial melt or the average source rock. In this case, calculated single-stage model ages could be very different from the "true time" of the source separation from the depleted mantle reservoir. The most dramatic case is shown by highly differentiated granitic rocks with the "lanthanide tetrad effect" (Jahn et al., 2001; Jahn, 2010). The $^{147}Sm/^{144}Nd$ ratios of these rocks often show values higher than the chondritic (0.1967) or even depleted mantle (0.2137) values, hence leading to negative or future model ages. To overcome this problem, a two-stage model was proposed (DePaolo et al., 1991), in which the protolith of a granitic rock is assumed to have evolved in a milieu with the average "continental" Sm/Nd ratio ($^{147}Sm/^{144}Nd = 0.118$, or $f_{Sm/Nd} = -0.4$) for the period from its initial separation from the depleted mantle reservoir to the time of partial melting. As many granitic melts have undergone fractional crystallization, the two-stage model ages may be more meaningful than the single-stage ages. Therefore, two types of model ages are presented in Table 4.

Please cite this article in press as: Jahn, B.-m., et al. Emplacement ages, geochemical and Sr–Nd–Hf isotopic characterization of Mesozoic to early Cenozoic granitoids of the Sikhote-Alin Orogenic Belt, Russian Far East: Crustal growth and regional tectonic evolution. Journal of Asian Earth Sciences (2015), http://dx.doi.org/10.1016/j.jseaes.2015.08.012

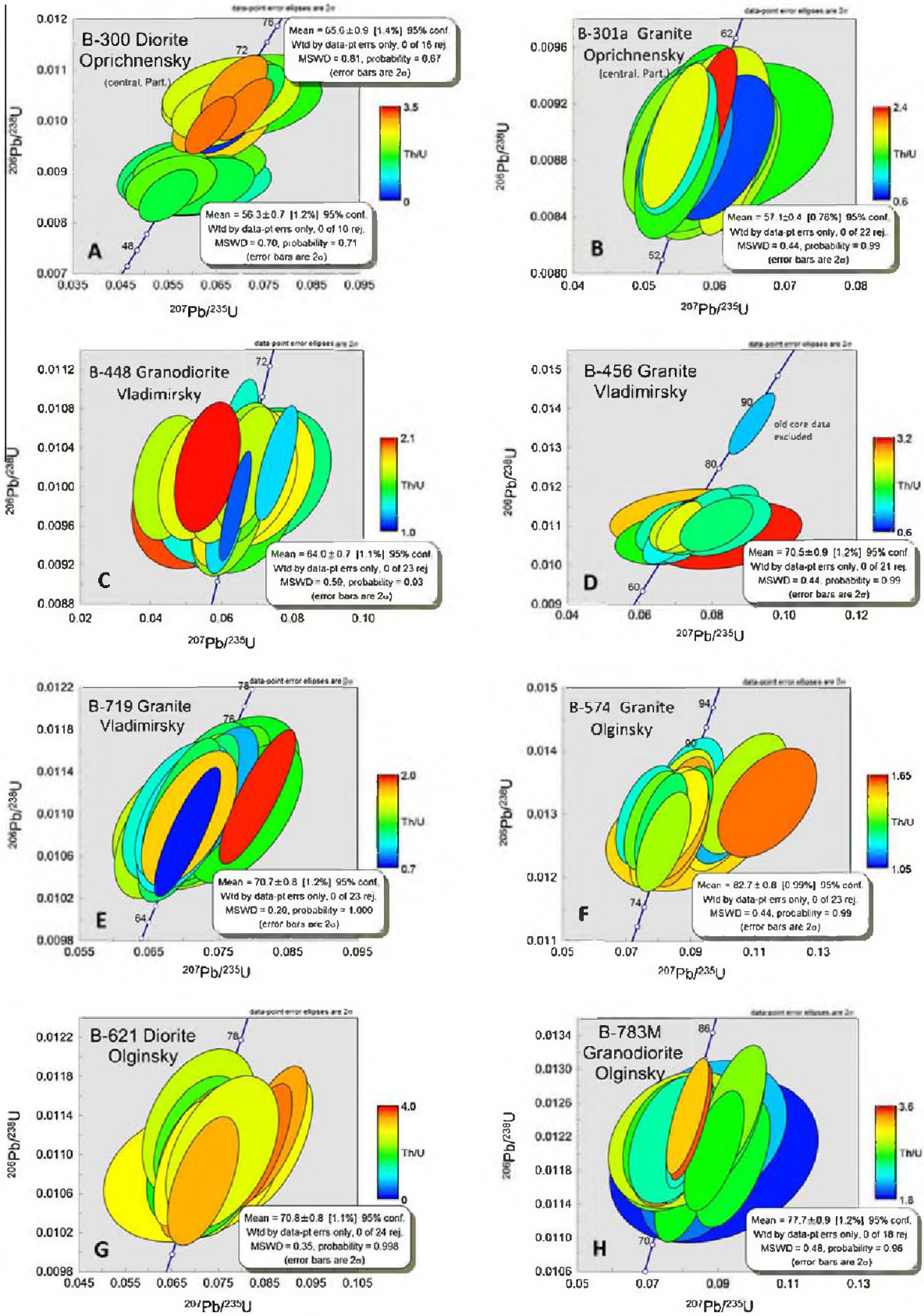


**Fig. 4.** Zircon U–Pb Concordia plots for 24 granitoid samples from the Sikhote-Alin orogenic belt. The calculated ages are based on $^{206}Pb/^{238}U$ ratios. The number of outliers (rejects) is indicated, but in most cases the number is zero. The color code represents Th/U ratios in individual spots of zircon analyses.

Please cite this article in press as: Jahn, B.-m., et al. Emplacement ages, geochemical and Sr–Nd–Hf isotopic characterization of Mesozoic to early Cenozoic granitoids of the Sikhote-Alin Orogenic Belt, Russian Far East: Crustal growth and regional tectonic evolution. Journal of Asian Earth Sciences (2015), http://dx.doi.org/10.1016/j.jseaes.2015.08.012

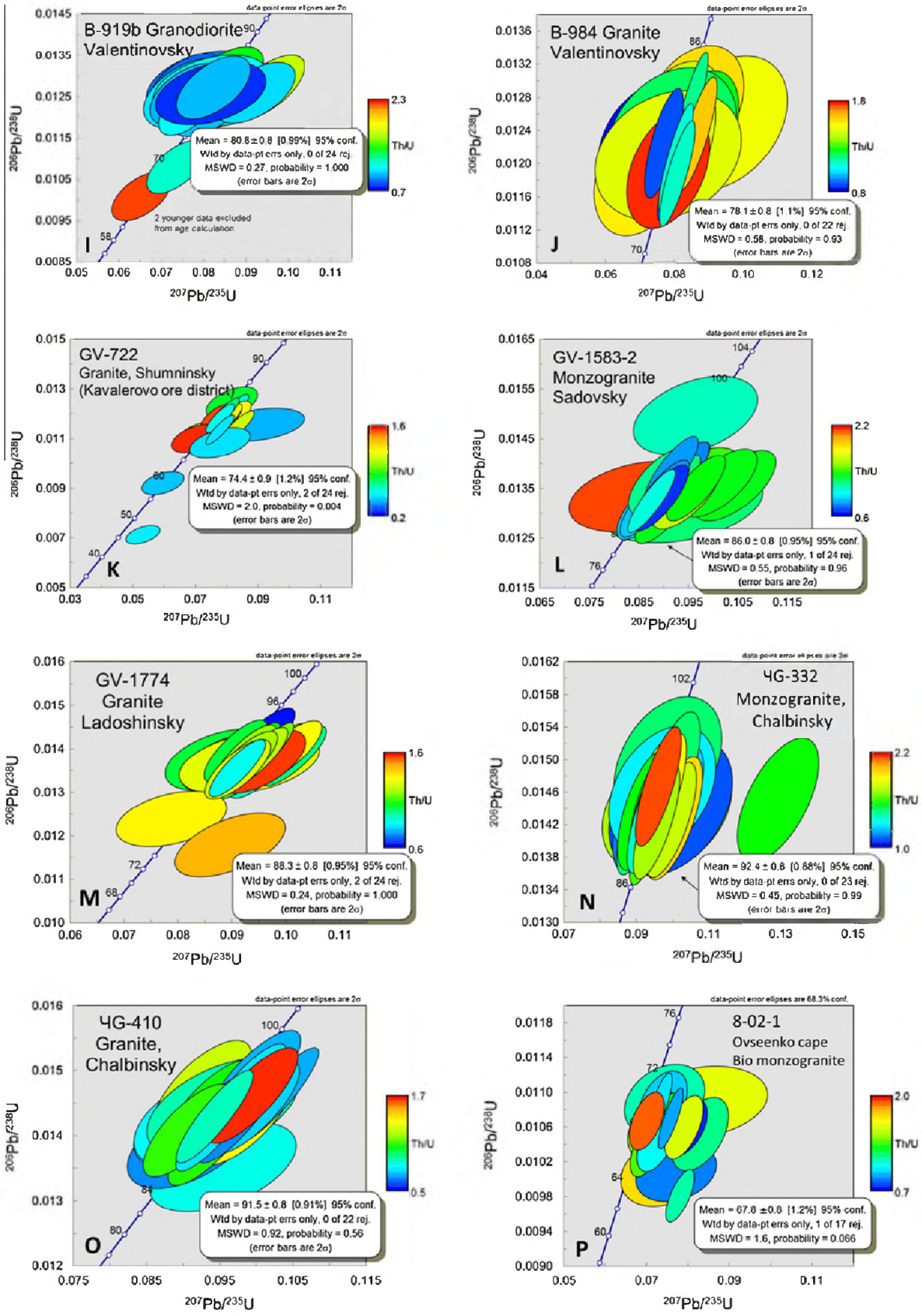


**Fig. 4** (*continued*)

Please cite this article in press as: Jahn, B.-m., et al. Emplacement ages, geochemical and Sr–Nd–Hf isotopic characterization of Mesozoic to early Cenozoic granitoids of the Sikhote-Alin Orogenic Belt, Russian Far East: Crustal growth and regional tectonic evolution. Journal of Asian Earth Sciences (2015), http://dx.doi.org/10.1016/j.jseaes.2015.08.012

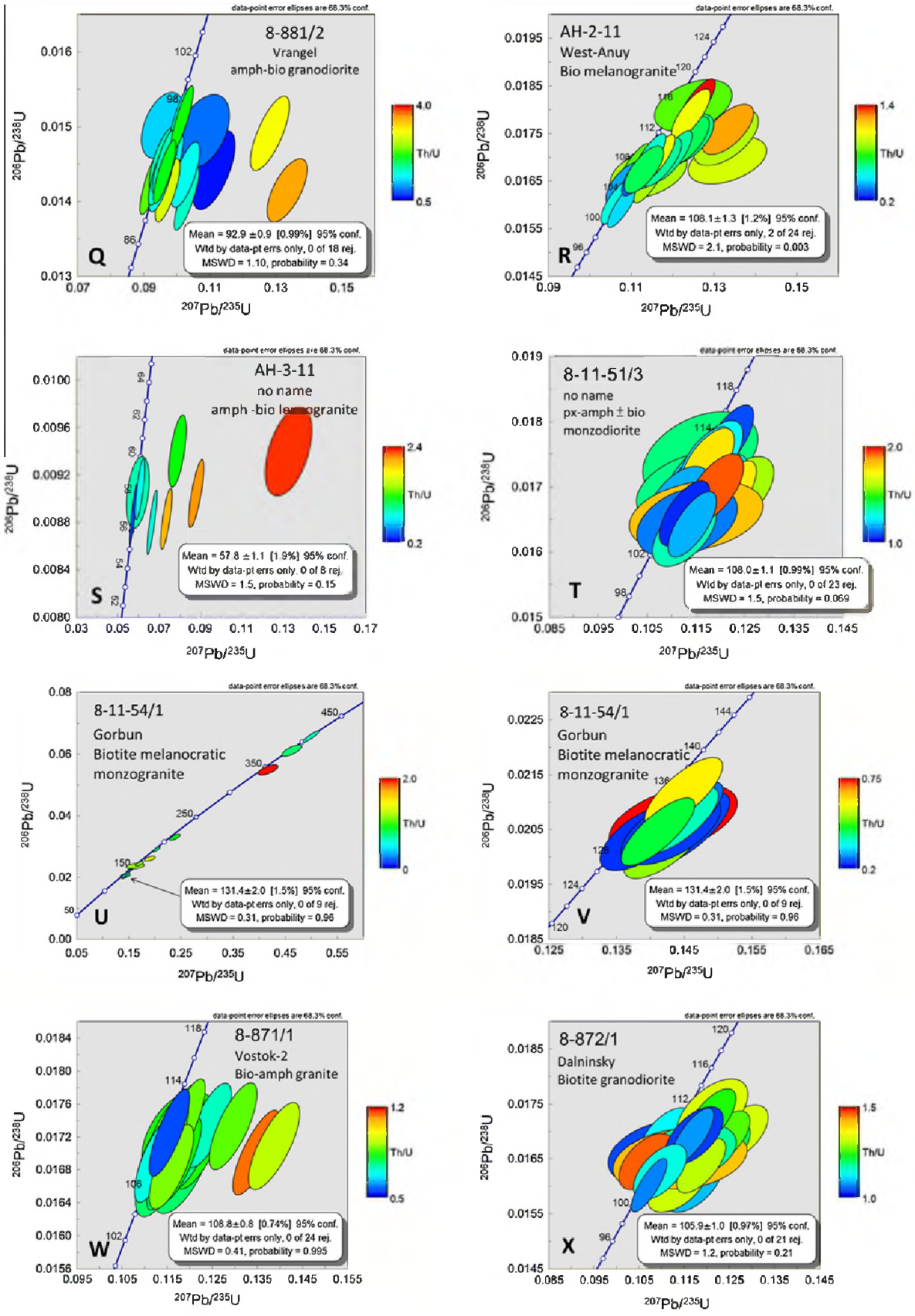


**Fig. 4** (*continued*)

Please cite this article in press as: Jahn, B.-m., et al. Emplacement ages, geochemical and Sr–Nd–Hf isotopic characterization of Mesozoic to early Cenozoic granitoids of the Sikhote-Alin Orogenic Belt, Russian Far East: Crustal growth and regional tectonic evolution. Journal of Asian Earth Sciences (2015), http://dx.doi.org/10.1016/j.jseaes.2015.08.012

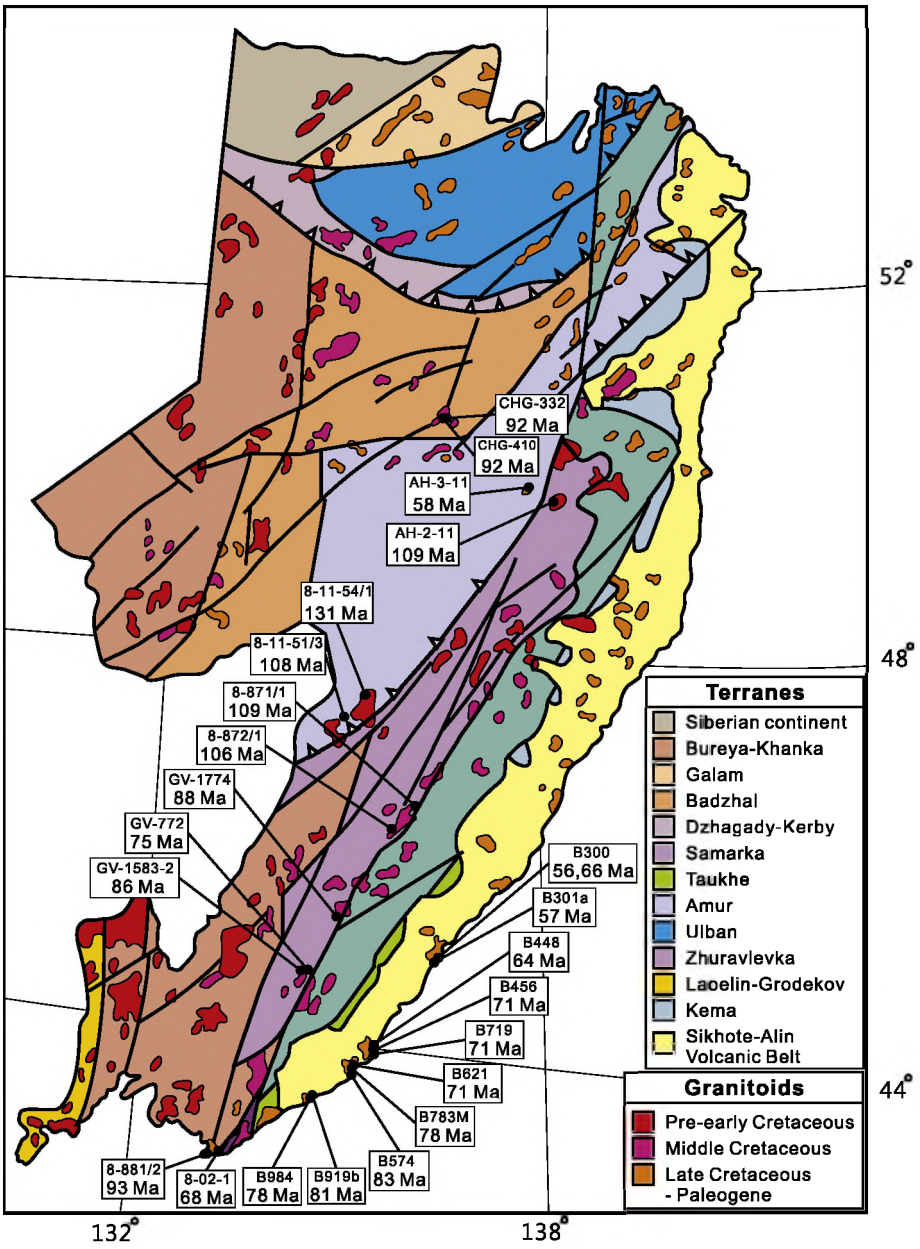


**Fig. 5.** Summary of zircon ages of all the 24 granitoid samples from the Primorye and Khabarovsk regions.

### 5.4. Zircon Hf isotopic data

Zircon Hf isotopic compositions of the granitoids are given in Table 5, and further illustrated in Fig. 10. Fig. 10A shows that (1) the majority of the analyzed zircon domains are characterized by positive $\varepsilon_{Hf}(t)$ values, and (2) all individual samples have a range of zircon $\varepsilon_{Hf}(t)$ values, as commonly observed in granitic rocks. The range of values is beyond the analytical uncertainty of 0.5–1.0 epsilon unit. Note that the whole data set appear to suggest a faint trend of increasing $\varepsilon_{Hf}(t)$ values as the emplacement age gets younger. However, such a trend is absent in the whole-rock $\varepsilon_{Nd}(t)$ values (Fig. 10B). On the other hand, the Hf isotopic data of three granitoids occurring in the Central Sikhote-Alin Fault zone (GV-722, GV-1774, and GV-1583-2) appears to show an opposite trend; that is, the $\varepsilon_{Hf}(t)$ values decrease with the younging of granitic intrusions.

## 6. Discussion

### 6.1. Significance of zircon ages and major thermal events in the Primorye region

As demonstrated earlier, the clear magmatic zoning, the range of Th/U ratios (>0.5) in zircon crystals and the clustering of concordant data points provide a strong argument for zircon crystallization in magmas. Thus, the zircon ages represent the emplacement time of the granitoid intrusions. The new age data indicate that the most important tectonothermal events of the Sikhote-Alin Orogenic Belt occurred in the Cretaceous. Note that the magmatic events are often accompanied by important mineralizations (e.g., Gonevchuk et al., 2010; Rodionov et al., 2010).

The granitic intrusive events in different tectonic units may be summarized as follows. The granitic rocks from the southeastern

Please cite this article in press as: Jahn, B.-m., et al. Emplacement ages, geochemical and Sr–Nd–Hf isotopic characterization of Mesozoic to early Cenozoic granitoids of the Sikhote-Alin Orogenic Belt, Russian Far East: Crustal growth and regional tectonic evolution. Journal of Asian Earth Sciences (2015), http://dx.doi.org/10.1016/j.jseaes.2015.08.012

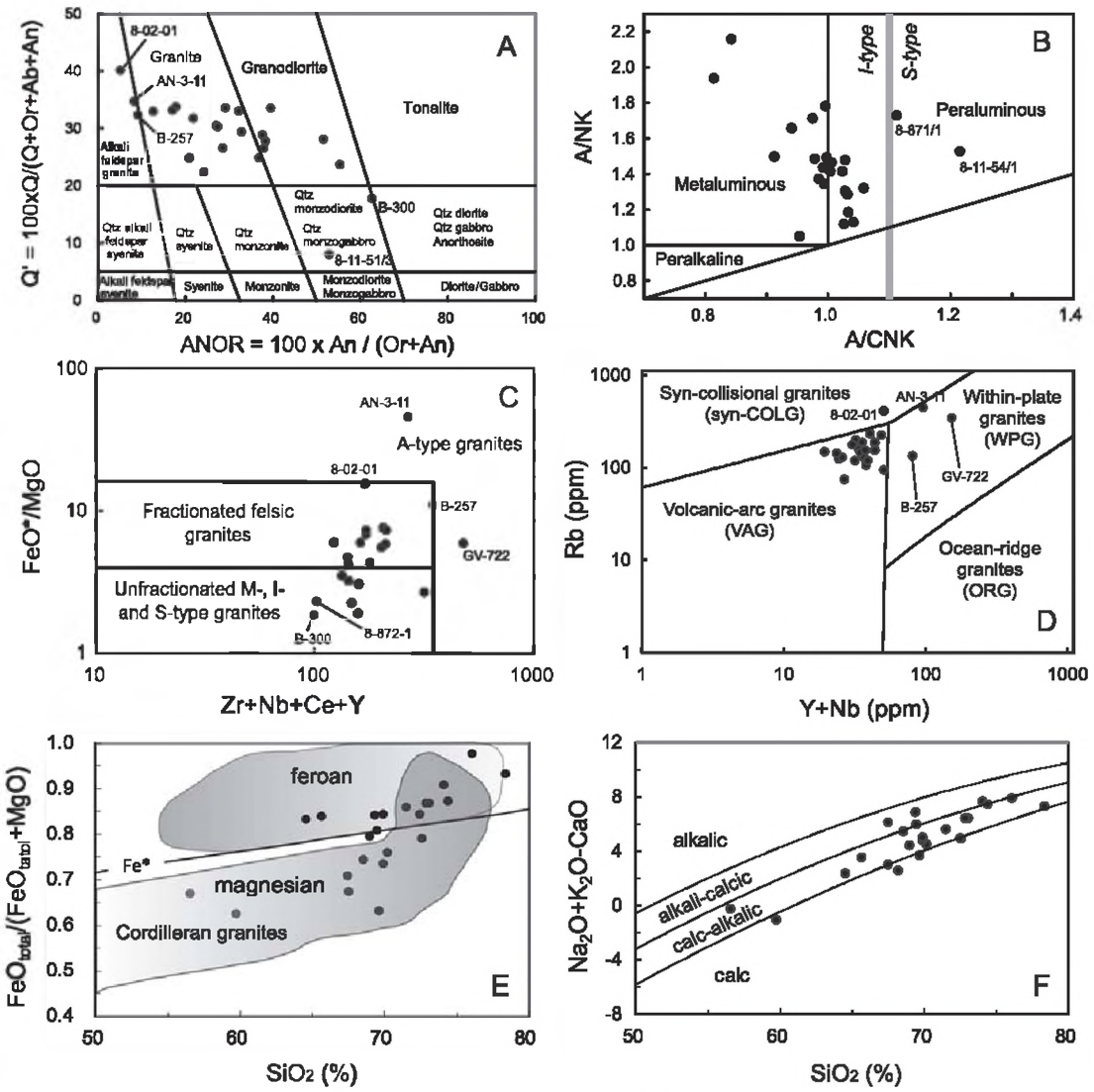


**Fig. 6.** Geochemical characterization of the granitoid samples from Sikhote-Alin. (A) The normative Q'-ANOR plot of Streckeisen and Le Maitre (1979) shows that most samples fall in the fields of granite and granodiorite, with a few in alkali-feldspar granite and quartz monzogranite. (B) Most samples have A/NK values >1.0 and A/CNK less than 1.1, thus they may be classified into I-type granitoids. A, C, N, K = molecular proportion of $Al_2O_3$, CaO, $Na_2O$, and $K_2O$, respectively. (C) In the FeO*/MgO vs (Zr + Nb + Ce + Y) plot of Whalen et al. (1987), most samples are not A-type granitoids but show variable degrees of fractional crystallization. (D) A trace element discrimination diagram of Pearce et al. (1984) suggests that the majority of granitic samples formed in an arc setting except three samples which fall in the field of "within-plate granites". (E) In the $FeO_{total}/(FeO_{total} + MgO)$ vs $SiO_2$ plot of Frost et al. (2001), most granitic samples fall in the "magnesian" or "Cordilleran-type" granites. Samples in the "ferroan" field include some A-type granitoids or alkali feldspar granites. The fit to the boundary line Fe* is $FeO_{total}/(FeO_{total} + MgO) = 0.486 + 0.0046 \times SiO_2(\%)$. (F) In the MALI vs $SiO_2$ diagram of Frost et al. (2001), the majority of granitic samples fall in the "calc-alkalic" field, and only three in the "alkali-calcic" field. MALI is the modified alkali-lime index and is equal to $Na_2O + K_2O - CaO$.

coastal areas were emplaced in the late Cretaceous to early Eocene (83–56 Ma), and they intruded into the early Cretaceous accretionary complex of the Tauka Terrane. The granitoids that occur along, or close to, the Central Sikhote-Alin Fault zone were emplaced in Middle to Late Cretaceous, from 109 to 75 Ma, and they intruded into the Jurassic to early Cretaceous accretionary complex of the Samarka Terrane. The other granitoids, including those occurring in the Khabarovsk Region, were emplaced from 131 to 58 Ma in the turbidite basin of the Amur Terrane (=Zhuravlevka Terrnae). It may be concluded that the granitoids of Sikhote-Alin were mainly generated and emplaced in the Cretaceous, from 131 to 57 Ma.

Despite that the overall zircon geochronology is rather straightforward, sample 8-11-54/1 (biotite-bearing monzogranite) shows a more complicated age pattern (Fig. 4U and V). The presence of inherited zircon grains suggests that the protolith of this rock contained a late Precambrian to early Paleozoic crustal component, or the granitoid magma has assimilated some crustal material during igneous differentiation. This seems to be corroborated by its negative $\varepsilon_{Nd}(t)$ value of −4.1 (Table 5).

The tectonothermal events are also recorded in the explosive eruptions of felsic magmas in the East Sikhote-Alin Volcanic-Plutonic Belt (ESAVPB). Grebennikov and Popov (2014) summarized that the "ignimbrite" or silicic volcanism occurs in two types – (1) voluminous plateau silicic volcanism filling large depressions, and (2) small caldera-type ignimbrites, formed by collapse of their roof into the magma generation zone. In fact, the two coastal terranes of accretionary complexes (Kema and Taukha) are extensively covered by felsic volcanic rocks. Grebennikov and Popov (2014) also noted that the voluminous plateau ignimbrites from

Please cite this article in press as: Jahn, B.-m., et al. Emplacement ages, geochemical and Sr–Nd–Hf isotopic characterization of Mesozoic to early Cenozoic granitoids of the Sikhote-Alin Orogenic Belt, Russian Far East: Crustal growth and regional tectonic evolution. Journal of Asian Earth Sciences (2015), http://dx.doi.org/10.1016/j.jseaes.2015.08.012

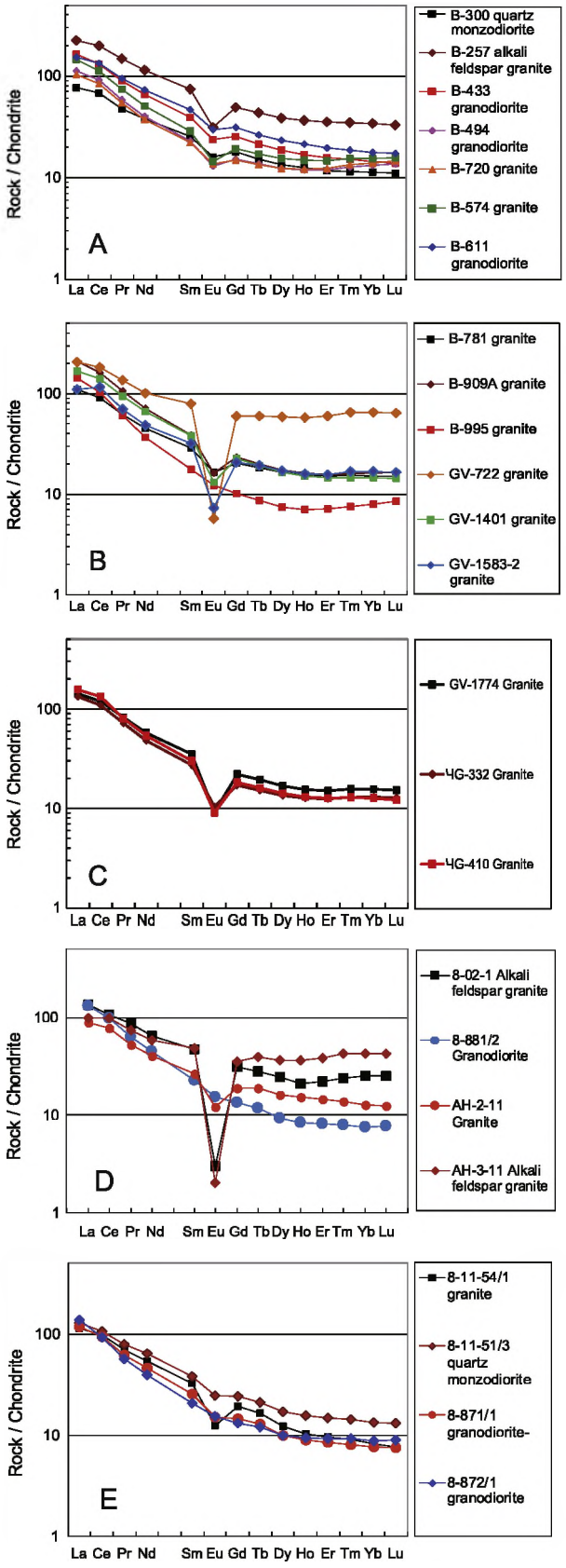


**Fig. 7.** Chondrite-normalized REE patterns of the granitoids from Sikhote-Alin. Chondrite values are from Sun and McDonough (1989).

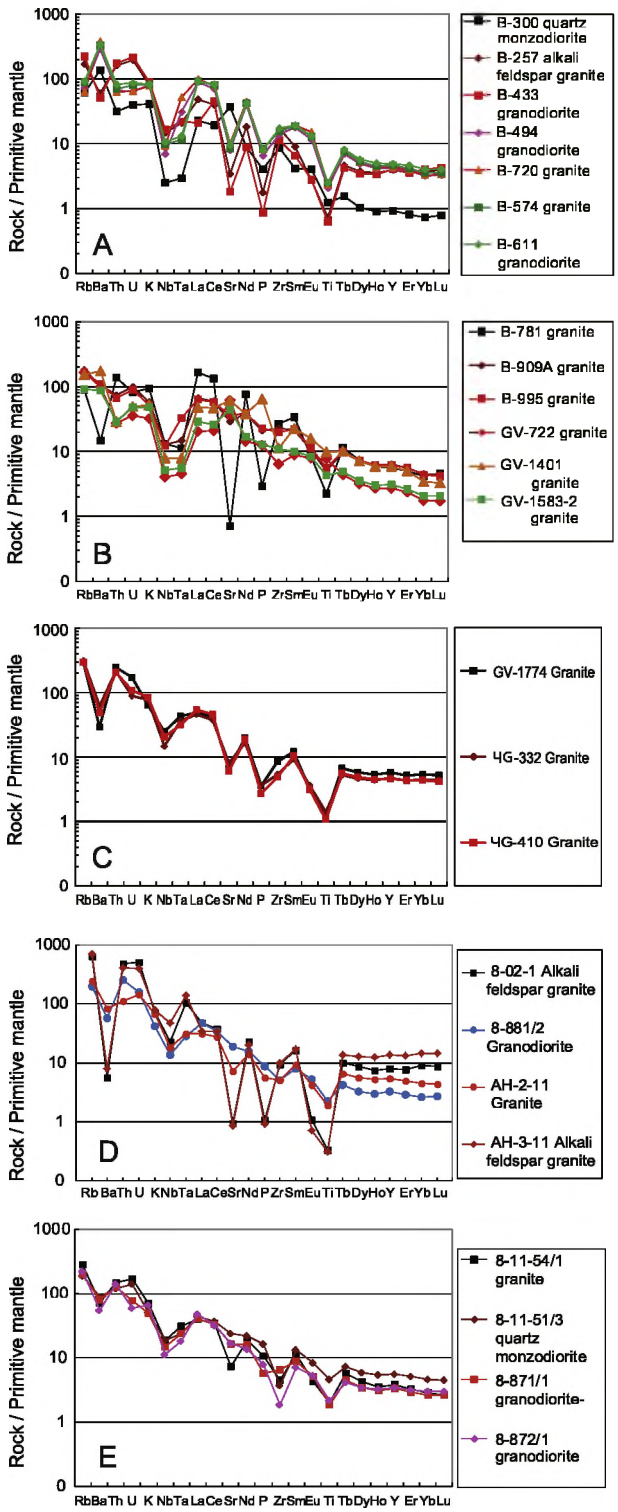


**Fig. 8.** Primitive mantle-normalized spidergrams of the granitoids from Sikhote-Alin. Primitive-mantle values are from Sun and McDonough (1989).

the ESAVB constitute a significant part of the Silicic Large Igneous Province (SLIP) that covers the Russian Far East along the coastal areas of the Japan and Okhotsk Seas.

In the ESAVPB, three large ignimbrite complexes occur – (1) the Primorsky, (2) the Siyanovsky-Levosobolevsky, and (3) the Bogopolsky Complexes. These "complexes" have a wide areal distribution but are not restricted to small areas. Therefore, it might be more appropriate to call the complexes as "sequences". The ignimbrites of the Primorye Region comprise mainly tuffs and ignimbrites, with subordinate rhyodacite and rhyolite lavas. The available age (Kurchavov, 1979; Mikhailov, 1989) and paleofloral

Please cite this article in press as: Jahn, B.-m., et al. Emplacement ages, geochemical and Sr–Nd–Hf isotopic characterization of Mesozoic to early Cenozoic granitoids of the Sikhote-Alin Orogenic Belt, Russian Far East: Crustal growth and regional tectonic evolution. Journal of Asian Earth Sciences (2015), http://dx.doi.org/10.1016/j.jseaes.2015.08.012

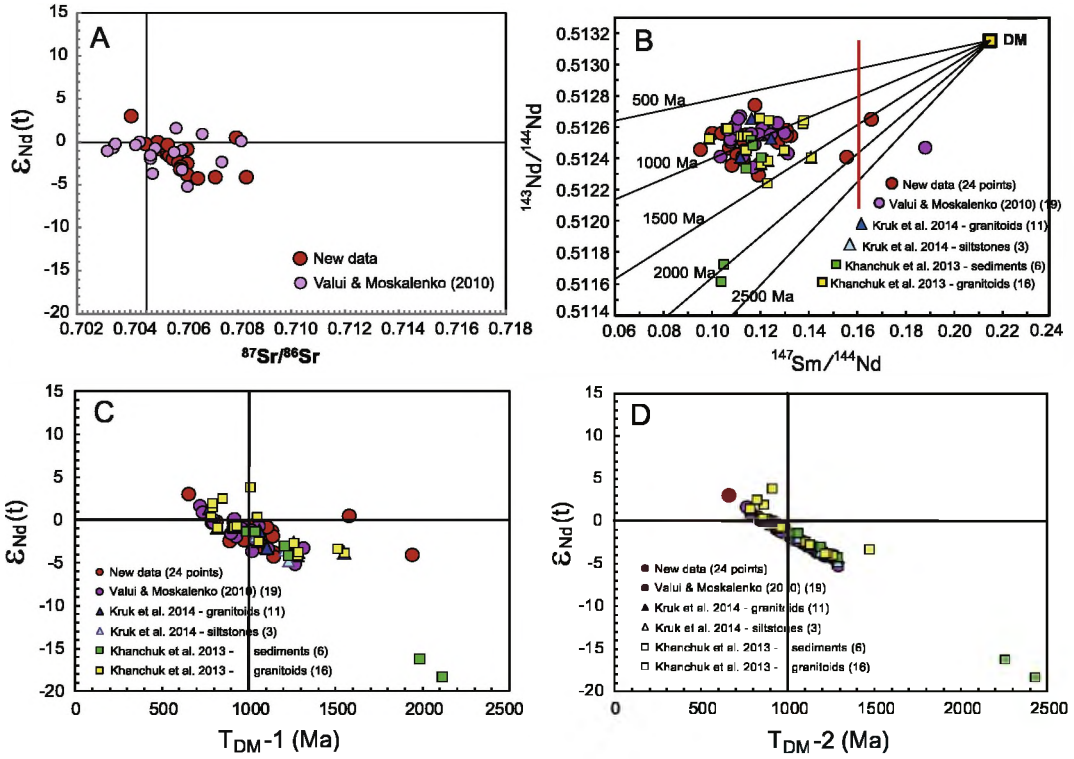


**Fig. 9.** Whole-rock Sr and Nd isotopic compositions of granitoids from Sikhote-Alin. The literature data (Valui and Moskalenko, 2010; Khanchuk et al., 2013; Kruk et al., 2014a) are used for comparison. (A) $\varepsilon_{Nd}(t)$ values vary from +3 to −6, with the majority from 0 to −5. Initial Sr isotopic ratios vary from 0.703 to 0.708. (B) Single-stage depleted-mantle model ages show a spread of values from 600 Ma to 1900 Ma, but (C) clustered around 1000 Ma. (D) Two-stage model ages vary from 600 to 1400 Ma.

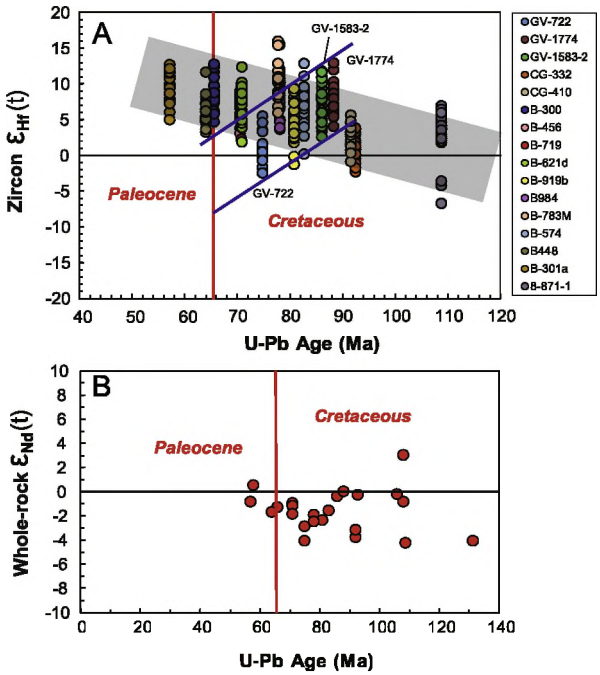


**Fig. 10.** (A) Zircon initial Hf isotopic compositions seem to show a weak increasing trend of $\varepsilon_{Hf}(t)$ values with the younging of granite intrusions. However, this trend is not demonstrated in the whole-rock Nd isotopic compositions (B). On the other hand, the Hf isotopic data of three granitoids from the Central Sikhote-Alin Fault zone (GV-722, GV-1774, and GV-1583-2) appears to show an opposite trend (blue lines); that is, the $\varepsilon_{Hf}(t)$ values decrease with the younging of granitic intrusions.

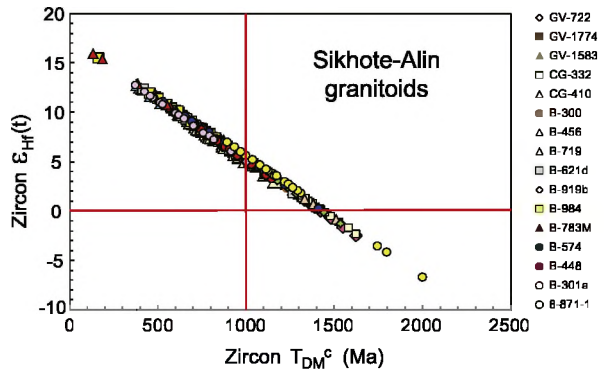


**Fig. 11.** A plot of crust-model ages ($T^{C}_{DM}$) of zircon grains vs $\varepsilon_{Hf}(t)$ values.

data (Nevolina, 1960) suggest that the volcanic rocks were erupted during the period of 90–82 Ma (Turonian-Campanian). The volcanic rocks are mainly of rhyodacitic to rhyolite in compositions ($SiO_2$ = 65–78%) and of "S-type" (granitoid equivalent) affinity, based on their A/CNK ratios or ASI index (Grebennikov and Popov, 2014).

The volcanic rocks of the Siyanovsky-Levosobolevsky Complex are welded tuffs and ignimbrites of dacitic to rhyodacitic compositions ($SiO_2$ = 67–71%). They are estimated to have erupted during the period of Maastrichtian to Paleocene (ca. 70–55 Ma; Grebennikov and Popov, 2014), but precise age data are lacking. The chemical compositions of the ignimbrites show that they are mainly of "S-type". By contrast, the volcanic rocks of the Bogopolsky Complex are characterized by two lithological facies; the early stage rocks are of S-type, whereas the late stage rocks are of A-type (Grebennikov and Popov, 2014). The volcanic rocks were erupted from the Paleocene to the early Eocene (ca. 60–50 Ma), based on Rb/Sr isochron ages of 60–53 Ma (Popov and Grebennikov, 2001) and K–Ar ages (Baskina and Favorskaya, 1969).

In conclusion, the three volcanic complexes or sequences have recorded three periods of volcanic eruptions: (1) 90–82 Ma, (2)

Please cite this article in press as: Jahn, B.-m., et al. Emplacement ages, geochemical and Sr–Nd–Hf isotopic characterization of Mesozoic to early Cenozoic granitoids of the Sikhote-Alin Orogenic Belt, Russian Far East: Crustal growth and regional tectonic evolution. Journal of Asian Earth Sciences (2015), http://dx.doi.org/10.1016/j.jseaes.2015.08.012

70–55 Ma, and (3) 60–50 Ma. In fact, these periods basically coincide with the intrusive episodes revealed by the present zircon U–Pb dating, even though the uncertainty of the volcanic chronology is higher.

### 6.2. Petrogenesis of the granitoids – geochemical and Sr–Nd–Hf isotopic constraints

The granitoids of the present study occur in different geologic terranes and were emplaced at different times. Therefore, they cannot be related by a differentiation process from a single parental magma, nor by different degrees of partial melting from a common source. However, their petrogenetic processes could be understood from, and constrained by, their geochemical and isotopic characteristics. The principal geochemical constraints are: (1) Based on the Q'-ANOR classification, the major rock types are granite and granodiorite, with three as alkali feldspar granite and two as quartz-monzodiorite (Fig. 6A). (2) The A/NK vs A/CNK plot (Fig. 6B) suggests that the majority (22/24) of granitoids are metaluminous to weakly peraluminous, thus they belong to the "I-type" genetic category; only two with A/CNK > 1.1 belong to the "S-type". Surprisingly, this is in strong contrast with the chemical nature of the ignimbrites which are mainly "S-type" (Grebennikov and Popov, 2014). Note that peraluminous melts may form by melting of biotite-bearing metaluminous felsic rocks (Miller, 1985) or even by water-excess melting of mafic rocks (Ellis and Thompson, 1986), but not necessarily by melting of metasedimentary rocks. (3) The majority of the granitoids (21 out of 24) fall in the "volcanic-arc granites" (VAG) field (Fig. 6D), so they were most probably generated in a continental arc setting. (4) The FeO*/MgO or $FeO_{tot}$/($FeO_{tot}$ + MgO) ratios indicate that many rocks have undergone significant fractional crystallization (Fig. 6C and E). (5) Three rocks (B-257, GV-722, AH-3-11) fall in the field of "within-plate granites", but they are highly differentiated, show REE patterns with huge negative Eu anomalies and faint lanthanide tetrad effect (Figs. 7A and 8B, D). That is, they might not have been necessarily generated in a "within-plate" setting; their parental magmas could have been generated in a continental arc setting, like the other samples. Note that sample B-257 is equivalent to B-301a in the zircon age maps (Figs. 2 and 5), its occurrence in the coastal arc area cannot be related to an intraplate setting. (6) The spidergrams (Fig. 8A–E) show depletion or negative anomaly in Nb–Ta, Sr, P, Zr and Ti. The feature of "negative TNT (Ti–Nb–Ta) anomaly" is most characteristic of granitic rocks, island arc volcanic rocks and the continental crust in general. The anomaly is commonly attributed to the fractionation of accessory minerals, such as titanite and ilmenite (for Ti), magnetite, ilmenite and amphibole (for Nb–Ta), apatite (for P), zircon (for Zr), and some major phases, such as feldspars (for Sr). Fractionation of monazite, allanite and titanite could exert a huge effect in LREE depletion. Apparently, this did not occur as the REE patterns of the granitoids of interest do not show significant LREE depletion.

The whole-rock Sr–Nd and zircon Hf isotopic compositions provide the most stringent petrogenetic constraint. The calculated initial $^{87}Sr/^{86}Sr$ ratios ($I_{Sr}$ values) range from 0.7040 to 0.7083, and the initial $\varepsilon_{Nd}(t)$ values range from +3.0 to −6.0, but in most cases they are slightly negative (Fig. 9A). Single-stage Sm–Nd model ages vary between 655 and 1940 Ma and two-stage model ages range from 659 to 1370 Ma (Table 4; Fig. 9B and D). In comparison, zircon Hf isotopic data show that most analyzed zircon domains have positive $\varepsilon_{Hf}(t)$ values (Fig. 10A). Besides, the entire data-set appears to suggest an increasing trend of $\varepsilon_{Hf}(t)$ values as the emplacement age gets younger (Fig. 10A). Such a trend is lacking in the whole-rock Nd isotopic compositions (Fig. 10B). The zircon Lu–Hf model ages yielded a range of 200–2000 Ma, but the majority are from 500 to 1500 Ma (Fig. 11).

The display of a large range of $\varepsilon_{Hf}(t)$ values in zircon grains from the same sample is frequently observed in granitic rocks (e.g., Griffin et al., 2002; Jahn et al., 2014). A likely explanation is given as follows. Zircon crystallizes at a given time in an evolving granitic magma likely preserves its chemical and isotopic compositions in equilibrium with the magma at that time. The bulk composition of a magma chamber will change through fractional crystallization, but the crystallization process in a closed system will not modify the isotopic composition. A change of isotopic composition could only be achieved through an open-system behavior, such as influx of an external magma or assimilation of country rocks in the magma chamber. Zircon crystals formed at any given stage would register the Hf isotopic composition of the evolving magma at that stage. Since zircon crystals do not grow at the same time, the individual grains from a single rock might have recorded the Hf isotopic compositions of different stages of magma evolution.

Consequently, the Sr–Nd–Hf isotopic data suggest that the granitoid magmas of Sikhote-Alin were generated by partial melting of sources with significant proportions of mantle-derived materials intercalated with older continental crust components. The magma differentiation was probably accompanied by crustal assimilation as evidenced by the zircon Hf isotopic data. The mantle-derived materials could include the subducted oceanic basalt or underplated basaltic magma to the lower part of the Sikhote-Alin basement. In fact, fragments of the subducted oceanic plate are registered by seismic tomography at mantle depths as high-velocity objects (Bijwaard et al., 1998). The crustal component might be represented by the hidden older basement rocks and the accretionay complexes of terrigenous derivation. One might argue that "old basement rocks" do not exist in the Sikhote-Alin accretionary orogen; however, they are identifiable from the Nd–Hf isotopic point of view. Moreover, the crustal thickness beneath the Sikhote-Alin is 38 km (Rodnikov et al., 1996, 2008), and such a thick crust cannot be made up entirely of only accretionary complexes. Therefore, the existence of an old continental basement is hypothesized, as for the case of SW Japan (Jahn, 2010).

In a geochemical and Nd isotopic study of the Early Cretaceous granitoids of the Samarka terrane (130–98 Ma), Kruk et al. (2014a) found that the granitoids of the first stage (Khungari Group; 130–123 Ma) occur as a rather uniform melanogranite–granite association and are characterized by high K/Na, low Ca, and elevated $Al_2O_3$. They are akin to the S-type granites. Two Nd isotope analyses yielded $\varepsilon_{Nd}(t) = -4.1$ and $-3.7$, with Sm–Nd model ages ($T_{DM}$) of ~1.3 Ga. Granitoids of the second stage (Tatibi Group; 110–98 Ma) are more variable in composition and show a wider range of K/Na and A/CNK, higher CaO and lower $P_2O_5$ than granitoids of the first stage. They belong to S- and I-type granites. Six Sm–Nd isotopic analyses yielded $\varepsilon_{Nd}(t) = -0.7$ to $-3.8$, and $T_{DM}$ ages of 0.82–1.55 Ga. When geochemical and Nd isotopic data of the upper crustal rocks of the Samarka terrane (=sandstones and siltstones of the turbidite matrix of a Jurassic accretionary prism and intercalated basalts) are compared, the Early Cretaceous granitoids were considered to have been produced by partial melting of the Samarka accretionary prism (Kruk et al., 2014a). By contrast, the generation of the second stage granitoids involved underplating of basaltic magmas and triggered anatexis of a mixed rock assemblage including metabasaltic and metasedimentary rocks of accretionary complex. This produced a great diversity of granitoids from S- to I-type (Kruk et al., 2014a).

### 6.3. Juvenile crustal growth and comparison with other parts of the Western Pacific orogens

Generation and intrusion of granitoid magmas represent upward transport of crustal materials from the lower part of the

Please cite this article in press as: Jahn, B.-m., et al. Emplacement ages, geochemical and Sr–Nd–Hf isotopic characterization of Mesozoic to early Cenozoic granitoids of the Sikhote-Alin Orogenic Belt, Russian Far East: Crustal growth and regional tectonic evolution. Journal of Asian Earth Sciences (2015), http://dx.doi.org/10.1016/j.jseaes.2015.08.012

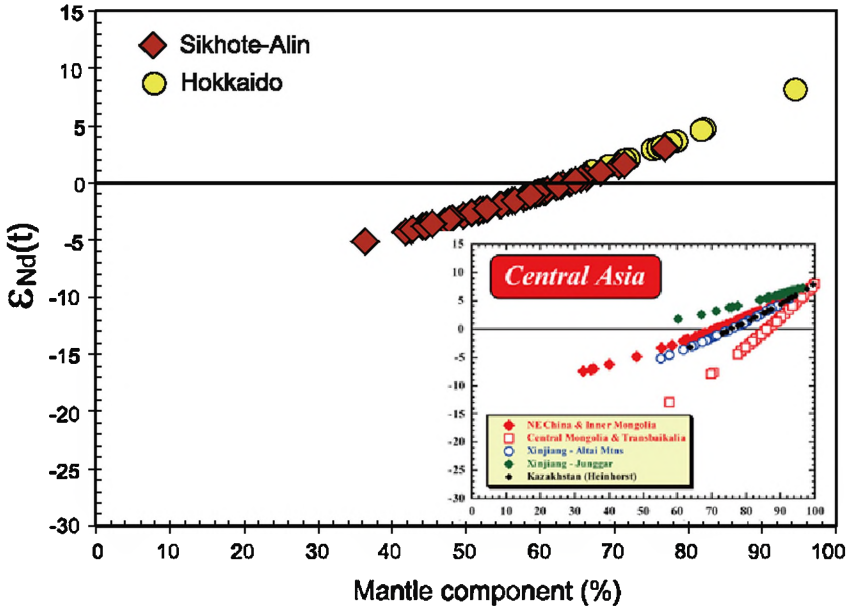


**Fig. 12.** Proportions of the mantle component vs. $\varepsilon_{Nd}(t)$ plot for the granitoids from Sikhote-Alin. The data of Hokkaido (Japan) and five terranes of the Central Asian Orogenic Belt are shown for comparison. The mantle component of the Sikhote-Alin samples varies from 36% to 77%.

crust and/or from the upper mantle. Anatexis of metasedimentary rocks may lead to the formation of peraluminous leucogranite, but such pure crustal melts are often limited in volume and in tectonic setting. Many lines of evidence advocate that generation of voluminous granitoid melts must have involved participation of mantle-derived liquid. The evidence includes (1) close association of granitic and basaltic rocks in orogenic belts in continental hot-spots and in regions of crustal extension; (2) petrological and geochemical arguments in favor of mixing of a mantle-derived component and crustal melt, including numerous mafic microgranular enclaves characteristic of many quartz diorite and granodiorite plutons of the studied region, and (3) thermal consideration and experimental demonstration of basalt-induced crustal melting (Huppert and Sparks, 1988). Thus, the generation of granitoid magmas implies an input of mantle material to the continental crust. Basaltic underplating to the lower crust and voluminous emplacement of basaltic sills are commonly considered to be the most effective way to trigger partial melting as well as to provide the mantle component to the granitoid liquids. If the source rocks are pre-existing metabasic rocks, the partial melts could become pure juvenile granitoids. Oxygen isotopic compositions (Valui et al., 2008) come to a similar conclusion regarding a significant contribution of juvenile protolith in the generation of granitoid rocks.

Using the Nd isotopic constraint, the proportion of the mantle component in the generation of the granitoids from Sikhote-Alin can be estimated. Fig. 12 shows a crude estimate of the proportion of the mantle (juvenile) to recycled components. The estimate was done using a simple two-component mixing calculation, assuming the two end-members to be a mantle-derived basalt (=mantle component) and an old continental crust (=crustal component). The data of the Cenozoic granitoids from Hokkaido (Jahn et al., 2014) and Paleozoic-to-Mesozoic granitoids from Central Asia (Jahn, 2004) are also shown for comparison. The mixing proportions for all granitoid samples can be calculated using the following equation:

$$X^m = Nd_c \times (\varepsilon^c - \varepsilon^r)/[\varepsilon^r \times (Nd_m - Nd_c) - (\varepsilon^m \times Nd_m - \varepsilon^c \times Nd_c)] \times 100$$

where $X^m$ = mantle-derived juvenile component (represented by basalt); $\varepsilon^c$, $\varepsilon^r$, $\varepsilon^m$ = Nd isotopic compositions of the crust, rock measured, and mantle component, respectively. $Nd_c$, $Nd_m$ = Nd concentration in the crust and mantle components, respectively. The inset of Fig. 12 was taken from Jahn (2004), and the assumed parameters used are: $\varepsilon^m = +8$, $\varepsilon^c = -12$ (NE China and Inner Mongolia), −30 (Central Mongolia and Transbaikalia), −15 (Altai Mountains), −4 (Junggar), −15 (Kazakhstan), $Nd_m = 15$ ppm, and $Nd_c = 25$ ppm. For the granitoids of Hokkaido and Sikhote-Alin, $\varepsilon^m = +10$ and $\varepsilon^c = -10$ were used; but we chose $Nd_c = 26.6$ ppm (average of 9 sedimentary rocks; Khanchuk et al., 2013; Kruk et al., 2014a) for the case of Sikhote-Alin.

Fig. 12 shows that the proportion of the mantle component in the granitoids of Sikhote-Alin varies from 77% to 36%. This represents a significant addition of juvenile crust to the Sikhote-Alin orogenic belt. However, the amount is lower than the granitoids from the Cenozoic accretionary terranes in Hokkaido (ca. 65–95%) and the Paleozoic accretionary terranes in the Central Asian Orogenic Belt. In any case, the overall range of slightly negative $\varepsilon_{Nd}(t)$ values (mostly from 0 to −4) requires a contribution of older crustal rocks in the granitoid generation. The large range of zircon Hf isotope compositions also supports a role of recycled crust in the generation and differentiation of granitic magmas.

In the above estimate of the mantle/crust proportion, the major sources of error come from the poor knowledge of the end members. Based on the peraluminous S-type character and negative $\varepsilon_{Nd}(t)$ values (−4.0 to −0.7), Kruk et al. (2014a) proposed that the Khungari group granitoids of the Samarka Terrane were produced by partial melting of the accretionary complex. The accretionary complex is characterized by sandstone, siltstone, mixed clastic layers, large olistoliths and plates of flints. Occasionally, basalt, gabbro, limestone, and meta-ophiolitic schist also occur (Eliseeva et al., 1976). The terrigenous matrix rocks contain radiolarians of Jurassic age (Kemkin and Khanchuk, 1992), whereas the siliceous rocks from inclusions are dated mainly at the Triassic–Early Jurassic or, less commonly, Paleozoic ages (Kemkin and Golozubov, 1997; Mazarovich, 1985; Volokhin et al., 2003).

Please cite this article in press as: Jahn, B.-m., et al. Emplacement ages, geochemical and Sr–Nd–Hf isotopic characterization of Mesozoic to early Cenozoic granitoids of the Sikhote-Alin Orogenic Belt, Russian Far East: Crustal growth and regional tectonic evolution. Journal of Asian Earth Sciences (2015), http://dx.doi.org/10.1016/j.jseaes.2015.08.012

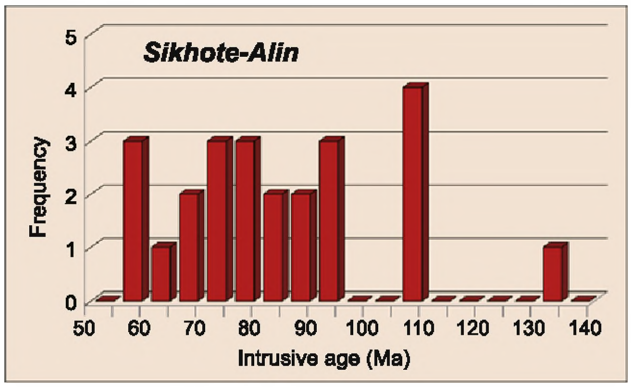


**Fig. 13.** Zircon age histogram for the Sikhote-Alin granitoids. A gap may be observed for the period from 130 to 110 Ma (magmatic quiescence period). The small gap of 110–95 Ma is probably an artifact because granitoids of 100–105 Ma have been recognized by conventional zircon dating of two granitoids from the Uspensk Intrusion (Khanchuk et al., 2008).

### 6.4. Tectonic implications

#### 6.4.1. Paleo-Pacific and Eurasian plate interaction

The formation and evolution of the East Asian continental margin have involved complicated tectonomagmatic processes, including subduction, accretion and magmatism. Furthermore, the tectonic processes are characterized by the "transform" nature or strike-slip displacement of individual terranes or blocks of different tectonic history (e.g., Abrajevitch et al., 2012; Isozaki et al., 2010; Kemkin, 2008; Khanchuk, 2001, 2006; Kirilova, 2003; Kojima, 1989; Maruyama et al., 1997; Tazawa, 2004; Zonenshain et al., 1990a,b). A large part of the Russian Far East is built up of accretionary complexes that formed along the convergent margin during the Cretaceous. A complex distribution of coeval complexes as well as juxtaposition of different age units indicates a considerable margin-parallel translation of terranes, which was represented by the sinistral strike-slip fault systems in the region, of which the Central Sikhote-Alin Fault is the most celebrated (e.g. Khanchuk, 2001, 2006; Otsuki, 1992; Sengor and Natal'in, 1996; Tazawa, 2004). A paleomagnetic study led Abrajevitch et al. (2012) to hypothesize that the West Sakhalin Basin has moved from sub-equatorial latitude during the early Cretaceous to about 40°N by the late Cretaceous. Similarly, the Nadanhada Terrane of NE China (or Nadanhada-Bikin Terrane in Fig. 1) was probably accreted to the Asian continental margin from low-latitude during the late Mesozoic (Mizutani and Kojima, 1992).

The tectonic evolution and crustal formation are intimately linked to the interaction between the Paleo-Pacific (=Izanagi) and Eurasian plates. Fig. 13 shows an apparent magmatic quiescence period between 130 and 110 Ma (Early Cretaceous). A second apparent gap between 105 and 95 Ma, based only on our zircon age data, cannot be taken for another quiescence period because two granitoids from the Uspensk Intrusion from South Primorye have been dated at 103 and 104 Ma by the conventional zircon U–Pb method (Khanchuk et al., 2008). The Early Cretaceous quiescence period may imply the lack of subduction activity due probably to a strike-slip or transformal plate interaction, as depicted from the tectonic analysis of Golozoubov (2006). However, the present database of 24 zircon ages (Fig. 13) is likely insufficient to reach a definite conclusion.

Nevertheless, the quasi-continuous magmatism in the Late Cretaceous (Fig. 13) indicates that the Paleo-Pacific plate subduction was active, and the apparent regular younging of granitic intrusion ages, from 80 to 56 Ma (Fig. 2), in the Taukha Terrane may in fact suggest an oblique subduction of the oceanic plate beneath the Eurasian continental margin. The subduction-induced magmatism

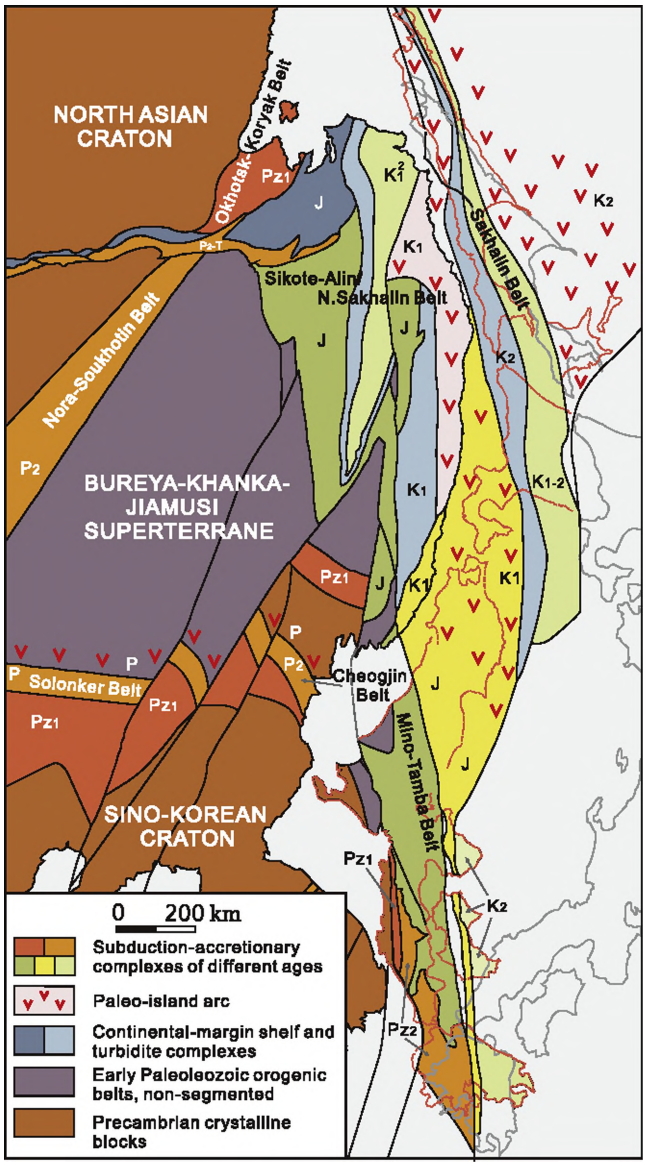


**Fig. 14.** A reconstructed terrane map of Khanchuk (2001) showing the correlation and geologic continuity between the Japanese Islands and Sikhote-Alin. Note that the "North Asian Craton" used by Khanchuk (2001) and shown in the upper left is equivalent to the more familiar "Siberian Craton".

produced not only granitic intrusion, but also abundant silicic volcanism accompanied by subordinate basaltic eruptions. An important implication from the present geochronological work is that during Late Cretaceous the Paleo-Pacific plate motion probably changed from a parallel or sub-parallel (magmatic quiescence) to oblique (active arc magmatism) relative to the continental margin of Sikhote-Alin. Late Cretaceous rapid sea-floor spreading at about 100 Ma (Larson, 1991; Larson and Pitman, 1972) induced highly active subduction and led to voluminous magmatism in the entire circum-Pacific areas (Jahn, 1974).

#### 6.4.2. Geological correlation between Sikhote-Alin and SW Japan

Finally, we discuss the problem of the geological correlation between the Sikhote-Alin and the Japanese Islands. Based on the lithostratigraphy, biostratigraphy (radiolarian assemblages) and geological structures, the Samarka terrane was correlated with the Nadanhada terrane in China and the Mino-Tamba belt in Japan (Fig. 14; Kojima, 1989; Khanchuk, 2001). These terranes represent fragments of the same Jurassic accretionary complex. Khanchuk

Please cite this article in press as: Jahn, B.-m., et al. Emplacement ages, geochemical and Sr–Nd–Hf isotopic characterization of Mesozoic to early Cenozoic granitoids of the Sikhote-Alin Orogenic Belt, Russian Far East: Crustal growth and regional tectonic evolution. Journal of Asian Earth Sciences (2015), http://dx.doi.org/10.1016/j.jseaes.2015.08.012

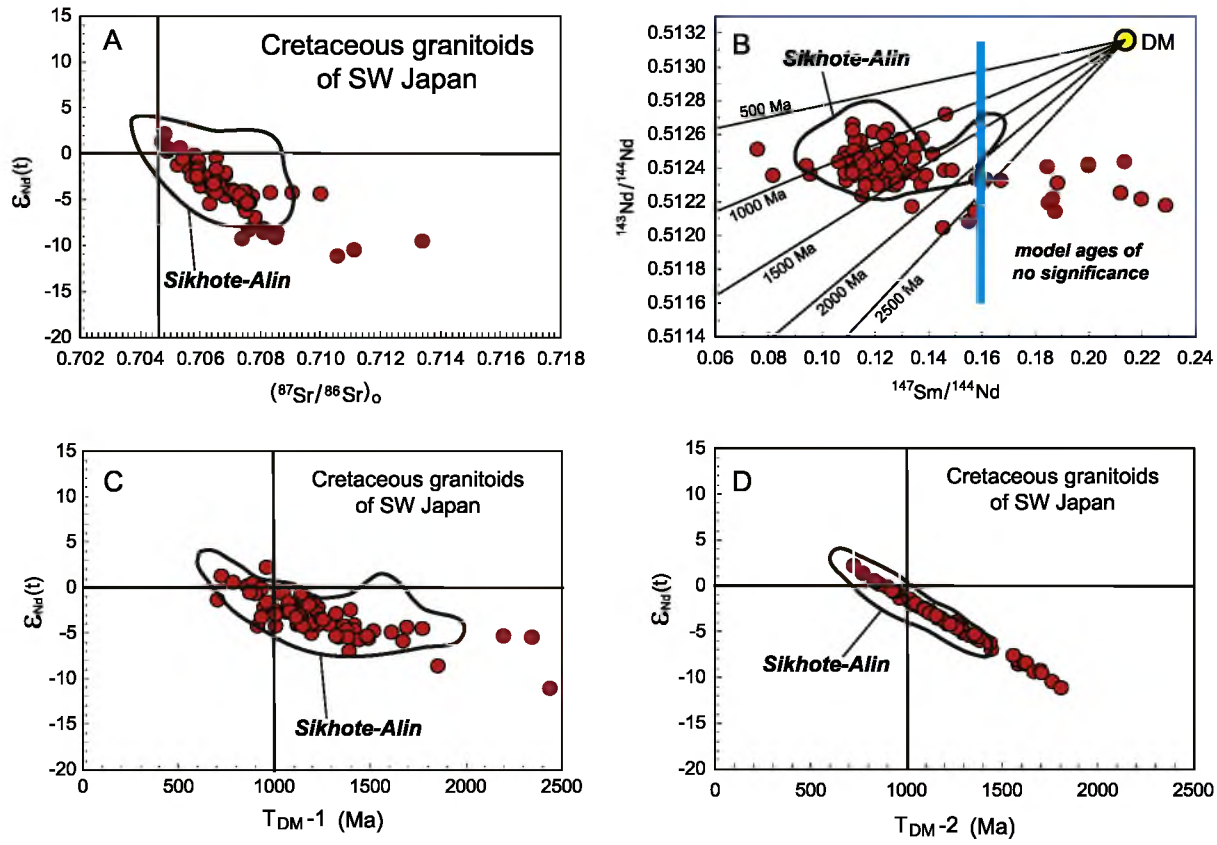


**Fig. 15.** Sr and Nd isotopic compositions of Cretaceous granitoids from SW Japan, with superposition of the envelopes of the Sikhote-Alin data sets. A remarkable similarity between the two sets of data isobserved. Data sources of SW Japan: Jahn (2010), Kagami et al. (1992), Arakawa and Shinmura (1995), Fujii et al. (2000), Iizumi et al. (2000), Ishioka and Iizumi (2003).

(2001) also considered that the Central Sikhote-Alin Fault and the Median and Tanakura Tectonic Lines (Japan) belong to the same Early Cretaceous Fault, and are comparable to the present San Andreas Fault in California. The Hida Belt could be correlated with the Sergeevka Terrane and the Khanka Block. The Taukha terrane may be a part of the Early Cretaceous subduction complex associated with the coeval arc volcanic rocks in NE Honshu and SW Hokkaido of Japan (Kiminami et al., 1992). Based on tectonic and faunal data, Matsukawa et al. (1997) proposed that the Jurassic to Early Cretaceous accretionary wedge and Early Cretaceous arc terranes (Taukha and others in NE Japan) were displaced from their original positions more than 1000 km northward and then accreted to the continental margin in the Albian time (113–100 Ma). Based on the age, lithology and structural position data of ophiolites and blueschists that occur in Sikhote-Alin and Japan, Ishiwatari and Tsujimori (2003) proposed a geologic continuation between Sikhote-Alin and Japan before the Miocene opening of the Japan Sea.

Evidence for the geologic correlations mentioned above may be strong for some cases but weak for the others. Geologic correlation could be made with two considerations: chronostratigraphic and lithostratigraphic. Based on the fossil assemblages and range of granitoid emplacement ages (Nakajima et al., 1990), the chronostratigraphic correlation between Sikhote-Alin and SW Japan could be well acceptable. However, we note that the similar Cretaceous age pattern is not unique to the two areas but is rampant in the Circum-Pacific regions. Therefore, the correlation has to be made with great care.

On the other hand, the whole-rock Sr–Nd isotopic data obtained for granitoid samples may be used to test the geologic correlation between Sikhote-Alin and SW Japan. The Sr–Nd isotopic data of Sikhote-Alin (Fig. 9) fall within the range of SW Japan (Jahn, 2010; Jahn et al., 2014), though the range of Sikhote-Alin is much smaller and does not show very negative values as seen in SW Japan. However, if only the data of Cretaceous granitoids are examined, a remarkable similarity between Sikhote-Alin and SW Japan is observed (Fig. 15). Therefore, the available age and isotopic signatures of granitoids lend support to the geologic correlation.

It has been hypothesized that the initial development of the Japanese accretionary orogen began in the early Paleozoic, in the eastern margin of Cathaysia, SE China (Isozaki, 1996, 1997; Isozaki et al., 2010; Maruyama et al., 1997). The proto-Japan (microcontinent) was rifted off after the Cretaceous. The available Sr–Nd isotope data of granitoids (e.g., Jahn, 2010 and references therein) and detrital zircon ages (Fujisaki et al., 2014) support the affinity of SW Japan to Cathaysia. If Sikhote-Alin can indeed be correlated with SW Japan and both formed a physical continuity as depicted in Fig. 14 (Khanchuk, 2001), we may also expect the initial development of Sikhote-Alin along Cathaysia. In any case, many lines of evidence support the correlation between the SW Japan and Sikhote-Alin accretionary orogens, but some of them can be challenged, particularly between the Taukha Terrane and NE Japan as advocated by Kiminami et al. (1992) and followed by many workers. The challenge comes mainly from the contrasting Sr–Nd isotopic signatures of granitoids from these two tectonic units (Jahn et al., in preparation).

## 7. Conclusions

Based on the newly obtained geochemical, isotopic and geochronological data, we present the following conclusions:

Please cite this article in press as: Jahn, B.-m., et al. Emplacement ages, geochemical and Sr–Nd–Hf isotopic characterization of Mesozoic to early Cenozoic granitoids of the Sikhote-Alin Orogenic Belt, Russian Far East: Crustal growth and regional tectonic evolution. Journal of Asian Earth Sciences (2015), http://dx.doi.org/10.1016/j.jseaes.2015.08.012

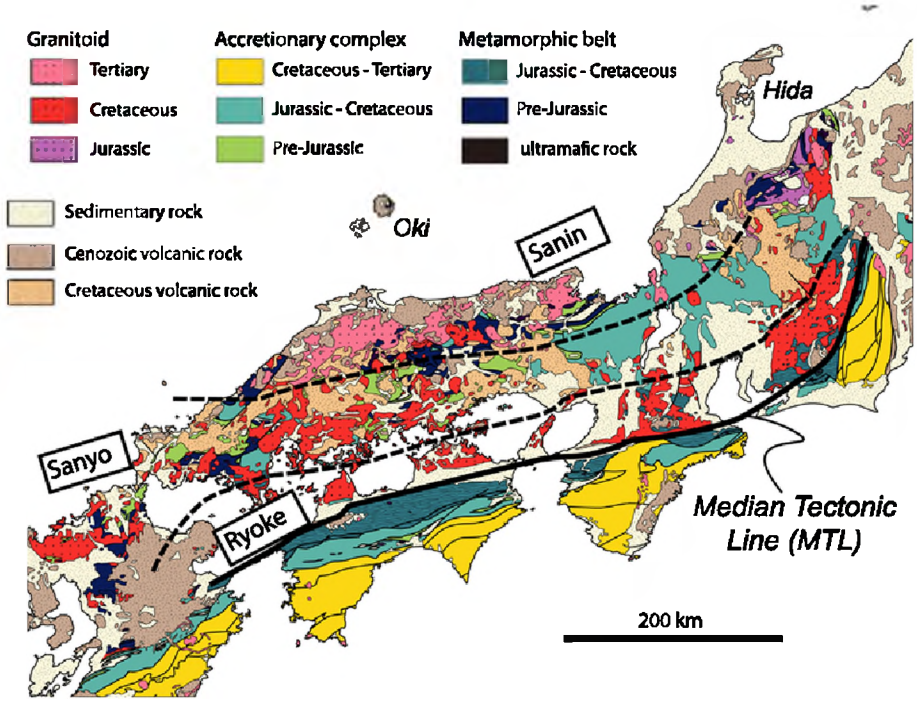


**Fig. A1.** General geologic map of SW Japan. The Median Tectonic Line (MTL) separates the granitoid-dominated terrane to the north from the Mesozoic-Cenozoic accretionary wedge to the south. The granitoid teranne is divided into three granitic belts (Ryoke, Sanyo and Sanin) based on the type of mineral deposits and oxygen fugacity (Ishihara, 1971).

1. Zircon dating revealed that granitoids of the Sikhote-Alin orogen were intruded from 130 to 56 Ma (Cretaceous to Paleogene). Granitoids in the coastal area were emplaced in the Taukha Terrane from 90 to 56 Ma, whereas those along the Central Sikhote-Alin Fault intruded the Samarka Terrane from 110 to 75 Ma. The "oldest" monzogranite (131 Ma) was emplaced to the west of the Central Sikhote-Alin Fault and within the Khanka Block. Thus, the most important tectonothermal events in the East Sikhote-Alin occurred in the Cretaceous.
2. Geochemical analysis indicates that most granitoids are I-type. Whole-rock Sr–Nd isotopic data suggest that the magmas were generated by partial melting of mixed source rocks including the subduction-related accretionary complex as well as unexposed Paleozoic-Proterozoic basement rocks. Zircon Hf isotopic data further indicate that zircon grains crystallized from mixed-source melts and that crustal assimilation took place during magmatic differentiation. Overall, the Sr–Nd–Hf isotopic data indicate a significant proportion of the mantle component (36–77%) in the generation of the granitoid rocks. This suggests an addition of juvenile crust in Sikhote-Alin.
3. The apparent regular change of granitic intrusion ages from 80 to 56 Ma in the Taukha Terrane was probably produced by oblique subduction of the Paleo-Pacific plate beneath the Eurasia continental margin.
4. Subduction-induced magmatism produced not only widespread granitoids, but also abundant silicic volcanic rocks. During the Late Cretaceous the Paleo-Pacific plate motion probably changed from a parallel or sub-parallel (=magmatic quiescence period) to oblique (active arc magmatism period) relative to the continental margin of Sikhote-Alin. We admit that the idea of the change of plate motion is speculative as the age and geochemical data do not provide an unequivocal support.
5. The geologic correlation between the Sikhote-Alin and SW Japan accretionary orogenic belts is supported by the present geochronologic and Sr–Nd isotopic study.

## Acknowledgments

We are deeply indebted to the following people and laboratories for their assistance in the acquisition of the data reported in this paper: Dunyi Liu (Beijing SHRIMP Center, for CL images), Sun-Lin Chung (NTU-Geosciences; chemical and zircon U–Pb and Hf isotope analyses), Chi-Yu Lee (NTU-Geosciences, major elements), and Wen-Yu Hsu (IES-AS; Sr–Nd isotope analyses). Ms. Jia-Ping Liao assisted in producing the U–Pb Concordia plots with color codes for Th/U ratios. A field excursion in southeastern Sikhote-Alin led by Galina Valui and Igor Alexandrov in September 2013 was very helpful. The Beijing SHRIMP Center (Dunyi Liu) and the University of Hong Kong (Min Sun) provided temporary shelters to BMJ in May 2014 and November 2014, respectively, for preparation of the manuscript. The early draft has been reviewed by Boris Litvinovsky and Igor Alexandrov. Their in-depth comments and suggestions are most appreciated. Constructive reviews by Profs. Gary Ernst, Alfred Kroner and Tatsuki Tsujimori have greatly improved the quality of this paper. BMJ acknowledges the support of NSC-Taiwan (MOST-Taiwan) through research projects of NSC-100-2923-M-002-010, NSC101-2116-M-002-003, NSC102-2116-M-002-031, MOST 104-2923-M-002-005.

## Appendix A. Brief geological description of SW Japan

The Japanese Islands have developed mainly through convergence between oceanic and continental plates along active margins (e.g., Isozaki, 1997; Isozaki et al., 2010). According to Isozaki et al. (2010), 9 belts of accretionary complex occur as thin subhorizontal fault-bounded units, i.e., nappe, and they show a clear downward and oceanward younging polarity. Numerous oceanic fragments derived from subducted oceanic plates, including deep-sea sediments and seamount basalts and reef limestone, were accreted to Japan. Furthermore, the Permo-Triassic tectonics is regarded as

Please cite this article in press as: Jahn, B.-m., et al. Emplacement ages, geochemical and Sr–Nd–Hf isotopic characterization of Mesozoic to early Cenozoic granitoids of the Sikhote-Alin Orogenic Belt, Russian Far East: Crustal growth and regional tectonic evolution. Journal of Asian Earth Sciences (2015), http://dx.doi.org/10.1016/j.jseaes.2015.08.012

most important because the basic framework of the Japanese orogenic belts was established and stabilized at that time (Isozaki, 1996). The occurrence of Permo-Triassic tectonic units is well developed in SW Japan and the Ryukyu Islands, but rarely recognized in NE Honshu and Hokkaido.

The Median Tectonic Line (MTL) is a prominent strike-slip fault running through most of SW Japan. It divides SW Japan into two zones: the "Inner Zone" on the back-arc side, and the "Outer Zone" on the fore-arc side (Fig. A1). In the Outer Zone, the post-Jurassic accretionary complexes are arranged to show oceanward younging from the Cretaceous to Miocene (Taira et al., 1988), and further to the present accretionary prism at the Nankai Trough. No collision-related Permo-Triassic units have been identified. The deep part of the accretionary complexes is exposed as a low-pressure to high-pressure regional metamorphic belt, which includes the eclogite-bearing Sanbagawa Belt. Conspicuous Miocene granitic rocks also occur on the Pacific side of SW Japan. These granitoids intruded into the Cretaceous and Tertiary accretionary complexes, and they were likely produced by remelting of the Shimanto accretionary complex (Shinjoe, 1997; Jahn, 2010).

In the Inner Zone (Fig. A1), Cretaceous to Paleogene granitoids are extensively distributed. Note that the majority of granitic intrusions were emplaced in the Cretaceous, and they intruded into the pre-Cretaceous accretionary complexes which include regional metamorphic rocks. Similar to Sikhote-Alin, the intrusive granitoids in SW Japan are associated with coeval rhyolites and ignimbrites even though much of the cover series has been eroded to expose the intrusive rocks. Besides, a few collisional belts, or non-accretionary units (Hida and Oki belts), occur in the northern part, and they are composed of polymetamorphic gneiss and schist complexes, with a Triassic regional metamorphism of intermediate pressure facies (Komatsu, 1990).

Ishihara (1971) made a detailed study of the granitoids and associated ore deposits. He divided the Inner Zone into three metallogenic provinces, from south to north, a Barren, a Tungsten, and a Molybdenum Province (see also Ishihara and Murakami, 2006). The three provinces correspond to the Ryoke, Sanyo and San-in Belts as delineated by Murakami (1974) on the basis of granite petrography and age data. The lithological types in the Inner Zone are more complicated than the granitoids and acid volcanic rocks alone. The Ryoke belt is a plutonic-metamorphic terrane that comprises pre-Cretaceous accretionary complexes with high-level granites and high-grade, but low P/T, metasediments with migmatites and gneissose granites. Granitic rocks are dominant over metamorphic rocks. The Ryoke and Sanyo granitoids were likely produced by Cretaceous subduction of the Kula-Pacific ridge (Nakajima, 1994). Isozaki et al. (2010) described that the Inner Zone is composed of a 15 km-thick lower crust of unknown composition, a 20 km-thick granitic upper crust and thin roof-pendants of the Paleozoic to Jurassic accretionary complex (AC) units on the surface. These AC units are characterized by subhorizontal stacking of multiply fault-bounded units, previously recognized "nappes", with a gentle dip angle toward the Eurasian continent.

In addition to granitoids, ophiolite complexes also occur widely in SE Japan (Ishiwatari and Tsujimori, 2001; Ishiwatari and Tsujimori, 2003; Fig. A2). They were emplaced from early Paleozoic to Cenozoic. In SW Japan the early Paleozoic Oeyama ophiolite occupies the highest structural position, and tectonically overlies the late Paleozoic Renge blueschist, the Yakuno ophiolite, and the Permian Akiyoshi (and Ultra-Tamba) accretionary complexes. These tectonic units are separated by thrust faults.

The Yakuno ophiolite is a rather complete succession composed of harzburgite tectonite, dunite–wehrlite–clinopyroxenite cumulate, metagabbro, amphibolite and metabasalt with abundant black shale. Study of radiolarian fossils from the black shale (Kurimoto and Makimoto, 1990) and radiometric dating (K–Ar on metagabbro (Shibata et al., 1977) and zircon U–Pb on plagiogranite (Herzig et al., 1997) indicate that the ophiolite formed in Early Permian (ca. 285 Ma) and was metamorphosed later during 240–280 Ma.

The Renge blueschist occurs as thin tectonic slices or blocks in serpentinite mélanges underlying the Oeyama ophiolite (Tsujimori, 1998), and has a phengite K–Ar age of 320 Ma (Tsujimori and Itaya, 1999).

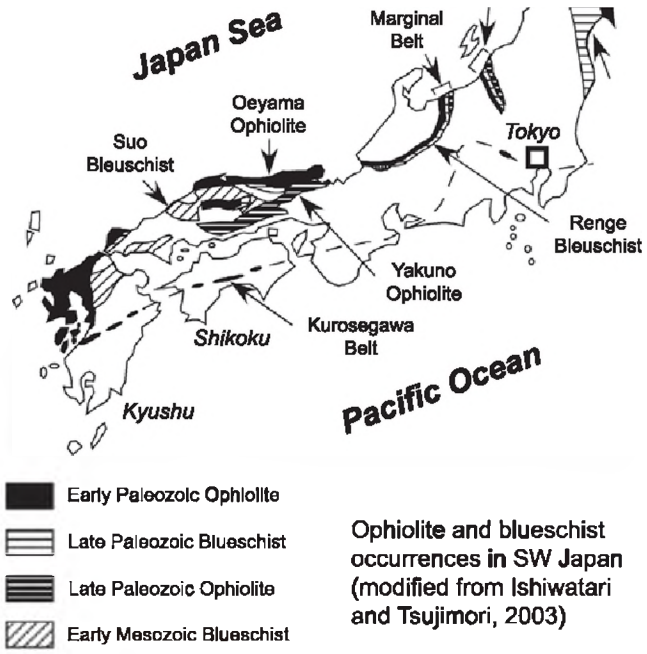


Fig. A2. Distribution of ophiolites and blueschists in SW Japan (modified from Ishiwatari and Tsujimori, 2003).

## References

Abrajevitch, A., Zyabrev, S., Didenko, A.N., Kodama, K., 2012. Paleomagnetsim of the West Sakhalin Basin: evidence for northward displacement during the Cretaceous. Geophys. J. Int. 190, 1439–1454.

Arakawa, Y., Shinmura, T., 1995. Nd–Sr isotopic and geochemical characteristics of two contrasting types of calc-alkaline plutons in the Hida belt, Japan. Chem. Geol. 124, 217–232.

Baskina, V.A., Favorskaya, M.A., 1969. Age of the igneous rocks of the Imansky block (East Sikhote-Alin) is fixed by the K–Ar method. DAN the USSR 184, 905–908 (in Russian).

Bijwaard, H., Spakman, W., Engdahl, E.R., 1998. Closing the gap between regional and travel time tomography. J. Geophys. Res. Solid Earth 103, 30055–30078.

Chiu, H.Y., Chung, S.L., Wu, F.Y., Liu, D., Liang, Y.H., Lin, I.J., Iizuka, Y., Xie, L.W., Wang, Y., Chu, M.F., 2009. Zircon U–Pb and Hf isotopic constraints from eastern Transhimalayan batholiths on the pre-collisional magmatic and tectonic evolution in southern Tibet. Tectonophysics 477, 3–19.

Chu, M.F., Chung, S.L., Song, B., Liu, D.Y., O'Reilly, S.Y., Pearson, N.L., 2006. Zircon U–Pb and Hf isotope constraints on the Mesozoic tectonics and crustal evolution of southern Tibet. Geology 34, 745–748.

DePaolo, D.J., Linn, A.M., Schubert, G., 1991. The continental crustal age distribution: methods of determining mantle separation ages from Sm–Nd isotopic data and application to the Southeastern United States. J. Geophys. Res. 96, 2017–2088.

Eliseeva, V.K., Lipman, R.Kh., Svyatogorova, N.N., 1976. New data on the stratigraphy of central Sikhote-Alin. Geologiya i Geofizika (Soviet Geol. Geophys.) 17, 30–43 (22–32).

Ellis, D.J., Thompson, A.B., 1986. Subsolidus and partial melting reactions in the quartz-excess $CaO+MgO+Al_2O_3+SiO_2+H_2O$ system under water-excess and water-deficient conditions to 10 kb: some implications for the origin of peraluminous melts from mafic rocks. J. Petrol. 27, 91–121.

Frost, B.R., Barnes, C.G., Collins, W.J., Arculus, R.J., Ellis, D.J., Frost, C.D., 2001. A geochemical classification for granitic rocks. J. Petrol. 42, 2033–2048.

Fujii, H., Tainosho, Y., Kagami, H., Kakiuchi, T., 2000. Sr–Nd isotopic systematics and geochemistry of the intermediate plutonic rocks from Ikoma mountains, Southwest Japan: Mesozoic magmatic activity in the Ryoke Belt. Island Arc 9, 37–45.

Fujisaki, W., Isozaki, Y., Maki, K., Sakata, S., Hirata, T., Maruyama, S., 2014. Age spectra of detrital zircon of the Jurassic clastic rocks of the Mino-Tanba AC belt

Please cite this article in press as: Jahn, B.-m., et al. Emplacement ages, geochemical and Sr–Nd–Hf isotopic characterization of Mesozoic to early Cenozoic granitoids of the Sikhote-Alin Orogenic Belt, Russian Far East: Crustal growth and regional tectonic evolution. Journal of Asian Earth Sciences (2015), http://dx.doi.org/10.1016/j.jseaes.2015.08.012

in SW Japan: constraints to the provenance of the mid-Mesozoic trench in East Asia. J. Asian Earth Sci. 88, 62–73.
Geology of the USSR, 1971. Primorsky Region. Part 1. Geological Structure, vol. 32. Nedra, Moscow, 695 p (in Russian).
Golozoubov, V.V., 2006. Tectonics of the Jurassic and Lower Cretaceous Complexes of the North-Western Framing of Pacific Ocean. Dal'nauka, Vladivostok, 239 p. (in Russian).
Golozoubov, V.V., Khanchuk, A.I., 1996. Taukha and Zhuravlevka terranes of South Sikhote-Alin – fragments of the Early Cretaceous margin of Asia. Russian J. Pac. Geol. 12, 203–220.
Gonevchuk, V.G., 2002. Tin-bearing System of the Far East: Magmatism and Ore Genesis. Dalnauka, Vladivostok, 296p (in Russian).
Gonevchuk, V.G., Gonevchuk, G.A., Korostelev, P.G., Semenyak, B.I., Seltmann, R., 2010. Tin deposits of the Sikhote-Alin and adjacent areas (Russian Far East) and their magmatic association. Aust. J. Earth Sci. 57, 777–802.
Gonevchuk, V.G., Gonevchuk, G.A., Lebedev, V.A., Orekhov, A.A., 2011. Association of monzonitic rocks of the Kavalerovo ore district (Primorye): geochronology and genesis. Russian J. Pac. Geol. 30, 20–31.
Goolaerts, A., Mattielli, N., de Jong, J., Weis, D., Scoates, J.S., 2004. Hf and Lu isotopic reference values for the zircon standard 91500 by MC-ICP-MS. Chem. Geol. 206, 1–9.
Grebennikov, A.V., Popov, V.K., 2014. Petrochemical aspects of the Late Cretaceous and Paleogene igmimbrite volcanism of East Sikhote-Alin. Russian J. Pac. Geol. 8, 38–55.
Griffin, W.L., Wang, X., Jackson, S.E., Pearson, N.J., O'Reilly, S.Y., Xu, X., Zhou, X., 2002. Zircon chemistry and magma mixing, SE China: in-situ analysis of Hf isotopes, Tonglu and Pingtan igneous complexes. Lithos 61, 237–269.
Griffin, W.L., Pearson, N.J., Belousova, E.A., Saeed, A., 2006. Comment: Hf-isotope heterogeneity in zircon 91500. Chem. Geol. 233, 358–363.
Gvozdev, V.I., 2010. Ore-magmatic Systems of Skarn Scheelite–Sulfide Deposits in Eastern Russia. Dal'nauka, Vladivostok (in Russian).
Herzig, C.T., Kimborough, D.L., Hayasaka, Y., 1997. Early Permian zircon uranium–lead ages for plagiogranites in the Yakuno ophiolite, Asago district, Southwest Japan. Island Arc 6, 396–403.
Huppert, H.E., Sparks, R.S., 1988. The generation of granitic magmas by intrusion of basalt into continental crust. J. Petrol. 29, 599–624.
Iizumi, S., Imaoka, T., Kagami, H., 2000. Sr–Nd isotope ratios of gabbroic and dioritic rocks in a Cretaceous-Paleogene granite terrain, Southwest Japan. Island Arc 9, 113–127.
Ishihara, S., 1971. Modal and chemical composition of the granitic rocks related to the major molybdenum and tungsten deposits in the inner zone of southwest Japan. J. Geol. Soc. Jpn 77, 441–452.
Ishihara, S., Murakami, H., 2006. Fractionated ilmenite-series granites in Southwest Japan: source magma for REE-Sn-W mineralizations. Resour. Geol. 56, 245–256.
Ishioka, J., Iizumi, S., 2003. Petrochemical and Sr–Nd isotope investigations of Cretaceous intrusive rocks and their enclaves in the Togouchi-Yoshiva district, northwest Hiroshima prefecture, SW Japan. Geochem. J. 37, 449–470.
Ishiwatari, A., Tsujimori, T., 2003. Paleozoic ophiolites and blueschists in Japan and Russian Primorye in the tectonic framework of East Asia: a synthesis. Island Arc 12, 190–206.
Isozaki, Y., 1996. Anatomy and genesis of a subduction-related orogen: a new view of geotectonic subdivision and evolution of the Japanese islands. Island Arc 5, 289–320.
Isozaki, Y., 1997. Constrasting two types of orogen in Permo-Triassic Japan: accretionary versus collisional. Island Arc 6, 2–24.
Isozaki, Y., Aoki, K., Nakama, T., Yanai, S., 2010. New insight into a subduction-related orogeny: a reappraisal of the geotectonic framework and evolution of the Japanese Islands. Gondwana Res. 18, 82–105.
Jahn, B.M., 1974. Mesozoic thermal events in southeast China. Nature 248, 480–483.
Jahn, B.M., 2004. The Central Asian Orogenic Belt and growth of the continental crust in the Phanerozoic. In: Malpas, J., Fletcher, C.J.N., Ali, J.R., Aitchison, J.C. (Eds.), Aspects of the Tectonic Evolution of China, vol. 226. Geological Society of London Special Publications, pp. 73–100.
Jahn, B.M., 2010. Accretionary orogen and evolution of the Japanese Islands – implications from a Sr–Nd isotopic study of the Phanerozoic granitoids from SW Japan. Am. J. Sci. 310, 1210–1249.
Jahn, B.M., Wu, F.Y., Chen, B., 2000a. Massive granitoid generation in Central Asia: Nd isotope evidence and implication for continental growth in the Phanerozoic. Episodes 23, 82–92.
Jahn, B.M., Wu, F.Y., Chen, B., 2000b. Granitoids of the Central Asian Orogenic Belt and continental growth in the Phanerozoic. Trans. Royal Soc. Edinburgh: Earth Sci. 91, 181–193.
Jahn, B.M., Wu, F., Capdevila, R., Martineau, F., Zhao, Z., Wang, Y., 2001. Highly evolved juvenile granites with tetrad REE patterns: the Woduhe and Baerzhe granites from the Great Xing'an Mountains in NE China. Lithos 59, 171–198.
Jahn, B.M., Capdevila, R., Liu, D.Y., Vernon, A., Badarch, G., 2004. Sources of Phanerozoic granitoids in the transect Bayanhongor-Ulaan Baatar, Mongolia: geochemical and Nd isotopic evidence, and implications for Phanerozoic crustal growth. J. Asian Earth Sci. 23, 629–653.
Jahn, B.M., Litvinovsky, B.A., Zanvilevich, A.N., Reichow, M., 2009. Peralkaline granitoid magmatism in the Mongolian-Transbaikalian Belt: evolution, petrogenesis and tectonic significance. Lithos 113, 521–539.
Jahn, B.M., Usuki, M., Usuki, T., Chung, S.L., 2014. Generation of Cenozoic granitoids in Hokkaido (Japan): constraints from zircon geochronology, Sr–Nd–Hf isotopic and geochemical analyses, and implications for crustal growth. Am. J. Sci. 314, 704–750.
Kagami, H., Iizumi, S., Tainosho, Y., Owada, M., 1992. Spatial variations of Sr and Nd isotope ratios of Cretaceous-Paleogene granitoid rocks, SW Japan Arc. Contrib. Miner. Petrol. 112, 165–177.
Kemkin, I.V., 2008. Structure of terranes in a Jurassic accretionary prism in the Sikhote-Alin-Amur area: implications for the Jurassic geodynamic history of the Asian eastern margin. Russ. Geol. Geophys. 49, 759–770.
Kemkin, I.V., Golozubov, V.V., 1997. The first find of the Early Jurassic radiolarians in the cherty allochthons of the Samarka accretionary prism (Southern Sikhote-Alin). Russian J. Pac. Geol. 13, 1111–1118.
Kemkin, I.V., Khanchuk, A.I., 1992. New data on the age of the paraautochthone of the Samarka accretionary complex, southern Sikhote-Alin'. Dokl. Akad. Nauk 324, 847–851.
Kemkin, I.V., Khanchuk, A.I., 1994. Jurassic accretionary prism in the southern Sikhote Alin. Geol. Pac. Ocean 10, 831–846.
Kemkin, I.V., Taketani, Y., 2008. Structure and age of lower structural unit of Taukha terrane of Late Jurassic-Early Cretaceous accretionary prism, southern Sikhote-Alin. Island Arc 17, 517–530.
Khanchuk, A.I., 2001. Pre-Neogene tectonics of the Sea-of-Japan region: a view from the Russian side. Earth Sci. (Chikyu Kagaku) 55, 275–291.
Khanchuk, A.I. (Ed.), 2006. Geodynamics, Magmatism, and Metallogeny of Eastern Russia, Book 1. Dal'nauka, Vladivostok, 572 pp, (in Russian).
Khanchuk, A.I., Kemkin, I.V., 2003. The Mesozoic geodynamic evolution of the Japan Sea region. Bull. DVO RAN 6, 99–116.
Khanchuk, A.I., Panchenko, I.V., Kemkin, I.V., 1988. Geodynamic Evolution of Sikhote-Alin and Sakhalin in the Paleozoic and Mesozoic. Far East Branch of the USSR Academy of Sciences, Vladivostok, 56 pp.
Khanchuk, A.I., Ratkin, V.V., Ryazantseva, M.D., Golozubov, V.V., Gonokhova, N.G., 1996. Geology and Mineral Deposits of Primorskiy Krai. Dalnauka, Vladivostok, 61 pp.
Khanchuk, A.I., Kruk, N.N., Valui, G.A., Nevolin, P.L., Moskalenko, E.Yu., Fugzan, M.M., Kirnozova, T.I., Travin, A.V., 2008. The Uspensk intrusion in South Primorye as a reference petrotype for granitoids of the transform continental margins. Dokl. Earth Sci. 421, 734–737.
Khanchuk, A.I., Vovna, G.M., Kiselev, V.I., Mishkin, M.A., Lavrik, S.N., 2010. First results of zircon LA-ICP-MS U-Pb dating of the rocks from the granulite complex of Khanka Massif in the Primorye Region. Dokl. Earth Sci. 434, 1164–1167.
Khanchuk, A.I., Kruk, N.N., Golozubov, V.V., Kovach, V.P., Serov, P.A., Kholodnov, V.V., Gvozdev, V.I., Kasatkin, S.A., 2013. The nature of the continental crust of Sikhote-Alin as evidenced from the Nd isotopy of rocks of Southern Primorie. Dokl. Earth Sci. 451, 809–813.
Kiminami, K., Niida, K., Ando, H., Kito, N., Iwata, K., Miyashita, S., Tajika, J., Sakakibara, M., 1992. Cretaceous-Paleogene arc-trench systems in Hokkaido. In: Adachi, M., Suzuki, K. (Eds.), 29th IGC Field Trip Guide Book, I: Paleozoic and Mesozoic Terranes, Basement of the Japanese Island Arcs, pp. 1–43.
Kirilova, G.L., 2003. Cretaceous tectonics and geological environments in East Russia. J. Asian Earth Sci. 21, 967–977.
Kojima, S., 1989. Mesozoic terrane accretion in Northeast China, Sikhote-Alin and Japan regions. Palaeogeogr. Palaeoclimatol. Palaeoecol. 69, 213–232.
Kojima, S., Kemkin, I.V., Kametaka, M., Ando, A., 2000. A correlation of accretionary complexes of southern Sikhote-Alin of Russia and the Inner Zone of Southwest Japan. Geosci. J. 4, 175–185.
Komatsu, M., 1990. Hida "Gaien" Belt and Joetsu Belt. In: Ichikawa, K., Mizutani, S., Hara, I., Hada, S., Yao, A. (Eds.), Pre-Cretaceous Terranes of Japan, Publication of IGCP Project 224: Pre-Jurassic Evolution of Eastern Asia, Osaka, Nippon Insatsu Shuppan, pp. 25–40.
Kruk, N.N., Simanenko, V.P., Gvozdev, V.I., Golozubov, V.V., Kovach, V.P., Serov, P.I., Kholodnov, V.V., Moskalenko, E.Yu., Kuibida, M.L., 2014a. Early Cretaceous granitoids of the Samarka terrane (Sikhote-Alin): geochemistry and sources of melts. Russ. Geol. Geophys. 55, 216–236.
Kruk, N.N., Simanenko, V.P., Golozubov, V.V., Kovach, V.P., Vladimirov, V.G., Kasatkin, S.A., 2014b. Geochemistry of rocks in the Anuy metamorphic dome, Sikhote-Alin: composition of the protoliths and the possible nature of metamorphism. Geochem. Int. 52, 229–246.
Krimskii, R.Sh., Pavlov, V.A., Rub, M.G., Belyatskii, V.B., Levskii, L.K., 1998. Rb–Sr and Sm–Nd isotopic systematics of the granitoids and ores of the Vostok-2 scheelite deposit, Primorie. Petrology 6, 1–11.
Kurchavov, A.M., 1979. Lateral Variability of Volcanic Rocks: On the Example of Southern Primorye. Nauka, Moscow, 145 p (in Russian).
Kurimoto, C., Makimoto, H., 1990. Geology of Fukuchiyama Area. 1:50,000 Scale Quadrangle Map. Geological Survey of Japan, Tsukuba (in Japanese with English abstract).
Larson, R.L., 1991. Latest pulse of Earth: evidence for a mid-Cretaceous superplume. Geology 19, 547–550.
Larson, R.L., Pitman, W.C., 1972. World-wide correlation of Mesozoic magnetic anomalies, and its implications. Geol. Soc. Am. Bull. 83, 3645–3662.
Lin, I.J., Chung, S.L., Chu, C.H., Lee, H.Y., Gallet, S., Wu, G., Ji, J., Zhang, Y., 2012. Geochemical and Sr–Nd isotopic characteristics of Cretaceous to Paleogene granitoids and volcanic rocks, SE Tibet: petrogenesis and tectonic implications. J. Asian Earth Sci. 53, 131–150.
Lin, T.-H., Chung, S.-L., Kumar, A., Wu, F.-Y., Chiu, H.-Y., Lin, I.-J., 2013. Linking a prolonged Neo-Tethyan magmatic arc in South Asia: zircon U–Pb and Hf isotopic constraints from the Lohit batholith, NE India. Terra Nova 25, 453–458.
Malinovsky, A.I., Golozoubov, V.V., Simanenko, V.P., 2006. The Kema island-arc terrane, Eastern Sikhote-Alin: formation settings and geodynamics. Dokl. Earth Sci. 410, 1026–1029.

Please cite this article in press as: Jahn, B.-m., et al. Emplacement ages, geochemical and Sr–Nd–Hf isotopic characterization of Mesozoic to early Cenozoic granitoids of the Sikhote-Alin Orogenic Belt, Russian Far East: Crustal growth and regional tectonic evolution. Journal of Asian Earth Sciences (2015), http://dx.doi.org/10.1016/j.jseaes.2015.08.012

Malinovsky, A.I., Golozoubov, V.V., Simanenko, V.P., Simanenko, L.F., 2008. Kema terrane: a fragment of a back-arc basin of the Early Cretaceous Moneron-Samarga island-arc system, East Sikhote-Alin range, Russian Far East. Island Arc 17, 285–304.
Maruyama, S., 1997. Pacific-type orogeny revisited: Miyashiro-type orogeny proposed: The. Island Arc 6, 91–120.
Maruyama, S., Isozaki, Y., Kimura, G., Terabayashi, M., 1997. Paleogeographic maps of the Japanese islands: plate tectonic synthesis from 750Ma to the present. Island Arc 6, 121–142.
Matsukawa, M., Takahashi, O., Hayashi, K., Ito, M., Konovaloy, V.P., 1997. Early Cretaceous paleogeography of Japan, based on tectonic and faunal data. Mem. Geol. Soc. Jpn. 48, 29–42.
Melnikov, N.G., Golozubov, V.V., 1980. Olistostromal thickness and consedimentation tectonic covers in the Sikhote-Alin. Geotectonics 4, 95–106 (in Russian).
Mazarovich, A.O., 1985. Tectonic Development of the Southern Primor'e in Paleozoic and Early Mesozoic. Nauka, Moscow, 103 p (in Russian).
Mikhailov, V.A., 1989. Magmatism of the Voclanotectonic Structures of the Southern East Sikhote-Alin Volcanic Belt. Dalnauka, Vladivostok, 171 p (in Russian).
Miller, C.F., 1985. Are strongly peraluminous magmas derived from politic sedimentary sources? J. Geol. 93, 673–689.
Mizutani, S., Kojima, S., 1992. Mesozoic radiolarian biostratigraphy of Japan and collage tectonics along the eastern continental margin of Asia. Paleogeogr. Paleoclimatol. Paleoecol. 96, 3–22.
Moskalenko, E.Yu., Kruk, N.N., Valui, G.A., 2011. New data on the geology and geochemistry of granitoids of the Uspenky massif, southern Primorye. Russian J. Pac. Geol. 30, 80–92.
Murakami, N., 1974. Some problems concerning late Mesozoic to early Tertiary igneous activity on the inner side of Southwest Japan. Pac. Geol. 8, 139–151.
Nakajima, T., 1994. The Ryoke plutonometamorphic belt: crustal section of the Cretaceous Eurasian continental margin. Lithos 33, 51–66.
Nakajima, T., Shirahase, T., Shibata, K., 1990. Along-arc lateral variation of Rb–Sr and K–Ar ages of Cretaceous granitic rocks in Southwest Japan. Contrib. Miner. Petrol. 104, 381–389.
Natal'in, B.A., 1991. Mesozoic accretionary and collisional tectonics of the USSR South Far east. Geol. Pac. Ocean 5, 3–23.
Natal'in, B.A., Faure, M., Monie, P., Borukaev, Ch.B., Prikhod'ko, V.S., Vrublevskii, A.A., 1994. The Anyui metamorphic dome, Sikhote-Alin, and its significance for the Mesozoic geodynamic evolution of Eastern Asia. Tikhookeanskaya Geol. 6, 3–25.
Nevolina, S.I., 1960. New finds of Cretaceous and Tertiary floras in Primorye. Inform. Sbornik Prmiorsk. Geol. Upravlenit 1, 41–44 (in Russian).
Otsuki, K., 1992. Oblique subduction, collision of microcontinents and subduction of oceanic ridge: their implications on the Cretaceous tectonics of Japan. Island Arc 1, 51–63.
Parfenov, L.M., 1984. Continental Margins and Island Arcs of the Mesozoides of Northeastern Asia. Nauka, Novosibirsk, 192 pp.
Pearce, J.A., Harris, N.W., Tindle, A.G., 1984. Trace element discrimination diagrams for the tectonic interpretation of granitic rocks. J. Petrol. 25, 956–983.
Popov, V.K., Grebennikov, A.V., 2001. The new data about age of effusions in the Bogopolsky suite in Primorski Krai. Pac. Geol. 3, 47–54 (in Russian).
Rodionov, S.M., Khanchuk, A.I., Obolenskiy, A.A., Ogasawara, M., Seminskiy, Z.V., Prokopiev, A.V., Timofeev, V.F., Nokleberg, W.J., 2010. Middle Jurassic through Quaternary metallogenesis and tectonics of northeast Asia. In: Nokleberg, W.J. (Ed.), Metallogenesis and Tectonics of Northeast Asia. U.S. Geological Survey Professional Paper 1765, 138 pp (Chapter 8).
Rodnikov, A.G., Rodkin, M.V., Stroev, P.A., Ueda, S., Isedsaki, N., Siki, T., 1996. Deep structure and geophysical fields along the Philippine Sea Geotravers. Fisika Zemli. 12, 100–108.
Rodnikov, A.G., Sergeyeva, N.A., Zabarinskaya, L.P., Filatova, N.I., Piip, V.B., Rashidov, V.A., 2008. The deep structure of active continental margins of the Far East (Russia). Russian J. Earth Sci. 10 (ES4002), 2008. http://dx.doi.org/10.2205/2007ES000224, 23 pages.
Rub, M.G., Pavlov, V.A., Gladkov, N.G., Jashukhin, O.I., 1982. Tungsten-Bearing and Tin-Bearing Granitoids of Some Regions in USSR. Nauka, Moscow, 263 p, (in Russian).
Sakhno, V.G., 2001. Late Mesozoic-Cenozoic Continental Volcanism of East Asia. Dalnauka, Vladivostok, 336 p. (in Russian).
Sakhno, V.G., Kovalenko, S.V., Alenicheva, A.A., 2011. Monzonitic magmatism of the porphyry copper deposit Lazurnoe: U–Pb and K–Ar-dating and magma genesis from evidence isotopic and geochemical study (Primor'e, Russia). Doklady AN 438, 82–90 (in Russian).
Sato, K., Kovalenko, S.V., Romanovsky, N.P., Nedachi, M., Berdnikov, N.V., Ishihara, T., 2004. Crustal control on the redox state of granitoid magmas: tectonic implications from the granitoid and metallogenic provinces in the circum-Japan Sea Region. Trans. Royal Soc. Edinburgh, Earth Sci. 95, 319–337.
Sato, K., Rodionov, S.M., Vrublevsky, A.A., 2006. Lermonotovskoe tungsten deposit: the oldest mineralization in the Sikhote-Alin orogen, Far East Russia. Resour. Geol. 56, 257–266.
Sengor, A.M.C., Natal'in, B.A., Burtman, V.S., 1993. Evolution of Altaid tectonic collage and Paleozoic crustal growth in Eurasia. Nature 364, 299–307.
Sengor, A.M.C., Natal'in, B.A., 1996. Turkic-type orogeny and its role in the making of the continental crust. Annu. Rev. Earth Planet. Sci. 24, 263–337.
Shibata, K., Igi, S., Uchiumi, S., 1977. K–Ar ages of hornblendes from gabbroic rocks in Southwest Japan. Geochem. J. 11, 57–64.
Shinjoe, H., 1997. Origin of the granodiorite in the forearc region of SW Japan: melting of the Shimanto accretionary prism. Chem. Geol. 134, 237–255.
Simanenko, V.P., Khanchuk, A.I., Golozoubov, V.V., 2002. The first data on geochemistry of Albian-Cenomanian volcanism in the Southern Primorye, Russian Far East. Geochem. Int. 40, 86–90.
Soloviev, S.G., 1995. Geologo-genetic features of the tungsten deposit Skrytoe in the Central Sikhote-Alin (Russia). Geol. Ore Deposits 37, 142–158 (in Russian).
Soloviev, S.G., Krivoshchekov, N.N., 2011. Vostok-2 gold-base metal-tungsten skarn deposit, Central Sikhote-Alin, Russia. Geol. Ore Deposits 53, 478–500.
Streckeisen, A., Le Maitre, R.W., 1979. A chemical approximation to the modal QAPF classification of the igneous rocks. Neues Jahrbuch für Mineralogie, Abhandlungen 136, 169–206.
Sun, S.S., McDonough, W.E., 1989. Chemical and isotopic systematics of oceanic basalts: implications for mantle composition and processes. In: Karthika, A.D., Norry, M.J. (Eds.), Magmatism in the Ocean Basins, vol. 42. Geological Society of London Special Publications, pp. 313–345.
Taira, A., Katto, J., Tashiro, M., Okamura, M., Komada, K., 1988. The Shimanto Belt in Shikoku, Japan—evolution of cretaceous to Miocene accretionary prism. Mod. Geol. 12, 5–46.
Tazawa, J., 2004. The strike-slip model: a synthesis on the origin and tectonic evolution of the Japanese Islands. J. Geol. Soc. Jpn. 110, 503–517.
Tsujimori, T., 1998. Geology of the Osayama serpentinite melange in the central Chugoku Mountains, southwestern Japan: 320 Ma blueschist-bearing serpentinite melange beneath the Oeyama ophiolite. J. Geol. Soc. Jpn 104, 213–231 (in Japanese with English abstract).
Tsujimori, T., Itaya, T., 1999. Blueschist-facies metamorphism during the Paleozoic orogeny in southwestern Japan: phengite K–Ar ages of blueschistfacies tectonic blocks in a serpentinite mélange beneath early Paleozoic Oeyama ophiolite. Island Arc 8, 190–205.
Utkin, V.P., 1980. Fault Displacements and Their Research Procedure. Nauka, Moscow, 144 p.
Valui, G.A., 2004. Petrologic features of granitoids of the East Sikhote-Alin volcanic Belt. Tikhookean. Geol. 23, 37–51.
Valui, G.A., 2014. Petrology of Granitoids and Differentiation of Melts Under Shallow-depth Conditions (East-Sikhote-Alinsky Volcanic Belt). Dalnauka, Vladivostok, 245 pp. (in Russian).
Valui, G.A., Moskalenko, E.Yu., Strizhkova, A.A., Sayadyan, G.R., 2008. Oxygen isotopes in the Cretaceous-Paleogene granites of Primorye and some problems of their genesis. Russian J. Pac. Geol. 2, 150–157.
Valui, G.A., Moskalenko, E.Yu., 2010. First data on the isotopes of Sm–Nd and Sr for Cretaceous-Paleogene granitoids of Primor'e and some problems of their genesis. Dokl. Earth Sci. 435, 1516–1519.
Volokhin, Yu. G., Mikhailik, E.V., Burii, G.I., 2003. Triassic Siliceous Association of the Southern Sikhote-Alin. Dal'nauka, Vladivostok, 252 pp. (in Russian).
Whalen, J.B., Currie, K.L., Chappell, B.W., 1987. A-type granites: geochemical characteristics, discriminations and petrogenesis. Contrib. Miner. Petrol. 95, 407–419.
Whitney, D.L., Evans, B.W., 2010. Abbreviations for names of rock-forming minerals. Am. Mineral. 95, 185–187.
Wilde, S., 2015. Final amalgamation of the Central Asian Orogenic Belt in NE China: Paleo-Asian Ocean closure versus Paleo-Pacific plate subduction—a review of the evidence. Tectonophysics, in press. http://dx.doi.org/10.1016/j.tecto.2015.05.006.
Wilde, S.A., Dorsett-Bain, H.L., Liu, J.L., 1997. The identification of a Late Pan-African granulite facies event in northeastern China: SHRIMP U–Pb zircon dating of the Mashan Group at Liu Mao, Heilongjiang Province, China. Proceedings of the 30th IGC: Precambrian Geology and Metamorphic Petrology, vol. 17. VSP International Science Publishers, Amsterdam, pp. 59–74.
Wilde, S.A., Zhang, X.Z., Wu, F.Y., 2000. Extension of a newly-identified 500 Ma metamorphic terrain in Northeast China: further U–Pb SHRIMP dating of the Mashan Complex, Heilongjiang Province, China. Tectonophysics 328, 115–130.
Wilde, S.A., Wu, F.Y., Zhang, X.Z., 2003. Late Pan-African magmatism in northeastern China: SHRIMP U–Pb zircon evidence from granitoids in the Jiamusi Massif. Precambr. Res. 122, 311–327.
Wilde, S.A., Wu, F.Y., Zhao, G.C., 2010. The Khanka Block, NE China, and its significance to the evolution of the Central Asian Orogenic Belt and continental accretion. In: Kusky, T.M., Zhai, M.G., Xiao, W.J. (Eds.), The Evolved Continents: Understanding Processes of Continental Growth, vol. 338. Geological Society of London, Special Publication, pp. 117–137.
Woodhead, J.D., Hergt, J.M., 2005. A preliminary appraisal of seven natural zircon reference materials for in situ Hf isotope determination. Geostand. Geoanal. Res. 29, 183–195.
Woodhead, J., Hergt, J., Shelley, M., Eggins, S., Kemp, R., 2004. Zircon Hf-isotope analysis with an excimer laser, depth profiling, ablation of complex geometries, and concomitant age estimation. Chem. Geol. 209, 121–135.
Wu, F.Y., Sun, D.Y., Jahn, B.M., Wilde, S., 2004. A Jurassic garnet-bearing granitic pluton from NE China showing tetrad REE patterns. J. Asian Earth Sci. 23, 731–744.
Wu, F.Y., Yang, Y.H., Xie, L.W., Yang, J.H., Xu, P., 2006. Hf isotope compositions of the standard zircons and baddeleyites used in U–Pb geochronology. Chem. Geol. 234, 105–126.
Wu, F.Y., Sun, D.Y., Ge, W.C., Zhang, Y.B., Grant, M.L., Wilde, S.A., Jahn, B.M., 2011. Geochronology of the Phanerozoic granitoids in northeastern China. J. Asian Earth Sci. 41, 1–30.

Please cite this article in press as: Jahn, B.-m., et al. Emplacement ages, geochemical and Sr–Nd–Hf isotopic characterization of Mesozoic to early Cenozoic granitoids of the Sikhote-Alin Orogenic Belt, Russian Far East: Crustal growth and regional tectonic evolution. Journal of Asian Earth Sciences (2015), http://dx.doi.org/10.1016/j.jseaes.2015.08.012

Xie, L.W., Zhang, Y.B., Zhang, H.H., Sun, J.F., Wu, F.Y., 2008. *In situ* simultaneous determination of trace elements, U–Pb and Lu–Hf isotopes in zircon and baddeleyite. Chin. Sci. Bull. 53, 1565–1573.

Zonenshain, L.P., Kuzmin, M.I., Natapov, L.M., 1990a. Plate Tectonics of the USSR Territory, vol. 2. Nedra, Moscow, p. 334.

Zonenshain, L.P., Kuzmin, M.I., Natapov, L.M., 1990b. Geology of the USSR. A Plate Tectonic Synthesis, vol. 21. AGU Publications, 242 pp.

Zhou, J.B., Wilde, S.A., Zhao, G.C., Zhang, X.Z., Zheng, C.Q., Wang, H., Zeng, W.S., 2010. Pan-African metamorphic and magmatic rocks of the Khanka Massif, NE China: further evidence regarding their affinity. Geol. Mag. 147, 737–749.

Zhou, J.B., Wilde, S.A., Zhang, X.Z., Ren, S.M., Zheng, C.Q., 2011. Pan-African metamorphic rocks of the Erguna block in the Great Xing'an Range, NE China: evidence for the timing of magmatic and metamorphic events and their tectonic implications. Tectonophysics 499, 105–177.

Zhou, J.B., Wilde, S.A., 2013. The crustal accretion history and tectonic evolution of the NE China segment of the Central Asian Orogenic Belt. Gondwana Res. 23, 1365–1377.

Please cite this article in press as: Jahn, B.-m., et al. Emplacement ages, geochemical and Sr–Nd–Hf isotopic characterization of Mesozoic to early Cenozoic granitoids of the Sikhote-Alin Orogenic Belt, Russian Far East: Crustal growth and regional tectonic evolution. Journal of Asian Earth Sciences (2015), http://dx.doi.org/10.1016/j.jseaes.2015.08.012